

✓

Spatio-temporal Dynamics of Heterogeneously Distributed Populations

by

Alisa S. Vadasz

Submitted in part fulfilment of the requirements for the degree of

Doctor of Philosophy (PhD) in Engineering

in the Department of Chemical Engineering in the Faculty of Engineering

at the University of Durban-Westville

Promoter: Prof. M. Carsky

Department of Chemical Engineering

Co-promoter: Prof. A.S. Gupthar

Department of Biochemistry

September 2003

DECLARATION

The Registrar (Academic)

UNIVERSITY OF DURBAN-WESTVILLE

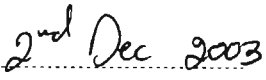
Dear Sir/Mme

I, Alisa S. Vadasz , REG.NO.: 9509479, hereby declare that the thesis entitled

Spatio-temporal Dynamics of Heterogeneously Distributed Populations

is the result of my own investigation and research and that it has not been submitted in part or in full for any other degree or to any other University.


.....
Signature


.....
Date

Acknowledgments

I wish to express my sincere gratitude to all those who provided me encouragement and assistance during the course of this study. Special appreciation is extended to:

Professor M. Carsky from Chemical Engineering Department and Professor A.S. Gupthar from Biochemistry Department for their invaluable guidance and advice as supervisors of this research.

Professor P. Vadasz the Chair of Mechanical Engineering at Northern Arizona University, AZ, USA, my husband and advisor, for his constant enthusiastic involvement, support, guidance, and assistance.

Professor N. M. Ijumba, the Dean of Engineering for his interest and moral support.

Professor M. Ariatti from Biochemistry Department for his constant interest, support and assistance whenever it was required.

Mr. Prem Ramlachan (Diggers) from Public Affairs, the Office of International Relations for his administrative guidance and help.

My dear endless supporting and encouraging family, Peter, my husband, and Johnathan, Nataly and Gabriel, my children.

SYNOPSIS

A theoretical account of investigating the growth dynamics in heterogeneously distributed populations is presented. The study presents the derivation of analytical solutions to the problem of growth of populations in space and in time. It has applications in a variety of fields, from microbial cell growth in Microbiology and Biochemistry, via animal population and vegetation growth in Ecology, and eventually in human cell growth of normal and abnormal (such as benign and malignant cells) tissues. The analytical solutions are compared to numerical solutions obtained via standard differential equations solvers showing a very good match within the parameter windows where the analytical solutions are expected to be valid. The novelty of this work focuses on four aspects: *(i)* expanding the application of a Neoclassical Model derived originally to deal with growth that is spatially homogeneous within the spatially heterogeneous problem, *(ii)* undertaking a linear stability analysis of the stationary points corresponding to the Neoclassical Model as applied to the heterogeneous problem, *(iii)* providing an analytical weak nonlinear solution to the spatially homogeneous problem and comparing the results to a numerical solution, and *(iv)* deriving a weak nonlinear solution to the spatially heterogeneous problem and comparing the results to a numerical solution. The Neoclassical Model applied to the spatially homogeneous problem was shown to capture all qualitative features that appear in growth experiments and a large number of quantitative results were shown to match very well their corresponding experiments. This work presents the first application of this model to the spatially heterogeneous problem providing linear stability analyses and analytical solutions by using the weak nonlinear method of solution.

KEY WORDS : Microbial Growth, Population Dynamics, Turing Instabilities,
Spatially Heterogeneous Growth, Neoclassical Theory.

Short Title: Growth Dynamics in Heterogeneous Populations

Table of Contents

	Page
DECLARATION	i
ACKNOWLEDGMENTS	ii
SYNOPSIS	iii
TABLE OF CONTENTS	iv
LIST OF FIGURES	ix
LIST OF TABLES	xviii
NOMENCLATURE	xix
CHAPTER 1 INTRODUCTION	1
1.1 Motivation and Background	1
1.2 Literature Survey	3
1.2.1 Growth Dynamics in Homogeneously Distributed Populations	3

1.2.2 The Neoclassical Model	10
Evaluation of the net average body mass, $m(u)$	21
Units and Dimensions	25
Monotonic Growth with LGM as a Particular Case	25
Analysis and Solution of the Equation Governing Monotonic Growth	26
Non-Monotonic Growth	35
1.2.3 Growth Dynamics in Heterogeneously Distributed Populations	39
Linear Stability Analysis	41
1.3 Summary of Unanswered Questions and Problems	45
 CHAPTER 2 PROBLEM FORMULATION	 46
2.1 Governing Equations and Boundary Conditions	46
2.2 Transforming the Equations into a Dimensionless Form	49
 CHAPTER 3 STATIONARY SOLUTIONS, MULTIPLICITY AND PARAMETER CONTROL	 53
3.1 Stationary Solutions	53
3.1.1 Derivation of Stationary Solutions	53
3.1.2 Conditions for u_{s1} to be biologically meaningful, i.e. non-negative ($u_{s1} \geq 0$)	55
3.1.3 Conditions for u_{s2} to be biologically meaningful, i.e. non-negative ($u_{s2} \geq 0$)	56
3.1.4 Additional Stationary Solutions	56
3.2 Multiplicity of Solutions	57
3.3 Stability Criteria and Parameter Control	58

CHAPTER 4 LINEAR STABILITY ANALYSIS TO SPATIALLY HOMOGENEOUS PERTURBATIONS (SHoP)	61
4.1 Linear Stability of the Nontrivial Stationary Solutions $(u_{s1,2}, v_{s1,2})$	61
4.2 Linear Stability of the Trivial Stationary Solution $(u_{so} = 0, v_{so})$	76
4.3 Explicit Stability Conditions to Spatially Homogeneous Perturbations (SHoP)	78
4.3.1 <i>General Derivation</i>	78
4.3.2 <i>The case corresponding to: $\beta_1 > 0$ & $\varphi_o < 0$</i>	79
<i>Deriving the explicit condition for (4-72)</i>	79
<i>Deriving the explicit condition for (4-73)</i>	80
4.3.3 <i>The case corresponding to: $\beta_1 < 0$ & $\varphi_o > 0$</i>	84
<i>Deriving the explicit condition for (4-72)</i>	84
<i>Deriving the explicit condition for (4-73)</i>	84
4.3.4 <i>The case corresponding to: $\beta_1 > 0$ & $\varphi_o > 0$</i>	88
4.3.5 <i>The case corresponding to: $\beta_1 < 0$ & $\varphi_o < 0$</i>	90
4.3.6 <i>Summary of Stability Conditions to SHoP</i>	93
4.3.7 <i>Procedure to Identify Windows of Parameter Values that Provide Necessary Conditions for Linear Stability to SHoP</i>	95
 CHAPTER 5 WEAK NONLINEAR SOLUTION FOR THE SPATIALLY HOMOGENEOUS PROBLEM	 97
5.1 Governing Equations for the Spatially Homogeneous Problem	97
5.2 Asymptotic Expansion, Scales and Parameters	99
5.3 Leading Order Solution at $O(1)$	102
5.4 Solution at Order $O(\varepsilon)$	103
5.5 Solution at Order $O(\varepsilon^2)$	106
5.6 Solvability Condition at Order $O(\varepsilon^3)$	111
5.7 Amplitude Equation, Bifurcation Structure and Solution	114
5.8 Complete Weak Nonlinear Solution and Numerical Method of Solution	119

5.9 Results and Discussion	121
5.9.1 - <i>An Example Demonstrating the Comparison between the Weak Nonlinear Method with the Linear Stability Analysis using a Numerical Solution for Benchmarking</i>	121
5.9.2 - <i>A Comparison between the Weak Nonlinear Results and a Numerical Solution for Benchmarking</i>	124
 CHAPTER 6 LINEAR STABILITY ANALYSIS TO SPATIALLY HETEROGENEOUS PERTURBATIONS (SHEP)	 130
6.1 Linear Stability of the Nontrivial Stationary Solutions $(u_{SI,2}, v_{SI,2})$	130
6.2 Summary of Stability Conditions	146
6.3 Conditions for Occurrence of Turing Instability	148
 CHAPTER 7 WEAK NONLINEAR SOLUTION FOR THE SPATIALLY HETEROGENEOUS PROBLEM	 149
7.1 Governing Equations for the Spatially Heterogeneous Problem	149
7.2 Asymptotic Expansion, Scales and Parameters	150
7.3 Solution at Leading $O(1)$	152
7.4 Order Solution at Order $O(\varepsilon)$	153
7.5 Solution at Order $O(\varepsilon^2)$	155
7.6 Solvability Condition at Order $O(\varepsilon^3)$	159
7.7 Amplitude Equation, Bifurcation Structure and Solution	162
7.8 Complete Weak Nonlinear Solution	165
7.9 Numerical Method of Solution	166
7.10 Results and Discussion	169
 CHAPTER 8 DISCUSSION AND CONCLUSIONS	 191
 REFERENCES	 192

APPENDICES	197
Appendix 1: Derivation of the Right-Hand-Side of eq. (5-41)	197
Appendix 2: Derivation of the Right-Hand-Side of eq. (5-43)	199
Appendix 3: Derivation of the Resonant Terms on the Right-Hand-Side of eq. (5-64)	201
Appendix 4: Derivation of the Right-Hand-Side of eq. (7-29)	203
Appendix 5: Derivation of the Right-Hand-Side of eq. (7-31)	205

List of Figures

	Page
Figure 1.1: Comparison of the LGM solution with experimental results for yeast cells based on Pearl (1927), after data from Carlson (1913) (here redrawn using the tabulated data from Pearl, 1927). (a) Cell concentration (normalized and dimensionless) versus time; (b) the <i>ln</i> curve of the cell concentration versus time.	4
Figure 1.2: The phase diagram for the solution of the LGM compared to: (a) concave and convex curves representing shapes that were obtained in different experiments. (b) Richards family of curves.	8
Figure 1.3: Typical colonies of <i>Saccharomyces cerevisiae</i> strains T206, T206q, VIN7 and Y217, respectively, growing on the differentiation medium WLN, used as the control group (A.S. Vadasz, 2000).	13
Figure 1.4: Typical challenged colonies of <i>Saccharomyces cerevisiae</i> strains growing on the differentiation medium WLN. Samples of sensitive strains, VIN7 and Y217, separately mixed with both the killer, T206, and the killer cured, T206q, respectively (A.S. Vadasz, 2000).	14
Figure 1.5: A methylene blue agar plate of the sensitive strain VIN7 challenged by both T206 ₁ and T206q growing in the liquid media. T206 ₂ sample was taken from a YMA plate. T206 ₁ and T206 ₂ showed the same growth pattern of the killer toxin effect, which was not observed for the cured strain, T206q (A.S. Vadasz, 2000).	15

Figure 1.6: Agarose gel electrophoresis of total nucleic acids the K_2 killer strain *Saccharomyces cerevisiae* T206 and its cured derivative, (T206q) (A.S. Vadasz, 2000). 16

Figure 1.7: Scanning Electron Microscope images of *Saccharomyces cerevisiae* wine strains growing under severe nutrient limitation. (a) Bipolar budding (pb) of daughter cells, which stay attached to elongated mother cells, forming pseudohyphae. (b) Pseudohyphae (ph) forage for limited nutrients (A.S. Vadasz, 2000). 17

Figure 1.8: Scanning Electron Microscope images of *Saccharomyces cerevisiae* wine strains growing on a stress medium, 3% grape juice agar, showing that undamaged cells are covered by protected sheaths (ps) (a and b), a net-like structure (b) and also revealing an invasive cell growth pattern (c and d) (A.S. Vadasz, 2000). 17

Figure 1.9: TEM images of *Saccharomyces cerevisiae* wine strains growing under severe nutrient limitation (a) forming transport vesicle of materials in or out of cell, and (b & c) releasing materials, which are potential nutrients or/and toxins (A. S. Vadasz, 2000). 18

Figure 1.10: Micrographs of sensitive *S. cerevisiae* cells damaged by a K_2 killer toxin (A.S. Vadasz, 2000). 18

Figure 1.11: Experimental results of total viable cell concentration and differentiation between the Y217 and VIN7 strains of yeast grown as a mixed culture in pure water. (a) Cell differentiation data; (b) Total viable cells (A.S. Vadasz, 2000). 19

Figure 1.12: Neoclassical model results (earlier version) for competition showing damped oscillations in the concentration of the surviving species and the extinction of the other species; survival of one species and extinction of the other; coexistence of both species (A.S. Vadasz, 2000). 20

Figure 1.13: Experimental results of the total viable cell biomass as a function of cell concentration for the T206 strain of yeast grown in 5% grape juice medium ($1\text{ MCell} = 10^6\text{ Cells}$), (Vadasz, P., Vadasz, A.S. 2002 a,b). 23

Figure 1.14: Experimental results of the total viable cell biomass as a function of cell concentration for the T206 strain of yeast grown in a rich medium. (a) Experimental results over the whole domain. (b) Detail around the origin ($1\text{ MCell} = 10^6\text{ Cells}$), (Vadasz, P., Vadasz, A.S. 2002 a,b). 24

Figure 1.15: Phase diagram for the solution of monotonic growth corresponding to $R > 1$, in terms of the specific growth rate \dot{U}/U versus the population number U , for $R = 5$ (Vadasz, P., Vadasz, A.S. 2002 a,b). 33

Figure 1.16: The effect of the initial growth rate on Lip and Lag . Analytical results in the time domain based on the Neoclassical Theory (Vadasz, P., Vadasz, A.S. 2002 a,b) for $R = 2$, subject to initial conditions of $U_o = 0.1$ and different small values of \dot{U}_o . 34

Figure 1.17: The solution to Growth followed by Decay according to the Logistic Growth Model (LGM). Initial conditions: $u_o = 0.05\delta$. The growth switches to decay at $(u/\delta) = 0.5$. 36

Figure 1.18: Numerical results of the Neoclassical Model (Vadasz, P., Vadasz, A.S. 2002 a,b) applied to the case of growth followed by decay, compared with experimental data from Pearl (1927). The parameter values for the numerical solution are $u_o = 2$, $\dot{u}_o = 1.5$, $v = -0.04$, $\mu = -1.2$, $r_m = 0.035$, $(k/m_o) = 8 \cdot 10^{-5}$, $b = 12$ and $\gamma = -1.6 \cdot 10^3$ in units consistent with Pearl (1927). 38

Figure 1.19: “ Snapshot after mixing an oscillating yeast extract to homogeneity. Reduced purine nucleotides yield dark structures. It is the first experimental demonstration that a biochemical system in homogeneous phase might break spatial homogeneity and evolve to spatial-temporal order” (reproduced from Haken, 1979, after Boiteux & Hess, 1978). 39

Figure 2.1: Dimensional representation of the problem formulation for growth dynamics in spatially heterogeneous populations. 47

Figure 2.2: Dimensionless representation of the problem formulation for growth dynamics in spatially heterogeneous populations. 51

Figure 4.1: Qualitative description of overdamped conditions identified to be applicable for $0 < \Delta_A < \psi_A^2/4$. 68

Figure 4.2: Qualitative description of critically damped conditions identified to be applicable for $0 < \Delta_A = \psi_A^2/4$. 68

Figure 4.3: Qualitative description of underdamped conditions identified to be applicable for $\Delta_A > \psi_A^2/4 > 0$. 69

Figure 4.4: Qualitative description of neutrally stable conditions identified to be applicable for $\psi_A = 0$ and $\Delta_A > 0$. 69

Figure 4.5: Qualitative description of monotonically unstable conditions identified to be applicable for $\psi_A > 0$ and $0 < \Delta_A < \psi_A^2/4$. 72

Figure 4.6: Qualitative description of monotonically unstable conditions identified to be applicable for $\psi_A > 0$ and $0 < \Delta_A = \psi_A^2/4$. 72

Figure 4.7: Qualitative description of monotonically unstable conditions identified to be applicable for $\psi_A > 0$ and $\Delta_A > \psi_A^2/4 > 0$.	73
Figure 5.1: Bifurcation diagram identifying a forward Hopf bifurcation.	117
Figure 5.2: Numerical solution showing the apparent exponential divergence of the amplitude for $\gamma_o = 1$ and $R = 5$, $\beta_o = 2.56 > \beta_{o,cr} = 2.5$. Short term results.	122
Figure 5.3: Numerical solution showing the finite amplitude results for $\gamma_o = 1$ and $R = 5$, $\beta_o = 2.56 > \beta_{o,cr} = 2.5$. Long term results.	122
Figure 5.4: Numerical solution showing the post-transient results $1500 < t < 1680$, for $\gamma_o = 1$ and $R = 5$, $\beta_o = 2.56 > \beta_{o,cr} = 2.5$.	123
Figure 5.5: Numerical results compared to the weak nonlinear solution for $\gamma_o = 1$ and $R = 5$, $\beta_o = 2.56 > \beta_{o,cr} = 2.5$.	124
Figure 5.6: Numerical results compared to the weak nonlinear solution for $\gamma_o = 1$ and $R = 5$, $\beta_o = 2.56 > \beta_{o,cr} = 2.5$. Quantitative comparison shows a very good match for time range $0 < t < 250$. For small times, i.e. small amplitudes the match looks better than for longer times.	126
Figure 5.7: Numerical results compared to the weak nonlinear solution for $\gamma_o = 1$ and $R = 5$, $\beta_o = 2.56 > \beta_{o,cr} = 2.5$. Quantitative comparison shows a quantitative deterioration in accuracy for time range $1500 < t < 1680$. For long times, i.e. large amplitudes the accuracy of the weak nonlinear results is somewhat compromised in both the frequency of oscillations as well as the amplitude value.	127
Figure 5.8: Numerical results compared to the weak nonlinear solution for $\gamma_o = 1$ and $R = 5$, $\beta_o = \beta_{o,cr} = 2.5$.	128

Figure 5.9: Numerical results compared to the weak nonlinear solution for $\gamma_o = 1$ and $R = 5$, $\beta_o = \beta_{o,cr} = 2.5$. Inset into the post-transient time range $350 < t < 420$. 129

Figure 6.1: Characteristic (neutral) curves corresponding to $\beta_1 = 2$, $\varphi_o < 0$, $Rn\varphi_o = -2$, $Rn\Delta_A = 4$. 138

Figure 6.2: Characteristic (neutral) curves corresponding to $\beta_1 = 2$, $\varphi_o = 0$, $Rn\varphi_o = 0$, $Rn\Delta_A = 4$. 139

Figure 6.3: Characteristic (neutral) curves corresponding to $\beta_1 = 2$, $0 < \varphi_o < (\kappa_{as}^2)/Rn$, $Rn\varphi_o = 1.5$, $Rn\Delta_A = 4$. 140

Figure 6.4: Characteristic (neutral) curves corresponding to $\beta_1 = 2$, $0 < \varphi_o = (\kappa_{as}^2)/Rn$, $Rn\varphi_o = 2$, $Rn\Delta_A = 4$. 141

Figure 6.5: Characteristic (neutral) curves corresponding to $\beta_1 = 2$, $0 < (\kappa_{as}^2)/Rn < \varphi_o$, $Rn\varphi_o = 2.5$, $Rn\Delta_A = 4$. 142

Figure 6.6: Characteristic (neutral) curves corresponding to $\beta_1 = -1.5$, $\varphi_o > 0$, $Rn\varphi_o = 2$, $Rn\Delta_A = 4$. 143

Figure 6.7: Characteristic (neutral) curves corresponding to $\beta_1 = -2$, $\varphi_o < 0$, $Rn\varphi_o = -1.7$, $Rn\Delta_A = 4$. 144

Figure 6.8: Characteristic (neutral) curves corresponding to $\beta_1 = -2$, $\varphi_o < 0$, $Rn\varphi_o = -2.3$, $Rn\Delta_A = 4$. 145

Figure 7.1: Bifurcation diagram identifying a forward pitchfork bifurcation. 164

Figure 7.2: Graphical representation of the numerical grid used in the numerical solution. 168

Figure 7.3: Graphical representation of the steady state weak nonlinear solution $u(x)$ compared to the numerical results for a sub-critical value of Gn , i.e. $Gn = 5 < Gn_{cr} = 5.70269$. The solution stabilizes at the stationary solution $u_s = 0.225$. 171

Figure 7.4: Graphical representation of the steady state weak nonlinear solution $v(x)$ compared to the numerical results for a sub-critical value of Gn , i.e. $Gn = 5 < Gn_{cr} = 5.70269$. The solution stabilizes at the stationary solution $v_s = -1.51875$. 172

Figure 7.5: Graphical representation of the steady state weak nonlinear solution v vs. u on the phase plane compared to the numerical results for a sub-critical value of Gn , i.e. $Gn = 5 < Gn_{cr} = 5.70269$. The solution stabilizes at the stationary solution $u_s = 0.225$, $v_s = -1.51875$. 173

Figure 7.6: Graphical representation of the steady state weak nonlinear solution $u(x)$ compared to the numerical results for a slightly super-critical value of Gn , i.e. $Gn = 5.71 > Gn_{cr} = 5.70269$. 174

Figure 7.7: Graphical representation of the steady state weak nonlinear solution $v(x)$ compared to the numerical results for a slightly super-critical value of Gn , i.e. $Gn = 5.71 > Gn_{cr} = 5.70269$. 175

Figure 7.8: Graphical representation of the steady state weak nonlinear solution v vs. u on the phase plane compared to the numerical results for a slightly super-critical value of Gn , i.e. $Gn = 5.71 > Gn_{cr} = 5.70269$. 176

Figure 7.9: Graphical representation of the difference between the steady state weak nonlinear solution and to the numerical results expressed by $\Delta u(x)$, for a slightly super-critical value of Gn , i.e. $Gn = 5.71 > Gn_{cr} = 5.70269$. The difference is less than $\pm 2 \cdot 10^{-3}$. 177

Figure 7.10: Graphical representation of the steady state weak nonlinear solution $u(x)$ compared to the numerical results for a super-critical value of Gn , i.e. $Gn = 7 > Gn_{cr} = 5.70269$. 178

Figure 7.11: Graphical representation of the steady state weak nonlinear solution $v(x)$ compared to the numerical results for a super-critical value of Gn , i.e. $Gn = 7 > Gn_{cr} = 5.70269$. 179

Figure 7.12: Graphical representation of the steady state weak nonlinear solution v vs. u on the phase plane compared to the numerical results for a super-critical value of Gn , i.e. $Gn = 7 > Gn_{cr} = 5.70269$. 180

Figure 7.13: Graphical representation of the difference between the steady state weak nonlinear solution and to the numerical results expressed by $\Delta u(x)$, for a super-critical value of Gn , i.e. $Gn = 7 > Gn_{cr} = 5.70269$. The difference is less than $\pm 8 \cdot 10^{-3}$. 181

Figure 7.14: Graphical representation of the steady state weak nonlinear solution $u(x)$ compared to the numerical results for a large super-critical value of Gn , i.e. $Gn = 15 > Gn_{cr} = 5.70269$. The breakdown of the accuracy of the weak nonlinear solution is evident. 182

Figure 7.15: Graphical representation of the steady state weak nonlinear solution $v(x)$ compared to the numerical results for a large super-critical value of Gn , i.e. $Gn = 15 > Gn_{cr} = 5.70269$. The breakdown of the accuracy of the weak nonlinear solution is less evident in the solution for $v(x)$. 183

Figure 7.16: Graphical representation of the steady state weak nonlinear solution v vs. u on the phase plane compared to the numerical results for a large super-critical value of Gn , i.e. $Gn = 15 > Gn_{cr} = 5.70269$. The breakdown of the accuracy of the weak nonlinear solution is evident. 184

Figure 7.17: Graphical representation of the steady state numerical results of $u(x)$ for a large super-critical value of Gn , i.e. $Gn = 20 > Gn_{cr} = 5.70269$. 185

Figure 7.18: Graphical representation of the steady state numerical results of $v(x)$ for a large super-critical value of Gn , i.e. $Gn = 20 > Gn_{cr} = 5.70269$. 186

Figure 7.19: Graphical representation of the steady state numerical results v vs. u on the phase plane for a large super-critical value of Gn , i.e. $Gn = 20 > Gn_{cr} = 5.70269$. 187

Figure 7.20: Graphical representation of the steady state weak nonlinear solution $u(x)$ compared to the numerical results for a super-critical value of Gn , i.e. $Gn = 25 > Gn_{cr} = 5.70269$. The second Fourier mode in the solution is evident and is captured also by the weak nonlinear solution although its accuracy suffers due to the large distance from Gn_{cr} . 188

Figure 7.21: Graphical representation of the steady state weak nonlinear solution $v(x)$ compared to the numerical results for a super-critical value of Gn , i.e. $Gn = 25 > Gn_{cr} = 5.70269$. The second Fourier mode in the solution is evident and is captured also by the weak nonlinear solution although its accuracy suffers due to the large distance from Gn_{cr} . 189

Figure 7.22: Graphical representation of the steady state weak nonlinear solution v vs. u on the phase plane compared to the numerical results for a large super-critical value of $Gn = 25 > Gn_{cr} = 5.70269$. 190

List of Tables

	Page
Table 4.1: Stability Table and type of qualitative regimes	75
Table 4.2: Explicit Stability Table for u_{s_0}, v_{s_0}	93
Table 4.3: Explicit Stability Table for u_{s_1}, v_{s_1}	94
Table 4.4: Explicit Stability Table for u_{s_2}, v_{s_2}	94

Nomenclature

Latin Symbols

A - amplitude in the weak nonlinear solution.

B - amplitude in the weak nonlinear solution.

C - amplitude in the weak nonlinear solution.

D_* - diffusivity of the population in the growth medium.

D - amplitude in the weak nonlinear solution.

E - amplitude in the weak nonlinear solution.

Gn - growth dimensionless number, eq. (2-8), (primitive parameter).

H_* - breadth of the domain.

k - cell or organism's nutrient storage capacity, eq. (1-8).

L_* - length of the domain.

L - aspect ratio of the domain, or dimensionless length, equals L_*/H_* .

M - total population net viable biomass, eq. (1-9).

m - net average viable body mass, eq. (1-10).

m_o - constant related to the total population net viable biomass, eq. (1-9).

m_1 - constant related to the total population net viable biomass, eq. (1-9).

N - spatial grid points in the numerical solution.

r_m - viable biomass ratio, equals m_1/m_o .

R - viable biomass dimensionless number, equals $r_m\delta$, (primitive parameter).

Rn - resource dimensionless number, eq. (2-8), (primitive parameter).

Sn - storage dimensionless number, eq. (2-8).

SHeP – Spatially Heterogeneous Perturbations.

SHoP – Spatially Homogeneous Perturbations.

r - absolute value of the complex amplitude.

t - time.

u - population number (or population concentration).

v - nutrient (or resource) consumption/utilization rate.

x - horizontal space coordinate in the direction measuring the length.
 y - horizontal space coordinate in the direction measuring the breadth.
 z - vertical space coordinate in the direction measuring the depth.

Greek Symbols

α - nutrient diffusivity in the growth medium, eq. (2-1).
 β - parameters defined by eq. (3-26).
 β_o - primitive parameter defined by eq. (2-14).
 γ - parameter/s defined by eq. (2-11).
 χ - relaxation time in the weak nonlinear amplitude equation to SHeP
 δ - carrying capacity of the environment.
 Δ - determinant of matrices A or B , eqs. (4-22) and (6-15), respectively.
 ε - asymptotic expansion parameter, $\varepsilon \ll 1$.
 φ_o - primitive parameter, eq. (2-9).
 η - amplitude equation parameter, eq. (5-78).
 κ - wave number.
 λ - eigenvalues.
 μ - maximum specific growth rate, eq. (1-2).
 θ - phase angle.
 σ_o - frequency of oscillations.
 τ - slow time scale, equals $\varepsilon^2 t$.
 ψ - trace of matrices A or B , eqs. (4-21) and (6-14), respectively.

Subscripts

* - dimensional values.
 A - related to matrix A , eq. (4-14).
 B - related to matrix B , eq. (6-10).
 S - stationary solution.
 l - corresponding to order $O(\varepsilon)$ in the asymptotic expansion.

2 - corresponding to order $O(\varepsilon^2)$ in the asymptotic expansion.

3 - corresponding to order $O(\varepsilon^3)$ in the asymptotic expansion.

Superscripts

$(\cdot)^*$ - complex conjugate.

CHAPTER 1

INTRODUCTION

1.1 Motivation and Background

Growth dynamics is a topic that has a wide variety of applications in different fields, from microbial cell growth in Microbiology and Biochemistry, via animal population and vegetation growth in Ecology, and eventually even in human cell growth (benign as well as malignant cells). Therefore, there are a variety of industries and services that are substantially impacted by the advancement of knowledge in this field. The food and beverage industries use this knowledge to control their processes. In the food industry the potential ability to control the *Lag* phase of microbial growth has the direct implication of increasing the shelf time of food products, leading to substantial financial savings, reduced prices of products and increasing the safety levels in consuming these products. In the beverage industry, e.g. wine production, different strains of yeast (*Saccharomyces cerevisiae*) are being used in the fermentation process. A better understanding of the yeast growth dynamics may improve the relevant processes, increase their efficiency, leading eventually to a better and cheaper product. In Ecology, it is paramount to understand the natural processes of population dynamics in order to reach correct conclusions regarding possible threats of extinction of a particular species and consequent requirements of otherwise undesirable human intervention. The latter is sometimes necessary in order to keep ecological balance. In particular, the fish industry in oceans and seas is extremely vulnerable to abnormal demands that may adversely impact the availability of fish in the years that follow such demands. In Medicine, the ability to understand, predict, and eventually control malignant cell growth might hold potentially the solution to cure or efficient treatment of a large number of diseases. All the examples given above have one common factor namely they all are related to population growth. The objective is to find the population number at all future times, given an initial population number (and possibly its initial growth rate) and the environmental factors

such as nutrient availability, pH, ambient temperature, etc., assuming that the spatial distribution of the population is uniform. The latter uniformity can be accomplished by forcing a well-mixed environment or can naturally occur under certain circumstances.

Since the early works of Malthus (1798), Pearl (1927) and Verhulst (1838) a large amount of work has been done in order to address the understanding of the problem of population dynamics and growth. Nevertheless, there is still disagreement in the scientific community regarding the lack of one universal law of nature that governs population growth as well as regarding the relevant mechanisms that control the latter.

While the topic of growth dynamics in homogeneously distributed populations has been dealt with since the nineteenth century, the corresponding problem of growth in heterogeneously distributed populations started receiving the required attention only in the second half of the twentieth century with the seminal work of Turing, (1952). The objective in this type of problem is to find the population number and its spatial distribution at all future times, given an initial spatial distribution of the population (and possibly its initial growth rate distribution), boundary conditions, and environmental factors.

1.2 Literature Survey

1.2.1 Growth Dynamics in Homogeneously Distributed Populations

Thomas Robert Malthus (1798) suggested the first theory of population growth in his essay “*An essay on the principle of population*”. His theory can be represented by the following equation

$$\frac{du}{dt} = \beta u \quad , \quad (1-1)$$

where u is the population number that yields an exponential solution of the form $u = u_0 e^{\beta t}$, where u_0 is the initial population number and β is the Malthusian specific growth rate. The exponential, unlimited, growth was a concern as it is natural to expect any population to arrive eventually at some finite population number. This problem was resolved by Pearl (1927). He suggested a very simple theory for population growth and applied it for a wide variety of experimental data indicating in some cases an outstanding fit. The Logistic Growth Model (LGM) suggested independently by Pearl (1927) was derived earlier by Verhulst (1838) but was practically forgotten and overlooked for almost ninety years. It essentially suggests that the concentration of a particular population be governed by the following equation

$$\frac{du}{dt} = \mu \left(1 - \frac{u}{\delta} \right) u \quad , \quad (1-2)$$

where u is the population number or the viable cell concentration, δ is the carrying capacity of the environment, and μ is the maximum specific growth rate. It can be observed that eq.(1-2) reduces to Malthus’s equation (1-1) when $(u/\delta) \ll 1$ and $\mu = \beta$. The distinction between the two constants μ and β will be discussed later in the context of the Neoclassical Theory. Equation (1-2) can be presented also in the following equivalent form proposed by Edelstein-Keshet (1988).

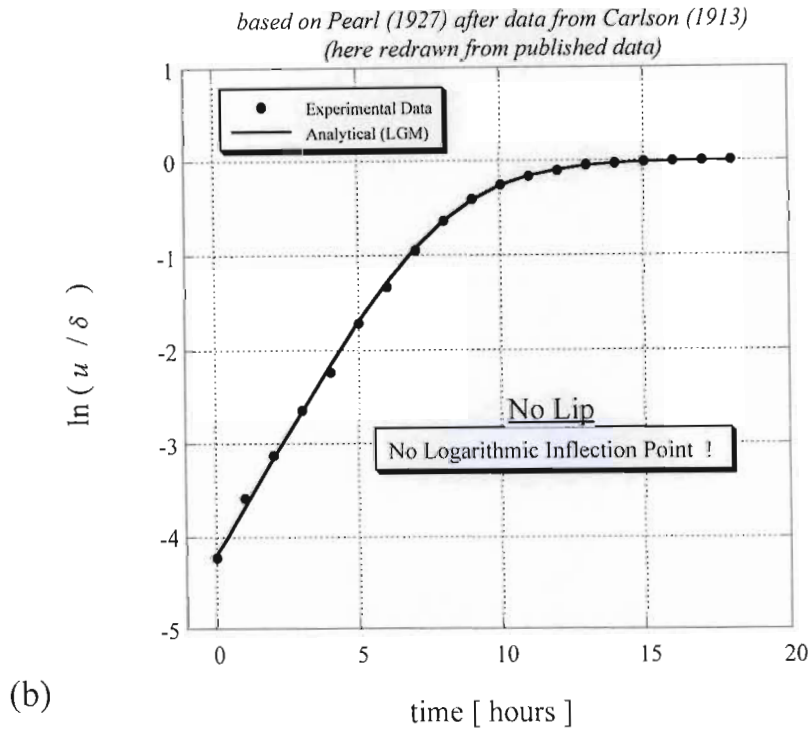
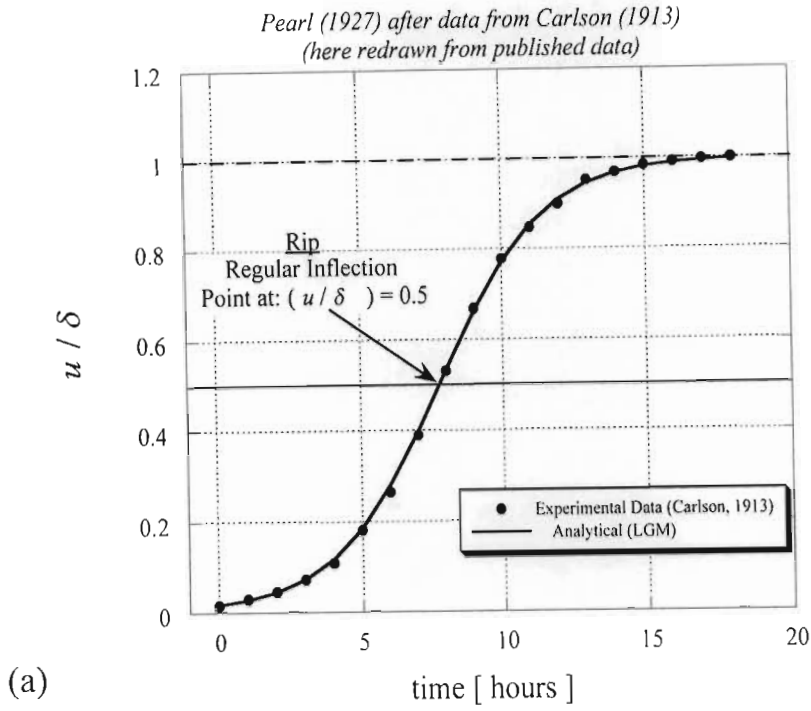


Figure 1.1: Comparison of the LGM solution with experimental results for yeast cells based on Pearl (1927), after data from Carlson (1913) (here redrawn using the tabulated data from Pearl, 1927). (a) Cell concentration (normalized and dimensionless) versus time; (b) the \ln curve of the cell concentration versus time.

$$\frac{du}{dt} = \mu u - \nu u^2 \quad , \quad (1-3)$$

where $\nu = \mu/\delta$. From the equation presented in this form, (1-3), it can be observed that the first term contributes to Malthusian growth, while the second term, νu^2 , contributes to inhibiting growth and is proportional to the number of encounters between each pair of individuals in the population. It reflects the effect of crowding and intra-specific competition on the population growth. The analytical solution to equation (1-2) expressed in the form,

$$u = \frac{\delta}{1 + \left(\frac{\delta}{u_0} - 1 \right) e^{-\mu t}} \quad , \quad (1-4)$$

where u_0 is the initial population or cell concentration, yields the familiar “S” shaped logistic curve leading asymptotically towards the stationary point $u = \delta$. The trivial stationary value $u = 0$ is unstable for $\mu > 0$. Pearl (1927) showed an excellent match between the LGM solution expressed by eq. (1-4) and experimental results for yeast cells reported by Carlson (1913). Pearl’s tabulated data have been redrawn here and they are presented in Figure 1.1a clearly confirming his claim of an excellent match. In addition, plotting the natural logarithm of the cell concentration versus time yields the graphical result presented in Figure 1.1b. From this figure it is clearly observed that the *regular inflection point (Rip)* that was recovered in Figure 1.1a at $u = 0.5\delta$ disappears when presenting the result in terms of $\ln(x)$ versus time. The LGM cannot recover a *logarithmic inflection point (Lip)*. It is important to observe the solution on a phase diagram in terms of the specific growth rate \dot{u}/u versus u , which can be simply drawn by using equation (1-2). This phase diagram is presented in Figure 1.2a, showing that the LGM solution lies on a straight line in this plane.

On the other hand there is substantial experimental evidence that the shape of the solution on the same phase diagram deviates significantly from the linear curve, e.g. Smith (1963). Concave as well as convex shapes, some of them indicating a maximum, were identified experimentally, as presented in Fig.1.2a by the gray curves. Additional models were developed in an attempt to describe the new experimental results. Gompertz model (Gompertz, 1825) and alternatively a model developed by Smith (1963) were proposed in order to recover the concave shapes,

while the convex curves and their possible maximum were explained among others in terms of the Alee effect (Alee, 1931). Some researchers were unhappy with the fact that Gompertz's model as well as models recovering the Alee effect do not produce a stationary point identical to the one obtained from the LGM. The argument was that if δ is indeed the carrying capacity of the environment it should depend on the environment only and all solutions in the same environment should eventually stabilize to the same value δ . As a result, Richards family of growth curves (Richards, 1959) was proposed to address this problem. They constitute a slight modification of the LGM in the form

$$\frac{du}{dt} = \mu \left[1 - \left(\frac{u}{\delta} \right)^\kappa \right] u, \quad (1-5)$$

where κ is a positive constant parameter that controls the concavity/convexity of the specific growth curve on the phase diagram, i.e. for $\kappa > 1$ the curves are convex, while for $\kappa < 1$ they are concave with the LGM recovered when $\kappa = 1$ (see Figure 1.2b). Despite their different curvature all Richards' growth curves cross the u axis at $u = \delta$ and the (\dot{u}/u) axis at $(\dot{u}/u) = \mu$, identically to the LGM.

In addition, substantial evidence accumulated from other, more recent, experimental results indicating that an inflection point is recovered on the logarithm of the cell concentration curve (see Baranyi and Roberts 1993, 1994, for a discussion on this topic). While it is obvious that there is a link between this *logarithmic inflection point* (*Lip*) and the existence of a *Lag Phase*, this link does not necessarily go both ways. This means that when a *Lag Phase* exists, a *logarithmic inflection point* (*Lip*) is to be obviously expected; however if a *logarithmic inflection point* (*Lip*) is recovered it does not necessarily mean that a *Lag Phase* must exist. One way to incorporate a "*Lag Phase*" in a Logistic Growth Model was proposed by Hutchinson (1948) and Wangersky and Cunningham (1957). Hutchinson's model was developed in an attempt to correct the fact that in equation (1-2) the concentration dependent regulatory mechanism represented by the factor $[1 - u/\delta]$ operates instantaneously. By considering that these regulatory effects are likely to operate with some built-in time lag, whose characteristic magnitude may be denoted by t_o , one can incorporate explicitly such time delays in the LGM equation. More realistically, the regulatory

term is likely to depend not on the population at the time exactly t_0 earlier, but rather on some smooth average over past populations (e.g. May, 1973). There is a major objection to using the proposed delay-model. This objection comes from the fact that even with such a delay the model recovers a lag in the inhibition stage and not during the growth stage as the experiments suggest. It is therefore more plausible to expect from any model to capture a lag without an explicitly imposed time delay which might indeed be present in some cases in addition to a non-autonomous natural response.

Other formulations of growth models were proposed as variations of the LGM equation (1-2) by considering different forms of the specific growth rate. In general this can be presented in the form

$$\frac{du}{dt} = u\mu f(u) \quad , \quad (1-6)$$

where $\mu f(u)$ is the specific growth rate and different forms of the function $f(u)$ have been proposed. Edelstein-Keshet (1988) proposes for a sufficiently smooth function to consider its Taylor series form $f(u) = a_1 + a_2u + a_3u^2 + a_4u^3 + \dots$. Baranyi and Roberts (1994), for example, preferred to use a Richards' family of growth curves (Richards, 1959) as presented in eq. (1-5).

Baranyi and Roberts (1994) suggested a new model originally proposed by Baranyi, Roberts and McClure (1993) to resolve the problem of lack of recovery of a *Lag Phase* and an inflection point in the logarithm of the cell concentration curve by the LGM and its different variations. They realized that the only way that a recovery of both the *Lag Phase* and the *logarithmic inflection point (Lip)* can be accomplished, while leading to the LGM stationary point, is via a non-autonomous model. They, therefore, suggested including a time dependent adjustment function $a(t)$ in the form

$$\frac{du}{dt} = u\mu a(t)f(u) \quad , \quad (1-7)$$

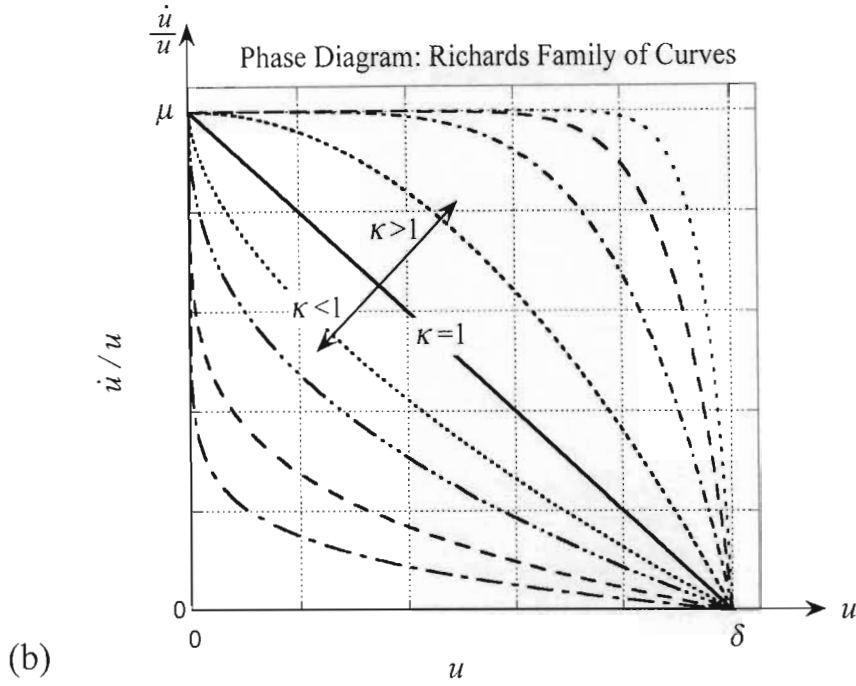
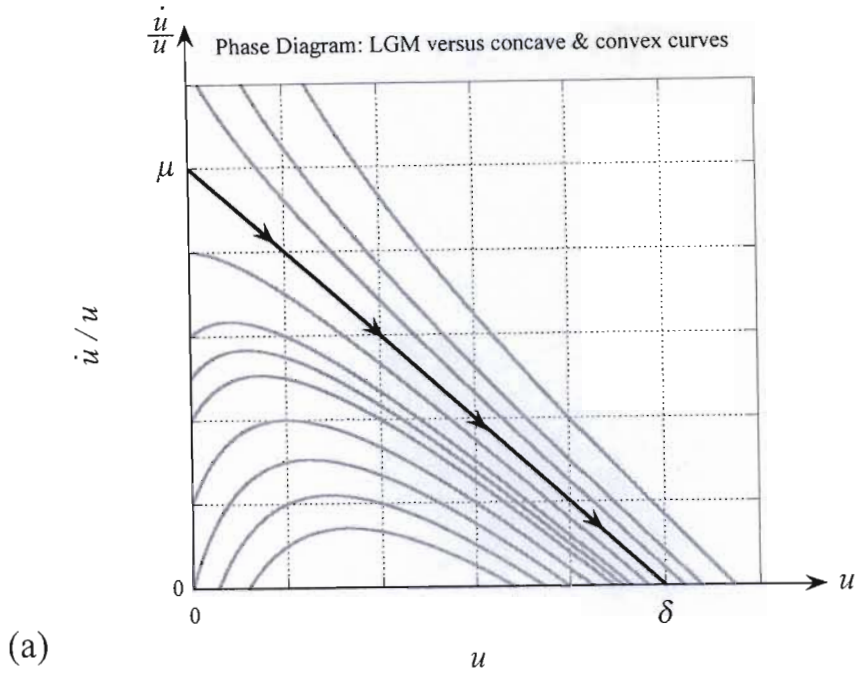


Figure 1.2: The phase diagram for the solution of the LGM compared to: (a) concave and convex curves representing shapes that were obtained in different experiments. (b) Richards family of curves.

where $f(u)$ takes one of the forms of the Richards' family of growth curves (Richards, 1959) discussed above. They present different forms of the adjustment function, $a(t)$ which recover different forms of previously proposed models as well as the *Lag Phase* and the *logarithmic inflection point (Lip)*. The major limitation of this proposed model is the fact that it is non-autonomous, i.e. it requires for each experiment to evaluate an adjustment function, which depends on time explicitly. Non-autonomous models are indeed acceptable in natural environments where daily or other time variations of temperature, pH as well as other medium parameters occur, therefore imposing on the growth parameters a time dependence. However the motivation provided by Baranyi and Roberts (1994) for suggesting a non-autonomous model was for recovering the microbial growth in a well controlled batch culture experiment for a constant environment, and in particular in recovering the “*Lag Phase*”. Their argument is that the “*Lag Phase*” is a result of cell history from growing previously in another environment, prior to being inoculated and grown in the actual environment. This is indeed the process that typical batch experiments follow. However, other explanations for the existence of the “*Lag Phase*” support the view that it is essentially linked to the time delay needed for the cells to transfer available nutrition from the medium into the cell before they can use it for growth and cell division.

Traditional and modern theories of growth of populations essentially associate the *LAG*, *LIP* as well as oscillations to delay effects (as previously presented) and more specifically to structured phenomena, such as age structure in populations. While age-structured (or other structurally distributed) models are basically correct, they cannot capture correctly the *LAG Phase* effect because the latter occurs at the early growth phases while the former models may produce a delay at the final growth phases. In addition the age-structured models require as input a LIFE TABLE that includes explicitly the birth rate and the death rate at any given time. However, if we know the birth rates \dot{u}_b and the death rates \dot{u}_d then by definition we know the growth rate $\dot{u} = \dot{u}_b - \dot{u}_d$. The growth rate can be simply integrated to yield the total population number at all times given some initial population value u_o , in the form $u = u_o + \int (\dot{u}_b - \dot{u}_d) dt$. The major difficulty is however that one has no way to know the growth rate, let alone knowing the birth and death rates. Therefore, structured

models are useful when the size of each structured component is required, e.g. the age distribution of a population versus time as well as the size of a population at different age groups. However, the growth of the total population as a whole is needed as an input to the latter models.

Another way of incorporating cell history effects in such models while keeping them autonomous was proposed via an inertial mechanism by Ginzburg (1986) and Akçakaya *et al.* (1988).

One is faced with substantial experimental evidence that shows excellent qualitative and quantitative match with the solution of the LGM on one hand. On the other hand, other experimental results indicate substantial qualitative and quantitative discrepancies between the LGM solution and the experimental data. These are, for example, the lack of recovery of a *Lag Phase* and *logarithmic inflection point (Lip)*, as well as the inability of the LGM and its modified versions to recover *overshooting* and *oscillations*.

1.2.2 The Neoclassical Model

Earlier versions of the Neoclassical Model were used to investigate the growth of populations sharing and competing over a common ecological niche (Vadasz, 2000, Vadasz *et al.*, 2001, 2002a,b, 2003). The computational results were compared to experiments and the experimental results were used to improve the model and place the theory on a sound basis. Different strains of yeast were used for this purpose in isolation (pure culture) as well as in mixtures. The typical colonies grew on differential medium (WLN) (Figures 1.3 and 1.4, respectively). Some strains of yeast, called “killer” (K), secrete into the growth medium toxins, which are lethal to other yeast strains, called “sensitive” (S) (Vadasz *et al.*, 2000). The toxin as well as the immunity to it is coded by a viral double stranded RNA (dsRNA), which inhabits the killer-yeast cells. Therefore, the killer-yeast is immune against the toxin that it produces and releases. The early version of the Neoclassical Model of competition was applied to the interaction between a killer and a sensitive strain of yeast growing in a mixed culture and in pure water. The sensitive wine yeast Y217 was challenged

with the K_2 killer yeast T206 at a killer : sensitive (K/S) cell ratio of approximately 1:100 and 1:1, respectively. The pure cultures were used as the controls of the mixed ones in order to differentiate the relative survival of each strain in the mixed cultures, while growing in the exact set of conditions. Filtration aimed to wash out spores. The major two conclusions from these experiments were that: (i) Coexistence of both strains as well as extinction of one of them was recovered experimentally as well as computationally; some results seem to depend on initial conditions. (ii) Oscillations in the cell count of both, the individual cell concentration as well as in the total viable cell count, were recovered experimentally as well as computationally (Figures 1.11 and 1.12).

Genetic alteration of the viral double - stranded RNA that inhabits a K_2 killer yeast, was induced by cycloheximide treatment in order to delete the ability of the killer strain to produce its viral killer toxin, and therefore used as a killer control (Vadasz, 2000). This allowed to compare the competition capabilities between the killer-yeast and its cured strain. The success of the curing process was regularly tested on methylene blue agar plates of sensitive cells challenged by both killer and killer-cured, (Figure 1.5). Also, nucleic acids (DNA and RNA) from both killer and killer cured strains were isolated by modifying the method of Fried and Fink (1978). Agarose gel electrophoresis analyses supported the curing (Figure 1.6).

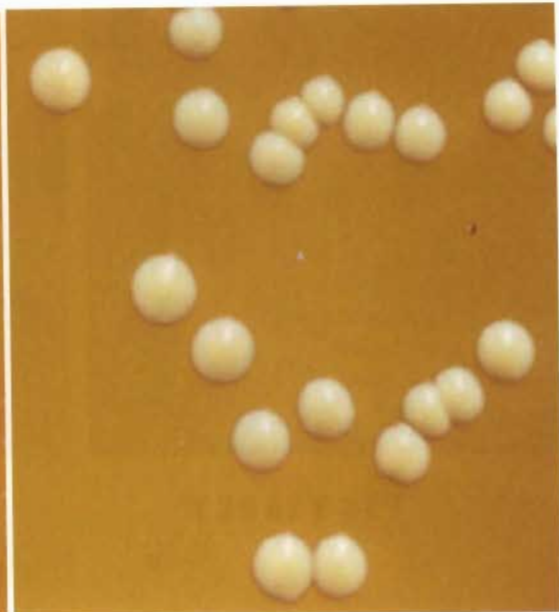
These results indicate spectacular potential in integrating biological and particularly genome-related methods with computational, modeling, and engineering approaches for investigating the mechanisms underlying the growth of micro-organisms and their interaction with the environment. As an example, one of the results obtained by growing individual strains (pure cultures) of yeast cells under nutritional stress, such as in pure water, showed that the yeast populations can produce growth curves qualitatively similar to those obtained while growing in environments enriched by nutrients. These results were somewhat surprising, as it was difficult to explain how cells can grow without nutrition. Following the levels of metabolites cells secrete into the medium, such as ethanol, and examinations of these cells under the Scanning Electron Microscope (SEM) and the Transmission Electron Microscope (TEM) (Figures 1.7 and 1.10) support some possible explanations.

Materials are released into the medium by the viable cells and from damaged and dead cells are potential nutrients (such as ethanol) or/and toxins (Figures 1.9 – 1.10).

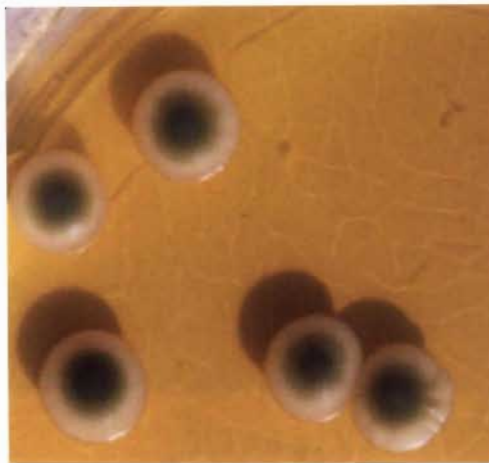
Cells growing under severe nutritional limitations show typical phenotypic changes (cell elongation, bipolar budding, invasive growth, pseudohyphal formation, aggregation and mucoid matrix formation as well as sporulation, Figures 1.7 – 1.8).



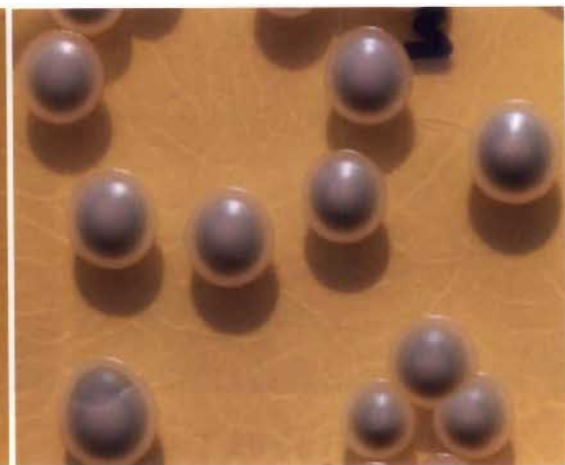
T 2 0 6



T 2 0 6 q

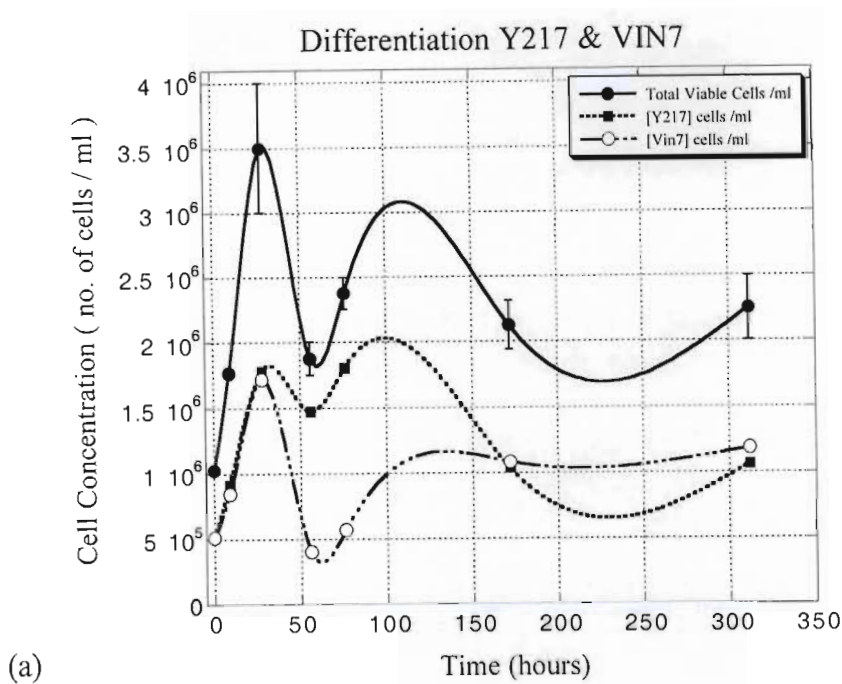


V I N 7

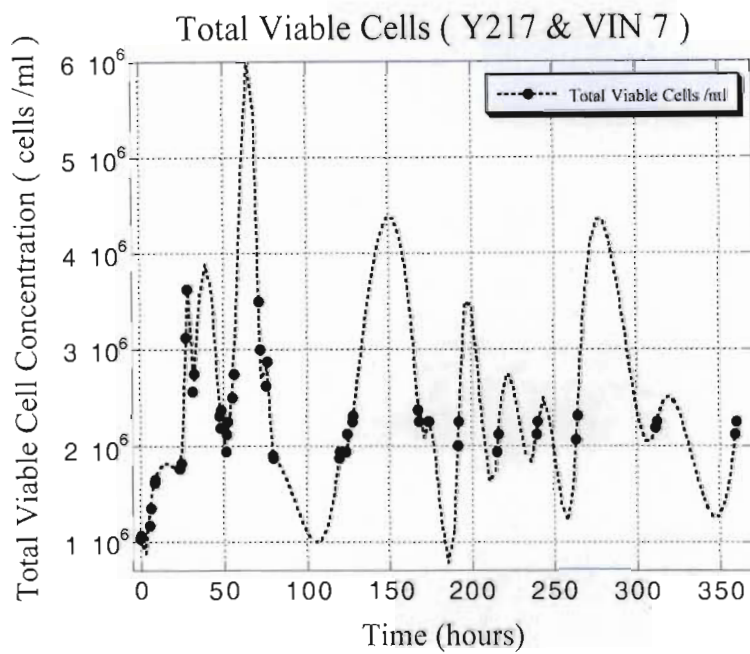


Y 2 1 7

Figure 1.3: Typical colonies of *Saccharomyces cerevisiae* strains T206, T206q, VIN7 and Y217, respectively, growing on the differentiation medium WLN, used as the control group (A.S. Vadasz, 2000).



(a)



(b)

Figure 1.11: Experimental results of total viable cell concentration and differentiation between the Y217 and VIN7 strains of yeast grown as a mixed culture in pure water. (a) Cell differentiation data; (b) Total viable cells (A.S. Vadasz, 2000).

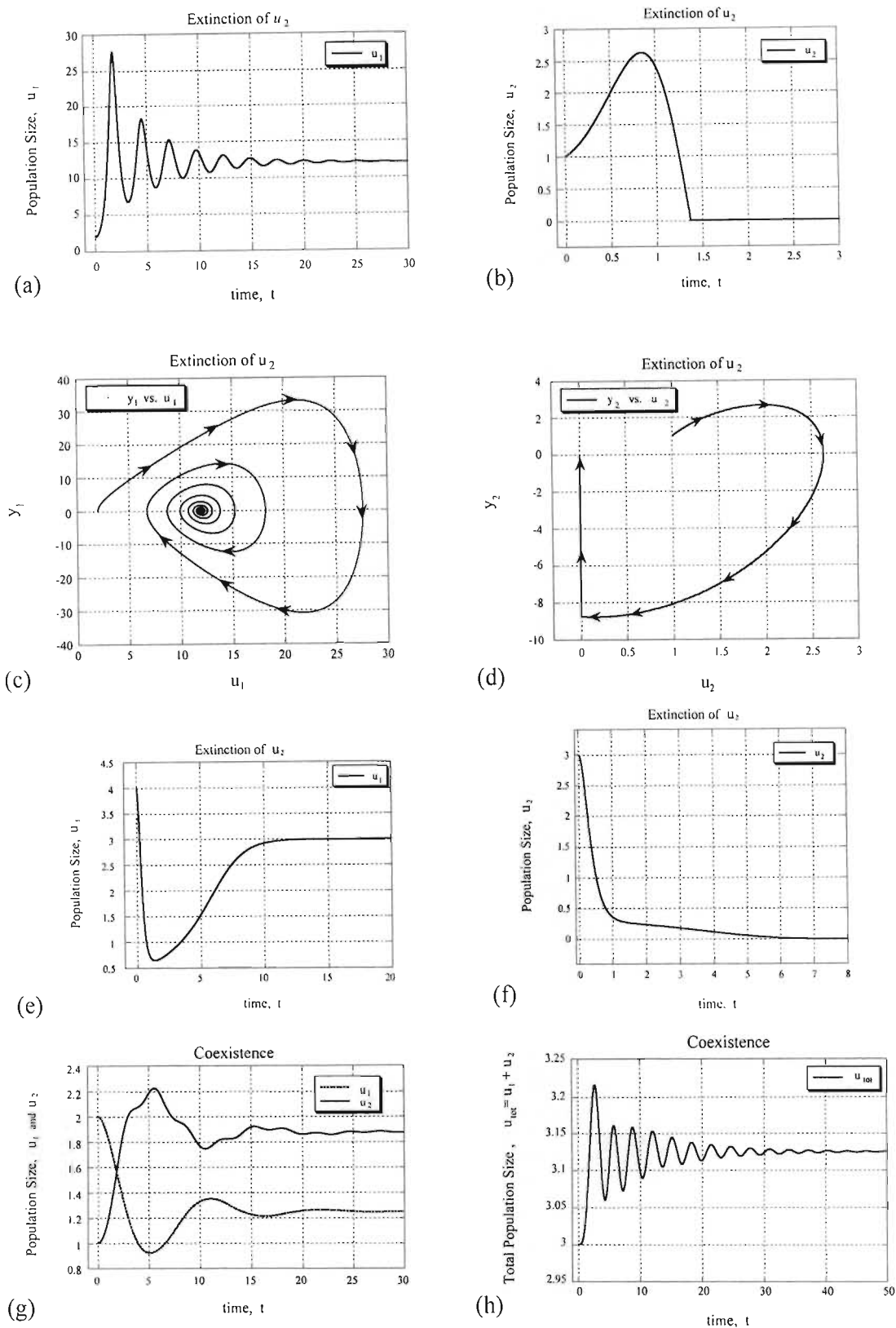


Figure 1.12: Neoclassical model results (earlier version) for competition showing damped oscillations in the concentration of the surviving species and the extinction of the other species; survival of one species and extinction of the other; coexistence of both species (A.S. Vadasz, 2000).

The mathematical model that was developed by Vadasz, P., Vadasz, A.S. (2002 a,b) is expressed in the form

$$\left\{ \begin{array}{l} \frac{du}{dt} = \mu \left[1 - \frac{u}{\delta} + \frac{(v - \mu)}{\mu(1 + r_m u)} \right] u \\ \frac{dv}{dt} = \gamma - \frac{k}{m_o} u \end{array} \right. \quad (1-8)$$

(a) (b)

where u is the population number, and v represents the nutrient (or resource) consumption/utilization rate. The denominator in the third term of eq. (1-8a) represents the net average biomass, hence the third term is a representation of the excess nutrient consumption/utilization per unit of biomass in the population. (see Vadasz, P., Vadasz, A.S. 2002 a,b for details). The other symbols represent: k is the cell or organism's nutrient storage capacity, m_o is linked to the net average biomass (see next paragraph and Figures 1.13 and 1.14), γ is the nutrient consumption/utilization acceleration, μ is the maximum specific growth rate of the Logistic Growth Model (Pearl, 1927, Verhulst, 1838), and δ is the carrying capacity of the environment.

Evaluation of the net average body mass, $m(u)$: The conceptual derivation of the net average body mass (or net viable cell's biomass, in case of cells) was presented by Vadasz, P., Vadasz, A.S. (2002a,b). It's results show that the total population net body mass, M , is related to the population number by the following linear relationship

$$M(u) = m_o + m_1 u \quad , \quad (1-9)$$

where m_o and m_1 are constants. Note that m_o has units of $[kg]$ (or $[kg/m^3]$ for cells) in SI units, while m_1 has units of $[kg/individual]$ (or $[kg/Cell]$ in case of cells), in SI units. The net average body mass (or net viable cell's biomass, in case of cells), $m(u)$, is obtained by dividing the total population net body mass, M , by the population number, u , in the form

$$m(u) = \frac{M(u)}{u} = \frac{m_o + m_1 u}{u} = \frac{m_o}{u} + m_1 = m_o \frac{(1 + r_m u)}{u}, \quad (1-10)$$

where $r_m = m_1/m_o$, and the units of r_m are [*individual*⁻¹] (or [(*Cell*/*m*³)⁻¹] in case of cells), in SI units. The most important result from this relationship is the fact that the constant m_o is generally not zero. For large populations in number, i.e. if $u \gg m_o/m_1$ the impact of m_o on the net average body mass is small, while for small numbers of population, i.e. if $u \ll m_o/m_1$, the contribution of m_1 becomes negligible. In addition one needs to be aware that $m(u)$ is the net average body mass which means that this is the gross average body mass less the amount of mass stored in the body, either as potential life, i.e. during pregnancy, or as nutrient storage.

There is experimental evidence from Vadasz (2000) that the linear approximation for the total viable cell biomass in the case of yeast cells does indeed apply. The main problem is that in experiments one cannot distinguish between the total gross viable cell biomass and the total net biomass, i.e. deducting the biomass stored either as nutrient storage or as “potential life” storage from the measured quantity. Nevertheless relationships are presented in Figures 1.13 and 1.14 between the measured total viable cells’ biomass and the viable cells’ concentration corresponding to the T206 strain of *Saccharomyces cerevisiae* grown in a 5% grape juice medium as well as in a nutrient rich environment, respectively. It is evident from Figures 1.13 and 1.14 that the linear relationship approximately holds, except for the very end of the curve. There, at high concentration levels, the relationship occasionally shows a multiplicity result that may be related to the storage effect, which becomes more pronounced at high population numbers, as indicated above. The most important result, however, from these figures is the fact that both show the existence of $m_o \neq 0$, i.e. the curve, whether linear or not, does not cross the u axis at $M_g = 0$ (see detail in Figure 1.14b presenting the rich medium results, zoomed into the region close to the origin). While, the linear relationship may very well represent a first order approximation of some more complex relationship, the constant non-zero term, m_o , is generic.

The linear relationship presented in eq. (1-9) was used in the derivations of the Neoclassical Theory, leading eventually to the derivation of equation (1-8).

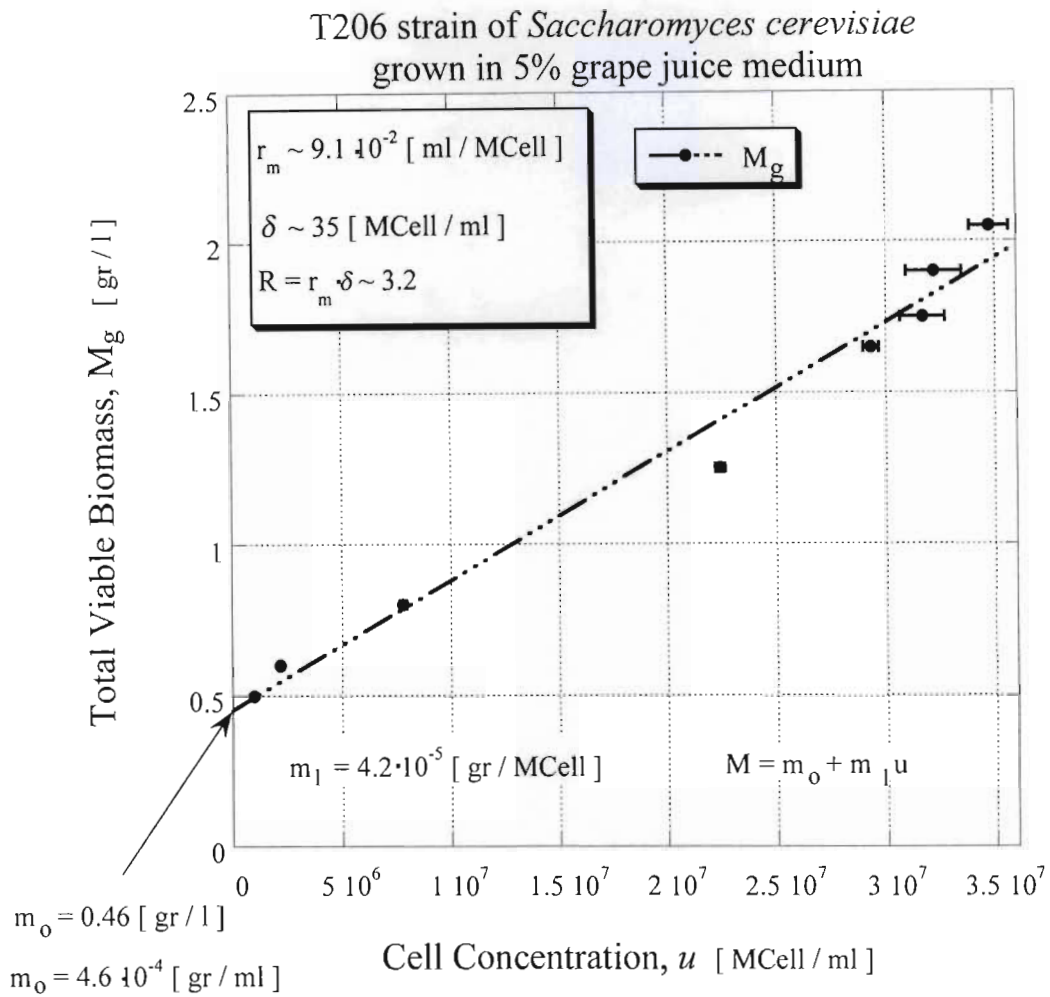


Figure 1.13: Experimental results of the total viable cell biomass as a function of cell concentration for the T206 strain of yeast grown in 5% grape juice medium (1 MCell = 10^6 Cells), (Vadasz, P., Vadasz, A.S. 2002 a,b).

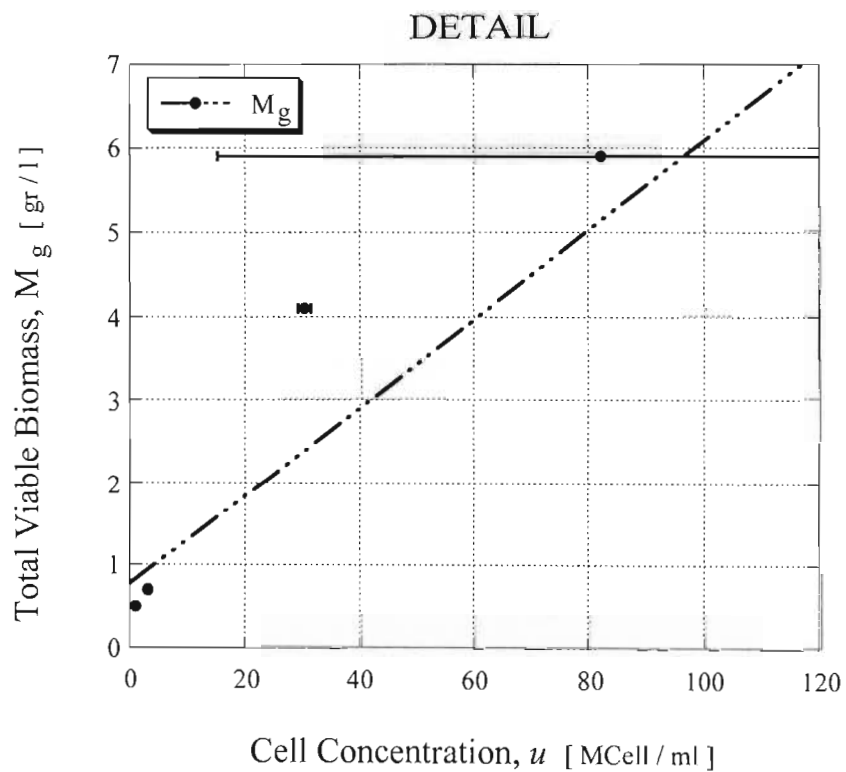
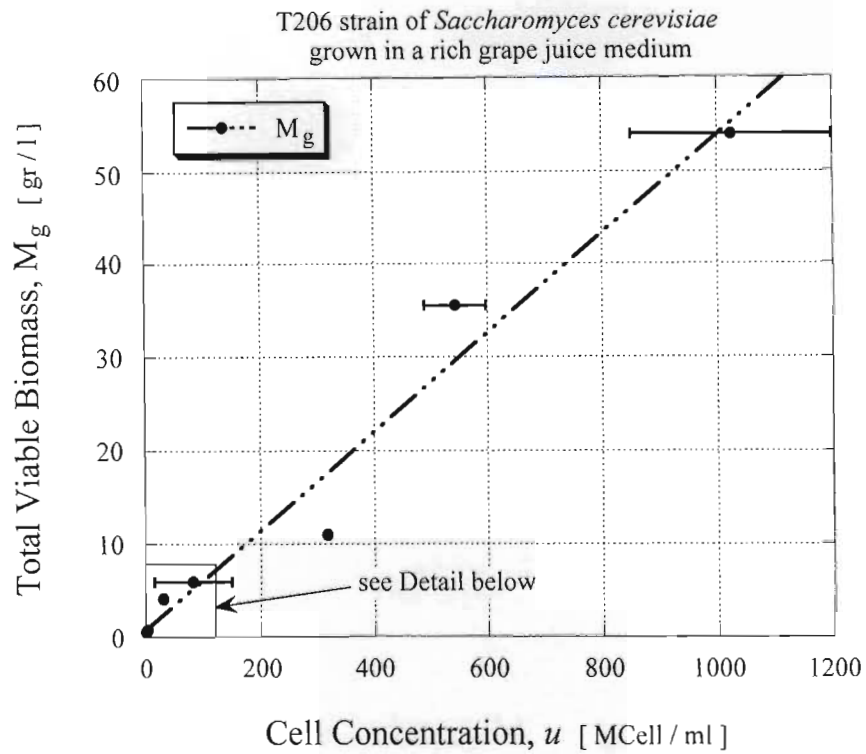


Figure 1.14: Experimental results of the total viable cell biomass as a function of cell concentration for the T206 strain of yeast grown in a rich medium. (a) Experimental results over the whole domain. (b) Detail around the origin ($1 \text{ MCell} = 10^6 \text{ Cells}$), (Vadasz, P., Vadasz, A.S. 2002 a,b).

The explicit definition of v , corresponding to the specific form of $m(u)$ used from eq. (1-10) to obtain eq. (1-8), is

$$v = \mu + (1 + r_m u) \left[\frac{\dot{u}}{u} + \mu \left(\frac{u}{\delta} - 1 \right) \right] \quad (1-11)$$

Units and Dimensions: When dealing with population dynamics as a general phenomenon it covers a wide range of scales, starting with the size of the individual in the population where the size scale ranges from $1 \mu m$ in case of cells and up to more than $1m$ in case of animals and humans. The corresponding time scales also vary substantially from an order of magnitude of $1hour$ in case of cells up to $60 years$ and even more in case of animals and humans. Each particular field dealing with one kind of population uses the most convenient technical units that fit best the typical scales of the population concerned. Hence, it is difficult in a study that deals generally with all types of populations to adopt a unified scale that fits all these fields. In this study the SI units were adopted to identify the units corresponding to different terms in the equations in general, but the technical units particular to a specific field are being used whenever experimental data relevant to such a specific field are presented. It sounds indeed ridiculous to speak about cells in kg and m (meters), however for the purpose of unifying the units as relevant to the equations that were derived the SI units were found appropriate. Nevertheless, when dealing with specific populations their corresponding technical units were selected as the most appropriate ones. With this in mind, the units of the population number u are [*individual*], or its corresponding concentration if the system deals with concentration of populations, the units of m are [$kg/individual$] and k in [$N/(m \cdot individual)$].

Monotonic Growth with LGM as a Particular Case: A particular special case is obtained from these equations when $\gamma = 0$ and $k = 0$, or when both γ as well as k are very small compared to the other terms in eq. (1-8). Subject to these conditions, equation (1-8b) yields $v = v_o = \text{constant}$. The value of this integration constant v_o

corresponds to the value of v at $t=0$ and can be established explicitly by using the definition of v from equation (1-11), in the form

$$v_o = \mu + (1 + r_m u_o) \left[\frac{\dot{u}_o}{u_o} + \mu \left(\frac{u_o}{\delta} - 1 \right) \right] \quad , \quad (1-12)$$

where u_o is the initial population number at $t=0$, and $\dot{u}_o = (du/dt)_{t=0}$ is the initial growth rate at $t=0$. Note that v_o has units of specific growth rate, i.e. $[s^{-1}]$ in SI units, identical to the units of μ . Then, with $v = v_o$, the system of two first order differential equations (1-8a) and (1-8b) reduces to one first order differential equation obtained by substituting eq. (1-12) into (1-8a), to yield

$$\frac{du}{dt} = \mu \left[1 - \frac{u}{\delta} + \frac{(v_o - \mu)}{\mu(1 + r_m u)} \right] u \quad , \quad (1-13)$$

Equation (1-13) represents **the equation governing all types of monotonic growth**. It is obvious that when $u_o = \mu$ equation (1-13) collapses to the special case of the LGM, eq. (1-2). However, for this to happen, a particular relationship on the initial conditions needs to be imposed, i.e.

$$\frac{\dot{u}_o}{u_o} = \mu \left(1 - \frac{u_o}{\delta} \right) \quad , \quad (1-14)$$

as can be observed from eq. (1-12).

A new equation for monotonic growth was obtained, eq. (1-13), as a special, mathematically degenerated, case of the more general equation governing population growth.

Analysis and Solution of the Equation Governing Monotonic Growth:

Monotonic growth is regularly obtained in laboratory experiments, whether in batch or continuous environments and is also observed in nature. Overshooting and oscillations, or growth followed eventually by decay, are also phenomena that were captured experimentally in the lab or in nature. However, it seems that there are sufficient circumstances when at least the initial growth phases are monotonic, followed sometimes at a slower (i.e. longer) time scale by non-monotonic behaviour

such as overshooting and decay. For monotonic growth, one first order equation was derived, i.e. eq. (1-13), which was obtained from the second order equation (1-8) as a mathematically degenerated case. As a result, the only memory that this equation has that it originated from a second order system of differential equations is the term v_o (defined in eq. (1-12)), which depends on two initial conditions, i.e. on the initial population number u_o as well as on the initial growth rate \dot{u}_o . The first stage in understanding the monotonic growth behaviour according to eq. (1-13) is to plot the solution on a phase diagram, in terms of the specific growth rate (\dot{u}/u) versus the population number u by using eq. (1-13). There are a variety of regimes, linked to the behaviour of the solution, that depend on different ranges of the parameters, r_m, v_o, μ and δ . The analysis can nevertheless be simplified by presenting equation (1-13) in a dimensionless form. Using δ as a characteristic value for the population number, μ^{-1} as a characteristic time, and μ as a characteristic value for the specific growth rate we can transform the dimensional variables and parameters into their following corresponding dimensionless form

$$U = \frac{u}{\delta} \quad ; \quad \tau = \mu t \quad ; \quad V_o = \frac{v_o}{\mu} \quad ; \quad R = r_m \delta \quad , \quad (1-15)$$

where U is the dimensionless population number, τ is the dimensionless time, while V_o and R are the dimensionless counterparts of v_o and r_m , respectively. Transforming equation (1-13) into a dimensionless form by using the dimensionless variables defined in eq. (1-15) yields

$$\frac{dU}{d\tau} = \left[1 - U + \frac{(V_o - 1)}{(1 + RU)} \right] U \quad , \quad (1-16)$$

while transforming the definition of v_o in eq.(1-12) into its corresponding dimensionless form produces

$$V_o = 1 + (1 + RU_o) \left[\frac{\dot{U}_o}{U_o} + (U_o - 1) \right] \quad , \quad (1-17)$$

where the initial dimensionless growth rate is defined as $\dot{U}_o = (dU/d\tau)_{\tau=0}$. Equation (1-16), due to its dimensionless form reduced the number of parameters from 4 to 2. By using eq. (1-16) the analysis simplifies substantially. A thorough and complete analysis of equation (41) covering all possible regimes is being presented elsewhere

(see Vadasz, P. and Vadasz, A., 2002a,b). The main relevant aspects of this analysis are presented here briefly. In general, one can separate the parameter domain into two distinct regimes, namely $R < 1$ and $R > 1$. This can be observed by presenting eq. (1-16) in the form

$$\frac{\dot{U}}{U} = \frac{[-RU^2 + (R-1)U + V_o]}{(1+RU)}, \quad (1-18)$$

where $\dot{U} = (dU/d\tau)$. The case when $R = 1$ is a degenerated case of eq. (1-18), which leads to the non-trivial stationary point $U_{2s} = \sqrt{V_o/R}$. While the possibility of negative R values is not excluded, only positive values of R are considered here. However, the value of V_o may certainly be negative as well. Nevertheless, for this particular degenerated case, when $R = 1$, only positive V_o values lead to a non-trivial stationary solution. If $V_o < 0$ in this case, the solution tends to extinction, i.e. to $U_{1s} = 0$, which becomes the only stationary point and is globally stable.

The solution for $R < 1$ and $R > 1$ produces a rich variety of curves on the phase diagram. The presentation here is restricted to the regime corresponding to $R > 1$. The growth regime corresponding to $R > 1$ is presented on phase diagrams in Figure 1.15 in terms of the specific growth rate (\dot{U}/U) versus the population number U . The positive U axis consists of a continuous distribution of stationary points, which are globally stable. Any point on the phase plane represents a possible initial condition. Once such a point is set (i.e. an initial condition for both U_o as well as \dot{U}_o), the solution follows the corresponding curve that passes through that point towards a stationary point in the direction indicated by the arrows.

A maxima on any curve in the (\dot{U}/U) versus U phase diagram, indicates the existence of a *logarithmic inflection point (Lip)* and possibly a *Lag*. For a *Lip* to exist, the following condition has to apply $[d^2(\ln U)/d\tau^2]_{lip} = 0$ at the *logarithmic inflection point*. This, however, implies

$$\left\{ \frac{d}{d\tau} \left[\frac{d(\ln U)}{d\tau} \right] \right\}_{lip} = \left\{ \frac{d}{d\tau} \left[\dot{U} \frac{d(\ln U)}{dU} \right] \right\}_{lip} = \left[\frac{d}{d\tau} \left(\frac{\dot{U}}{U} \right) \right]_{lip} = \left[\dot{U} \frac{d}{dU} \left(\frac{\dot{U}}{U} \right) \right]_{lip} = 0 \quad (1-19)$$

that holds only if $\left[d(\dot{U}/U)/dU \right]_{lip} = 0$, i.e. when (\dot{U}/U) has a maximum on the (\dot{U}/U) versus U phase diagram, unless $\dot{U} = 0$ the latter identifying a stationary point rather than a *Lip*.

The straight line corresponding to the LGM solution, which occurs when $V_o = 1$ and divides the phase plane into two regions, can be observed in Figure 1.15. Actually, the location of this line corresponding to the LGM is invariant to any changes in the value of R . Its location on the phase plane is therefore constant. This is an important property of the LGM. From Figure 1.15 it is evident that the region corresponding to $V_o > 1$ the curves are concave. However, the region corresponding to $V_o < 1$ can be further divided into four important zones, as follows:

$$(i) \quad \text{Zone I:} \quad \frac{(R-1)}{R} < V_o < 1$$

$$(ii) \quad \text{Zone II:} \quad 0 < V_o < \frac{(R-1)}{R}$$

$$(iii) \quad \text{Zone III:} \quad -\frac{(R-1)^2}{4R} < V_o < 0$$

$$(iv) \quad \text{Zone IV:} \quad V_o < -\frac{(R-1)^2}{4R}$$

In Zone I the curves are convex but there is no possibility of a *logarithmic inflection point*, as the curves have no maxima in the non-negative U domain. In Zone II a *logarithmic inflection point* exists but no *Lag* is possible. In Zone III both a *Lip* as well as a *Lag* become possible. In Zone IV (not shown in the figure) the solution leads always to extinction, i.e. the trivial stationary point $U_{ls} = 0$ becomes the only globally stable solution. The reason for the possibility of a *Lag* in Zone III is the existence of additional positive but unstable stationary points in this Zone to the left of point A in Figure 1.15. When the initial conditions are sufficiently close to one of these unstable stationary points which can be described mathematically as “ghosts”, the solution spends a relatively long time to escape from its neighbourhood. This implies that if $0 < \dot{U}_o < 1$, i.e. \dot{U}_o is positive but sufficiently small, and $U_o < U_A$, then a *Lag* exists. The value of U_A is given by $U_A = (R-1)/2R$. It is this type of “ghost”-like behaviour

(see Strogatz (1994) for a discussion on “ghosts”) that causes a *Lag* to exist. The location of the *logarithmic inflection point* was evaluated by using the condition derived in eq. (1-19) with eq. (1-18) and is presented in the form

$$U_{lip} = -\frac{1}{R} + \left[\frac{(1-V_o)}{R} \right]^{1/2} . \quad (1-20)$$

The locus of all *logarithmic inflection points* in Zones II and III was found to lie on the straight line

$$\left(\frac{\dot{U}}{U} \right)_{lip} = -2U_{lip} + \frac{(R-1)}{R} , \quad (1-21)$$

as indicated on Figure 1.15.

Equation (1-16) has a closed form solution that can be obtained by direct integration in terms of its corresponding stationary points. The first stationary point is the trivial one $U_{1s} = 0$. The non-trivial stationary points are obtained by solving equation (1-16) for steady state, i.e. $(\dot{U}/U) = 0$, leading to the following algebraic equation for these stationary points, U_{2s} and U_{3s} .

$$RU_s^2 - (R-1)U_s - V_o = 0 . \quad (1-22)$$

The roots of equation (1-22) are

$$U_{2,3s} = \frac{1}{2} \left[\frac{(1-R)}{R} \pm \sqrt{\Delta_o} \right] , \quad (1-23)$$

where $U_{2s} \geq U_{3s}$ and the discriminant Δ_o was found to be

$$\Delta_o = \frac{(1-R)^2}{R^2} \left[1 + \frac{4V_o R}{(1-R)^2} \right] . \quad (1-24)$$

While the negative stationary points are of no interest to population growth (there is no meaning to negative population number) their importance here is in the sense that they affect mathematically the transient solution. The closed form solution to equation (1-16) can be finally presented by defining the following parameter

$$\alpha = \frac{[1 + R(2V_o - 1)]}{R\sqrt{\Delta_o}} \quad . \quad (1-25)$$

Then, the solution can be expressed in terms of U_{2s}, U_{3s} and α in the form

$$\ln \left[\frac{U |U - U_{3s}|^{(\alpha-1)/2}}{|U - U_{2s}|^{(\alpha+1)/2}} \right] = V_o \tau + C_1 \quad , \quad (1-26)$$

where C_1 is an integration constant that is related to the initial conditions by the following relationship

$$C_1 = \ln \left[\frac{U_o |U_o - U_{3s}|^{(\alpha-1)/2}}{|U_o - U_{2s}|^{(\alpha+1)/2}} \right] \quad . \quad (1-27)$$

Equation (1-26) represents the closed form solution to eq. (1-16) for monotonic growth. However, it is presented in implicit form and it is not possible to derive an explicit equation for U as a function of τ . Nevertheless, this is in no way a problem because one can use the property of the solution being monotonic and evaluate τ as a function of U by using equation (1-26) for values of $U_o \leq U \leq U_{2s}$ when U_{2s} is the stable positive stationary point, or for values of $0 \leq U \leq U_o$ when $U_{1s} = 0$ is the stable stationary point. Note that when U_{3s} is non-negative (the points on the U axis to the left of U_A in Figure 1.15) it is always globally unstable as can be observed from Figure 1.15. The monotonic behaviour of the solution guaranties that for each value of U there is one and only one value of τ . By using this procedure one can vary the values of U within the range indicated above and obtain the corresponding values of τ , producing therefore the numerical values needed for plotting the resulting solution of U as a function of τ .

The analytical closed form solution linked with the computational procedure described above was used to produce results that demonstrate the recovery of solutions that exhibit a *logarithmic inflection point (Lip)* and a *Lag phase*. The impact of the initial conditions U_o, \dot{U}_o and of the parameter R on the *Lag* duration Λ , and on the *Lip* location in time, τ_{lip} , was also investigated from these solutions. There is no problem to evaluate the value of τ_{lip} by substituting eq. (1-20) into eq. (1-26), however it is more difficult to evaluate the *Lag* duration Λ because of the subjective definition of the *Lag*. While different *Lag* definitions were proposed in the

professional literature, e.g. Pirt (1975), Baranyi and Roberts (1994), the definition used here is one that is consistent with the findings that the *Lag* is essentially related to the existence of unstable stationary points. The *Lag* duration Λ is therefore defined as the amount of time that elapses until the solution reaches a value, which is by a certain percentage above the corresponding unstable stationary point U_{3S} . This implies that $U_{\Lambda} = bU_{3S}$, where $b > 1$ is a constant that specifies by how far U_{Λ} is from U_{3S} . We define the dimensionless *Lag* duration, Λ , as the time needed for the solution to reach the value U_{Λ} for any predetermined value of b . This definition is very similar to the way one defines the time needed for a monotonic solution to reach steady state.

In the computation results presented in Figure 1.16 a value of 2.5% above U_{3S} was used as the *Lag* threshold, i.e. $b = 1.025$. The corresponding dimensional definition of *Lag* duration, λ , is naturally converted by using eq. (1-15) for time scaling, i.e. $\lambda = \Lambda/\mu$. Therefore, as a natural consequence of the adopted scaling, this dimensional definition of *Lag* duration is inversely proportional to the maximum specific growth rate μ , as discussed by Baranyi and Roberts (1994). The results of the solution in the time domain, obtained by using eq. (1-26) subject to initial conditions of $U_o = 0.1$ and different small values of \dot{U}_o ranging from 10^{-7} and up to $5 \cdot 10^{-3}$ are presented in Figure 1.16 corresponding to a value of $R = 2$. The figure shows the effect of the initial growth rate on the *Lip* as well as the *Lag*. The accurate evaluated location of the *Lag* and *Lip* is presented in the figure by the indicated points. As indeed expected, the smaller the initial growth rate \dot{U}_o the longer the *Lag* duration Λ and the larger the value of τ_{lip} . For the curves corresponding to $\dot{U}_o = 10^{-3}$ and $\dot{U}_o = 5 \cdot 10^{-3}$ there is no *Lag*, although the *Lip* exists.

The Neoclassical Theory (Vadasz, P., Vadasz, A.S. 2002 a,b) was shown to capture all experimentally observed features, from Pearl's Logistic Growth Model (Pearl, 1927), Malthusian growth (Malthus, 1798), the existence of a *LIP* and possibly a *LAG* (under certain conditions), the Alee effect (Alee, 1931), concave and convex curves on the phase diagram, Gizburg's law of biological inertia (Ginzburg, 1986, Akçakaya *et al.*, 1988), and even the Gompertz model (Gompertz, 1825) which is commonly used in modeling tumor growth. In addition the theory captures effects of

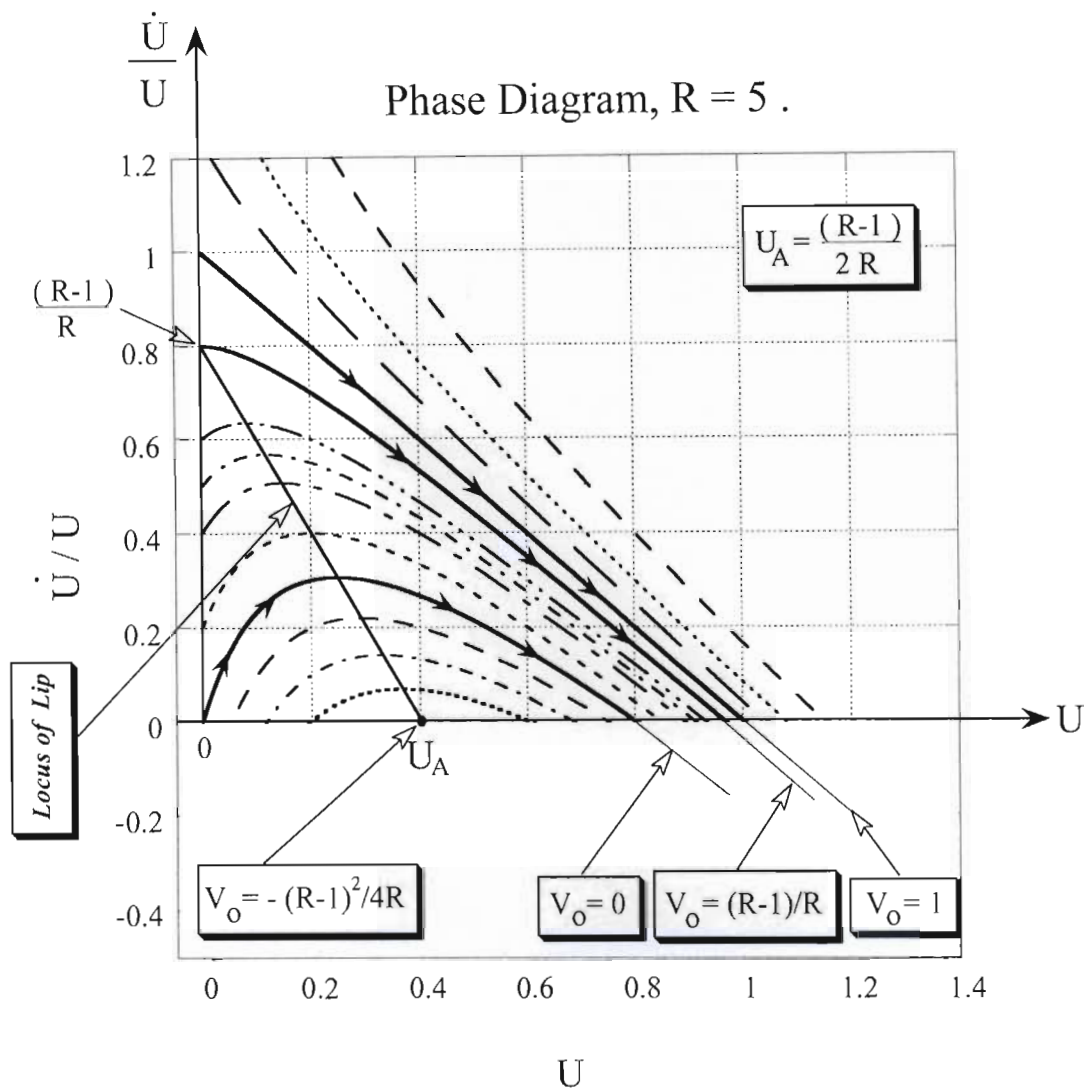


Figure 1.15: Phase diagram for the solution of monotonic growth corresponding to $R > 1$, in terms of the specific growth rate \dot{U}/U versus the population number U , for $R = 5$ (Vadasz, P., Vadasz, A.S. 2002 a,b).

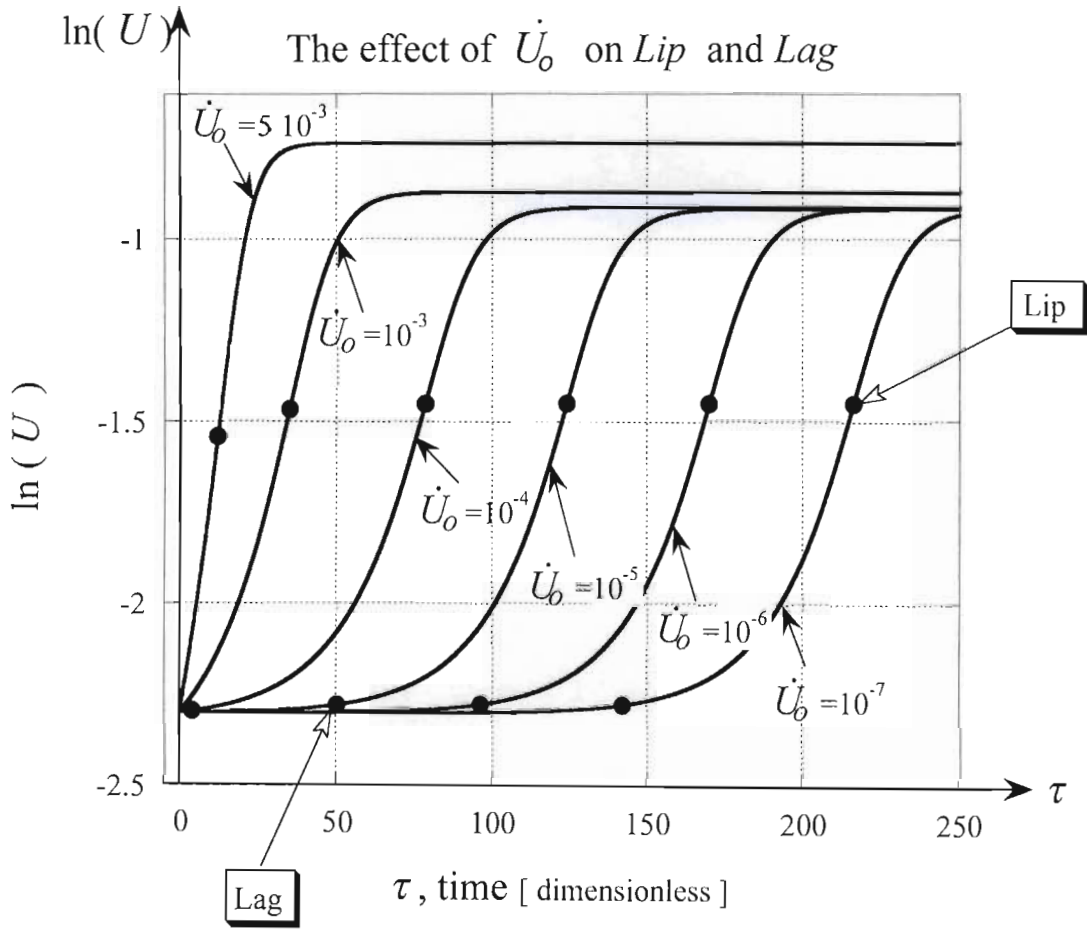


Figure 1.16: The effect of the initial growth rate on *Lip* and *Lag*. Analytical results in the time domain based on the Neoclassical Theory (Vadasz, P., Vadasz, A.S. 2002 a,b) for $R = 2$, subject to initial conditions of $U_o = 0.1$ and different small values of \dot{U}_o .

oscillations observed experimentally among others by Boiteux and Hess (1978), Davey *et al.* (1996) and Haken (1979), as well as growth followed by decay that was experimentally reported by Pearl (1927) and is a well known textbook case in Microbiology. Nevertheless the latter is not covered in the best population dynamics textbooks and reviews (see Edelstein-Keshet, 1988, Krebs, 1978, May, 1973, 1978, 1981, 1995 and Pielou, 1969).

Non-Monotonic Growth: Pearl (1927) compared his proposed LGM to experimental results of growth of yeast cells based on Carlson (1913), and the growth of the fly *Drosophila melanogaster* that he performed in his lab. In the second case, for the fly *Drosophila*, he repeated his experiment in three different types of environmental conditions. The first was applied to an isolated environment of finite size (bottles) with an initial finite amount of non-renewable nutrition. The second was similar to the first but additional nutrition was provided when the original amount was used up, a condition that Pearl identifies as a sub-optimal nutritional level. The third type consisted of a very carefully designed and controlled environment in order to create optimal nutritional levels. In the first type of experiment an initial growth was observed followed by a decline in population levels as the food supply diminished, leading to extinction. Nevertheless, the LGM equation (1-2) and solution (1-4) can not recover a solution that initially grows and eventually decays without a discontinuity in the growth rate. The only way the LGM can describe growth followed by decay is by switching the value of the parameter μ from positive to negative at some point in time. The first problem with such an approach is that it is difficult to even contemplate how to establish this value of t_d where the growth stops and the decay starts. The solution of the LGM corresponding to such a sudden change in the value of μ is presented in Figure 1.17, where a “cusp” is evident from the graph. Even when the solution of the growth part (part “G” in Figure 1.17) reaches almost the stationary point and the graph then may look smoother this “cusp” still exists. The existence of this cusp is because just prior to the decay the growth rate is positive, $\dot{u} > 0$, even if it is very small, while immediately after the decay started the growth rate is negative $\dot{u} < 0$. The growth rate does not vanish identically anywhere,

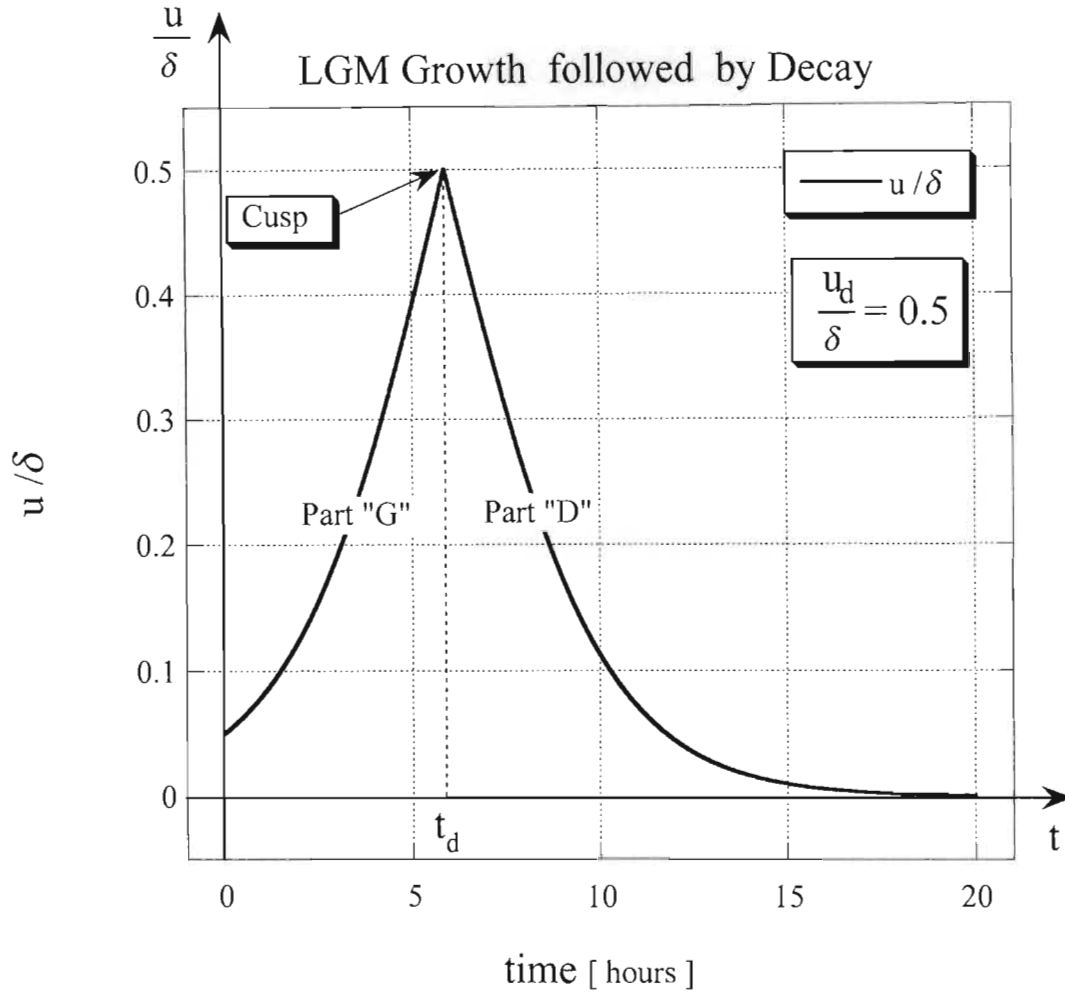


Figure 1.17: The solution to Growth followed by Decay according to the Logistic Growth Model (LGM). Initial conditions: $u_0 = 0.05\delta$. The growth switches to decay at $(u/\delta) = 0.5$.

not even at the transition point, as would have been expected on a smooth transition from growth to decay. Note that $\dot{u} \neq 0$ at any finite time value according to the LGM. Furthermore, any curve representing monotonic growth will produce similar results and therefore only a non-monotonic solution is able to produce a smooth transition from growth to decay. Growth followed by decay according to the computational results using the Neoclassical Model represented by eq. (1-8) are compared with corresponding experimental results presented by Pearl (1927) in Figure 1.18 showing an excellent match.

In the second type of experiment Pearl succeeded to reproduce the LGM curve. It is however the third type which is of interest as Pearl (1927) reports that in this carefully controlled experiment “...*the population first grows up to a maximum or asymptotic level, just as in the second type of experiment But in this case the population can be kept at this asymptotic level as long as the experimenter desires. A striking result, however, is that during the growth period and thereafter **there are violent oscillations of the populations in size, about its mean position given by the fitted curve.** In fact these waves in the size of the population, produced by oscillations in the birth and death rates, are perhaps the most characteristic feature of population experiments of this particular type. It has not been so far possible to devise any method of holding these populations in a steady state at the level of the asymptote, when there is at all times an abundance of fresh food...*”.

More recent experimental results reconfirm the existence of overshooting and oscillations either in spatially homogeneous yeast growth media (Davey *et al.*, 1996) as well as in spatio-temporal experiments of Boiteaux and Hess (1978), Haken (1979). The latter are also features that were recovered qualitatively as well as quantitatively by the Neoclassical Model (see Vadasz, P., Vadasz, A.S. 2002 a,b).

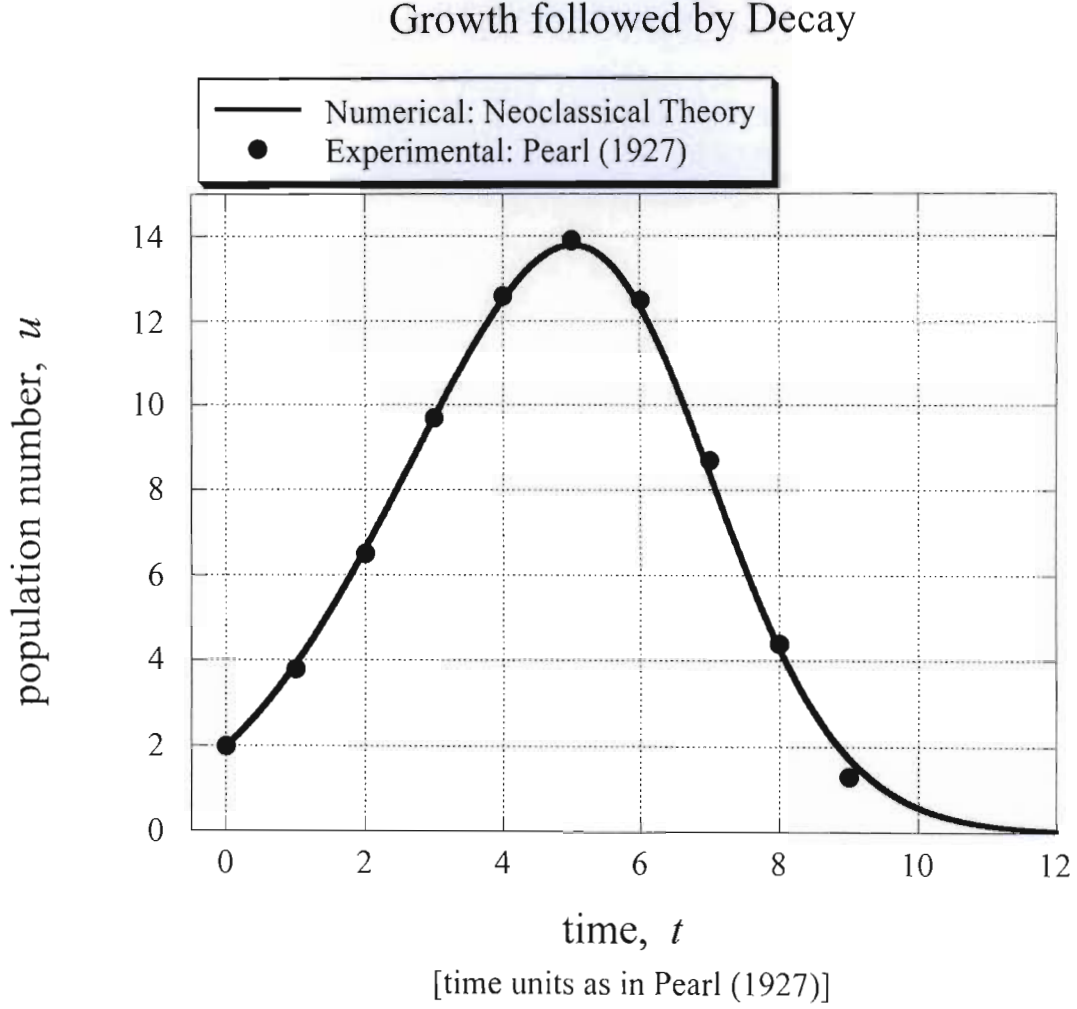


Figure 1.18: Numerical results of the Neoclassical Model (Vadasz, P., Vadasz, A.S. 2002 a,b) applied to the case of growth followed by decay, compared with experimental data from Pearl (1927). The parameter values for the numerical solution are $u_o = 2$, $\dot{u}_o = 1.5$, $v = -0.04$, $\mu = -1.2$, $r_m = 0.035$, $(k/m_o) = 8 \cdot 10^{-5}$, $b = 12$ and $\gamma = -1.6 \cdot 10^3$ in units consistent with Pearl (1927).

1.2.3 Growth Dynamics in Heterogeneously Distributed Populations

At least two interacting chemicals, or a microorganism interacting with one chemical are needed for spatial pattern formation to occur. Diffusion in a chemical system can actually have a destabilizing influence. The latter is contrary to intuition since diffusion usually has a smoothing effect on spatial variations of a concentration field and would therefore be considered stabilizing. The instability caused by diffusion can promote growth of structure at a particular wavelength. This provides a mechanism for producing patterns. Pattern formation in a chemical system will not occur unless the diffusion coefficients differ substantially. The difficulty of satisfying this condition for chemicals in solution partially explains why nearly 40 years have lapsed after Turing's paper (Turing, 1952) before the experimental confirmation of his theoretical predictions was undertaken successfully, although initial findings were available as early as 1978 (see Fig. 1.19, Haken, 1979, after Boiteux & Hess, 1978).

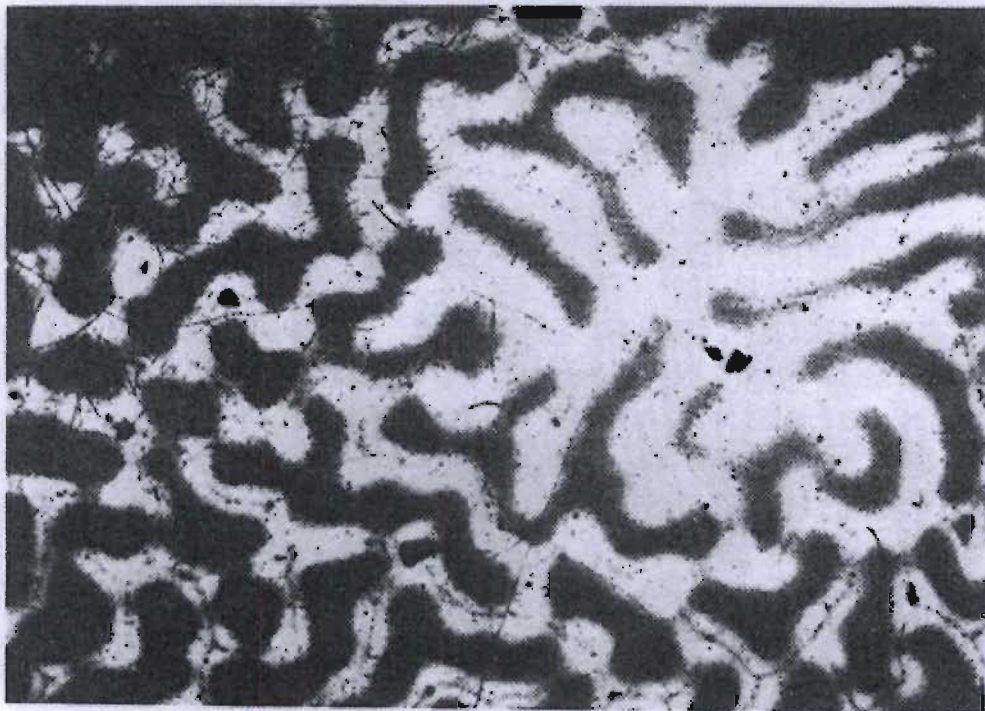


Figure 1.19: “ Snapshot after mixing an oscillating yeast extract to homogeneity. Reduced purine nucleotides yield dark structures. It is the first experimental demonstration that a biochemical system in homogeneous phase might break spatial homogeneity and evolve to spatial-temporal order” (reproduced from Haken, 1979, after Boiteux & Hess, 1978).

Most of the studies of Turing instabilities (Turing, 1952) deal with linear stability analysis identifying the conditions for occurrence of such instabilities and direct numerical solution to the governing equations. These studies deal with the theory of pattern formation via diffusion-driven instabilities as applied in biology (Meinhardt, 1982, Murray, 1989), chemistry (Epstein and Showalter 1996), and physics (Cross and Hohenberg, 1993). A mechanism for the morphogenetic development of pattern and form from a homogeneous mass of cells is provided in developmental biology (e.g. Murray, 1989). In ecology it is also used to explain the spatial structure in populations and communities (Segel and Jackson, 1975, Allen, 1975, Levin and Segel 1976, Mimura and Murray, 1978, Kot, 1989, Neubert Kot and Lewis, 1995, Rohani and Ruxton, 1999, Wilson *et al.*, 1999). Turing instabilities have been recovered experimentally in chemical systems (Castets *et al.*, 1990), claimed in insect host-parasitoid systems (Maron and Harrison, 1997) and semiarid vegetation (Klausmeir, 1999) as well as in yeast populations by Boiteaux and Hess (1978), Haken (1979) as presented in Figure 1.19. Among the most recent studies the work of Neubert, Caswell and Murray (2002) suggests that “reactivity” is necessary for Turing instabilities (Turing, 1952). “Reactivity” is defined by the authors mathematically as the maximum amplification rate, over all initial perturbations, immediately following the perturbation. It is related to the transient initial growth of a perturbation prior to its eventual decay.

The existing analytical work on Turing instabilities does not go as far as obtaining a complete analytical solution to the problem and therefore is limited to producing stability conditions only. Complete analytical results even when their accuracy is limited to a narrow parameter range can provide a tool for validation of numerical solutions and can identify the conditions for occurrence or prevention of Turing instability, a tool much needed in planning experiments.

The general problem formulation for Turing instability is represented by the following equations

$$\begin{cases} \frac{\partial u_*}{\partial t} = D_* \nabla_*^2 u_* + f_1(u_*, v_*) & (a) \\ \frac{\partial v_*}{\partial t} = \alpha_* \nabla_*^2 v_* + f_2(u_*, v_*) & (b) \end{cases} \quad (1-28)$$

where $u_*(x_*, y_*, z_*, t_*)$ is the population number, and $v_*(x_*, y_*, z_*, t_*)$ represents the nutrient (or resource) consumption/utilization rate; both are functions of time as well as spatial coordinates x_* , y_* and z_* . The asterisk subscript, $*$, stands to indicate **dimensional** quantities. Eventually the equations will be rendered **dimensionless** and hence dropping the latter subscript. The functions $f_1(u_*, v_*)$ and $f_2(u_*, v_*)$ are typically nonlinear, however stability analyses are by definition linear and therefore in linear stability analyses these functions take the specific form

$$f_1(u_*, v_*) = a_{11}u_* + a_{12}v_* \quad (1-29)$$

$$f_2(u_*, v_*) = a_{21}u_* + a_{22}v_*$$

Nevertheless, the distinction between different models as far as the linear stability analysis is concerned is the fact that the coefficients a_{11}, a_{12}, a_{21} and a_{22} in eq. (1-29) are functions of the constant stationary (or equilibrium) solutions that are obtained from the solution of the typically nonlinear algebraic equations $f_1(u_*, v_*) = 0$ and $f_2(u_*, v_*) = 0$.

Linear Stability Analysis: The objective of the linear stability analysis is to identify the conditions of stability of stationary solutions u_{*s} and v_{*s} that are obtained by setting the nonlinear functions $f_1(u_*, v_*)$ and $f_2(u_*, v_*)$ equal to zero, i.e.

$$f_1(u_{*s}, v_{*s}) = 0 \text{ and } f_2(u_{*s}, v_{*s}) = 0 \quad (1-30)$$

These stationary solutions may be stable to all small perturbations, unstable to Spatially Homogeneous Perturbations (SHoP) or unstable to Spatially Heterogeneous Perturbations (SHeP). Assuming small perturbations (u_*, v_*) around these stationary solutions in the form

$$u_* = u_{*s} + \varepsilon u_{*1} \text{ and } v_* = v_{*s} + \varepsilon v_{*1} \quad (1-31)$$

where $\varepsilon \ll 1$ stands only to indicate that the perturbations are very small. Substituting (1-31) into equation (1-28) and linearizing the resulting equations yields

$$\begin{cases} \frac{\partial u_{*1}}{\partial t_*} = D_* \nabla_*^2 u_{*1} + a_{11} u_{*1} + a_{12} v_{*1} & (a) \\ \frac{\partial v_{*1}}{\partial t_*} = \alpha_* \nabla_*^2 v_{*1} + a_{21} u_{*1} + a_{22} v_{*1} & (b) \end{cases} \quad (1-32)$$

where a_{11} , a_{12} , a_{21} , and a_{22} are the coefficients resulting from the linearization of the functions $f_1(u_*, v_*)$ and $f_2(u_*, v_*)$, defined in the form

$$a_{11} = \frac{\partial f_1(u_*, v_*)}{\partial u_*}, \quad a_{12} = \frac{\partial f_1(u_*, v_*)}{\partial v_*} \quad (1-33)$$

$$a_{21} = \frac{\partial f_2(u_*, v_*)}{\partial u_*}, \quad a_{22} = \frac{\partial f_2(u_*, v_*)}{\partial v_*}$$

The solution to equations (1-32) for a two dimensional case (in the x_* , y_* directions in space) has the form

$$u_{*1} = B_* e^{\lambda_* t_*} e^{i(\kappa_{*x} x_* + \kappa_{*y} y_*)} \quad (1-34)$$

$$v_{*1} = C e^{\lambda_* t_*} e^{i(\kappa_{*x} x_* + \kappa_{*y} y_*)}$$

Substituting these solutions (1-34) into equations (1-32) leads to the following equations

$$\begin{cases} \lambda_* B e^{\lambda_* t_*} e^{i(\kappa_{*x} x_* + \kappa_{*y} y_*)} = (-\kappa_*^2 D_* B + a_{11} B + a_{12} C) e^{\lambda_* t_*} e^{i(\kappa_{*x} x_* + \kappa_{*y} y_*)} & (a) \\ \lambda_* C e^{\lambda_* t_*} e^{i(\kappa_{*x} x_* + \kappa_{*y} y_*)} = (-\kappa_*^2 \alpha_* C + a_{21} B + a_{22} C) e^{\lambda_* t_*} e^{i(\kappa_{*x} x_* + \kappa_{*y} y_*)} & (b) \end{cases} \quad (1-35)$$

or

$$\begin{cases} (\lambda_* + \kappa_*^2 D_* - a_{11}) u_{*1} - a_{12} v_{*1} = 0 & (a) \\ -a_{21} u_{*1} + (\lambda_* + \kappa_*^2 \alpha_* - a_{22}) v_{*1} = 0 & (b) \end{cases} \quad (1-36)$$

where $\kappa_*^2 = \kappa_{*x}^2 + \kappa_{*y}^2$. The eigenvalue problem represented by the system of equations (1-36) can be expressed in the form

$$A_k \mathbf{w}_{*I} = \lambda_* \mathbf{w}_{*I} \quad (1-37)$$

where the perturbation vector \mathbf{w}_{*I} and the matrix A_k are defined in the form

$$\mathbf{w}_{*I} = \begin{bmatrix} u_{*1} \\ v_{*1} \end{bmatrix} ; \quad A_k = A - \kappa_*^2 D_{dc} = \begin{pmatrix} a_{11} - \kappa_*^2 D_* & a_{12} \\ a_{21} & a_{22} - \kappa_*^2 \alpha_* \end{pmatrix} \quad (1-38)$$

and where

$$A = \begin{pmatrix} a_{11} & a_{12} \\ a_{21} & a_{22} \end{pmatrix} \quad \text{and} \quad D_{dc} = \begin{pmatrix} D_* & 0 \\ 0 & \alpha_* \end{pmatrix} \quad (1-39)$$

It produces the characteristic quadratic equation for the eigenvalues λ_* , in the form

$$\lambda_*^2 - \left[(a_{11} + a_{22}) - \kappa_*^2 (D_* + \alpha_*) \right] \lambda_* - a_{12} a_{21} = 0 \quad (1-40)$$

or

$$\lambda_*^2 - \psi_{A_k} \lambda_* + \Delta_{A_k} = 0 \quad (1-41)$$

where

$$\psi_{A_k} = \text{trace}(A_k) = (a_{11} + a_{22}) - \kappa_*^2 (D_* + \alpha_*) \quad (1-42)$$

and

$$\Delta_{A_k} = \det(A_k) = (a_{11} - \kappa_*^2 D_*) (a_{22} - \kappa_*^2 \alpha_*) - a_{12} a_{21} \quad (1-43)$$

The solution to the characteristic equation (1-41) is

$$\lambda_{*,1,2} = \frac{\psi_{A_k}}{2} \left[1 \pm \sqrt{1 - \frac{4\Delta_{A_k}}{\psi_{A_k}^2}} \right] \quad (1-44)$$

For the perturbations to grow resulting in destabilizing the stationary solution at least one of the eigenvalues must have a positive real part. From eq. (18) the following condition can be derived identifying when the real parts of both eigenvalues are negative (meaning that the perturbations decay and the stationary solution is stable)

$$\psi_{A_k} = \text{trace}(A_k) = (a_{11} + a_{22}) - \kappa_*^2 (D_* + \alpha_*) < 0 \quad (1-45)$$

$$\Delta_{A_k} = \det(A_k) = (a_{11} - \kappa_*^2 D_*) (a_{22} - \kappa_*^2 \alpha_*) - a_{12} a_{21} > 0 \quad (1-46)$$

Inequality (1-46) enforces the condition that the square-root in eq. (1-44) is real and less than 1 (or imaginary) causing the square brackets to be positive, while inequality

(1-45) causes the eigenvalues to be negative. To have spatial heterogeneity while diffusion is present one assumes that a stable stationary state is present in the absence of diffusion. By setting $D_* = 0$ and $\alpha_* = 0$ in inequalities (1-45) and (1-46) yields the linear stability conditions to small Spatially Homogeneous Perturbations (SHoP) in the form

$$\psi_A = \text{trace}(A) = a_{11} + a_{22} < 0 \quad (1-47)$$

$$\Delta_A = \det(A) = a_{11}a_{22} - a_{12}a_{21} > 0 \quad (1-48)$$

Since $a_{11} + a_{22} < 0$ and the diffusion coefficients are both positive by definition in the spatially heterogeneous case, i.e. $D_* > 0$ and $\alpha_* > 0$, inequality (1-45) is automatically satisfied. Then, Turing instability occurs when for some wavenumber κ ,

$$\Delta_{A_\kappa} = \det(A_\kappa) = (a_{11} - \kappa^2 D_*)(a_{22} - \kappa^2 \alpha_*) - a_{12}a_{21} \leq 0 \quad (1-49)$$

This condition is being investigated further in Chapters 4 and 6, and especially for the particular system considered in this study.

1.3 Summary of Unanswered Questions and Problems

Since the spatially homogeneous population growth problem seems to be better represented by the Neoclassical Model and because the linear stability of the corresponding spatially heterogeneous problem is substantially affected by the stationary points it becomes appealing in using the Neoclassical Model in the context of the heterogeneous system. The latter allows the investigation of Turing instabilities in terms of the stationary points corresponding to the Neoclassical Model. Furthermore, the linear stability analysis is only a partial tool in understanding the growth dynamics in both the spatially homogeneous as well as the spatially heterogeneous problems. Therefore, using an expanded analytical tool in the form of the weak nonlinear method of solution is anticipated to produce analytical solutions to these nonlinear problems and thus providing a higher level of insight into the mechanisms controlling the growth dynamics. The work presented here will focus on these four major developments, namely

- (i) using the Neoclassical Model within the spatially heterogeneous problem,
- (ii) undertaking a linear stability analysis of the stationary points corresponding to the Neoclassical Model as applied to the heterogeneous problem,
- (iii) providing an analytical weak nonlinear solution to the spatially homogeneous problem and comparing the results to a numerical solution, and
- (iv) deriving a weak nonlinear solution to the spatially heterogeneous problem and comparing the results to a numerical solution.

CHAPTER 2

PROBLEM FORMULATION

2.1 Governing Equations and Boundary Conditions

The objective in the spatially heterogeneous problem is to find the population number and its spatial distribution at all future times, given an initial spatial distribution of the population, its initial growth rate distribution, boundary conditions, and environmental factors. Since the aim in the present study is to take the theoretical understanding of the spatially heterogeneous problem beyond just linear stability, the precise form of the non-linear functions $f_1(u,v)$ and $f_2(u,v)$ in equation (1-28) are essential beyond the establishment of the stationary solutions. The proposed system here is an extension of the corresponding homogeneous case represented by eq. (1-8) and takes the form

$$\left\{ \begin{array}{l} \frac{\partial u_*}{\partial t_*} = D_* \nabla_*^2 u_* + \mu_* \left[1 - \frac{u_*}{\delta_*} + \frac{(v_* - \mu_*)}{\mu_* (1 + r_m u_*)} \right] u_* \\ \frac{\partial v_*}{\partial t_*} = \alpha_* \nabla_*^2 v_* + \gamma_* - \frac{k_*}{m_o} u_* + \varphi_o v_* \end{array} \right. \quad (2-1)$$

where $u_*(t_*, x_*, y_*, z_*)$ is the viable population number (cell concentration), D_* is the diffusivity of this population in the growth medium, $v_*(t_*, x_*, y_*, z_*)$ is the excess consumption/utilization rate of an abiotic resource (e.g. nutrient), α_* is the nutrient diffusivity in the growth medium, k_* is the cell or organism's nutrient storage capacity, m_o is linked to the net average biomass (see eqs. (1-9) and (1-10) and Figures 1.13 and 1.14), γ_* is the nutrient consumption/utilization acceleration, μ_* is the maximum specific growth rate of the Logistic Growth Model (Pearl, 1927; Verhulst, 1838), and δ_* is the carrying capacity of the environment. Equation (2-1) is presented in a dimensional form and the asterisks linked to its variables and

parameters stand to indicate dimensional quantities. The symbol $\nabla_*^2 \equiv \partial^2/\partial x_*^2 + \partial^2/\partial y_*^2 + \partial^2/\partial z_*^2$ stands for the dimensional Laplacian operator.

The corresponding units for the variables and parameters presented in eq. (2-1) are as follows

$$\begin{aligned}
 u_* &\rightarrow \left[\frac{\text{Cell}}{m^3} \right], \quad \delta_* \rightarrow \left[\frac{\text{Cell}}{m^3} \right], \quad r_{m*} \rightarrow \left[\left(\frac{\text{Cell}}{m^3} \right)^{-1} \right], \quad k_* \rightarrow \left[\frac{N \cdot m^3}{m \cdot \text{Cell}} \right] = \left[\frac{kg \cdot m^3}{s^2 \cdot \text{Cell}} \right], \\
 v_* &\rightarrow [s^{-1}], \quad \mu_* \rightarrow [s^{-1}], \quad \gamma_* \rightarrow [s^{-2}], \quad \varphi_{o*} \rightarrow [s^{-1}], \quad t_* \rightarrow [s], \\
 (x_*, y_*, z_*) &\rightarrow [m], \quad m_{o*} \rightarrow [kg], \quad D_* \rightarrow \left[\frac{m^2}{s} \right], \quad \alpha_* \rightarrow \left[\frac{m^2}{s} \right]
 \end{aligned} \tag{2-2}$$

While the problem as formulated in eq. (2-1) deals with a three-dimensional medium, the reduction to a two dimensional one (2-D) is desirable, possible and realistic, if considering for example growth of populations over particular surfaces, or growth of cells in a very shallow layer of medium. Then the Laplacian operator considered will become two-dimensional and be defined in the form $\nabla_*^2 \equiv \partial^2/\partial x_*^2 + \partial^2/\partial y_*^2$. A two dimensional rectangular domain that is considered here is presented in Figure 2.1.

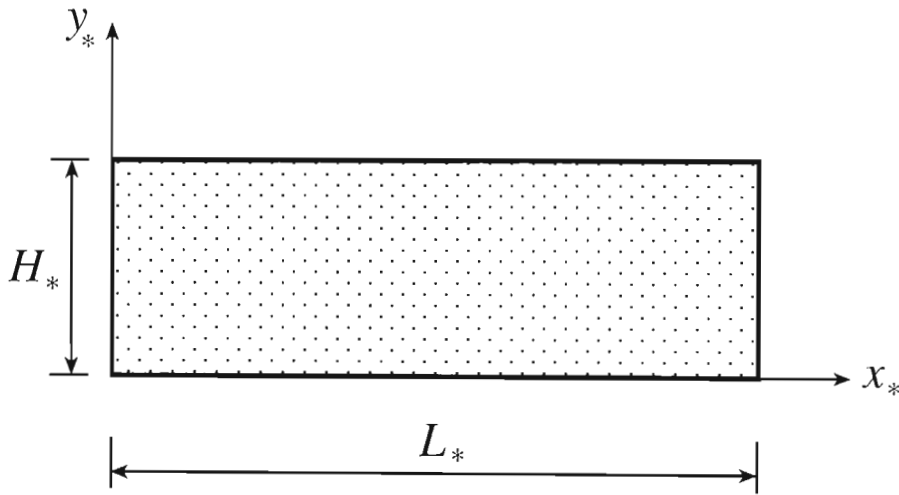


Figure 2.1: Dimensional representation of the problem formulation for growth dynamics in spatially heterogeneous populations.

The boundary conditions considered in this study are of total isolation of the domain from its surroundings. Since the population and nutrient flux assumes the form of Fick's law of diffusion, i.e. $J_{*u} \equiv -D_* \nabla_* u_*$ and $J_{*v} \equiv -\alpha_* \nabla_* v_*$, the isolation boundary conditions take the form

$$\left(\frac{\partial u_*}{\partial x_*} \right)_{x_* = 0, L} = \left(\frac{\partial u_*}{\partial y_*} \right)_{y_* = 0, H} = 0 \quad (a)$$

(2-3)

$$\left(\frac{\partial v_*}{\partial x_*} \right)_{x_* = 0, L} = \left(\frac{\partial v_*}{\partial y_*} \right)_{y_* = 0, H} = 0 \quad (b)$$

Equations (2-1) and the boundary conditions (2-3) consist of the mathematical representation of the problem considered in this study.

2.2 Transforming the Equations into a Dimensionless Form

The objective of this section is to transform eq. (2-1) into a dimensionless form. The reason for the latter is the advantage obtained from such a transformation, which is threefold. First, it reduces the number of constant parameters and simplifies the following analysis. Second, it reveals the dimensionless groups that control the physical and biological aspects of the problem. Third, it may, subject to certain conditions, normalize at least some of the variables of the problem.

By using the dimensions of the parameters and variables listed in eq. (2-2) one may select the following way to transform the dependent and independent variables in eq. (2-1) into their dimensionless form

$$u = \frac{u_*}{\delta_*}, \quad v = \frac{v_*}{\mu_*}, \quad t = \mu_* t_*,$$

$$x = \frac{x_*}{H_*}, \quad y = \frac{y_{**}}{H_*}, \quad z = \frac{z_*}{H_*}, \quad L = \frac{L_*}{H_*} \quad (2-4)$$

$$R = r_m \delta_*, \quad \varphi_o = \frac{\varphi_{o*}}{\mu_*}, \quad \gamma = \frac{\gamma_*(u_*)}{\mu_*^2}$$

where symbols without an asterisk stand to indicate dimensionless variables and parameters. By using eq. (2-4) one can replace the variables and parameters in eq. (2-1) in the form

$$u_* = \delta_* u, \quad v_* = \mu_* v, \quad t_* = \frac{t}{\mu_*},$$

$$x_* = H_* x, \quad y_* = H_* y, \quad z_* = H_* z, \quad L_* = H_* L \quad (2-5)$$

$$r_{m*} = \frac{R}{\delta_*}, \quad \varphi_{o*} = \mu_* \varphi_o, \quad \gamma_*(u_*) = \mu_*^2 \gamma$$

Substituting eq. (2-4) into eq. (2-1) yields

$$\left\{ \begin{array}{l} \mu_* \delta_* \frac{\partial u}{\partial t} = \frac{D_* \delta_*}{H_*^2} \nabla^2 u + \mu_* \left[1 - \frac{u \delta_*}{\delta_*} + \frac{\mu_* (\nu - 1)}{\mu_* (1 + r_{m*} \delta_* u)} \right] \delta_* u \quad (a) \\ \mu_*^2 \frac{\partial v}{\partial t} = \frac{\alpha_* \mu_*}{H_*^2} \nabla^2 v + \mu_*^2 \gamma - \frac{k_* \delta_*}{m_{o*}} u + \mu_*^2 \varphi_o v \quad (b) \end{array} \right. \quad (2-6)$$

Dividing now eq. (2-6a) by $(\mu_* \delta_*)$ and eq. (2-6b) by μ_*^2 , substituting $R = r_{m*} \delta_*$, and canceling alike terms produces the following equation

$$\left\{ \begin{array}{l} \frac{\partial u}{\partial t} = \frac{D_*}{\mu_* H_*^2} \nabla^2 u + \left[1 - u + \frac{(\nu - 1)}{(1 + R u)} \right] u \quad (a) \\ \frac{\partial v}{\partial t} = \frac{\alpha_*}{\mu_* H_*^2} \nabla^2 v + \gamma - \frac{k_* \delta_*}{\mu_*^2 m_{o*}} u + \varphi_o v \quad (b) \end{array} \right. \quad (2-7)$$

The only dimensional parameters (symbols with asterisks) appear grouped together as coefficients to different terms. It can be verified by using their units from eq. (2-2) that each combined group is dimensionless as well. One can therefore define the following dimensionless numbers to represent these dimensionless groups in the form

$$Gn = \frac{\mu_* H_*^2}{D_*}, \quad Rn = \frac{\mu_* H_*^2}{\alpha_*}, \quad Sn = \frac{k_* \delta_*}{\mu_*^2 m_{o*}} \quad (2-8)$$

where Gn represents a Growth Number, Rn is a Resource Number, and Sn is a Storage Number. Substituting these dimensionless groups into eq. (2-7) leads to the dimensionless form of these equations, which is fully equivalent to eq. (2-1), in the form

$$\left\{ \begin{array}{l} \frac{\partial u}{\partial t} = \frac{1}{Gn} \nabla^2 u + \left[1 - u + \frac{(\nu - 1)}{(1 + R u)} \right] u \quad (a) \\ \frac{\partial v}{\partial t} = \frac{1}{Rn} \nabla^2 v + \gamma - Sn u + \varphi_o v \quad (b) \end{array} \right. \quad (2-9)$$

where $R = r_{m*} \delta_*$ is a Biomass Number.

The rectangular geometry of the dimensionless domain in 2-D is presented in Figure 2.2.

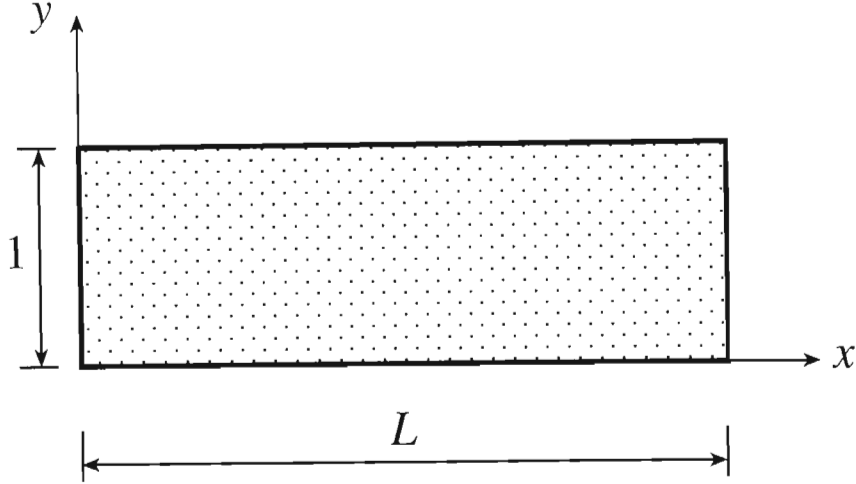


Figure 2.2: Dimensionless representation of the problem formulation for growth dynamics in spatially heterogeneous populations.

The dimensionless boundary conditions take the form

$$\left(\frac{\partial u}{\partial x}\right)_{x=0,L} = \left(\frac{\partial u}{\partial y}\right)_{y=0,1} = 0 \quad (a) \quad (2-10)$$

$$\left(\frac{\partial v}{\partial x}\right)_{x=0,L} = \left(\frac{\partial v}{\partial y}\right)_{y=0,1} = 0 \quad (b)$$

Now one can test the accomplishment of the first objective in transforming the equations into a dimensionless form by comparing the number of parameters controlling the dimensional and dimensionless problems, respectively. If one assumes that γ_* is constant, the dimensional problem is controlled by 9 parameters in eq. (2-1), namely $D_*, \mu_*, \delta_*, r_m^*, \alpha_*, \gamma_*, k_*, m_o^*, \varphi_o^*$, and 2 geometrical parameters in the boundary conditions eq. (2-3), namely H_* and L_* , a total number of 11 parameters. In contrast, the dimensionless problem is controlled by 6 parameters in eq. (2-9), namely $Gn, R, Rn, \gamma, Sn, \varphi_o$, and one parameter in the boundary conditions eq. (2-10), namely L , a total number of 7 parameters. This transformation resulted in a significant reduction of the total number of parameters from 11 to 7. In this study γ is assumed

to be a function of the population number u , and in the absence of accurate data a linear relationship is assumed in the form

$$\gamma = \gamma_o + \gamma_1 u \quad (2-11)$$

Substituting eq. (2-11) into eq. (2-9) one obtains

$$\begin{cases} \frac{\partial u}{\partial t} = \frac{1}{Gn} \nabla^2 u + \left[1 - u + \frac{(v-1)}{(1+R u)} \right] u & (a) \\ \frac{\partial v}{\partial t} = \frac{1}{Rn} \nabla^2 v + \gamma_o + \gamma_1 u - Sn u + \varphi_o v & (b) \end{cases} \quad (2-12)$$

and using the notation

$$\beta_o = Sn - \gamma_1 \quad (2-13)$$

leads to the final dimensionless form of the equations governing the spatio-temporal dynamics of heterogeneously distributed populations in the form

$$\begin{cases} \frac{\partial u}{\partial t} = \frac{1}{Gn} \nabla^2 u + \left[1 - u + \frac{(v-1)}{(1+R u)} \right] u & (a) \\ \frac{\partial v}{\partial t} = \frac{1}{Rn} \nabla^2 v + \gamma_o - \beta_o u + \varphi_o v & (b) \end{cases} \quad (2-14)$$

Equation (2-14) and the boundary conditions (2-10) subject to a selected form of initial conditions, e.g. $(u)_{t=0} = u_{in}(x, y)$, $(v)_{t=0} = v_{in}(x, y)$ constitute the final formulation of the problem considered in this study.

CHAPTER 3

STATIONARY SOLUTIONS, MULTIPLICITY AND PARAMETER CONTROL

3.1 Stationary Solutions

3.1.1 Derivation of Stationary Solutions

To obtain the stationary (i.e. time independent) solutions one substitutes in eq. (2-14) the condition that the stationary solution is time independent, i.e. $(\partial u/\partial t) = 0$ and $(\partial v/\partial t) = 0$ to obtain for a 2-D domain

$$\begin{cases} \frac{\partial^2 u}{\partial x^2} + \frac{\partial^2 u}{\partial y^2} = -Gn \left[1 - u + \frac{(v-1)}{(1+R u)} \right] u & (a) \\ \frac{\partial^2 v}{\partial x^2} + \frac{\partial^2 v}{\partial y^2} = Rn [\beta_o u - \varphi_o v - \gamma_o] = 0 & (b) \end{cases} \quad (3-1)$$

One possible set of solutions to eq. (3-1) is

$$u = u_s = \text{constant} \ \& \ v = v_s = \text{constant} \quad (3-2)$$

The set of solutions consistent with (3-2) are not only time independent but also spatially uniform. They are obtained from eq.(3-1) by setting $\partial^2 u/\partial x^2 = \partial^2 u/\partial y^2 = 0$ and $\partial^2 v/\partial x^2 = \partial^2 v/\partial y^2 = 0$ that yields

$$\begin{cases} \left[1 - u_s + \frac{(v_s-1)}{(1+R u_s)} \right] u_s = 0 & (a) \\ \beta_o u_s - \varphi_o v_s - \gamma_o = 0 & (b) \end{cases} \quad (3-3)$$

that can be presented in the following alternative forms

$$\begin{cases} \left[(1 - u_s)(1 + R u_s) + v_s - 1 \right] u_s = 0 & (a) \\ \beta_o u_s - \varphi_o v_s - \gamma_o = 0 & (b) \end{cases} \quad (3-4)$$

and

$$\begin{cases} \left[(R - 1)u_s - R u_s^2 + v_s \right] u_s = 0 & (a) \\ \beta_o u_s - \varphi_o v_s - \gamma_o = 0 & (b) \end{cases} \quad (3-5)$$

The different solutions to the nonlinear algebraic eqs. (3-5) are the following three solutions.

First Solution: the Trivial Solution (u_{so}, v_{so})

$$u_{so} = 0 \quad \& \quad v_{so} = -\frac{\gamma_o}{\varphi_o} \quad (3-6)$$

Second and Third Solutions: the Non Trivial Solutions $(u_{s1,2}, v_{s1,2})$

From eq. (3-5a) one gets

$$v_s = u_s(R u_s - R + 1) \quad (3-7)$$

which upon substituting into eq. (3-5b) leads to a quadratic algebraic equation for u_s in the form

$$u_s^2 + \frac{[\varphi_o(1 - R) - \beta_o]}{\varphi_o R} u_s + \frac{\gamma_o}{\varphi_o R} = 0 \quad (3-8)$$

The solution to eq. (3-8) has the form

$$u_{s1,2} = \frac{[\beta_o + \varphi_o(R - 1)]}{2\varphi_o R} \left[1 \pm \sqrt{1 - \frac{4\gamma_o\varphi_o R}{[\varphi_o(1 - R) - \beta_o]^2}} \right] \quad (3-9)$$

For simplicity of using this solution in the following derivations the following notation is used

$$S = \sqrt{1 - \frac{4\gamma_o\varphi_o R}{[\varphi_o(1 - R) - \beta_o]^2}} \quad (3-10)$$

Then the stationary solutions (3-9) and (3-7) become

$$u_{s1} = \frac{[\beta_o + \varphi_o(R-1)](1+S)}{2\varphi_o R} \quad (3-11)$$

$$v_{s1,2} = \frac{[\beta_o + \varphi_o(R-1)]\{[\beta_o + \varphi_o(R-1)](1+S) - 2(R-1)\varphi_o\}}{4\varphi_o^2 R} \quad (3-12)$$

$$u_{s2} = \frac{[\beta_o + \varphi_o(R-1)](1-S)}{2\varphi_o R} \quad (3-13)$$

$$v_{s2} = \frac{[\beta_o + \varphi_o(R-1)]\{[\beta_o + \varphi_o(R-1)](1-S) - 2(R-1)\varphi_o\}}{4\varphi_o^2 R} \quad (3-14)$$

Not the whole parameter domain is consistent with these solutions. While the value of v_s can be allowed to be negative, the value of u_s must be non-negative because there is no biological meaning to negative population values. The next step is to derive the conditions for the stationary solutions of u_{s1} and u_{s2} to be non-negative.

3.1.2 Conditions for u_{s1} to be biologically meaningful, i.e. non-negative ($u_{s1} \geq 0$)

Imposing the constraint that $u_{s1} \geq 0$ and using eq. (3-11) leads to

$$\frac{1}{2R} \left[\frac{\beta_o}{\varphi_o} + (R-1) \right] (1+S) \geq 0 \quad (3-15)$$

Since $R > 0$ and $S \geq 0$ by definition, the condition (3-15) is reduced to

$$\frac{\beta_o}{\varphi_o} \geq 1 - R \quad (3-16)$$

The latter condition implies

$$\begin{cases} \beta_o \geq \varphi_o(1-R) & \forall \varphi_o > 0 & (a) \\ \beta_o \leq (-\varphi_o)(R-1) & \forall \varphi_o < 0 & (b) \end{cases} \quad (3-17)$$

Conditions (3-16) or its alternative form (3-17) indicate the parameter window when $u_{s1} \geq 0$.

3.1.3 Conditions for u_{s2} to be biologically meaningful, i.e. non-negative ($u_{s2} \geq 0$)

Similarly, for $u_{s2} \geq 0$ and using eq.(3-13) leads to

$$\frac{1}{2R} \left[\frac{\beta_o}{\phi_o} + (R-1) \right] (1-S) \geq 0 \quad (3-18)$$

and using the fact that $R > 0$ and $S \geq 0$ by definition, the condition (3-18) is reduced to

$$\frac{\beta_o}{\phi_o} + (R-1) \geq 0 \quad \text{and} \quad (1-S) > 0 \quad (3-19)$$

or

$$\frac{\beta_o}{\phi_o} + (R-1) \leq 0 \quad \text{and} \quad (1-S) < 0 \quad (3-20)$$

The latter implies

$$\begin{cases} \frac{\beta_o}{\phi_o} \geq (1-R) & \forall S < 1 & (a) \\ \frac{\beta_o}{\phi_o} \leq (1-R) & \forall S > 1 & (b) \end{cases} \quad (3-21)$$

Conditions (3-21) indicate the parameter window when $u_{s2} \geq 0$. The interesting result from eq. (3-16) and (3-21) indicates that for $S > 1$ when the stationary solution u_{s1} becomes biologically meaningless the other solution u_{s2} just becomes meaningful.

3.1.4 Additional Stationary Solutions

One may expect additional solutions that are functions of x and y leading to spatial heterogeneity. Identifying these solutions and their stability is the objective of this study.

3.2 Multiplicity of Solutions

The stationary constant solutions presented in section 3.1 are regular solutions. Some limiting cases that cause the governing equations to degenerate may yield additional special solutions that have been consistently captured experimentally. One such example is the widespread occurrence of monotonic solutions as evidenced by the large number of experiments that capture this type of monotonic growth. From the problem formulated in this study monotonic growth is a mathematically degenerated case when $\gamma_o = \gamma_1 = 0$, $Sn = \varphi_o = 0$ and $Rn \rightarrow \infty$ (in reality this means $Rn \gg 1$ implying for example a very small resource diffusivity in the medium), or when γ_o, γ_1, Sn and φ_o are very small and Rn is very large compared to the other terms in eq. (2-14b). Subject to these conditions, equation (2-14b) yields $v = v_o = \text{constant}$. The value of this integration constant v_o corresponds to the value of v at $t = 0$ and can be established explicitly by using the definition of v from equation (1-11) and its dimensionless transformation eq. (2-4), in the form

$$v_o = 1 + (1 + Ru_o) \left[\frac{\dot{u}_o}{u_o} + (u_o - 1) \right] \quad , \quad (3-22)$$

where u_o is the initial population number at $t = 0$, and $\dot{u}_o = (du/dt)_{t=0}$ is the initial growth rate at $t = 0$. Then, with $v = v_o$, the system of two first order partial differential equations (2-14a) and (2-14b) reduces to one first order partial differential equation obtained by substituting eq. (3-22) into (2-14a), to yield

$$\frac{\partial u}{\partial t} = \frac{1}{Gn} \nabla^2 u + \left[1 - u + \frac{(v_o - 1)}{(1 + Ru)} \right] u \quad , \quad (3-23)$$

The constant stationary solutions of eq. (3-23) correspond to the stationary solutions of the degenerated monotonic form linked to the Neoclassical Model, i.e.

$$u_{1NCS} = 0 \quad , \quad (3-24)$$

$$u_{2,3NCS} = \frac{1}{2} \left[\frac{(1 - R)}{R} \pm \sqrt{\Delta_o} \right] \quad ,$$

where $u_{2S} \geq u_{3S}$ and the discriminant Δ_o is

$$\Delta_o = \frac{(1-R)^2}{R^2} \left[1 + \frac{4\nu_o R}{(1-R)^2} \right] . \quad (3-25)$$

The latter solutions represent one example of degenerated forms of the governing equations that may lead to special constant stationary solutions that at least in the context of the homogeneous problem represent results that are captured frequently in experiments. The objective of the present study is to focus on the general problem as is anticipated to occur in spatially heterogeneous populations without special emphasis on the degenerated special cases. Nevertheless, one should be fully aware of the further possibilities due to the multiplicity of constant stationary solutions, some of them being degenerated special cases.

3.3 Stability Criteria and Parameter Control

There are a considerable number of possibilities concerning the ultimate solution that materializes under different circumstances. One of the multiple constant stationary solutions may turnout to be stable to both Spatially Homogeneous Perturbations (SHoP) as well as to Spatially Heterogeneous Perturbations (SHeP). Some of these stationary solutions may turnout to be linearly unstable to Spatially Homogeneous Perturbations (SHoP) but stable to Spatially Heterogeneous Perturbations (SHeP) in which case another type of time dependent (usually oscillatory) but spatially uniform solution takes over. Alternatively, one of these stationary solutions may be unstable to both Spatially Homogeneous Perturbations (SHoP) as well as to Spatially Heterogeneous Perturbations (SHeP). In the latter case it is difficult to establish which solution is to materialize and why. It may very well depend on the initial conditions although there is no method available to indicate how to distinguish and establish which initial conditions lead to what solution.

In order to make sure that the latter possibility does not complicate the analysis presented in this study, the work here will be focused on the pre-condition that the constant stationary solutions (u_{s0}, v_{s0}) , (u_{s1}, v_{s1}) and (u_{s2}, v_{s2}) are stable to SHoP when their stability to SHeP is investigated. This means that small Spatially Homogeneous Perturbations (SHoP) around these stationary solutions decay while

small Spatially Heterogeneous Perturbations (SheP) around these solutions may very well grow into a spatial pattern leading to a Turing type of instability.

The first step in this analysis is therefore to identify the conditions for stability of the constant stationary solutions (u_{s0}, v_{s0}) , (u_{s1}, v_{s1}) and (u_{s2}, v_{s2}) to SHoP. Then a weak nonlinear method of solution will demonstrate the qualitative as well as quantitative form of spatially homogeneous solutions that are obtained when the stability conditions are not fulfilled. The analytical weak nonlinear results are compared with a standard numerical solution in order to identify quantitatively the domain of validity of the weak nonlinear solution. Then the linear stability analysis to SHep is undertaken to identify the conditions when Turing instabilities eventually materialize. In contrast with the other available stability analyses that produce the simple stability conditions in terms of the parameters of the linearized equations, the present analysis focuses much attention to convert these conditions into a form that depends exclusively on the primitive parameters of the original system of governing equations. It is obvious that the stability conditions presented in section 1.2.3, eqs. (1-45) and (1-46) depend on the parameters of the linearized system (1-32). However, their link to the primitive parameters of the original nonlinear problem is not explicitly given by the conditions expressed in eqs. (1-45) and (1-46). The latter are being developed in this study considering the specific nonlinear problem formulated in eq. (2-14). It turns-out that the connection between these two types of parameters occurs via the dependence of the parameters in the linearized equations on the stationary solutions.

The latter dependence appears via different complicated algebraic functions that for simplicity are represented in the following notation that is being used throughout the following chapters. This useful notation is presented in the form

$$\beta_1 = \left[\frac{R(1-u_s)}{(1+Ru_s)} - 1 \right] u_s = \frac{[R(1-2u_s)-1]u_s}{(1+Ru_s)} = [R(1-2u_s)-1]\beta_2 = \beta_2\beta_3 ; \quad (a)$$

$$\beta_2 = \frac{u_s}{(1+Ru_s)} = \frac{u_s}{\beta_4} ; \quad (b)$$

$$\beta_3 = (R-2Ru_s-1) = [R(1-2u_s)-1] ; \quad (c)$$

$$\beta_4 = (1+Ru_s) ; \quad (d)$$

(3-26)

$$\beta_5 = \beta_3 - Ru_s = (R-3Ru_s-1) = [R(1-3u_s)-1] ; \quad (e)$$

$$\beta_6 = (3Ru_s - R + 1) = [R(3u_s - 1) + 1] = -\beta_5 ; \quad (f)$$

$$\beta_1 = \beta_2\beta_3 ; \quad (g)$$

$$u_s = \beta_2\beta_4 ; \quad (h)$$

where u_s represents any of the constant stationary solutions that their stability is being investigated.

CHAPTER 4

LINEAR STABILITY ANALYSIS TO SPATIALLY HOMOGENEOUS PERTURBATIONS (SHoP)

4.1 Linear Stability of the Nontrivial Stationary Solutions $(u_{SI,2}, v_{SI,2})$

For undertaking the linear stability of the stationary solutions $(u_{SI,2}, v_{SI,2})$ to small Spatially Homogeneous Perturbations (SHoP) one considers the system of equations (2-14) corresponding to conditions of very large values of Gn and Rn , i.e. mathematically meaning $Gn \rightarrow \infty$ and $Rn \rightarrow \infty$. This transforms eq. (2-14) into the following spatially homogeneous form

$$\left\{ \begin{array}{l} \frac{du}{dt} = \left[1 - u + \frac{(v-1)}{(1+Ru)} \right] u \quad (a) \\ \frac{dv}{dt} = \gamma_o - \beta_o u + \varphi_o v \quad (b) \end{array} \right. \quad (4-1)$$

Equation (4-1) can be presented in the following equivalent form that is more convenient for the following derivations

$$\left\{ \begin{array}{l} (1+Ru) \frac{du}{dt} = [(1-u)(1+Ru) + v-1] u \quad (a) \\ \frac{dv}{dt} = \gamma_o - \beta_o u + \varphi_o v \quad (b) \end{array} \right. \quad (4-2)$$

which expands further into

$$\left\{ \begin{array}{l} (1 + R u) \frac{du}{dt} = [(R-1)u - R u^2 + v] u \quad (a) \\ \frac{dv}{dt} = \gamma_o - \beta_o u + \varphi_o v \quad (b) \end{array} \right. \quad (4-3)$$

By introducing small perturbations $(\varepsilon u_1, \varepsilon v_1)$ around the stationary solutions (u_s, v_s) in the form

$$u = u_s + \varepsilon u_1 \quad \text{and} \quad v = v_s + \varepsilon v_1 \quad (4-4)$$

where $\varepsilon \ll 1$ stands only to indicate that the perturbations are very small, and substituting (4-4) into (4-3) yields

$$\left\{ \begin{array}{l} [1 + R(u_s + \varepsilon u_1)] \frac{d(u_s + \varepsilon u_1)}{dt} = [(R-1)(u_s + \varepsilon u_1) - R(u_s + \varepsilon u_1)^2 + (v_s + \varepsilon v_1)] (u_s + \varepsilon u_1) \quad (a) \\ \frac{d(v_s + \varepsilon v_1)}{dt} = \gamma_o - \beta_o (u_s + \varepsilon u_1) + \varphi_o (v_s + \varepsilon v_1) \quad (b) \end{array} \right. \quad (4-5)$$

Expanding the expressions in eq. (4-5) taking into account that the stationary solutions (u_s, v_s) are time independent and therefore $du_s/dt = 0$ and $dv_s/dt = 0$, leads to

$$\left\{ \begin{array}{l} \varepsilon(1 + R u_s) \frac{du_1}{dt} + \varepsilon^2 R u_1 \frac{du_1}{dt} = \{ [(R-1)u_s - R u_s^2 + v_s] u_s + \varepsilon [(R-1-2R u_s) u_1 + v_1] u_s - \varepsilon^2 R u_s u_1^2 \} + \{ \varepsilon [(R-1)u_s - R u_s^2 + v_s] u_1 + \varepsilon^2 [(R-1-2R u_s) u_1 + v_1] u_1 - R \varepsilon^3 u_1^3 \} \quad (a) \\ \varepsilon \frac{dv_1}{dt} = \gamma_o - \beta_o u_s + \varphi_o v_s + \varepsilon (-\beta_o u_1 + \varphi_o v_1) \quad (b) \end{array} \right. \quad (4-6)$$

Obviously, from eqs. (3-5) and (3-7) the stationary solutions $(u_{s1,2}, v_{s1,2})$ satisfy the following conditions

$$(R-1)u_s - R u_s^2 + v_s = 0 \quad (4-7)$$

$$\beta_o u_s - \varphi_o v_s - \gamma_o = 0 \quad (4-8)$$

which when introduced into eq. (4-6) yields

$$\left\{ \begin{array}{l} \varepsilon(1 + Ru_s) \frac{du_1}{dt} + \varepsilon^2 Ru_1 \frac{du_1}{dt} = \varepsilon[(R - 1 - 2Ru_s)u_s u_1 + u_s v_1] + \quad (a) \\ \varepsilon^2 \{[(R - 1 - 2Ru_s)u_1 + v_1]u_1 - Ru_s u_1^2\} - \varepsilon^3 Ru_1^3 \quad (4-9) \\ \varepsilon \frac{dv_1}{dt} = \varepsilon(-\beta_o u_1 + \varphi_o v_1) \quad (b) \end{array} \right.$$

The linearization applied in any linear stability analysis assumes small perturbations, expressed by the fact that $\varepsilon \ll 1$. Therefore one can neglect in eq. (4-9) terms that are $O(\varepsilon^2)$ or smaller, e.g. $O(\varepsilon^3)$. This approximation transforms eq. (4-9) into the following linearized form

$$\left\{ \begin{array}{l} \varepsilon(1 + Ru_s) \frac{du_1}{dt} = \varepsilon[(R - 1 - 2Ru_s)u_s u_1 + u_s v_1] \quad (a) \\ \varepsilon \frac{dv_1}{dt} = \varepsilon(-\beta_o u_1 + \varphi_o v_1) \quad (b) \end{array} \right. \quad (4-10)$$

Dividing eq. (4-10) by $(1 + Ru_s)$ yields

$$\left\{ \begin{array}{l} \frac{du_1}{dt} = \frac{[R(1 - 2u_s) - 1]u_s}{(1 + Ru_s)} u_1 + \frac{u_s}{(1 + Ru_s)} v_1 \quad (a) \\ \frac{dv_1}{dt} = -\beta_o u_1 + \varphi_o v_1 \quad (b) \end{array} \right. \quad (4-11)$$

From the notation (3-26a,b) one recognizes in eq. (4-11) the terms for β_1 and β_2 . Replacing this notation leads to the linear stability equations

$$\left\{ \begin{array}{l} \frac{du_1}{dt} = \beta_1 u_1 + \beta_2 v_1 \quad (a) \\ \frac{dv_1}{dt} = -\beta_o u_1 + \varphi_o v_1 \quad (b) \end{array} \right. \quad (4-12)$$

or in the equivalent vector/matrix form

$$\frac{dw_1}{dt} = A w_1 \quad (4-13)$$

where $w_1 = [u_1, v_1]^T$, and the matrix A stands for

$$A = \begin{bmatrix} \beta_1 & ; & \beta_2 \\ -\beta_o & ; & \varphi_o \end{bmatrix} \quad (4-14)$$

The linear system (4-12) has solutions of the following form

$$u_1 = B e^{\lambda t} \quad (a) \quad (4-15)$$

$$v_1 = C e^{\lambda t} \quad (b)$$

which upon substitution into eq. (4-12) produces the following equations

$$\lambda B e^{\lambda t} = (\beta_1 B + \beta_2 C) e^{\lambda t} \quad (a) \quad (4-16)$$

$$\lambda C e^{\lambda t} = (-\beta_o B + \varphi_o C) e^{\lambda t} \quad (b)$$

or

$$\lambda B = \beta_1 B + \beta_2 C \quad (a) \quad (4-17)$$

$$\lambda C = -\beta_o B + \varphi_o C \quad (b)$$

One way to solve this system is to express C in terms of B from eq. (4-17a) in the form

$$C = \frac{(\lambda - \beta_1)}{\beta_2} B \quad (4-18)$$

and substituting this value of C into eq. (4-17b) in the form

$$[\lambda(\lambda - \beta_1) + \beta_o \beta_2 - \varphi_o(\lambda - \beta_1)] B = 0 \quad (4-19)$$

which upon expansion produces the following characteristic equation for the eigenvalues of the linear problem

$$\lambda^2 - (\beta_1 + \varphi_o)\lambda + (\beta_o \beta_2 + \varphi_o \beta_1) = 0 \quad (4-20)$$

It can be recognized that the coefficient terms appearing in eq. (4-20) represent the trace, ψ_A , and the determinant, Δ_A , of the coefficient matrix A as follows

$$\psi_A = \text{trace}(A) = \beta_1 + \varphi_o \quad (4-21)$$

$$\Delta_A = \det(A) = \beta_1 \varphi_o + \beta_o \beta_2 \quad (4-22)$$

Equation (4-20) can therefore be represented in terms of the trace ψ_A and the determinant Δ_A of the coefficient matrix A as follows

$$\lambda^2 - \psi_A \lambda + \Delta_A = 0 \quad (4-23)$$

Its solution for the eigenvalues is

$$\lambda_{1,2} = \frac{\psi_A}{2} \left[1 \pm \sqrt{1 - \frac{4\Delta_A}{\psi_A^2}} \right] \quad (4-24)$$

The solution to the linear system takes therefore the final form

$$u_1 = B_1 e^{\lambda_1 t} + B_2 e^{\lambda_2 t} \quad (a) \quad (4-25)$$

$$v_1 = C_1 e^{\lambda_1 t} + C_2 e^{\lambda_2 t} \quad (b)$$

When λ is complex, i.e. $\lambda = \lambda_r \pm i\lambda_i$, the solution takes the form

$$u_1 = e^{\lambda_r t} (B e^{i\lambda_i t} + B^* e^{-i\lambda_i t}) = e^{\lambda_r t} [B_1 \sin(\lambda_i t) + B_2 \cos(\lambda_i t)] \quad (a) \quad (4-26)$$

$$v_1 = e^{\lambda_r t} (C e^{i\lambda_i t} + C^* e^{-i\lambda_i t}) = e^{\lambda_r t} [C_1 \sin(\lambda_i t) + C_2 \cos(\lambda_i t)] \quad (b)$$

where B^* represents the constant complex conjugate of B , and C^* represents the constant complex conjugate of C .

The eigenvalues (4-24) combined with the form of the solutions (4-25) and (4-26) provide the conditions for small perturbations $\varepsilon(u_1, v_1)$ around the stationary solutions $(u_{S1,2}, v_{S1,2})$ to grow or decay. When λ is real and negative or complex with a negative real part the perturbations decay and the corresponding stationary solution (u_{S1}, v_{S1}) or (u_{S2}, v_{S2}) is stable, while if λ is real and positive or complex with a positive real part the perturbations grow exponentially and the corresponding stationary solution is unstable. The linear stability analysis can not provide an answer regarding what solution will eventually materialize when the stationary solution is unstable. Naturally, the unlimited exponential growth is not typically an acceptable realistic solution. The weak nonlinear method of solution will provide the answers to this question in chapter 5. From eq. (4-23) it is obvious that for stability of the stationary solutions $(u_{S1,2}, v_{S1,2})$ to SHoP one needs to impose the conditions

$$\psi_A < 0 \quad \& \quad \Delta_A > 0 \quad (4-27)$$

The latter guarantees that the eigenvalues λ are real and negative or complex conjugates with a negative real part.

One can summarize these results by describing the different qualitative solutions obtained from the linear stability analysis in the form

(i) $(u_{S1,2}, v_{S1,2})$ are *stable* to SHoP if:

$$\psi_A < 0 \quad \& \quad \Delta_A > 0 \quad (4-28)$$

Within this regime that satisfies inequalities (4-28) one can identify the following qualitatively different sub-regimes:

$$(a) \text{ If } 0 < \Delta_A < \frac{\psi_A^2}{4} \text{ (which is equivalent to } 0 < \frac{4\Delta_A}{\psi_A^2} < 1 \text{)} \quad (4-29)$$

then λ_1 and λ_2 are real and negative, conditions identified as *overdamped* oscillations. Their qualitative graphical representation is presented in Fig. 4.1.

$$(b) \text{ If } 0 < \Delta_A = \frac{\psi_A^2}{4} \text{ (which is equivalent to } 0 < \frac{4\Delta_A}{\psi_A^2} = 1 \text{)} \quad (4-30)$$

then $\lambda_1 = \lambda_2 < 0$ (i.e. real, equal and negative), conditions identified as *critically damped* oscillations. The solution for this case of equal eigenvalues has the form

$$u_1 = (B_1 + B_2 t)e^{\lambda_1 t} = (B_1 + B_2 t)e^{\lambda_2 t} \quad (a) \quad (4-31)$$

$$v_1 = (C_1 + C_2 t)e^{\lambda_1 t} = (C_1 + C_2 t)e^{\lambda_2 t} \quad (b)$$

Their qualitative graphical representation is presented in Fig. 4.2.

$$(c) \text{ If } \Delta_A > \frac{\psi_A^2}{4} > 0 \text{ (which is equivalent to } \frac{4\Delta_A}{\psi_A^2} > 1 > 0 \text{)} \quad (4-32)$$

then λ_1 and λ_2 are a pair of complex conjugate eigenvalues in the form

$$\lambda_1 = \lambda_r + i\lambda_i, \text{ and } \lambda_2 = \lambda_r - i\lambda_i, \quad (4-33)$$

with

$$\lambda_r = \frac{\psi_A}{2} < 0 \text{ and } \lambda_i = \frac{\psi_A}{2} \sqrt{\frac{4\Delta_A}{\psi_A^2} - 1} \quad (4-34)$$

conditions identified as *underdamped* oscillations. Their qualitative graphical representation is presented in Fig. 4.3.

(ii) $(u_{s1,2}, v_{s1,2})$ are *neutrally stable* to SHoP if:

$$\psi_A = 0 \quad \& \quad \Delta_A > 0 \quad (4-35)$$

For this regime the eigenvalues equation has the form

$$\lambda^2 + \Delta_A = 0 \quad (4-36)$$

leading to the following eigenvalues solution

$$\lambda_{1,2} = \pm i\sqrt{\Delta_A} \quad \forall \Delta_A > 0 \quad (\lambda_r = 0, \lambda_i = \sqrt{\Delta_A}) \quad (4-37)$$

conditions identified as *neutrally stable* oscillations because the real part of the eigenvalues is zero and therefore perturbations neither decay nor grow. Their qualitative graphical representation is presented in Fig. 4.4.

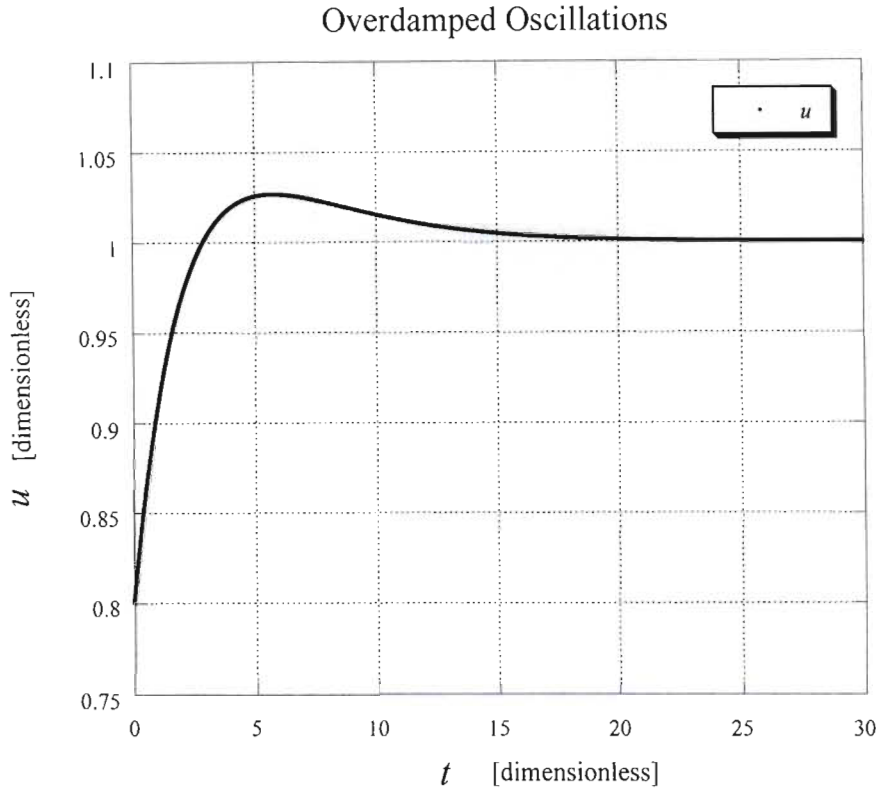


Figure 4.1: Qualitative description of overdamped conditions identified to be applicable for $0 < \Delta_A < \psi_A^2/4$.

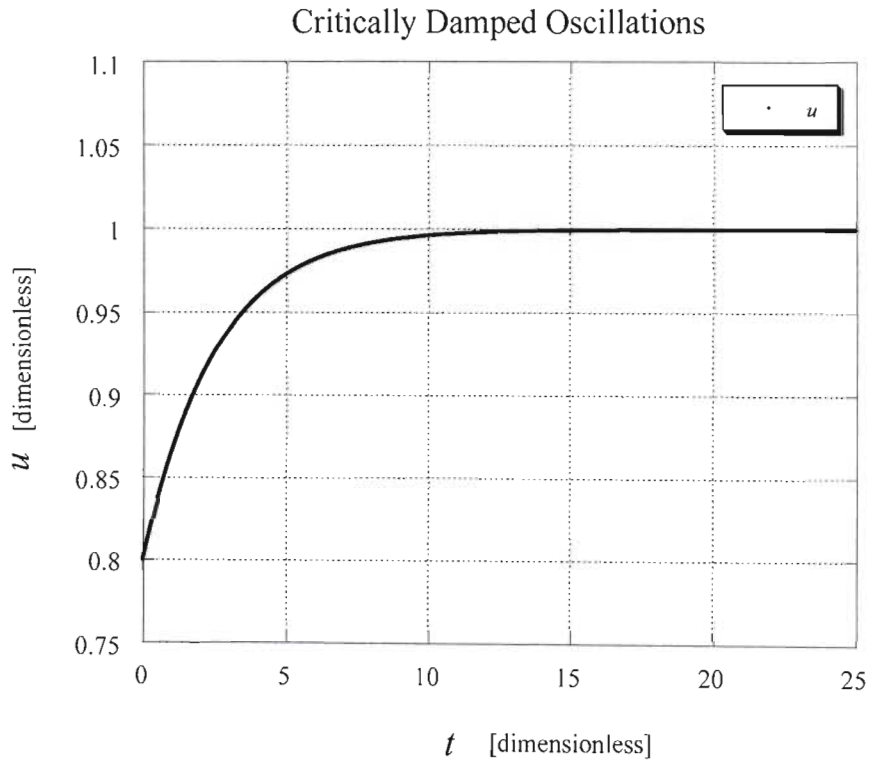


Figure 4.2: Qualitative description of critically damped conditions identified to be applicable for $0 < \Delta_A = \psi_A^2/4$.

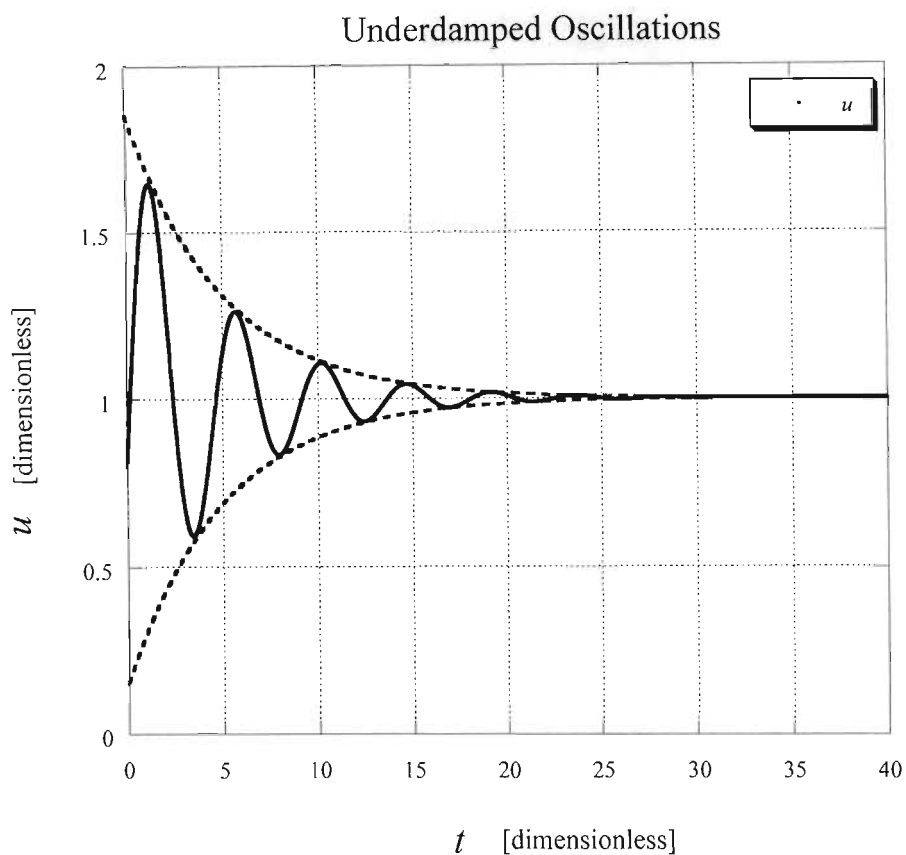


Figure 4.3: Qualitative description of underdamped conditions identified to be applicable for $\Delta_A > \psi_A^2/4 > 0$.

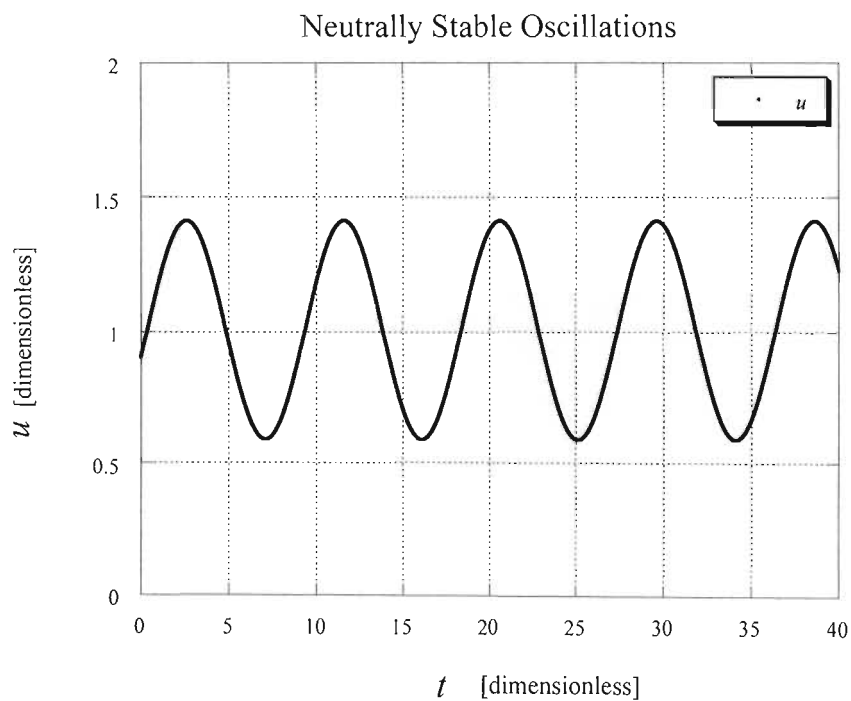


Figure 4.4: Qualitative description of neutrally stable conditions identified to be applicable for $\psi_A = 0$ and $\Delta_A > 0$.

(iii) $(u_{sl,2}, v_{sl,2})$ are *unstable* to SHoP if:

$$\psi_A < 0 \quad \& \quad \Delta_A < 0 \quad (4-38)$$

For this regime the eigenvalues solution has the form

$$\lambda_1 = \frac{\psi_A}{2} \left[1 + \sqrt{1 - \frac{4 \Delta_A}{\psi_A^2}} \right] = \frac{\psi_A}{2} \left[1 + \sqrt{1 + \frac{4 |\Delta_A|}{\psi_A^2}} \right] < 0 \quad \forall \Delta_A < 0 \quad (4-39)$$

$$\lambda_2 = \frac{\psi_A}{2} \left[1 - \sqrt{1 - \frac{4 \Delta_A}{\psi_A^2}} \right] = \frac{\psi_A}{2} \left[1 - \sqrt{1 + \frac{4 |\Delta_A|}{\psi_A^2}} \right] > 0 \quad \forall \Delta_A < 0 \quad (4-40)$$

leading to a monotonically diverging solution because both eigenvalues are real, one negative ($\lambda_1 < 0$) and one positive ($\lambda_2 > 0$), the latter causing the perturbation to diverge and grow exponentially. These conditions are identified as *unstable monotonically diverging*.

(iv) $(u_{sl,2}, v_{sl,2})$ are *neutrally stable* to SHoP if:

$$\psi_A < 0 \quad \& \quad \Delta_A = 0 \quad (4-41)$$

For this regime the eigenvalues are

$$\lambda_1 = \psi_A < 0 \quad (4-42)$$

$$\lambda_2 = 0 \quad (4-43)$$

leading to a monotonically neutrally stable solution, because the perturbations decay due to $\lambda_1 < 0$ but neither decay nor grow due to $\lambda_2 = 0$. These conditions are identified as *monotonically neutrally stable*.

(v) $(u_{sl,2}, v_{sl,2})$ are *unstable* to SHoP if:

$$\psi_A > 0 \quad \& \quad \Delta_A > 0 \quad (4-44)$$

Within this regime that satisfies inequalities (4-44) one can identify the following qualitatively different sub-regimes:

$$(a) \text{ If } 0 < \Delta_A < \frac{\psi_A^2}{4} \text{ (which is equivalent to } 0 < \frac{4\Delta_A}{\psi_A^2} < 1 \text{)} \quad (4-45)$$

then λ_1 and λ_2 are real and positive, conditions identified as *monotonically diverging*. Their qualitative graphical representation is presented in Fig. 4.5.

$$(b) \text{ If } 0 < \Delta_A = \frac{\psi_A^2}{4} \text{ (which is equivalent to } 0 < \frac{4\Delta_A}{\psi_A^2} = 1 \text{)} \quad (4-46)$$

then the eigenvalues $\lambda_1 = \lambda_2 > 0$ are real, equal and positive, conditions identified as *monotonically diverging* as well. Their qualitative graphical representation is presented in Fig. 4.6.

$$(c) \text{ If } \Delta_A > \frac{\psi_A^2}{4} > 0 \text{ (which is equivalent to } \frac{4\Delta_A}{\psi_A^2} > 1 > 0 \text{)} \quad (4-47)$$

then λ_1 and λ_2 are a pair of complex conjugate eigenvalues in the form

$$\lambda_1 = \lambda_r + i\lambda_i, \text{ and } \lambda_2 = \lambda_r - i\lambda_i, \quad (4-48)$$

with

$$\lambda_r = \frac{\psi_A}{2} > 0 \text{ and } \lambda_i = \frac{\psi_A}{2} \sqrt{\frac{4\Delta_A}{\psi_A^2} - 1} \quad (4-49)$$

conditions identified as *oscillatory diverging*. Their qualitative graphical representation is presented in Fig. 4.7.

(vi) A degenerated case is obtained if:

$$\psi_A = 0 \quad \& \quad \Delta_A = 0 \quad (4-50)$$

(vii) $(u_{Sl,2}, v_{Sl,2})$ are *unstable* to SHoP if:

$$\psi_A > 0 \quad \& \quad \Delta_A = 0 \quad (4-51)$$

then λ_1 and λ_2 are real, and

$$\lambda_1 = \psi_A > 0 \text{ and } \lambda_2 = 0. \quad (4-52)$$

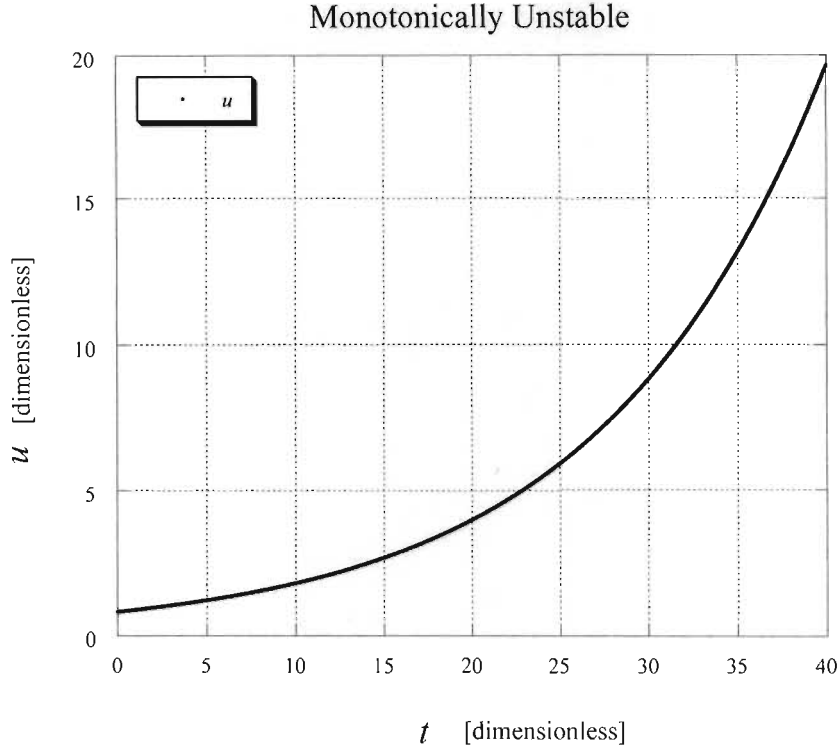


Figure 4.5: Qualitative description of monotonically unstable conditions identified to be applicable for $\psi_A > 0$ and $0 < \Delta_A < \psi_A^2/4$.

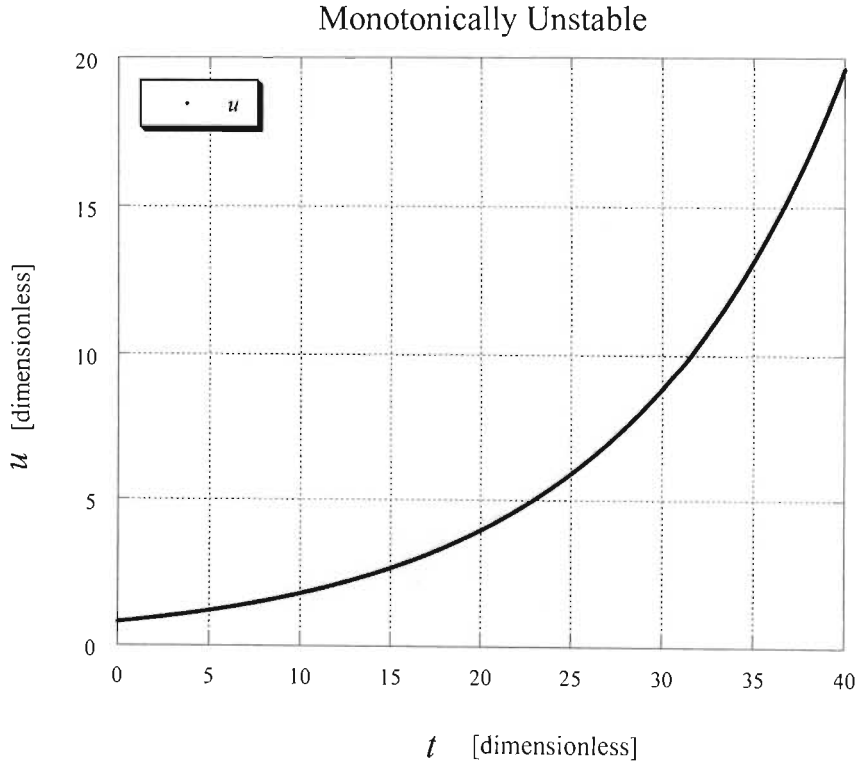


Figure 4.6: Qualitative description of monotonically unstable conditions identified to be applicable for $\psi_A > 0$ and $0 < \Delta_A = \psi_A^2/4$.

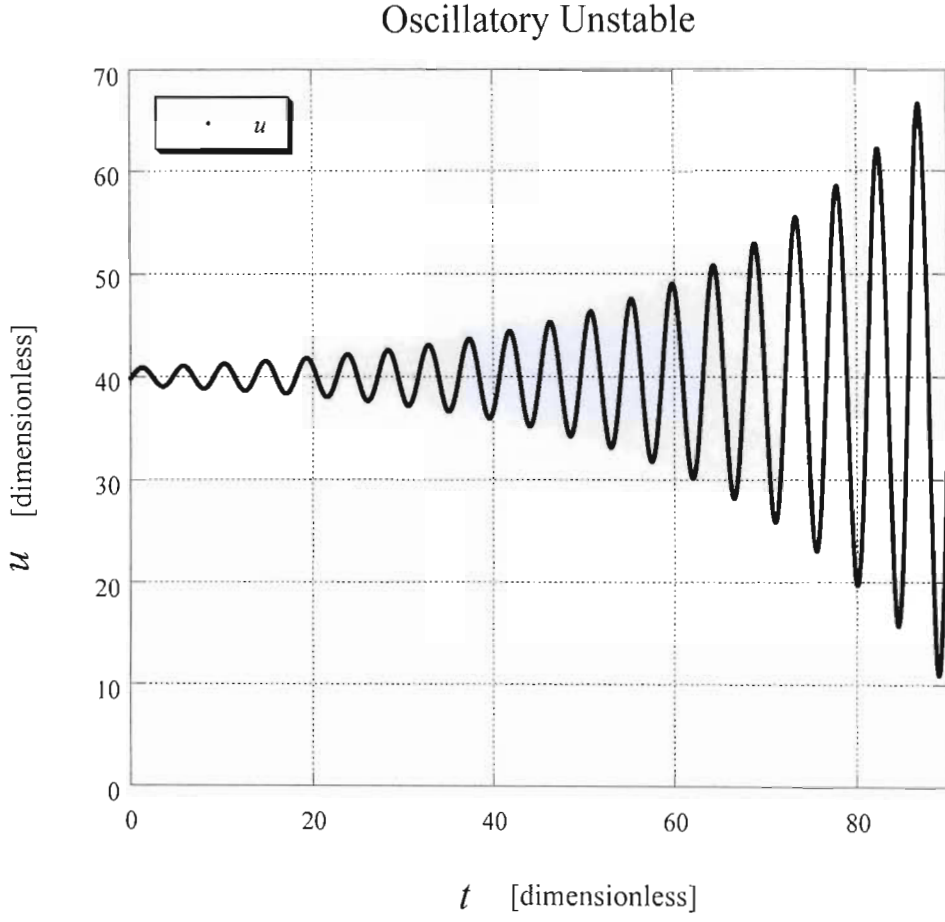


Figure 4.7: Qualitative description of monotonically unstable conditions identified to be applicable for $\psi_A > 0$ and $\Delta_A > \psi_A^2/4 > 0$.

(viii) $(u_{S1,2}, v_{S1,2})$ are *unstable* to SHoP if:

$$\psi_A = 0 \quad \& \quad \Delta_A < 0 \quad (4-53)$$

then λ_1 and λ_2 are real, and equal to

$$\lambda_{1,2} = \pm \sqrt{|\Delta_A|} \quad . \quad (4-54)$$

(ix) $(u_{S1,2}, v_{S1,2})$ are *unstable* to SHoP if:

$$\psi_A > 0 \quad \& \quad \Delta_A < 0 \quad (4-55)$$

then λ_1 and λ_2 are real, and equal to

$$\lambda_1 = \frac{\psi_A}{2} \left[1 + \sqrt{1 - \frac{4 \Delta_A}{\psi_A^2}} \right] = \frac{\psi_A}{2} \left[1 + \sqrt{1 + \frac{4 |\Delta_A|}{\psi_A^2}} \right] > 0 \quad \forall \quad \Delta_A < 0 \quad (4-56)$$

$$\lambda_2 = \frac{\psi_A}{2} \left[1 - \sqrt{1 - \frac{4 \Delta_A}{\psi_A^2}} \right] = \frac{\psi_A}{2} \left[1 - \sqrt{1 + \frac{4 |\Delta_A|}{\psi_A^2}} \right] < 0 \quad \forall \quad \Delta_A < 0 \quad (4-57)$$

The linear stability results presented in the previous 9 different combinations of positive, negative and zero values of ψ_A and Δ_A are summarized in the Stability Table 4.1

Table 4.1: Stability Table and type of qualitative regimes

	$\psi_A < 0$			$\psi_A = 0$	$\psi_A > 0$		
	<i>STABLE</i>			<i>NEUTRALLY</i>	<i>UNSTABLE</i>		
	$\Delta_A < \frac{\psi_A^2}{4}$	$\Delta_A = \frac{\psi_A^2}{4}$	$\Delta_A > \frac{\psi_A^2}{4}$	<i>STABLE</i>	$\Delta_A < \frac{\psi_A^2}{4}$	$\Delta_A = \frac{\psi_A^2}{4}$	$\Delta_A > \frac{\psi_A^2}{4}$
$\Delta_A > 0$	$\lambda_1 \text{ \& } \lambda_2$ real $\lambda_1 < 0 \text{ \& } \lambda_2 < 0$ overdamped (sink)	$\lambda_1 \text{ \& } \lambda_2$ real $\lambda_1 = \lambda_2 < 0$ critically damped (sink)	$\lambda_1 \text{ \& } \lambda_2$ pair of complex conjugates $\lambda_{1,2} = \lambda_r \pm i\lambda_i$ $\lambda_r < 0$ (converging spiral)	$\lambda_{1,2} = \pm i\sqrt{\Delta_A}$	$\lambda_1 \text{ \& } \lambda_2$ real $\lambda_1 > 0 \text{ \& } \lambda_2 > 0$ monotonically diverging (source)	$\lambda_1 \text{ \& } \lambda_2$ real $\lambda_1 = \lambda_2 > 0$ monotonically diverging (source)	$\lambda_1 \text{ \& } \lambda_2$ pair of complex conjugates $\lambda_{1,2} = \lambda_r \pm i\lambda_i$ $\lambda_r > 0$ (diverging spiral)
$\Delta_A = 0$	<i>Neutrally Stable</i> $\lambda_1 \text{ \& } \lambda_2$ real $\lambda_1 = \psi_A < 0, \lambda_2 = 0$			<i>Degenerated Case</i> $\lambda_1 = 0,$ $\lambda_2 = 0$	<i>Unstable</i> $\lambda_1 \text{ \& } \lambda_2$ real $\lambda_1 = \psi_A > 0, \lambda_2 = 0$ (Source)		
$\Delta_A < 0$	<i>Unstable Monotonically Diverging</i> $\lambda_1 \text{ \& } \lambda_2$ real $\lambda_1 < 0, \lambda_2 > 0$ (Source)			<i>Unstable Monotonically Diverging</i> $\lambda_1 \text{ \& } \lambda_2$ real $\lambda_{1,2} = \pm \sqrt{ \Delta_A }$ $\lambda_1 > 0,$ $\lambda_2 < 0$ (Source)	<i>Unstable Monotonically Diverging</i> $\lambda_1 \text{ \& } \lambda_2$ real $\lambda_1 > 0, \lambda_2 < 0$ (Source)		

4.2 Linear Stability of the Trivial Stationary Solution ($u_{so} = 0, v_{so}$)

The linear stability of the trivial stationary solution

$$u_{so} = 0 \quad \& \quad v_{so} = -\frac{\gamma_o}{\phi_o} \quad (4-58)$$

is undertaken in this section. The method is identical to the one applied for the nontrivial stationary solutions except that the values of $u_{so} = 0, v_{so} = -\gamma_o/\phi_o$ replace the ones for $(u_{s1,2}, v_{s1,2})$ in the definitions of $\beta_1, \beta_2, \beta_3, \beta_4, \beta_5$ and β_6 in eq. (3-26). Because $u_{so} = 0$ one obtains $\beta_1 = 0$ and $\beta_2 = 0$. By introducing small perturbations around the stationary solutions (u_{so}, v_{so}) in the form

$$u = u_{so} + \varepsilon u_1 \quad \text{and} \quad v = v_{so} + \varepsilon v_1 \quad (4-59)$$

where $\varepsilon \ll 1$ stands only to indicate that the perturbations are very small and substituting (4-58) and (4-59) into (4-3) yields the following linearized equations for the perturbations

$$\begin{cases} \frac{du_1}{dt} = -\frac{\gamma_o}{\phi_o} v_1 & (a) \\ \frac{dv_1}{dt} = -\beta_o u_1 + \phi_o v_1 & (b) \end{cases} \quad (4-60)$$

or in the equivalent vector/matrix form

$$\frac{d\mathbf{w}_1}{dt} = A \mathbf{w}_1 \quad (4-61)$$

where $\mathbf{w}_1 = [u_1, v_1]^T$, and the matrix A in this case stands for

$$A = \begin{bmatrix} 0 & ; & -\frac{\gamma_o}{\phi_o} \\ -\beta_o & ; & \phi_o \end{bmatrix} \quad (4-62)$$

The characteristic equation for the eigenvalues takes the form

$$\lambda^2 - \varphi_o \lambda - \frac{\beta_o \gamma_o}{\varphi_o} = 0 \quad (4-63)$$

It can be recognized that the coefficient terms appearing in eq. (4-63) represent the trace ψ_A and the determinant Δ_A of the coefficient matrix A as follows

$$\psi_A = \text{trace}(A) = \varphi_o \quad (4-64)$$

$$\Delta_A = \det(A) = -\frac{\beta_o \gamma_o}{\varphi_o} \quad (4-65)$$

The solution to eq. (4-63) for the eigenvalues is

$$\lambda_{1,2} = \frac{\psi_A}{2} \left[1 \pm \sqrt{1 - \frac{4\Delta_A}{\psi_A^2}} \right] = \frac{\varphi_o}{2} \left[1 \pm \sqrt{1 + \frac{4\beta_o \gamma_o}{\varphi_o^3}} \right] \quad (4-66)$$

For stability of u_{so}, v_{so} , the following conditions need to be enforced

$$\psi_A < 0 \quad \Rightarrow \quad \varphi_o < 0 \quad (4-67)$$

and

$$\Delta_A > 0 \quad \Rightarrow \quad -\frac{\beta_o \gamma_o}{\varphi_o} = \underbrace{\frac{\beta_o \gamma_o}{(-\varphi_o)}}_{\substack{>0 \\ \text{eq.} \\ (4-67)}} > 0 \quad \Rightarrow \quad \beta_o \gamma_o > 0 \quad (4-68)$$

One can conclude that the trivial solution u_{so}, v_{so} is stable to SHoP if

$$\varphi_o < 0 \quad \& \quad \beta_o \gamma_o > 0 \quad (4-69)$$

and u_{so}, v_{so} is unstable to SHoP if

$$\varphi_o > 0 \quad \text{or} \quad \beta_o \gamma_o < 0 \quad (4-70)$$

4.3 Explicit Stability Conditions to Spatially Homogeneous Perturbations (SHoP)

4.3.1 General Derivation

The linear stability conditions (4-69) that were obtained for the trivial solution u_{S_0}, v_{S_0} are expressed in terms of the primitive parameters of the original system, i.e. φ_o, β_o and γ_o . On the other hand the linear stability conditions (4-27) ($\psi_A < 0$ & $\Delta_A > 0$) for the nontrivial solutions $u_{S_{1,2}}, v_{S_{1,2}}$ are not expressed explicitly in terms of the primitive parameters of the original system. Even when one replaces into (4-27) the expressions for ψ_A and Δ_A it yields

$$\psi_A = \beta_1 + \varphi_o < 0 \quad \& \quad \Delta_A = \beta_1 \varphi_o + \beta_o \beta_2 > 0 \quad (4-71)$$

While these conditions depend explicitly on β_o and φ_o they also depend on these parameters and other primitive parameters of the original system (4-1) via the coefficients β_1 and β_2 . The latter are defined in eq. (3-26). The objective of this section is to derive the stability conditions for $u_{S_{1,2}}, v_{S_{1,2}}$, (4-71) explicitly in terms of the primitive parameters of the original system (4-1), or at least to find the necessary conditions for stability explicitly in terms of these primitive parameters.

One possibility that the first condition in (4-71) is fulfilled can be enforced by requiring β_1 and φ_o to have opposite signs, i.e.

$$\beta_1 \varphi_o < 0. \quad (4-72)$$

This is however a necessary condition (if the possibility of $\beta_1 < 0$ & $\varphi_o < 0$ does not apply) but certainly not a sufficient condition to guarantee that $\psi_A < 0$. It is however a very useful condition to use in deriving a procedure to identify the parameter window for linear stability of $u_{S_{1,2}}, v_{S_{1,2}}$ to SHoP. On the other hand, by using the fact that $\beta_2 > 0$, because $u_{S_{1,2}} > 0$ and by using the definition of β_2 from (3-26b), the second condition from (4-71) implies

$$\beta_o > -\frac{\beta_1 \varphi_o}{\beta_2} \quad (4-73)$$

One needs to consider first, two separate cases that are consistent with (4-72), i.e. (i) $\beta_1 > 0$ & $\varphi_o < 0$, and (ii) $\beta_1 < 0$ & $\varphi_o > 0$.

4.3.2 The case corresponding to: $\beta_1 > 0$ & $\varphi_o < 0$

Deriving the explicit condition for (4-72): Since for this case $\beta_1 > 0$ one needs to express this latter condition explicitly in terms of the system's primitive parameters and combine it with the derivation of (4-73) expressed also in terms of the system's primitive parameters. By using the definition of β_1 from eq. (3-26a) one obtains from $\beta_1 > 0$ the condition

$$R(1 - 2u_s) - 1 > 0 \quad (4-74)$$

By substituting into (4-74) the explicit expression for $u_{s1,2}$ from eqs. (3-11) and (3-13) it yields

$$(R-1) - \left(\frac{\beta_o}{\varphi_o} + R - 1 \right) (1 \pm S) > 0 \quad (4-75)$$

where $S = \sqrt{1 - 4\gamma_o\varphi_o R / [\varphi_o(1-R) - \beta_o]^2}$, from eq. (3-10), which upon further expansion leads to

$$-\left[\frac{\beta_o}{\varphi_o} \pm \left(\frac{\beta_o}{\varphi_o} + R - 1 \right) S \right] > 0 \quad (4-76)$$

or

$$\left[\frac{\beta_o}{\varphi_o} \pm \left(\frac{\beta_o}{\varphi_o} + R - 1 \right) S \right] < 0 \quad (4-77)$$

By indicating explicitly in (4-77) the fact that $\varphi_o < 0$ in the form

$$-\frac{\beta_o}{(-\varphi_o)} \pm \left(-\frac{\beta_o}{(-\varphi_o)} + R - 1 \right) S < 0 \quad (4-78)$$

or

$$-\frac{\beta_o}{(-\varphi_o)} (1 \pm S) \pm (R-1) S < 0 \quad (\text{equivalent to: } \beta_1 > 0) \quad (4-79)$$

yields a result that can be separated into a condition for u_{s1} and another one for u_{s2} , as represented by the \pm sign in (4-79). It is important to notice that S depends on γ_o in addition to φ_o, β_o and R , while γ_o does not affect the other terms. Therefore the value of S can be controlled via γ_o for any choice of φ_o, β_o and R .

Deriving the explicit condition for (4-73): The condition (4-79) that is equivalent to $\beta_1 > 0$ needs combining with $\beta_o > -\beta_1 \varphi_o / \beta_2$ (4-73). One can evaluate the ratio β_1 / β_2 by using the definitions given in eq. (3-26a,b) in the form

$$\frac{\beta_1}{\beta_2} = [R(1 - 2u_s) - 1] \quad . \quad (4-80)$$

Substituting this result (4-80) into the right hand side of (4-73) yields

$$-\frac{\beta_1 \varphi_o}{\beta_2} = (-\varphi_o)[R(1 - 2u_s) - 1] \quad (4-81)$$

leading to inequality (4-73) in the form

$$\beta_o > (-\varphi_o)[R(1 - 2u_s) - 1] \quad (4-82)$$

or alternatively for $\varphi_o < 0$

$$\frac{\beta_o}{(-\varphi_o)} > [R(1 - 2u_s) - 1] \quad . \quad (4-83)$$

$$-\frac{\beta_o}{(-\varphi_o)} + [R(1 - 2u_s) - 1] < 0 \quad . \quad (4-84)$$

By substituting into (4-83) the explicit expression for $u_{s1,2}$ from eqs. (3-11) and (3-13) and expanding it yields

$$\pm \left[\frac{\beta_o}{(-\varphi_o)} - (R - 1) \right] S < 0 \quad (\text{equivalent to: } \beta_o > -\beta_1 \varphi_o / \beta_2) \quad (4-85)$$

(i) *Stability condition for u_{s1} :*

Inequality (4-79) for u_{s1} is represented by accounting for the positive sign instead of the \pm sign in the form

$$-\frac{\beta_o}{(-\varphi_o)}(1+S) + (R-1)S < 0 \quad (4-86)$$

Since $S > 0$ by definition, this expression leads to

$$\frac{\beta_o}{(-\varphi_o)} > (R-1)\frac{S}{(1+S)} \quad (\text{equivalent to: } \beta_1 > 0) \quad (4-87)$$

representing the explicit condition for u_{s1} that is equivalent to $\beta_1 > 0$.

Inequality (4-85) for u_{s1} is represented by accounting for the positive sign instead of the \pm sign in the form

$$\left[\frac{\beta_o}{(-\varphi_o)} - (R-1) \right] S < 0 \quad (4-88)$$

Since $S > 0$ by definition, this expression leads to

$$\frac{\beta_o}{(-\varphi_o)} - (R-1) < 0 \quad (4-89)$$

or

$$\frac{\beta_o}{(-\varphi_o)} < (R-1) \quad (\text{equivalent to: } \beta_o > -\beta_1\varphi_o/\beta_2) \quad (4-90)$$

that can be expressed in the following alternative form which occasionally may turnout more convenient

$$\beta_o < (R-1)(-\varphi_o) \quad (\text{equivalent to: } \beta_o > -\beta_1\varphi_o/\beta_2) \quad (4-91)$$

representing the explicit condition for u_{s1} that is equivalent to $\beta_o > -\beta_1\varphi_o/\beta_2$. Conditions (4-87) and (4-91) are fully consistent with the requirement that u_{s1} be non-negative ($u_{s1} \geq 0$) in order to have a biologically meaningful solution, eq. (3-17).

Combining now condition (4-87) with (4-90) yields

$$\underbrace{(R-1) \frac{S}{(1+S)}}_{\beta_o > -\beta_1 \varphi_o / \beta_2} < \underbrace{\frac{\beta_o}{(-\varphi_o)}}_{\beta_1 > 0} < (R-1) \quad (4-92)$$

(ii) *Stability condition for u_{s2} :*

Inequality (4-79) for u_{s2} is represented by accounting for the negative sign instead of the \pm sign in the form

$$-\frac{\beta_o}{(-\varphi_o)}(1-S) - (R-1)S < 0 \quad (4-93)$$

leading to

$$\frac{\beta_o}{(-\varphi_o)}(S-1) < (R-1)S \quad (\text{equivalent to: } \beta_1 > 0) \quad (4-94)$$

Using $\gamma_o > 0$, which implies $S > 1$ (see definition of S in eq. (3-10) with $\gamma_o > 0$ and $\varphi_o < 0$) the latter condition can be expressed also in the form

$$\frac{\beta_o}{(-\varphi_o)} < (R-1) \frac{S}{(S-1)} \quad (\text{equivalent to: } \beta_1 > 0) \quad \forall S > 1 \text{ (or } \gamma_o > 0) \quad (4-95)$$

representing the explicit condition for u_{s2} , that is equivalent to $\beta_1 > 0$. It should be noted that for $S > 1$ the following ratio in eq. (4-95) applies

$$\frac{S}{(S-1)} > 1 \quad (4-96)$$

Inequality (4-85) for u_{s2} is represented by accounting for the negative sign instead of the \pm sign in the form

$$-\left[\frac{\beta_o}{(-\varphi_o)} - (R-1) \right] S < 0 \quad (4-97)$$

Since $S > 0$ by definition, this expression leads to

$$\frac{\beta_o}{(-\varphi_o)} - (R-1) > 0 \quad (4-98)$$

or

$$\frac{\beta_o}{(-\varphi_o)} > (R-1) \quad (\text{ equivalent to: } \beta_o > -\beta_1\varphi_o/\beta_2) \quad (4-99)$$

that can be expressed in the following alternative form which occasionally may turnout more convenient

$$\beta_o > (R-1)(-\varphi_o) \quad (\text{ equivalent to: } \beta_o > -\beta_1\varphi_o/\beta_2) \quad (4-100)$$

representing the explicit condition for u_{s2} that is equivalent to $\beta_o > -\beta_1\varphi_o/\beta_2$. From (4-99) expressed in the form $\beta_o/\varphi_o < 1-R$, combined with the condition for u_{s2} to be non-negative, i.e. $u_{s2} \geq 0$ presented in eq. (3-21), one concludes that ***the only possibility for a non-negative value of u_{s2} to be stable to SHoP is $S > 1$*** implying and supporting the assumption that $\gamma_o > 0$.

Combining now condition (4-95) with (4-99) yields

$$\underbrace{(R-1)}_{\beta_1 > 0} < \underbrace{\frac{\beta_o}{(-\varphi_o)}}_{\beta_o > -\beta_1\varphi_o/\beta_2} < \underbrace{(R-1)\frac{S}{(S-1)}}_{\beta_o > -\beta_1\varphi_o/\beta_2} \quad \forall S > 1 \text{ (i.e. } \forall \beta_o > 0) \quad (4-101)$$

4.3.3 The case corresponding to: $\beta_1 < 0$ & $\varphi_o > 0$

Deriving the explicit condition for (4-72): Since for this case $\beta_1 < 0$ one needs to express this latter condition explicitly in terms of the system's primitive parameters and combine it with the derivation of (4-73) expressed also in terms of the system's primitive parameters. By using the definition of β_1 from eq. (3-26a) one obtains from $\beta_1 < 0$ the condition

$$R(1 - 2u_s) - 1 < 0 \quad (4-102)$$

By substituting into (4-102) the explicit expression for $u_{s1,2}$ from eqs. (3-11) and (3-13) it yields

$$\frac{\beta_o}{\varphi_o} (1 \pm S) \pm (R - 1) S > 0 \quad (\text{equivalent to: } \beta_1 < 0) \quad (4-103)$$

where $S = \sqrt{1 - 4\gamma_o\varphi_o R / [\varphi_o(1 - R) - \beta_o]^2}$, from eq. (3-10). Equation (4-103) presents a result that can be separated into a condition for u_{s1} and another one for u_{s2} , as represented by the \pm sign in (4-103). Note that S depends on γ_o in addition to φ_o, β_o and R , while γ_o does not affect the other terms. Therefore the value of S can be controlled via γ_o for any choice of φ_o, β_o and R .

Deriving the explicit condition for (4-73): The condition (4-103) that is equivalent to $\beta_1 < 0$ needs combining with $\beta_o > -\beta_1 \varphi_o / \beta_2$ (4-73). Substituting (4-80) into the right hand side of (4-73) yields

$$-\frac{\beta_1 \varphi_o}{\beta_2} = \varphi_o [1 - R(1 - 2u_s)] \quad (4-104)$$

leading to inequality (4-73) in the form

$$\beta_o > \varphi_o [1 - R(1 - 2u_s)] \quad (4-105)$$

or alternatively for $\varphi_o > 0$

$$\frac{\beta_o}{\varphi_o} > [1 - R(1 - 2u_s)] \quad (4-106)$$

$$\frac{\beta_o}{\varphi_o} + R - 1 - 2Ru_s > 0 \quad . \quad (4-107)$$

By substituting into (4-107) the explicit expression for $u_{s1,2}$ from eqs. (3-11) and (3-13) and expanding it yields

$$\pm \left[\frac{\beta_o}{\varphi_o} + (R-1) \right] S < 0 \quad (\text{equivalent to: } \beta_o > -\beta_1\varphi_o/\beta_2) \quad (4-108)$$

(i) *Stability condition for u_{s1} :*

Inequality (4-103) for u_{s1} is represented by accounting for the positive sign instead of the \pm sign in the form

$$\frac{\beta_o}{\varphi_o}(1+S) + (R-1)S > 0 \quad (4-109)$$

Since $S > 0$ by definition, this expression leads to

$$\frac{\beta_o}{\varphi_o} > -(R-1)\frac{S}{(1+S)} \quad (4-110)$$

representing the explicit condition for u_{s1} that is equivalent to $\beta_1 < 0$.

Inequality (4-108) for u_{s1} is represented by accounting for the positive sign instead of the \pm sign in the form

$$\left[\frac{\beta_o}{\varphi_o} + (R-1) \right] S < 0 \quad (4-111)$$

Since $S > 0$ by definition, this expression leads to

$$\frac{\beta_o}{\varphi_o} + (R-1) < 0 \quad (4-112)$$

or

$$\frac{\beta_o}{\varphi_o} < (1-R) \quad (\text{equivalent to: } \beta_o > -\beta_1\varphi_o/\beta_2) \quad (4-113)$$

that can be expressed in the following alternative form which occasionally may turnout more convenient

$$\beta_o < (1-R) \varphi_o \quad (\text{equivalent to: } \beta_o > -\beta_1 \varphi_o / \beta_2) \quad (4-114)$$

representing the explicit condition for u_{s1} that is equivalent to $\beta_o > -\beta_1 \varphi_o / \beta_2$.

Condition (4-114) violates the requirement that u_{s1} be non-negative in order to be biologically meaningful, as expressed by eq. (3-17a) applicable to this case when $\varphi_o > 0$. Therefore, one concludes that any biologically meaningful stationary solution u_{s1} is unstable to SHoP if $\varphi_o > 0$.

(ii) *Stability condition for u_{s2} :*

Inequality (4-103) for u_{s2} is represented by accounting for the negative sign instead of the \pm sign in the form

$$\frac{\beta_o}{\varphi_o} (1-S) - (R-1) S > 0 \quad (4-115)$$

leading to

$$\frac{\beta_o}{\varphi_o} (1-S) > (R-1) S \quad (\text{equivalent to: } \beta_1 < 0) \quad (4-116)$$

Using $\gamma_o > 0$, which implies $S < 1$ (see definition of S in eq. (3-10) with $\gamma_o > 0$ and $\varphi_o > 0$) the latter condition can be expressed also in the form

$$\frac{\beta_o}{\varphi_o} > (R-1) \frac{S}{(1-S)} \quad (\text{equivalent to: } \beta_1 < 0) \quad \forall S < 1 \text{ (or } \gamma_o > 0 \text{)} \quad (4-117)$$

or

$$\beta_o > (R-1) \varphi_o \frac{S}{(1-S)} \quad (\text{equivalent to: } \beta_1 < 0) \quad \forall S < 1 \text{ (or } \gamma_o > 0 \text{)} \quad (4-118)$$

representing the explicit condition for u_{s2} , that is equivalent to $\beta_1 < 0$.

Inequality (4-108) for u_{s2} is represented by accounting for the negative sign instead of the \pm sign in the form

$$-\left[\frac{\beta_o}{\varphi_o} + (R-1) \right] S < 0 \quad (\text{equivalent to: } \beta_o > -\beta_1 \varphi_o / \beta_2) \quad (4-119)$$

Since $S > 0$ by definition, this expression leads to

$$\frac{\beta_o}{\varphi_o} + (R-1) > 0 \quad (4-120)$$

or

$$\frac{\beta_o}{\varphi_o} > (1-R) \quad (\text{equivalent to: } \beta_o > -\beta_1 \varphi_o / \beta_2) \quad (4-121)$$

that can be expressed in the following alternative form which occasionally may turnout more convenient

$$\beta_o > (1-R) \varphi_o \quad (\text{equivalent to: } \beta_o > -\beta_1 \varphi_o / \beta_2) \quad (4-122)$$

representing the explicit condition for u_{s2} that is equivalent to $\beta_o > -\beta_1 \varphi_o / \beta_2$. From (4-121) combined with the condition for u_{s2} to be non-negative, i.e. $u_{s2} \geq 0$ presented in eq. (3-21), one concludes that ***the only possibility for a non-negative value of u_{s2} to be stable to SHoP is $S < 1$*** implying and supporting the assumption that $\gamma_o > 0$.

Combining now condition (4-121) with (4-117) in the form

$$\frac{\beta_o}{\varphi_o} > -(R-1) \quad \& \quad \frac{\beta_o}{\varphi_o} > (R-1) \frac{S}{(1-S)} \quad \forall \quad S < 1 \quad (4-123)$$

needs the evaluation of the right hand sides of both conditions which produce the following inequalities

$$(R-1) \frac{S}{(1-S)} > -(R-1) \quad \forall \quad R > 1 \quad \& \quad 0 < S < 1, \quad (a) \quad (4-124)$$

$$(R-1) \frac{S}{(1-S)} < -(R-1) \quad \forall \quad R < 1 \quad \& \quad 0 < S < 1. \quad (b)$$

The latter inequalities (4-124) applied to (4-123) yield

$$\left\{ \begin{array}{ll} \underbrace{\frac{\beta_o}{\varphi_o} < (R-1) \frac{S}{(1-S)}}_{\beta_1 < 0} & \forall \quad R > 1 \quad (a) \\ \underbrace{\frac{\beta_o}{\varphi_o} > (1-R)}_{\beta_o > -\beta_1 \varphi_o / \beta_2} & \forall \quad R < 1 \quad (b) \end{array} \right. \quad \forall \quad S < 1 \quad (\text{i.e. } \forall \quad \beta_o > 0) \quad (4-125)$$

4.3.4 The case corresponding to: $\beta_1 > 0$ & $\varphi_o > 0$

For this parameter regime it is obvious that the stability condition (4-71) $\psi_A = \beta_1 + \varphi_o < 0$ is violated and therefore **for these parameters, $\beta_1 > 0$ & $\varphi_o > 0$, the stationary solutions $u_{s1,2}, v_{s1,2}$ are unstable to SHoP**. One is still interested to identify explicitly these conditions in terms of the primitive system parameters in order to identify explicitly the instability regime.

Deriving the explicit condition for $\beta_1 > 0$ & $\varphi_o > 0$: Since for this case $\beta_1 > 0$ & $\varphi_o > 0$ one needs to express this latter condition explicitly in terms of the system's primitive parameters. By using the definition of β_1 from eq. (3-26a) one obtains for $\beta_1 > 0$ the condition

$$\frac{\beta_o}{\varphi_o}(1 \pm S) \pm (R-1)S < 0 \quad (\text{equivalent to: } \beta_1 > 0) \quad (4-126)$$

where $S = \sqrt{1 - 4\gamma_o\varphi_o R / [\varphi_o(1-R) - \beta_o]^2}$, from eq. (3-10). Equation (4-126) presents a result that can be separated into a condition for u_{s1} and another one for u_{s2} , as represented by the \pm sign in (4-126). Note that S depends on γ_o in addition to φ_o, β_o and R , while γ_o does not affect the other terms. Therefore the value of S can be controlled via γ_o for any choice of φ_o, β_o and R .

(i) Condition for u_{s1} :

Inequality (4-126) for u_{s1} is represented by accounting for the positive sign instead of the \pm sign in the form

$$\frac{\beta_o}{\varphi_o}(1 + S) + (R-1)S < 0 \quad (4-127)$$

Since $S > 0$ by definition, this expression leads to

$$\frac{\beta_o}{\varphi_o} < -(R-1)\frac{S}{(1+S)} \quad \forall \beta_1 > 0 \quad (4-128)$$

representing the explicit condition for u_{s1} that is equivalent to $\beta_1 > 0$. Combining this condition with the requirement for a biological meaningful solution, $u_{s1} \geq 0$, from eq. (3-17a) corresponding to $\varphi_o > 0$, expressed in the form $\beta_o/\varphi_o \geq (1-R)$, $\forall \varphi_o > 0$ yields

$$-(R-1) \leq \frac{\beta_o}{\varphi_o} < -(R-1) \frac{S}{(1+S)} \quad (4-129)$$

or

$$-(R-1) \varphi_o \leq \beta_o < -(R-1) \varphi_o \frac{S}{(1+S)} \quad (4-130)$$

(ii) *Condition for u_{s2} :*

Inequality (4-126) for u_{s2} is represented by accounting for the negative sign instead of the \pm sign in the form

$$\frac{\beta_o}{\varphi_o} (1-S) - (R-1) S < 0 \quad (4-131)$$

Since $S > 0$ by definition, this expression leads to

$$\frac{\beta_o}{\varphi_o} (1-S) < (R-1) S \quad (4-132)$$

or

$$\begin{cases} \frac{\beta_o}{\varphi_o} < (R-1) \frac{S}{(1-S)} & \forall S < 1 \\ \frac{\beta_o}{\varphi_o} > (R-1) \frac{S}{(1-S)} & \forall S > 1 \end{cases} \quad (4-133)$$

representing the explicit condition for u_{s2} that is equivalent to $\beta_1 > 0$. Combining this condition with the requirement for a biological meaningful solution, $u_{s2} \geq 0$, from eq. (3-21) yields

$$\left\{ \begin{array}{ll} - (R-1) < \frac{\beta_o}{\varphi_o} < (R-1) \frac{S}{(1-S)} & \forall S < 1 \quad (a) \\ - (R-1) \underbrace{\frac{S}{(S-1)}}_{>1} < \frac{\beta_o}{\varphi_o} < - (R-1) & \forall S > 1 \quad (b) \end{array} \right. \quad (4-134)$$

or

$$\left\{ \begin{array}{ll} - (R-1) \varphi_o < \beta_o < (R-1) \varphi_o \frac{S}{(1-S)} & \forall S < 1 \quad (a) \\ - (R-1) \underbrace{\frac{S}{(S-1)}}_{>1} \varphi_o < \beta_o < - (R-1) \varphi_o & \forall S > 1 \quad (b) \end{array} \right. \quad (4-135)$$

4.3.5 The case corresponding to: $\beta_1 < 0$ & $\varphi_o < 0$

For this parameter regime it is obvious that the stability condition (4-71) $\psi_A = \beta_1 + \varphi_o < 0$ is fulfilled unconditionally and therefore for these parameters, $\beta_1 < 0$ & $\varphi_o < 0$, the conditions that need to be imposed are the stability condition (4-71): $\beta_o > -\beta_1 \varphi_o / \beta_2$, combined with $\beta_1 < 0$, which can be presented in the form

$$\pm \left[\frac{\beta_o}{(-\varphi_o)} - (R-1) \right] S < 0 \quad \text{for} \quad \beta_1 < 0 \quad (4-136)$$

and

$$\frac{\beta_o}{\varphi_o} (1 \pm S) \pm (R-1) S < 0 \quad \text{for} \quad \beta_o > -\beta_1 \varphi_o / \beta_2 \quad (4-137)$$

Equations (4-136) and (4-137) present results that can be separated into a condition for u_{S1} and another one for u_{S2} , as represented by the \pm sign in (4-136) and (4-137).

(i) Condition for u_{s1} :

Inequalities (4-136) and (4-137) for u_{s1} are represented by accounting for the positive sign instead of the \pm sign in the form

$$\left[\frac{\beta_o}{(-\varphi_o)} - (R-1) \right] S < 0 \quad \text{for} \quad \beta_1 < 0 \quad (4-138)$$

and

$$-\frac{\beta_o}{(-\varphi_o)}(1+S) + (R-1)S < 0 \quad \text{for} \quad \beta_o > -\beta_1\varphi_o/\beta_2 \quad (4-139)$$

Since $S > 0$ by definition, these expressions lead to

$$\frac{\beta_o}{(-\varphi_o)} < (R-1) \quad \text{for} \quad \beta_1 < 0 \quad (4-140)$$

and

$$\frac{\beta_o}{(-\varphi_o)} > (R-1)\frac{S}{(S+1)} \quad \text{for} \quad \beta_o > -\beta_1\varphi_o/\beta_2 \quad (4-141)$$

representing the explicit conditions for u_{s1} that are equivalent to $\beta_1 < 0$ and $\beta_o > -\beta_1\varphi_o/\beta_2$, in the form

$$-(R-1)\frac{S}{(S+1)} < \frac{\beta_o}{(-\varphi_o)} < (R-1) \quad (4-142)$$

This condition violates the requirement for a biological meaningful solution, $u_{s1} \geq 0$, from eq. (3-17b) corresponding to $\varphi_o < 0$, expressed in the form $\beta_o/(-\varphi_o) \geq (R-1)$, $\forall \varphi_o < 0$. The explicit parameter domain corresponding to $\varphi_o < 0$, $\beta_1 < 0$ and $u_{s1} \geq 0$ is an empty space. Therefore, **any biologically meaningful stationary solution u_{s1} does not exist if $\varphi_o < 0$ and $\beta_1 < 0$.**

(ii) Condition for u_{s2} :

Inequalities (4-136) and (4-137) for u_{s2} are represented by accounting for the negative sign instead of the \pm sign in the form

$$-\left[\frac{\beta_o}{(-\varphi_o)} - (R-1) \right] S < 0 \quad \text{for} \quad \beta_1 < 0 \quad (4-143)$$

and

$$\frac{\beta_o}{\varphi_o}(1-S) - (R-1)S < 0 \quad \text{for} \quad \beta_o > -\beta_1\varphi_o/\beta_2 \quad (4-144)$$

Since $S > 0$ by definition, these expressions lead to

$$\frac{\beta_o}{(-\varphi_o)} > (R-1) \quad \text{for} \quad \beta_1 < 0 \quad (4-145)$$

$$\left\{ \begin{array}{ll} \frac{\beta_o}{(-\varphi_o)} < (R-1) \underbrace{\frac{S}{(S-1)}}_{>1} & \forall S > 1 \\ \frac{\beta_o}{(-\varphi_o)} > (R-1) \underbrace{\frac{S}{(S-1)}}_{<0} & \forall S < 1 \end{array} \right. \quad \text{for} \quad \beta_o > -\beta_1\varphi_o/\beta_2 \quad (4-146)$$

representing the explicit conditions for u_{s2} that are equivalent to $\beta_1 < 0$ and $\beta_o > -\beta_1\varphi_o/\beta_2$, in the form

$$\left\{ \begin{array}{ll} (R-1) < \frac{\beta_o}{(-\varphi_o)} < (R-1) \underbrace{\frac{S}{(S-1)}}_{>1} & \forall S > 1 \quad \& \quad R > 1 \quad (a) \\ (R-1) \underbrace{\frac{S}{(S-1)}}_{>1} < \frac{\beta_o}{(-\varphi_o)} < (R-1) & \forall S > 1 \quad \& \quad R < 1 \quad (b) \\ \frac{\beta_o}{(-\varphi_o)} > (R-1) & \forall S < 1 \quad \& \quad R > 1 \quad (c) \\ \frac{\beta_o}{(-\varphi_o)} > (R-1) \underbrace{\frac{S}{(S-1)}}_{<0} & \forall S < 1 \quad \& \quad R < 1 \quad (d) \end{array} \right. \quad (4-147)$$

These conditions combined with the requirement for a biologically meaningful solution, $u_{s2} \geq 0$, from eq. (3-17b) corresponding to $\varphi_o < 0$, expressed in the form $\beta_o/(-\varphi_o) \leq (R-1)$, $\forall S < 1$ and $\beta_o/(-\varphi_o) \geq (R-1)$, $\forall S > 1$ yield the stability condition

$$(R-1) < \frac{\beta_o}{(-\varphi_o)} < (R-1) \underbrace{\frac{S}{(S-1)}}_{>1} \quad \forall S > 1 \quad \& \quad R > 1 \quad (4-148)$$

eliminating the possibilities of $S < 1$ and $R < 1$ as being inconsistent with a biologically meaningful solution, $u_{S2} \geq 0$. One may conclude that for $\beta_1 < 0$ and $\varphi_o < 0$ **a biologically meaningful solution $u_{S2} \geq 0$ exists only if $S > 1$ and it is stable to SHoP only if $R > 1$ and condition (4-148) is fulfilled.**

4.3.6 Summary of Stability Conditions to SHoP

The Linear Stability Conditions of (u_{So}, v_{So}) and $(u_{S1,2}, v_{S1,2})$ to SHoP derived in this chapter and expressed explicitly in terms of the primitive system's parameters are being summarized in Table 4.2 for u_{So}, v_{So} , in Table 4.3 for u_{S1}, v_{S1} , and in Table 4.4 for u_{S2}, v_{S2} .

Table 4.2: Explicit Stability Table for u_{So}, v_{So}

	$\varphi_o < 0$	$\varphi_o > 0$
$\beta_o \gamma_o > 0$	(u_{So}, v_{So}) stable to SHoP	(u_{So}, v_{So}) unstable to SHoP
$\beta_o \gamma_o < 0$	(u_{So}, v_{So}) unstable to SHoP	(u_{So}, v_{So}) unstable to SHoP

Table 4.3: Explicit Stability Table for u_{S1}, v_{S1}

	Explicitly Equivalent to:	$\varphi_o > 0$	$\varphi_o < 0$
$\beta_1 > 0$	$\frac{\beta_o}{\varphi_o} < -(R-1)\frac{S}{(1+S)}$	u_{S1} is unstable to SHoP	$u_{S1,2}$ is stable to SHoP if: $\underbrace{(R-1)\frac{S}{(1+S)}}_{\beta_o > -\beta_1\varphi_o/\beta_2} < \underbrace{\frac{\beta_o}{(-\varphi_o)}}_{\beta_1 > 0} < \underbrace{(R-1)}_{\beta_1 > 0}$
$\beta_1 < 0$	$\frac{\beta_o}{\varphi_o} > -(R-1)\frac{S}{(1+S)}$	Any biologically meaningful stationary solution u_{S1} is unstable to SHoP	Any biologically meaningful stationary solution u_{S1} does not exist if $\varphi_o < 0$ and $\beta_1 < 0$

 Table 4.4: Explicit Stability Table for u_{S2}, v_{S2}

	Explicitly Equivalent to:	$\varphi_o > 0$	$\varphi_o < 0$
$\beta_1 > 0$	$\frac{\beta_o}{\varphi_o} < (R-1)\frac{S}{(1-S)}, \forall S < 1$ $\frac{\beta_o}{\varphi_o} > (R-1)\frac{S}{(1-S)}, \forall S > 1$	u_{S2} is unstable to SHoP	$u_{S1,2}$ is stable to SHoP if: $\underbrace{(R-1)}_{\beta_1 > 0} < \underbrace{\frac{\beta_o}{(-\varphi_o)}}_{\beta_o > -\beta_1\varphi_o/\beta_2} < \underbrace{(R-1)\frac{S}{(S-1)}}_{\beta_1 > 0}, \forall S > 1$ Any biologically meaningful stationary solution u_{S2} is unstable to SHoP if: $S > 1$
$\beta_1 < 0$	$\frac{\beta_o}{\varphi_o} > (R-1)\frac{S}{(1-S)}, \forall S < 1$	Any biologically meaningful stationary solution u_{S1} is unstable to SHoP	A biologically meaningful solution $u_{S2} \geq 0$ exists only if $S > 1$ and it is stable to SHoP only if $R > 1$ and if: $(R-1) < \underbrace{\frac{\beta_o}{(-\varphi_o)}}_{>1} < \underbrace{(R-1)\frac{S}{(S-1)}}_{>1}, \forall S > 1, \forall R > 1$

4.3.7 Procedure to Identify Windows of Parameter Values that Provide Necessary Conditions for Linear Stability to SHoP

The following Procedure Sequence is useful in identifying windows of parameter values which provide necessary conditions for linear stability to SHoP. This Procedure Sequence applies to the parameter regime $\varphi_o < 0$ and $\beta_1 > 0$.

Procedure Sequence

- (1). Choose values of $R > 0$ and $\varphi_o < 0$.
- (2). Choose a value of S .
- (3). Choose $\beta_{o,b} < \beta_o < \beta_{o,t}$, where

$$\beta_{o,b} = \frac{(R-1)S}{(S+1)}(-\varphi_o) \text{ and } \beta_{o,t} = (R-1)(-\varphi_o).$$

- (4). Check the value of $\psi_A = \beta_1 + \varphi_o$ to establish if the stability condition $\psi_A = \beta_1 + \varphi_o < 0$ is satisfied. If it is satisfied go to next step. If it is not satisfied go back to (3) to choose a different value of β_o . The closer the value of β_o is to $\beta_{o,b}$ the closer β_1 is to 0.
- (5). Evaluate γ_o consistent with the value of S selected in step (2) by using the following relationship derived from the definition of S , eq. (3-10),

$$\gamma_o = \frac{(S^2 - 1)[\varphi_o(1 - R) - \beta_o]^2}{4R(-\varphi_o)}$$

Example:

(1). Choose values of $R > 0$ and $\varphi_o < 0$: $R = 10$, $\varphi_o = -0.4$

(2). Choose a value of S : $S = 2$

(3).
$$\beta_{o,b} = \frac{(R-1)S}{(S+1)}(-\varphi_o) = 2.4,$$

$$\beta_{o,t} = (R-1)(-\varphi_o) = 3.6$$

Choose: $2.4 < \beta_o < 3.6 \rightarrow \beta_o = 3$

(4).
$$u_{s1} = \frac{[\beta_o + \varphi_o(R-1)](1+S)}{2\varphi_o R} = 0.225 \rightarrow \beta_1 = \left[\frac{R(1-u_s)}{(1+Ru_s)} - 1 \right] u_s = 0.31154$$

The stability condition $\psi_A = \beta_1 + \varphi_o = 0.31154 - 0.4 = -0.08846 < 0$ is satisfied.

(5). Evaluate γ_o consistent with the value of S selected in step (2)

$$\gamma_o = \frac{(S^2 - 1)[\varphi_o(1-R) - \beta_o]^2}{4R(-\varphi_o)} = 0.0675$$

This set of primitive parameter values: $R = 10$, $\varphi_o = -0.4$, $S = 2$, $\beta_o = 3$, $\gamma_o = 0.0675$ is an example of a choice that guarantees stability of (u_{s1}, v_{s1}) to SHoP. Different other choices can be obtained by applying the Procedure Sequence listed above.

CHAPTER 5

WEAK NONLINEAR SOLUTION FOR THE SPATIALLY HOMOGENEOUS PROBLEM

5.1 Governing Equations for the Spatially Homogeneous Problem

As in the case of the linear stability analysis, here one needs to impose the condition that the stationary solution in the absence of diffusion is stable, for the heterogeneous solution to be at all possible. Since the interest in this study is to obtain a complete analytical solution to the non-linear problem and not only the linear stability, imposing the latter condition implies solving the following homogeneous problem, eq. (4-3), prior to attempting the solution to the heterogeneous case

$$\left\{ \begin{array}{l} (1 + R u) \frac{du}{dt} = [(R - 1) u - R u^2 + v] u \quad (a) \\ \frac{dv}{dt} = \gamma_o - \beta_o u + \varphi_o v \quad (b) \end{array} \right. \quad (5-1)$$

The objective of the present chapter is to analyze the solution as the values of the parameters vary in such a way that for $\Delta_A > 0$, ψ_A changes from negative when the stationary solution is stable via $\psi_A = 0$ to $\psi_A > 0$, when the stationary solution loses stability and another solution takes over. The analytical solution to eq. (5-1) is obtained by applying the weak nonlinear method of solution. It consists of expanding the dependent variables u and v in terms of a small parameter representing its distance from a critical value that is established by the linear stability analysis as shown in what follows. The special case when $\varphi_o = 0$ is particularly interesting and therefore is considered as a demonstration of the validity of the weak nonlinear method of solution. For this particular case when $\varphi_o = 0$ eq. (5-1) takes the form

$$\left\{ \begin{array}{l} (1 + R u) \frac{du}{dt} = [(R - 1)u - R u^2 + v] u \quad (a) \\ \frac{dv}{dt} = \gamma_o - \beta_o u \quad (b) \end{array} \right. \quad (5-2)$$

It produces one non-trivial stationary solution ($(du/dt) = 0$, $(dv/dt) = 0$) in the form

$$u_s = \frac{\gamma_o}{\beta_o} = \frac{1}{\xi} > 0, \quad v_s = [R u_s - R + 1] u_s = \left[\frac{R \gamma_o}{\beta_o} - R + 1 \right] \frac{\gamma_o}{\beta_o} \quad (5-3)$$

where $\xi = \beta_o / \gamma_o$. The particular conditions $\gamma_o > 0$ and consequently $\beta_o > 0$, the latter being necessary for dealing with a biologically meaningful stationary solution $u_s > 0$, are being considered.

5.2 Asymptotic Expansion, Scales and Parameters

Using β_o as the control parameter for the asymptotic expansion and its critical value $\beta_{o,cr}$, that is obtained from the linear stability solution corresponding to neutral stability, i.e. eq. (4-35) applied to the conditions when $\varphi_o = 0$ in the form

$$\psi_A = \beta_1 = 0 \quad \& \quad \Delta_A > 0 \quad (5-4)$$

yields explicitly upon substituting the expression for β_1 from (3-26a)

$$u_s = \frac{(R-1)}{2R} \quad \text{for neutrally stable conditions} \quad (5-5)$$

which combined with eq. (5-3) leads to the critical value of β_o in the form

$$\beta_{o,cr} = \frac{2R\gamma_o}{(R-1)} \quad \text{or} \quad \xi_{cr} = \frac{2R}{(R-1)} = \frac{\beta_{o,cr}}{\gamma_o} \quad (5-6)$$

One can now define the small expansion parameter $\varepsilon \ll 1$ in terms of the relative distance of β_o from its critical value $\beta_{o,cr}$ as follows

$$\varepsilon^2 = \frac{\beta_o - \beta_{o,cr}}{\beta_{o,cr}} \quad (5-7)$$

The expansion of the dependent variables u and v has therefore the form

$$u = u_s + \varepsilon u_1 + \varepsilon^2 u_2 + \varepsilon^3 u_3 + \dots \quad (5-8)$$

$$v = v_s + \varepsilon v_1 + \varepsilon^2 v_2 + \varepsilon^3 v_3 + \dots \quad (5-9)$$

Also the parameter β_o can be expanded by using the finite series obtained from eq. (5-7) in the form

$$\beta_o = \beta_{o,cr} + \varepsilon^2 \beta_{o,cr} \quad (5-10)$$

Introducing a slow time scale and hence replacing t with $t \rightarrow t + \tau$, where $\tau = \varepsilon^2 t$ represents the slow time scale, and substituting the expansions (5-8) and (5-9) into the equations (5-2) yields a hierarchy of differential equations at the different orders. The latter is obtained by grouping terms of like powers of ε . At the leading order one obtains the equations for the stationary solution, at order ε the equations are very

similar to the linear stability analysis equations and its solutions can be obtained up to the value of an unknown amplitude which is time dependent. At order ε^2 the solutions produce a homogeneous and a particular solution. Finally, at order ε^3 a solvability condition obtained by imposing the requirement for a finite amplitude solution provides an equation for the time evolution of the $O(\varepsilon)$ amplitude as well as for the frequency correction. The latter amplitude equation has a closed form solution that yields a complete analytical result to the problem, however its accuracy is very high only in the neighborhood of the critical value of β_o , i.e. around $\beta_o \approx \beta_{o,cr}$, such that $\varepsilon \ll 1$ (see eq. (5-7)) and not too far away from the stationary solution. As one moves away from $\beta_o \approx \beta_{o,cr}$, or when the amplitude becomes large so the solution moves quite far from the stationary point, the accuracy of the analytical solution obtained via the weak nonlinear method is gradually compromised. Nevertheless, the advantage of having a completely analytical solution to the nonlinear problem, even when it is limited in terms of accuracy around $\beta_o \approx \beta_{o,cr}$ and small amplitudes, is of great value. It allows to identify what solutions may occur under different conditions and not only to identify the linear stability conditions.

The following example shows the major difference between the linear stability results and the weak nonlinear solution, as well as a comparison of the weak nonlinear results with a direct numerical solution of equations (5-2). The latter was obtained by using a standard Runge-Kutta solver to double precision from the IMSL Library (1991) (DIVPRK) up to a desired tolerance for error control specified by the parameter *tol*. This comparison demonstrates the very high accuracy of the weak nonlinear method in the neighborhood of $\beta_o \approx \beta_{o,cr}$ and small amplitudes, and the loss of accuracy as the parameter value departs from $\beta_o \approx \beta_{o,cr}$ or when high amplitude oscillations occur.

Substituting expansions (5-8) and (5-9) as well as (5-10) and replacing t with $t \rightarrow t + \tau$, where $\tau = \varepsilon^2 t$, into the equations (5-2) yields

T040097



$$\begin{aligned}
& \varepsilon(1 + R u_s) \frac{d u_1}{d t} + \varepsilon^2 \left[(1 + R u_s) \frac{d u_2}{d t} + R u_1 \frac{d u_1}{d t} \right] + \\
& \varepsilon^3 \left[(1 + R u_s) \frac{d u_3}{d t} + R u_1 \frac{d u_2}{d t} + R u_2 \frac{d u_1}{d t} + (1 + R u_s) \frac{d u_1}{d \tau} \right] = \\
& \left[(R-1) u_s - R u_s^2 + v_s \right] u_s + \varepsilon \left[\beta_3 u_s u_1 + u_s v_1 \right] + \\
& \varepsilon^2 \left[\beta_3 u_s u_2 + u_s v_2 + \beta_5 u_1^2 + u_1 v_1 \right] + \\
& \varepsilon^3 \left[\beta_3 u_s u_3 + u_s v_3 + 2 \beta_5 u_1 u_2 - R u_1^3 + u_1 v_2 + u_2 v_1 \right]
\end{aligned} \tag{5-11}$$

$$\begin{aligned}
& \varepsilon \frac{d v_1}{d t} + \varepsilon^2 \frac{d v_2}{d t} + \varepsilon^3 \left[\frac{d v_3}{d t} + \frac{d v_1}{d \tau} \right] = (\gamma_o - \beta_{o,cr} u_s) - \\
& \varepsilon \beta_{o,cr} u_1 - \varepsilon^2 \beta_{o,cr} (u_s + u_2) - \varepsilon^3 \beta_{o,cr} (u_3 + u_1)
\end{aligned} \tag{5-12}$$

where β_3 and β_5 are defined in eq. (3-26).

By grouping now the terms containing like powers of ε and requiring that they balance each other in each of the equations (5-11) and (5-12) yields separate equations at the different orders.

5.3 Leading Order Solution at $O(1)$

By using the leading order, $O(1)$, terms in eqs (5-11) and (5-12) respectively, leads to

$$\left[(R-1)u_s - R u_s^2 + v_s \right] u_s = 0 \quad (5-13)$$

$$\gamma_o - \beta_{o,cr} u_s = 0 \quad (5-14)$$

producing the stationary solutions at the leading order in the form

$$v_s = (R u_s - R + 1) u_s \quad (5-15)$$

$$u_s = \frac{\gamma_o}{\beta_{o,cr}} \quad (5-16)$$

By substituting (5-6) into (5-16) yields the stationary solution in the following form

$$u_s = \frac{(R-1)}{2R} \quad (5-17)$$

$$v_s = -\frac{(R-1)^2}{4R} \quad (5-18)$$

5.4 Solution at Order $O(\varepsilon)$

At order $O(\varepsilon)$ one collects the terms in eqs (5-11) and (5-12) that correspond to the power of ε^1 leading to

$$\begin{cases} (1 + R u_s) \frac{d u_1}{dt} = \beta_3 u_s u_1 + u_s v_1 & (a) \\ \frac{d v_1}{dt} = -\beta_{o,cr} u_1 & (b) \end{cases} \quad (5-19)$$

Dividing eq. (5-19a) by $(1 + R u_s)$ and using the definition of β_1 and β_2 from eq. (3-26a,b) produces the linear set of equations

$$\begin{cases} \frac{d u_1}{dt} = \beta_1 u_1 + \beta_2 v_1 & (a) \\ \frac{d v_1}{dt} = -\beta_{o,cr} u_1 & (b) \end{cases} \quad (5-20)$$

Since at neutral stability conditions applicable to these equations $\beta_1 = 0$ according to eq. (5-4) and therefore by using eq. (3-26a) it implies also $\beta_3 = 0$, eq. (5-20) can be presented in the equivalent form

$$\begin{cases} \frac{d u_1}{dt} - \beta_2 v_1 = 0 & (a) \\ \frac{d v_1}{dt} + \beta_{o,cr} u_1 = 0 & (b) \end{cases} \quad (5-21)$$

The $O(\varepsilon)$ solutions to equations (5-21) have to account for the fact that they are evaluated at neutral stability and hence the real part of the eigenvalues vanishes, i.e. for $\lambda_{1,2} = \lambda_r \pm i\lambda_i$: $\lambda_r = 0$ and $\lambda_i = \sqrt{\Delta_A}$, where $\Delta_A = \beta_o \beta_2$. Otherwise at slightly supercritical values of β_o the solution will grow indefinitely, a result that one would like to avoid. It is for this reason that the amplitudes of the solutions at this order are allowed to vary over the slow time scale τ , while the value of $\lambda_r = 0$ is used at this order. With this latter argument applied, the solution to eq. (5-21) has the form

$$u_1 = B_1 e^{i\sigma_o t} + B_1^* e^{-i\sigma_o t} = b_{11} \sin(\sigma_o t) + b_{12} \cos(\sigma_o t) \quad (a) \quad (5-22)$$

$$v_1 = C_1 e^{i\sigma_o t} + C_1^* e^{-i\sigma_o t} = c_{11} \sin(\sigma_o t) + c_{12} \cos(\sigma_o t) \quad (b)$$

where the following notation replaces λ_i

$$\sigma_o = \lambda_i = \sqrt{\Delta_A} = \sqrt{\beta_{o,cr} \beta_2} \quad (5-23)$$

being the basic frequency of the oscillations, and where $B_1(\tau)$ and $B_1^*(\tau)$, $C_1(\tau)$ and $C_1^*(\tau)$ are complex conjugate amplitudes of u_1 and v_1 respectively. They depend on the slow time scale τ and their values are to be established from this weak nonlinear solution. To establish the value of the basic frequency σ_o explicitly one may use the definition of β_2 from eq. (3-26b) in connection with the stationary solution of $u_s = \gamma_o / \beta_{o,cr} = (R-1)/2R$ from eqs. (5-16) and (5-18) in the form

$$\beta_2 = \frac{u_s}{(1 + R u_s)} = \frac{\gamma_o}{(\beta_{o,cr} + R \gamma_o)} = \frac{(R-1)}{R(R+1)} \quad (5-24)$$

into the definition of σ_o to yield

$$\sigma_o = \sqrt{\frac{\gamma_o \beta_{o,cr}}{(\beta_{o,cr} + R \gamma_o)}} = \sqrt{\frac{2\gamma_o}{(R+1)}} \quad (5-25)$$

Substituting the solution (5-22) into the equations at this order (5-21) reconfirms the result for $\beta_{o,cr}$ from (5-6), which was obtained from the linear stability analysis.

The expression for the basic frequency is occasionally presented in terms of σ_o^2 , i.e.

$$\sigma_o^2 = \frac{2\gamma_o}{(R+1)} \quad (5-26)$$

In addition, substituting the solution (5-22) into the equations (5-21) produces relationships between the $O(\varepsilon)$ coefficients in the form

$$C_1 = i \frac{\sigma_o}{\beta_2} B_1; \quad C_1^* = -i \frac{\sigma_o}{\beta_2} B_1^* \quad (5-27)$$

$$B_1 C_1 = i \frac{\sigma_o}{\beta_2} B_1^2; \quad B_1^* C_1^* = -i \frac{\sigma_o}{\beta_2} B_1^{*2} \quad (5-28)$$

$$B_1 C_1^* = -i \frac{\sigma_o}{\beta_2} B_1 B_1^*; \quad B_1^* C_1 = i \frac{\sigma_o}{\beta_2} B_1 B_1^* \quad (5-29)$$

The ratio σ_o/β_2 , which appears in eqs. (5-27), (5-28) and (5-29) is evaluated to be

$$\frac{\sigma_o}{\beta_2} = \sqrt{\frac{2\gamma_o R^2 (R+1)}{(R-1)^2}} = \frac{R}{(R-1)} \sqrt{2\gamma_o (R+1)} \quad (5-30)$$

5.5 Solution at Order $O(\varepsilon^2)$

At order $O(\varepsilon^2)$ one collects the terms in eqs (5-11) and (5-12) that correspond to the power of ε^2 leading to

$$\begin{cases} (1 + R u_s) \frac{d u_2}{dt} = \beta_3 u_s u_2 + u_s v_2 + \beta_5 u_1^2 + u_1 v_1 - R u_1 \frac{d u_1}{dt} & (a) \\ \frac{d v_2}{dt} = -\beta_{o,cr} u_s - \beta_{o,cr} u_2 & (b) \end{cases} \quad (5-31)$$

Dividing eq. (5-31a) by $(1 + R u_s)$ and using the definitions of $\beta_1 = \beta_2 \beta_3$, $\beta_2 = u_s / \beta_4$ and $\beta_4 = (1 + R u_s)$ from eqs. (3-26 a,b,d), and the relationship $\beta_{o,cr} u_s = \gamma_o$ from eq. (5-16) transforms equation (5-31) into the form

$$\begin{cases} \frac{d u_2}{dt} = \beta_1 u_2 + \beta_2 v_2 + \frac{\beta_5}{\beta_4} u_1^2 + \frac{1}{\beta_4} u_1 v_1 - \frac{R}{\beta_4} u_1 \frac{d u_1}{dt} & (a) \\ \frac{d v_2}{dt} = -\beta_{o,cr} u_2 - \gamma_o & (b) \end{cases} \quad (5-32)$$

Equation (5-32) can then be presented in the form

$$\begin{cases} \left[\frac{d}{dt} - \beta_1 \right] u_2 - \beta_2 v_2 = \frac{\beta_5}{\beta_4} u_1^2 + \frac{1}{\beta_4} u_1 v_1 - \frac{R}{\beta_4} u_1 \frac{d u_1}{dt} & (a) \\ \frac{d v_2}{dt} + \beta_{o,cr} u_2 = -\gamma_o & (b) \end{cases} \quad (5-33)$$

By using now the fact that at neutral stability conditions applicable to these equations $\beta_1 = 0$ (eq. (5-4)) and $\beta_3 = 0$ (eq.(3-26a)) transforms eqs. (5-33) into the following reduced form

$$\begin{cases} \frac{d u_2}{dt} - \beta_2 v_2 = -R \beta_2 u_1^2 + \frac{1}{\beta_4} u_1 v_1 - \frac{R}{\beta_4} u_1 \frac{d u_1}{dt} & (a) \\ \frac{d v_2}{dt} + \beta_{o,cr} u_2 = -\gamma_o & (b) \end{cases} \quad (5-34)$$

where use was made of the fact that according to eqs. (3-26) with $\beta_3 = 0$ one obtains the relationship $\beta_5/\beta_4 = -R\beta_2$.

Equations (5-34) form a coupled linear system. From eq. (5-34) it is easy to observe that the left-hand-side operator of the equations is identical to the one that appears in eq. (5-21) at order $O(\varepsilon)$ and operates on u_1 and v_1 . The major difference is in the form of the right-hand-side terms. While at order $O(\varepsilon)$ the right-hand-side terms are zero and the equations are homogeneous, the $O(\varepsilon^2)$ equations (5-34) contain terms on their right-hand-side, which depend on the solution at $O(\varepsilon)$. Since the solution at order $O(\varepsilon)$ is known and given by eq. (5-22) it becomes possible to derive the analytical solution to eq. (5-34) at order $O(\varepsilon^2)$. It consists of the superposition between a homogeneous and a particular solution in the form

$$\begin{aligned} u_2 &= u_{2H} + u_{2P} & (a) \\ v_2 &= v_{2H} + v_{2P} & (b) \end{aligned} \tag{5-35}$$

where (u_{2H}, v_{2H}) is the homogeneous part of the solution and (u_{2P}, v_{2P}) represents the particular solution. The homogeneous part of the solution satisfies the system of equations

$$\begin{cases} \frac{du_{2H}}{dt} - \beta_2 v_{2H} = 0 \\ \frac{dv_{2H}}{dt} + \beta_{o,cr} u_{2H} = 0 \end{cases} \tag{5-36}$$

(a) (b)

while the particular solution satisfies the equations

$$\begin{cases} \frac{du_{2P}}{dt} - \beta_2 v_{2P} = -R\beta_2 u_1^2 + \frac{1}{\beta_4} u_1 v_1 - \frac{R}{\beta_4} u_1 \frac{du_1}{dt} \\ \frac{dv_{2P}}{dt} + \beta_{o,cr} u_{2P} = -\gamma_o \end{cases} \tag{5-37}$$

(a) (b)

Since the homogeneous part of the system (5-34) is identical to the equations solved at order $O(\varepsilon)$, the homogenous solution should also have an identical form as eq. (5-22), i.e.

$$u_{2H} = B_2 e^{i\sigma_o t} + B_2^* e^{-i\sigma_o t} = b_{21} \sin(\sigma_o t) + b_{22} \cos(\sigma_o t) \quad (a) \quad (5-38)$$

$$v_{2H} = C_2 e^{i\sigma_o t} + C_2^* e^{-i\sigma_o t} = c_{21} \sin(\sigma_o t) + c_{22} \cos(\sigma_o t) \quad (b)$$

where the relationship between the coefficients is similar to eq. (5-27) at order $O(\varepsilon)$ in the form

$$C_2 = i \frac{\sigma_o}{\beta_2} B_2; \quad C_2^* = -i \frac{\sigma_o}{\beta_2} B_2^* \quad (5-39)$$

To derive the particular solution one needs to decouple the equations (5-37a) and (5-37b) in order to obtain one equation for u_{2P} only, and another equation for v_{2P} only. Decoupling the equations is accomplished by using (5-37a) to express v_{2P} in terms of the other variables in the form

$$v_{2P} = \frac{\left[\frac{d u_{2P}}{dt} - \left(-R \beta_2 u_1^2 + \frac{1}{\beta_4} u_1 v_1 - \frac{R}{\beta_4} u_1 \frac{d u_1}{dt} \right) \right]}{\beta_2}, \quad (5-40)$$

and substitute it into eq. (5-37b) to yield

$$\frac{d^2 u_{2P}}{dt^2} + \sigma_o^2 u_{2P} = -R \beta_2 \left(\frac{d u_1^2}{dt} \right) + \frac{1}{\beta_4} \frac{d(u_1 v_1)}{dt} - \frac{R}{\beta_4} \frac{d}{dt} \left(u_1 \frac{d u_1}{dt} \right) - \beta_2 \gamma_o \quad (5-41)$$

where the relationship $\sigma_o^2 = \beta_2 \beta_{o,cr}$ from eq. (5-23) was substituted in (5-41).

Applying the same process on eq. (5-37b) to isolate u_{2P} yields

$$u_{2P} = - \frac{\left(\frac{d v_{2P}}{dt} - \gamma_o \right)}{\beta_{o,cr}} \quad (5-42)$$

which upon substitution into (5-37a) produces

$$\frac{d^2 v_{2P}}{dt^2} + \sigma_o^2 v_{2P} = R \sigma_o^2 u_1^2 - \frac{\beta_{o,cr}}{\beta_4} u_1 v_1 + \frac{R \beta_{o,cr}}{\beta_4} u_1 \frac{d u_1}{dt} \quad (5-43)$$

Equations (5-41) and (5-43) represent the decoupled form corresponding to the system (5-37). The explicit and tedious evaluation of the terms on the right-hand-side of eq. (5-41) is presented in Appendix 1, and the right-hand-side of eq. (5-43) is presented in Appendix 2. These terms act as forcing functions and they impact

directly on the form of the solutions u_{2P} and v_{2P} . The results from Appendices 1 and 2 are

$$RHS(5-41) = \left[\frac{2\sigma_o^2(\beta_2 R - 1)}{\beta_2 \beta_4} - i2\sigma_o R \beta_2 \right] B_1^2 e^{i2\sigma_o t} + \left[\frac{2\sigma_o^2(\beta_2 R - 1)}{\beta_2 \beta_4} + i2\sigma_o R \beta_2 \right] B_1^{*2} e^{-i2\sigma_o t} - \beta_2 \gamma_o \quad (5-44)$$

$$RHS(5-43) = \left[R\sigma_o^2 + \frac{i\sigma_o \beta_{o,cr}(R\beta_2 - 1)}{\beta_2 \beta_4} \right] B_1^2 e^{i2\sigma_o t} + \left[R\sigma_o^2 - \frac{i\sigma_o \beta_{o,cr}(R\beta_2 - 1)}{\beta_2 \beta_4} \right] B_1^{*2} e^{-i2\sigma_o t} + 2R\sigma_o^2 B_1 B_1^* \quad (5-45)$$

These forcing functions suggest particular solutions of the form

$$u_{2P} = B_{21} e^{i2\sigma_o t} + B_{22} e^{-i2\sigma_o t} + B_{20} \quad (a) \quad (5-46)$$

$$v_{2P} = C_{21} e^{i2\sigma_o t} + C_{22} e^{-i2\sigma_o t} + C_{20} \quad (b)$$

Substituting the particular solution (5-46a) and the RHS expressions (5-44) into (5-41) yields

$$\begin{aligned} -3\sigma_o^2 B_{21} e^{i2\sigma_o t} - 3\sigma_o^2 B_{22} e^{-i2\sigma_o t} + \sigma_o^2 B_{20} = \\ \left[\frac{2\sigma_o^2(\beta_2 R - 1)}{\beta_2 \beta_4} - i2\sigma_o R \beta_2 \right] B_1^2 e^{i2\sigma_o t} + \left[\frac{2\sigma_o^2(\beta_2 R - 1)}{\beta_2 \beta_4} + i2\sigma_o R \beta_2 \right] B_1^{*2} e^{-i2\sigma_o t} - \beta_2 \gamma_o \end{aligned} \quad (5-47)$$

Equating the terms on the left-hand-side with these on the right-hand-side of (5-47) yields the values of the coefficients of the particular solution in the form

$$B_{21} = \left[\frac{2(1 - \beta_2 R)}{3u_s} + i \frac{2\beta_2 R}{3\sigma_o} \right] B_1^2 \quad (5-48)$$

$$B_{22} = \left[\frac{2(1-\beta_2 R)}{3u_s} - i \frac{2\beta_2 R}{3\sigma_o} \right] B_1^{*2} \quad (5-49)$$

$$B_{20} = - \frac{\beta_2 \gamma_o}{\sigma_o^2} = - \frac{(R-1)}{2R} = -u_s \quad (5-50)$$

where use was made of eq. (3-26h), i.e. $\beta_2 \beta_4 = u_s$.

Substituting the particular solutions (5-46b) and the RHS expressions (5-45) into (5-43) yields

$$\begin{aligned} -3\sigma_o^2 C_{21} e^{i2\sigma_o t} - 3\sigma_o^2 C_{22} e^{-i2\sigma_o t} + \sigma_o^2 C_{20} = \\ \left[R\sigma_o^2 + \frac{i\sigma_o \beta_{o,cr} (R\beta_2 - 1)}{\beta_2 \beta_4} \right] B_1^2 e^{i2\sigma_o t} + \\ \left[R\sigma_o^2 - \frac{i\sigma_o \beta_{o,cr} (R\beta_2 - 1)}{\beta_2 \beta_4} \right] B_1^{*2} e^{-i2\sigma_o t} + 2R\sigma_o^2 B_1 B_1^* \end{aligned} \quad (5-51)$$

Equating the terms on the left-hand-side with these on the right-hand-side of (5-51) yields the values of the coefficients of the particular solution in the form

$$C_{21} = \left[-\frac{R}{3} + i \frac{\beta_{o,cr} (1 - R\beta_2)}{3\sigma_o u_s} \right] B_1^2 \quad (5-52)$$

$$C_{22} = \left[-\frac{R}{3} - i \frac{\beta_{o,cr} (1 - R\beta_2)}{3\sigma_o u_s} \right] B_1^{*2} \quad (5-53)$$

$$C_{20} = 2R B_1 B_1^* \quad (5-54)$$

The complete solution at this order becomes

$$u_2 = B_2 e^{i\sigma_o t} + B_2^* e^{-i\sigma_o t} + B_{21} e^{i2\sigma_o t} + B_{22} e^{-i2\sigma_o t} + B_{20} \quad (a) \quad (5-55)$$

$$v_2 = C_2 e^{i\sigma_o t} + C_2^* e^{-i\sigma_o t} + C_{21} e^{i2\sigma_o t} + C_{22} e^{-i2\sigma_o t} + C_{20} \quad (b)$$

where the values of the coefficients are defined in eqs.(5-48), (5-49), (5-50), (5-52), (5-53) and (5-54), and the relationship between the $O(\varepsilon^2)$ coefficients of the homogeneous solution is given by eq. (5-39).

5.6 Solvability Condition at Order $O(\varepsilon^3)$

At order $O(\varepsilon^3)$ one collects the terms in eqs (5-11) and (5-12) that correspond to the power of ε^3 leading to

$$\left[(1 + R u_s) \frac{d}{dt} - \beta_3 u_s \right] u_3 - u_s v_3 = 2\beta_5 u_1 u_2 - R u_1^3 + u_1 v_2 + u_2 v_1 - \quad (5-56)$$

$$R u_1 \frac{d u_2}{dt} - R u_2 \frac{d u_1}{dt} - (1 + R u_s) \frac{d u_1}{d\tau}$$

$$\frac{d v_3}{dt} + \beta_{o,cr} u_3 = -\beta_{o,cr} u_1 - \frac{d v_1}{d\tau} \quad (5-57)$$

By using now the fact that at neutral stability conditions applicable to these equations $\beta_1 = 0$ (eq. (5-4)) and $\beta_3 = 0$ (eq. (3-26a)), and dividing eq. (5-58) by $(1 + R u_s)$ and using the definitions of $\beta_1 = \beta_2 \beta_3$, $\beta_2 = u_s / \beta_4$ and $\beta_4 = (1 + R u_s)$, $\beta_5 = -R u_s$ from eqs. (3-26), and the relationship $\beta_{o,cr} u_s = \gamma_o$ from eq. (5-16), transforms eq. (5-56) into the following reduced form

$$\frac{d u_3}{dt} - \beta_2 v_3 = -2R\beta_2 u_1 u_2 - \frac{R}{\beta_4} u_1^3 + \frac{1}{\beta_4} u_1 v_2 + \frac{1}{\beta_4} u_2 v_1 - \quad (5-58)$$

$$\frac{R}{\beta_4} u_1 \frac{d u_2}{dt} - \frac{R}{\beta_4} u_2 \frac{d u_1}{dt} - \frac{d u_1}{d\tau}$$

Equations (5-58) and (5-57) can then be presented in the following form

$$\begin{cases} \frac{d u_3}{dt} - \beta_2 v_3 = RHS1 & (a) \\ \frac{d v_3}{dt} + \beta_{o,cr} u_3 = RHS2 & (b) \end{cases} \quad (5-59)$$

where $RHS1$ and $RHS2$ are terms on the right-hand-side of eqs.(5-59a,b), which depend on known solution from previous orders $O(\varepsilon)$ and $O(\varepsilon^2)$, and are defined from eqs. (5-58) and (5-57) in the form

$$RHS1 = -2R\beta_2 u_1 u_2 - \frac{R}{\beta_4} u_1^3 + \frac{1}{\beta_4} u_1 v_2 + \frac{1}{\beta_4} u_2 v_1 - \frac{R}{\beta_4} u_1 \frac{du_2}{dt} - \frac{R}{\beta_4} u_2 \frac{du_1}{dt} - \frac{du_1}{d\tau} \quad (5-60)$$

$$RHS2 = -\beta_{o,cr} u_1 - \frac{dv_1}{d\tau} \quad (5-61)$$

Equations (5-59) form a coupled linear system. From eq. (5-59) it is easy to observe that the left-hand-side operator of the equations is identical to the one that appears in eq. (5-21) at order $O(\varepsilon)$ and operates on (u_1, v_1) , and in eq.(5-34) at order $O(\varepsilon^2)$. The major difference is in the form of the right-hand-side terms. Since the solutions at orders $O(\varepsilon)$ and $O(\varepsilon^2)$ are known and given by eq. (5-22) and (5-55) it becomes possible to derive the analytical solution to eq. (5-59) at order $O(\varepsilon^3)$, provided the forcing terms on the right-hand-side do not have a functional form identical to the homogeneous solution. When some of the forcing terms on the right hand sides of eqs. (5-59) have functional forms identical to the homogeneous solution, i.e. $e^{i\sigma_o t}$ or $e^{-i\sigma_o t}$ they force particular solutions of the form $te^{i\sigma_o t}$ or $te^{-i\sigma_o t}$ (or equivalently $t \sin(\sigma_o t)$, $t \cos(\sigma_o t)$) that are not bounded and grow indefinitely. These are conditions recognized as resonance. In order for the solution to be finite one needs to impose the condition that the coefficients of these resonant terms vanish. As a first step the decoupling of equations (5-59a) and (5-59b) is required.

Decoupling equations (5-59a) and (5-59b) is accomplished by expressing v_3 from (5-59a) in the form

$$v_3 = \frac{1}{\beta_2} \frac{du_3}{dt} - \frac{1}{\beta_2} RHS1 \quad (5-62)$$

and substituting it into (5-59b) to yield

$$\frac{d^2 u_3}{dt^2} + \beta_{o,cr} \beta_2 u_3 = \frac{d(RHS1)}{dt} + \beta_2 (RHS2) \quad (5-63)$$

Substituting into eq. (5-63) the relationship $\sigma_o^2 = \beta_2 \beta_{o,cr}$ from eq. (5-23) yields

$$\frac{d^2 u_3}{dt^2} + \sigma_o^2 u_3 = \frac{d(RHS1)}{dt} + \beta_2 (RHS2) \quad (5-64)$$

Alternatively, expressing u_3 from (5-59b) in the form

$$u_3 = -\frac{1}{\beta_{o,cr}} \frac{dv_3}{dt} + \frac{1}{\beta_{o,cr}} RHS2 \quad (5-65)$$

and substituting it into (5-59a) yields

$$\frac{d^2 v_3}{dt^2} + \sigma_o^2 v_3 = -\frac{d(RHS2)}{dt} - \beta_{o,cr}(RHS1) \quad (5-66)$$

The interest in these derivations is to obtain the condition that guarantees a finite solution at this order, and not necessarily to derive this solution. Therefore the aim is to evaluate only the resonant terms in the right-hand-side of eq. (5-64) or (5-66). The explicit and tedious evaluation of the terms on the right-hand-side of eq. (5-64) is presented in Appendix 3. The results are

$$RHS(5-64) = \left\{ i\sigma_o \left[-\left(2R\beta_2 + i\frac{R\sigma_o}{\beta_4} \right) (B_1 B_{20} + B_1^* B_{21}) - \frac{dB_1}{d\tau} - \frac{3R}{\beta_4} B_1^2 B_1^* + \right. \right. \\ \left. \left. \frac{1}{\beta_4} (B_1 C_{20} + B_1^* C_{21} + B_{20} C_1 + B_{21} C_1^*) \right] + \beta_2 \left(-\frac{dC_1}{d\tau} - \beta_{o,cr} B_1 \right) \right\} e^{i\sigma_o t} + \quad (5-67)$$

c.c. + n.r.t.

where *c.c.* stands for “complex conjugate” terms, and *n.r.t.* stands for “non-resonant terms”. Substituting the relationships for the coefficients defined in eqs. (5-27), (5-39), (5-48), (5-50), (5-52) and (5-54) into (5-67) and equating these resonant terms to zero produces the following equation

$$\frac{dB_1}{d\tau} - \frac{\beta_2}{2} (2Ru_s + iR\sigma_o) B_1 + \frac{1}{2\beta_4} \left\{ \left[\frac{R}{3} - \frac{2R^2\beta_2}{3} + \frac{4R(1-R\beta_2)}{3} + \frac{2R^2u_s}{3(R-1)} \right] + \right. \\ \left. i \left[\frac{2R\sigma_o(1-R\beta_2)}{3u_s} + \frac{\sigma_o(1-R\beta_2)}{3\beta_2 u_s} + \frac{4R^2\beta_2 u_s}{3\sigma_o} \right] \right\} B_1^2 B_1^* = 0 \quad (5-68)$$

Equation (5-68), obtained as a solvability condition of the equations at order $O(\varepsilon^3)$, represents an equation for the time evolution of the amplitude of the solution at order $O(\varepsilon)$.

5.7 Amplitude Equation, Bifurcation Structure and Solution

The amplitude equation (5-68) can be presented in the simplified form

$$\frac{dB_1}{d\tau} = H_1 B_1 - H_2 B_1^2 B_1^* \quad (5-69)$$

by introducing the notation

$$H_1 = \frac{\beta_2}{2} (2R u_s + iR \sigma_o) B_1 \quad (5-70)$$

$$H_2 = \frac{1}{2\beta_4} \left\{ \left[\frac{R}{3} - \frac{2R^2\beta_2}{3} + \frac{4R(1-R\beta_2)}{3} + \frac{2R^2 u_s}{3(R-1)} \right] + \right. \\ \left. i \left[\frac{2R\sigma_o(1-R\beta_2)}{3u_s} + \frac{\sigma_o(1-R\beta_2)}{3\beta_2 u_s} + \frac{4R^2\beta_2 u_s}{3\sigma_o} \right] \right\} \quad (5-71)$$

A further simplification is accomplished by multiplying eq. (5-69) by ε^3 and reintroducing the original time scale by back-substitution of $\tau = \varepsilon^2 t$, to obtain

$$\frac{\varepsilon^2}{\varepsilon^2} \frac{d(\varepsilon B_1)}{dt} = \varepsilon^2 H_1 (\varepsilon B_1) - H_2 (\varepsilon^2 B_1^2) (\varepsilon B_1^*) \quad (5-72)$$

By introducing the notation

$$B = \varepsilon B_1 \quad \text{and} \quad B^* = \varepsilon B_1^* \quad (5-73)$$

into eq. (5-72) yields

$$\frac{dB}{dt} = \varepsilon^2 H_1 B - H_2 B^2 B^* \quad (5-74)$$

or the alternative form

$$\frac{dB}{dt} = (\varepsilon^2 H_1 - H_2 B B^*) B \quad (5-75)$$

To analyze and solve the amplitude equation (5-75) it is more convenient to introduce the polar representation of complex variables in the form

$$B = r e^{i\theta}, \quad B^* = r e^{-i\theta}, \quad B B^* = r^2, \quad r = |B| \quad (5-76)$$

Correspondingly, the values of the complex constants H_1 and H_2 are also separated into real and imaginary parts by using the following notation

$$H_1 = \chi\eta + ip, \quad H_2 = \chi + is \quad (5-77)$$

where χ , η , p and s are real constants defined from explicit simplifications of (5-70) and (5-71) in the form

$$\eta = \frac{(R+1)(R-1)^2}{8R^2}, \quad (5-78)$$

$$\chi = \frac{4R}{(R+1)^2} \quad (5-79)$$

$$p = \frac{(R-1)}{(R+1)} \sqrt{\frac{\gamma_o}{2(R+1)}}, \quad (5-80)$$

$$s = \sqrt{\frac{2}{\gamma_o(R+1)}} \left[\frac{4\gamma_o R^2(3R-1) + (R+1)(R-1)^4}{3(R+1)^2(R-1)^2} \right] \quad (5-81)$$

By substituting (5-76), (5-77), (5-78), (5-79), (5-80) and (5-81) into (5-75) yields two equations, one for the absolute value of the amplitude, r , and the second for the phase angle θ , in the form

$$\frac{dr}{dt} = \chi(\eta\epsilon^2 - r^2)r \quad (5-82)$$

$$\frac{d\theta}{dt} = p\epsilon^2 - sr^2 \quad (5-83)$$

Equation (5-83) represents also an expression for the frequency correction to the basic frequency σ_o , i.e. $\dot{\theta} = p\epsilon^2 - sr^2$.

The steady state solution to the amplitude equation (5-82) corresponding to the post-transient solution to u_1 and v_1 is obtained by setting the time derivative term in (5-82) equal to zero, in the form

$$(\eta\epsilon^2 - r^2)r = 0 \quad (5-84)$$

The solutions to (5-84) are

$$r_{(0)} = 0 \quad \forall \quad \beta_o \leq \beta_{o,cr} \quad (5-85)$$

corresponding to the case when the stationary solutions are stable, and

$$r^2 = \varepsilon^2 \eta \quad (5-86)$$

or

$$r_{1,2} = \pm \varepsilon \sqrt{\eta} \quad \forall \quad \beta_o \geq \beta_{o,cr} \quad (5-87)$$

corresponding to the case when the stationary solutions loose stability in the linear sense. Replacing the definition of ε in eq. (5-87) transforms the steady state solution to the form that is explicitly expressed in terms of β_o

$$r_{1,2} = \pm \sqrt{\frac{\eta (\beta_o - \beta_{o,cr})}{\beta_{o,cr}}} \quad (5-88)$$

The graphical description of the amplitude r following (5-88) is presented in Figure 5.1 representing a bifurcation diagram. Clearly, for $\beta_o \geq \beta_{o,cr}$ the expression under the square root is non-negative as long as $\eta > 0$. From equation (5-78) it is obvious that $\eta > 0$ and therefore the bifurcation is forward. The fact that the amplitude r represents the coefficients of a solution that oscillates in time identifies this type of bifurcation as a Hopf bifurcation. The frequency correction at steady state is obtained by substituting (5-86) into (5-83)

$$\dot{\theta} = (p - s \eta) \varepsilon^2 \quad (5-89)$$

The transient solution to eq. (5-82) is obtained by direct integration starting in representing the equation as

$$\int \frac{dr}{(\eta \varepsilon^2 - r^2) r} = \int \chi dt \quad (5-90)$$

producing after integration of both sides

$$\frac{1}{2\eta \varepsilon^2} \ln \left(\frac{r^2}{\eta \varepsilon^2 - r^2} \right) = \chi t + c_o \quad (5-91)$$

where c_o is the integration constant. Eq. (5-91) is further presented in the form

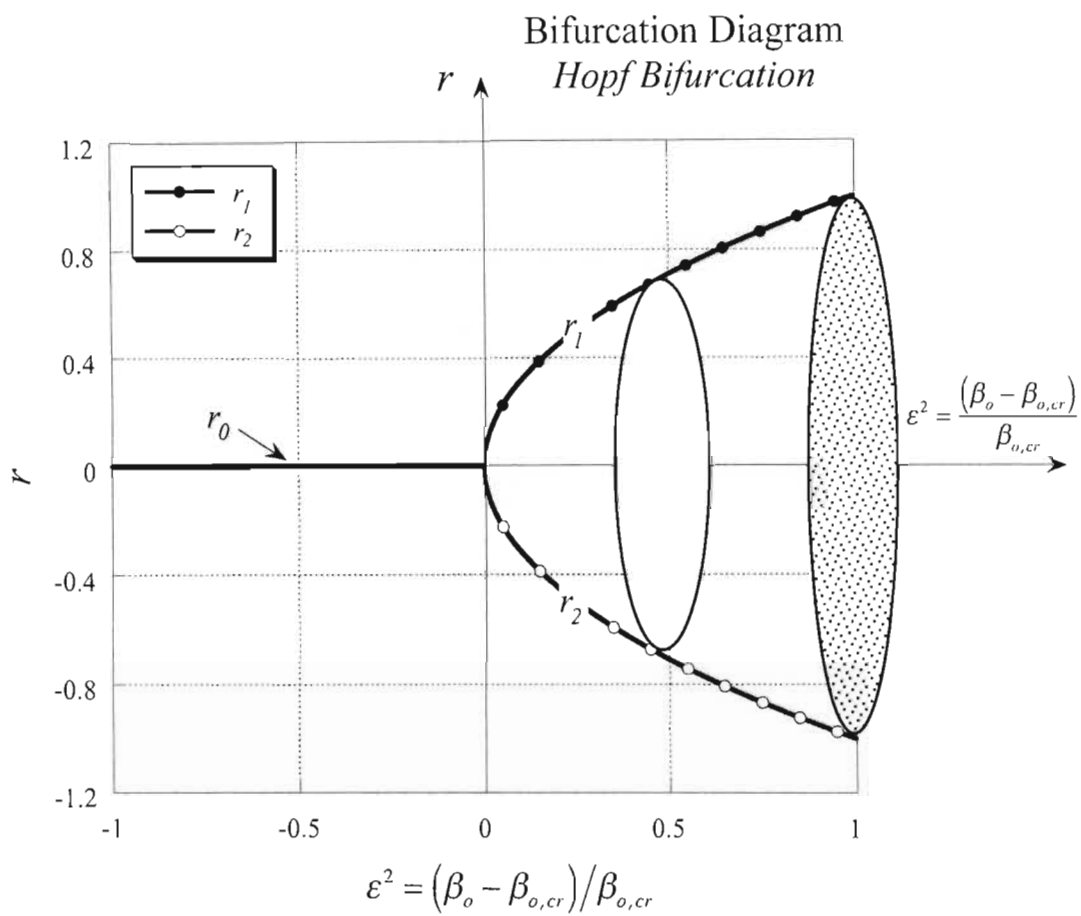


Figure 5.1: Bifurcation diagram identifying a forward Hopf bifurcation.

$$\ln\left(\frac{r^2}{\eta\epsilon^2 - r^2}\right) = 2\eta\epsilon^2\chi t + b_o \quad (5-92)$$

where b_o is the amended integration constant. From eq. (5-92) the transient solution of r can be derived algebraically in the form

$$r^2 = \frac{\eta\epsilon^2}{\left[1 + \left(\frac{\eta\epsilon^2}{r_o^2} - 1\right)\exp(-2\chi\eta\epsilon^2 t)\right]} \quad (5-93)$$

where r_o represents the initial conditions of r . The corresponding transient solution to the frequency correction $\dot{\theta}$, is obtained by substituting (5-93) into (5-83)

$$\dot{\theta} = p\epsilon^2 - \frac{\eta\epsilon^2}{\left[1 + \left(\frac{\eta\epsilon^2}{r_o^2} - 1\right)\exp(-2\chi\eta\epsilon^2 t)\right]} \quad (5-94)$$

and the phase angle θ , by integrating (5-94)

$$\theta = \int \left(p\epsilon^2 - \frac{\eta\epsilon^2}{\left[1 + \left(\frac{\eta\epsilon^2}{r_o^2} - 1\right)\exp(-2\chi\eta\epsilon^2 t)\right]} \right) dt \quad (5-95)$$

leading to the solution

$$\begin{aligned} \theta &= (p - s\eta)\epsilon^2 t - \frac{s}{2\chi} \ln\left[1 + \left(\frac{\eta\epsilon^2}{r_o^2} - 1\right)\exp(-2\chi\eta\epsilon^2 t)\right] + \theta_o + \frac{s}{2\chi} \ln\left(\frac{\eta\epsilon^2}{r_o^2}\right) = \\ &\theta_o + (p - s\eta)\epsilon^2 t + \frac{s}{2\chi} \ln\left[\frac{r^2}{r_o^2}\right] \end{aligned} \quad (5-96)$$

where θ_o represents the initial conditions for the phase angle.

5.8 Complete Weak Nonlinear Solution and Numerical Method of Solution

The complete weak nonlinear solution is obtained by replacing eqs. (5-76) and (5-27) into the $O(\varepsilon)$ solutions, eq. (5-22), in the form

$$\varepsilon u_1 = B_1 e^{i\sigma_o t} + B_1^* e^{-i\sigma_o t} = 2r \left[e^{i(\sigma_o t + \theta)} - e^{-i(\sigma_o t + \theta)} \right] = 2r \cos(\sigma_o t + \theta) \quad (5-97)$$

$$\varepsilon v_1 = C_1 e^{i\sigma_o t} + C_1^* e^{-i\sigma_o t} =$$

$$i \frac{\sigma_o}{\beta_2} (B_1 e^{i\sigma_o t} - B_1^* e^{-i\sigma_o t}) = \frac{\sigma_o}{\beta_2} r i \left[e^{i(\sigma_o t + \theta)} - e^{-i(\sigma_o t + \theta)} \right] = \quad (5-98)$$

$$= - \frac{2R\sigma_o(R+1)}{(R-1)} r \sin(\sigma_o t + \theta)$$

and using the amplitude solution for r and θ , from (5-93) and (5-96). Then, substituting these solutions into the expansions of u and v , (5-8) and (5-9), up to order $O(\varepsilon)$ yields

$$u = u_s + \varepsilon u_1 = \frac{(R-1)}{2R(1+\varepsilon^2)} + 2r \cos(\sigma_o t + \theta) \quad (5-99)$$

$$v = v_s + \varepsilon v_1 = - \frac{(R-1)^2(1+2\varepsilon^2)}{4R(1+\varepsilon^2)^2} - \frac{2R\sigma_o(R+1)}{(R-1)} r \sin(\sigma_o t + \theta) \quad (5-100)$$

where $\sigma_o = \sqrt{2\gamma_o/(R+1)}$ and $\beta_{o,cr} = 2R\gamma_o/(R-1)$.

Since the initial conditions are given in terms of u_o, v_o and in eqs. (5-99) and (5-100) the initial conditions are required in terms of r_o and θ_o , a conversion is necessary. The objective of this conversion is formulated in the following form: “given $u_o, v_o \rightarrow$ find r_o, θ_o ”. The equivalent initial conditions are being derived by using (5-99) and (5-100) at $t = 0$ in the form

$$u_o = \frac{(R-1)}{2R(1+\varepsilon^2)} + 2r_o \cos(\theta_o) \quad (5-101)$$

$$v_o = - \frac{(R-1)^2(1+2\varepsilon^2)}{4R(1+\varepsilon^2)^2} - \frac{2R\sigma_o(R+1)}{(R-1)} r_o \sin(\theta_o) \quad (5-102)$$

Then the solution to the algebraic system yields the expressions of r_o and θ_o in the form

$$r_o^2 = \frac{1}{4} \left\{ \left[u_o - \frac{(R-1)}{2R(1+\varepsilon^2)} \right]^2 + \frac{(R-1)^2}{2\gamma_o R^2 (R+1+2\varepsilon^2)} \left[v_o - \frac{(R-1)^2(1+2\varepsilon^2)}{4R(1+\varepsilon^2)^2} \right]^2 \right\} \quad (5-103)$$

$$\theta_o = \tan^{-1} \left\{ - \frac{(R-1) \left[4R(1+\varepsilon^2)^2 v_o + (R-1)^2(1+2\varepsilon^2) \right]}{2R\sigma_o(R+1+2\varepsilon^2)(1+\varepsilon^2) \left[R(2u_o(1+\varepsilon^2)-1) + 1 \right]} \right\} \quad (5-104)$$

For any initial conditions of u_o, v_o one can use eqs. (5-103) and (5-104) to establish their equivalent initial conditions in terms of r_o and θ_o , to be used in the weak nonlinear solution (5-99) and (5-100). The latter solution is analytically expressed and it is expected to be valid for values of $\varepsilon \ll 1$, meaning that β_o is in the neighborhood of $\beta_{o,cr}$. The next section provides examples of results obtained by using this weak nonlinear solution compared with numerical results.

5.9 Results and Discussion

5.9.1 - An Example Demonstrating the Comparison between the Weak Nonlinear Method with the Linear Stability Analysis using a Numerical Solution for Benchmarking

The linear stability analysis, which is the most widely used tool for analytical prediction, produces criteria for stability. As an example, for $\gamma_o = 1$ and $R = 5$ the critical value of β_o following eq. (5-6) is $\beta_{o,cr} = 2.5$. The linear stability analysis anticipates that all small perturbations to the stationary solution (5-17), (5-18) decay if the value of β_o is smaller than $\beta_{o,cr}$ and grow via oscillations that their amplitude diverges when $\beta_o > \beta_{o,cr}$. The latter occurs because the linear stability solutions (4-26) have the form

$$u_1 = e^{\lambda_r t} [B_1 \sin(\lambda_i t) + B_2 \cos(\lambda_i t)] \quad (a) \quad (5-105)$$

$$v_1 = e^{\lambda_r t} [C_1 \sin(\lambda_i t) + C_2 \cos(\lambda_i t)] \quad (b)$$

with $\lambda_r = \psi_A/2$. For $\gamma_o = 1$ and $R = 5$, $\beta_{o,cr} = 2.5$. Therefore for $\beta_o > 2.5$ $\lambda_r = \psi_A/2 > 0$ and the amplitude of the oscillations increases exponentially and diverges. The following numerical solution presented in Figure 5.2 demonstrates this anticipation based on the linear stability analysis by applying a direct numerical method of solution to equations (5-2). The latter was obtained by using a standard Runge-Kutta solver to double precision from the IMSL Library (1991) (DIVPRK) up to a desired tolerance for error control.

However, in reality, if the numerical solution is obtained for a sufficiently long time range the exponential divergence of the amplitude can be shown to be limited leading eventually to a finite amplitude as presented in Figure 5.3. From Figure 5.3 it is obvious that the amplitude does not diverge but rather stabilizes and the solution shows large amplitude oscillations at post-transient conditions which can be better observed by zooming within the post-transient time range $1500 < t < 1680$ as presented in Figure 5.4.

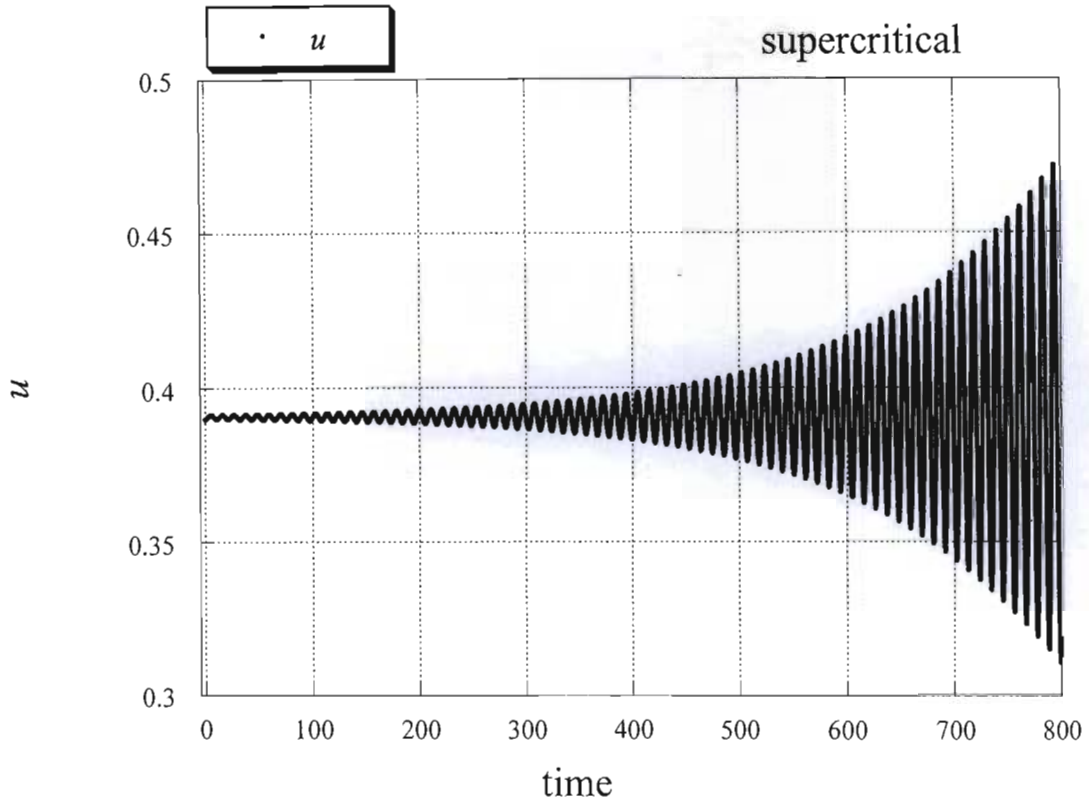


Figure 5.2: Numerical solution showing the apparent exponential divergence of the amplitude for $\gamma_o = 1$ and $R = 5$, $\beta_o = 2.56 > \beta_{o,cr} = 2.5$. Short term results.

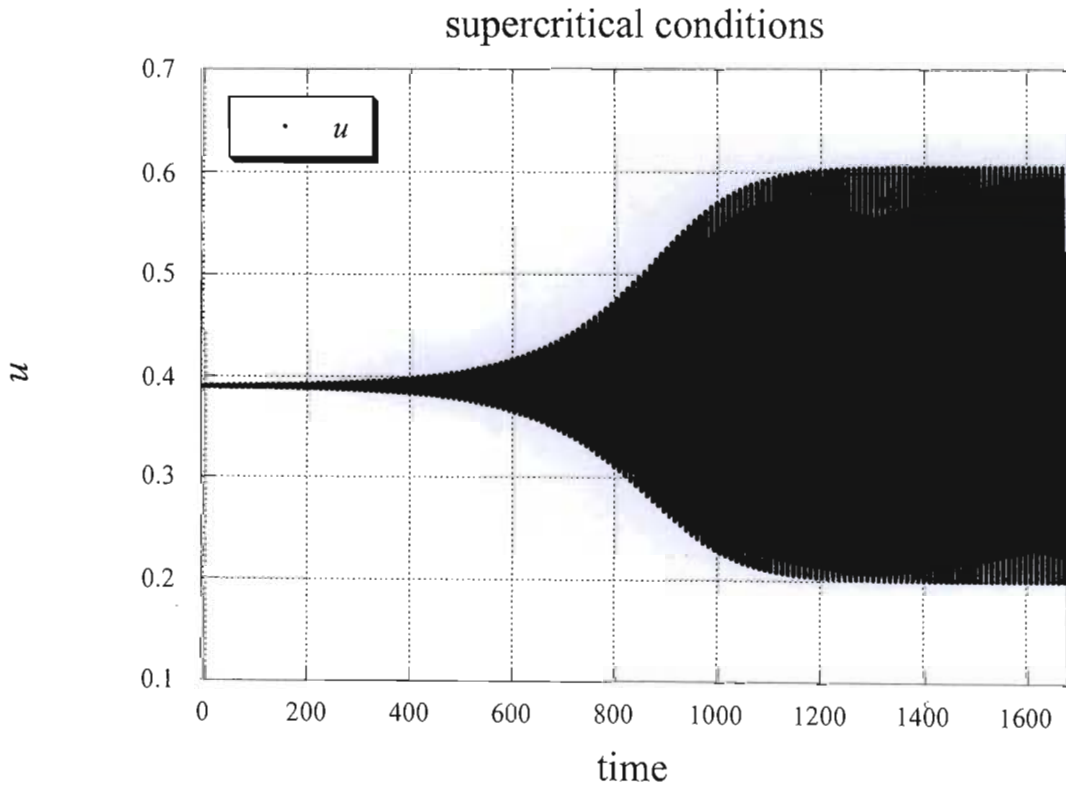


Figure 5.3: Numerical solution showing the finite amplitude results for $\gamma_o = 1$ and $R = 5$, $\beta_o = 2.56 > \beta_{o,cr} = 2.5$. Long term results.

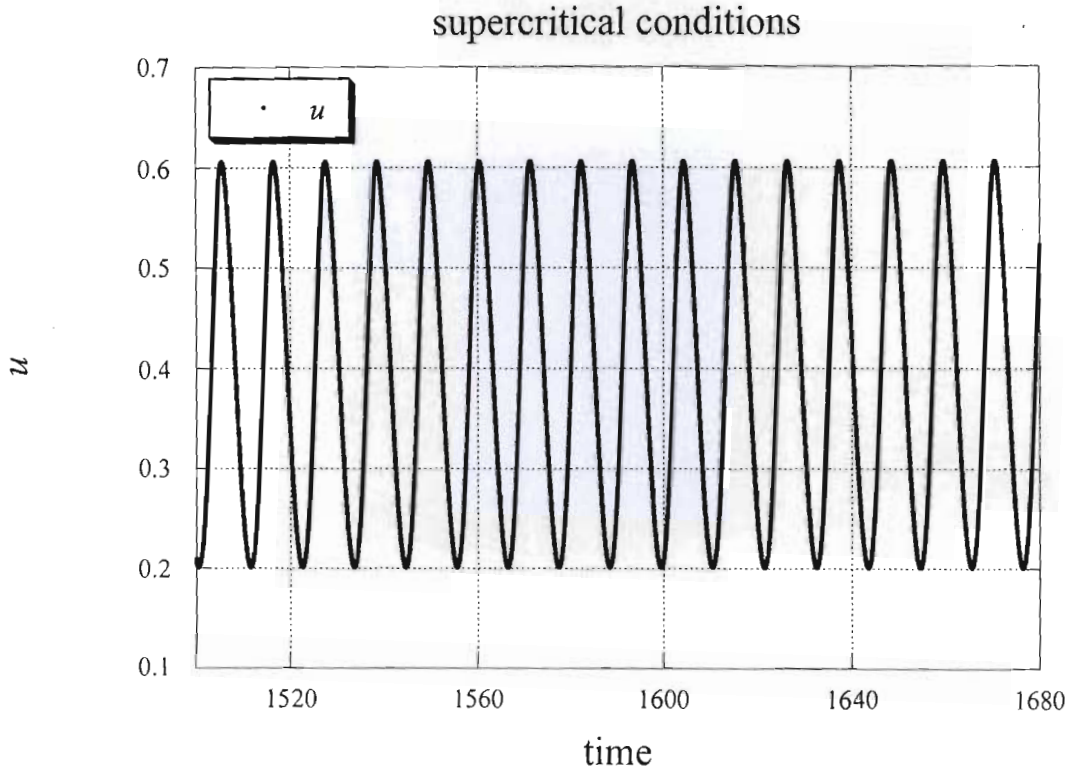


Figure 5.4: Numerical solution showing the post-transient results $1500 < t < 1680$, for $\gamma_o = 1$ and $R = 5$, $\beta_o = 2.56 > \beta_{o,cr} = 2.5$.

5.9.2 - A Comparison between the Weak Nonlinear Results and a Numerical Solution for Benchmarking

On the other hand the weak nonlinear method produces results based on eqs.(5-99) and (5-100) that are presented in Figure 5.5 in comparison to the accurate numerical results. Although the post-transient oscillations have large amplitudes (hence the weak nonlinear method is not so accurate in this parameter range) the comparison shows an excellent qualitative match, both solutions leading to finite amplitude oscillations at the post-transient state. It is difficult to observe the oscillations in Fig. 5.5, but the envelope of the solution is evident.

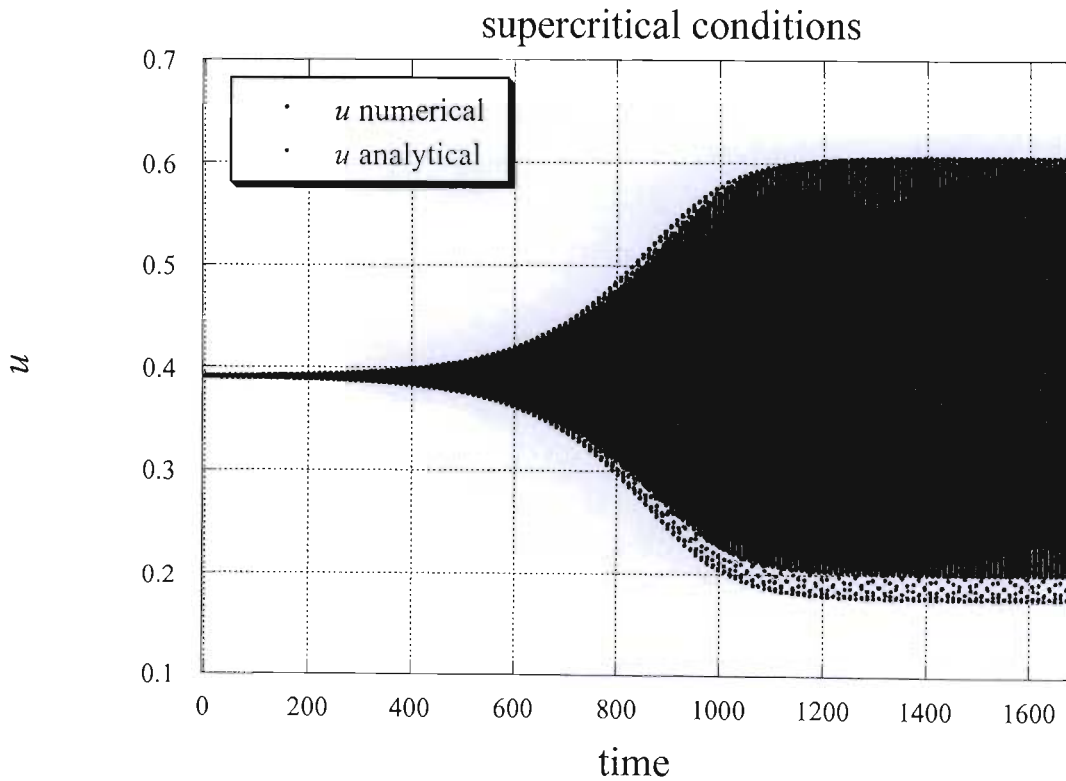


Figure 5.5: Numerical results compared to the weak nonlinear solution for $\gamma_o = 1$ and $R = 5$, $\beta_o = 2.56 > \beta_{o,cr} = 2.5$.

In addition, the quantitative comparison (Figures 5.6 and 5.7) shows also that the weak nonlinear solution is not far from the accurate numerical results. Obviously, the further away the value of β_o is from its critical value, $\beta_{o,cr} = 2.5$ and the larger the amplitude of the oscillations, the less accurate the weak nonlinear solution becomes.

However, for small amplitudes and in the neighborhood of $\beta_{o,cr} = 2.5$, the weak nonlinear results are expected to produce the only reliable analytical solution. Figures 5.7 and 5.8 show a comparison between the weak nonlinear results and numerical results obtained at $\beta_o = \beta_{o,cr} = 2.5$. Numerical values of u differ by less than 10^{-4} on average from the weak nonlinear ones.

The sample of results presented so far show the strength (and limitations) of using the weak nonlinear method of solution to obtain analytical results that can provide guidance of the parameter regimes where accurate numerical results or experiments are desirable.

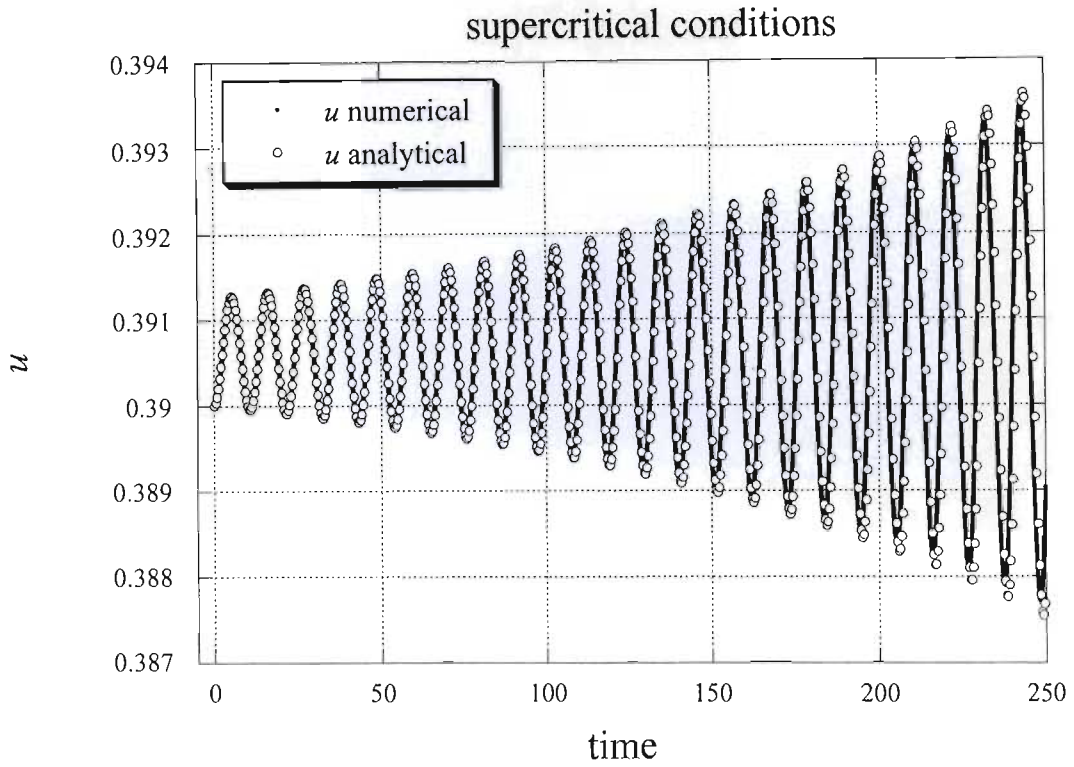


Figure 5.6: Numerical results compared to the weak nonlinear solution for $\gamma_o = 1$ and $R = 5$, $\beta_o = 2.56 > \beta_{o,cr} = 2.5$. Quantitative comparison shows a very good match for time range $0 < t < 250$. For small times, i.e. small amplitudes the match looks better than for longer times.

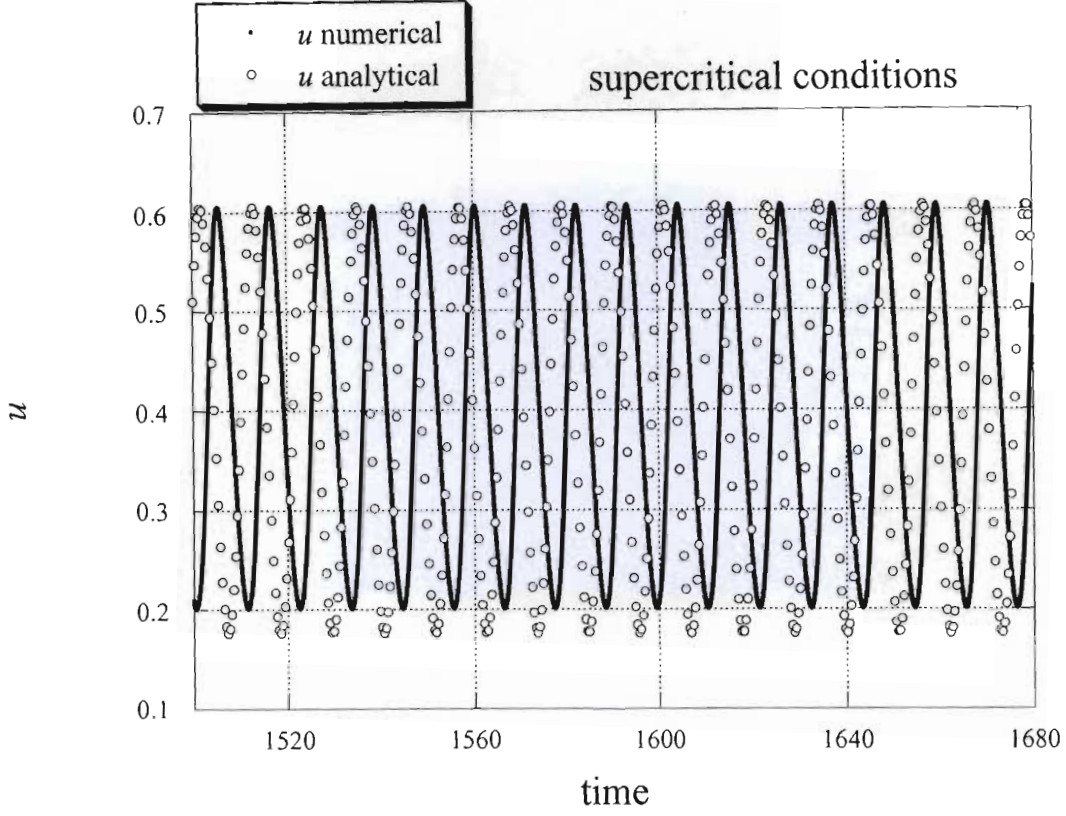


Figure 5.7: Numerical results compared to the weak nonlinear solution for $\gamma_o = 1$ and $R = 5$, $\beta_o = 2.56 > \beta_{o,cr} = 2.5$. Quantitative comparison shows a quantitative deterioration in accuracy for time range $1500 < t < 1680$. For long times, i.e. large amplitudes the accuracy of the weak nonlinear results is somewhat compromised in both the frequency of oscillations as well as the amplitude value.

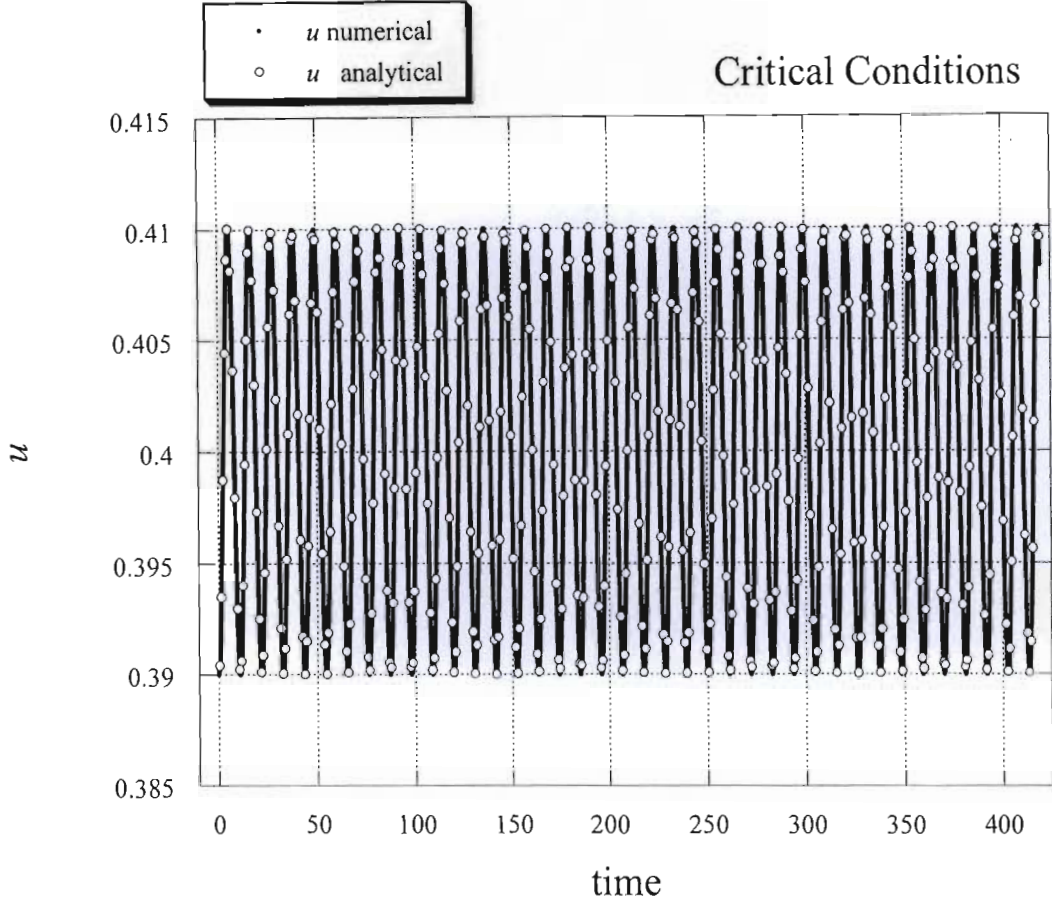


Figure 5.8: Numerical results compared to the weak nonlinear solution for $\gamma_o = 1$ and $R = 5$, $\beta_o = \beta_{o,cr} = 2.5$.

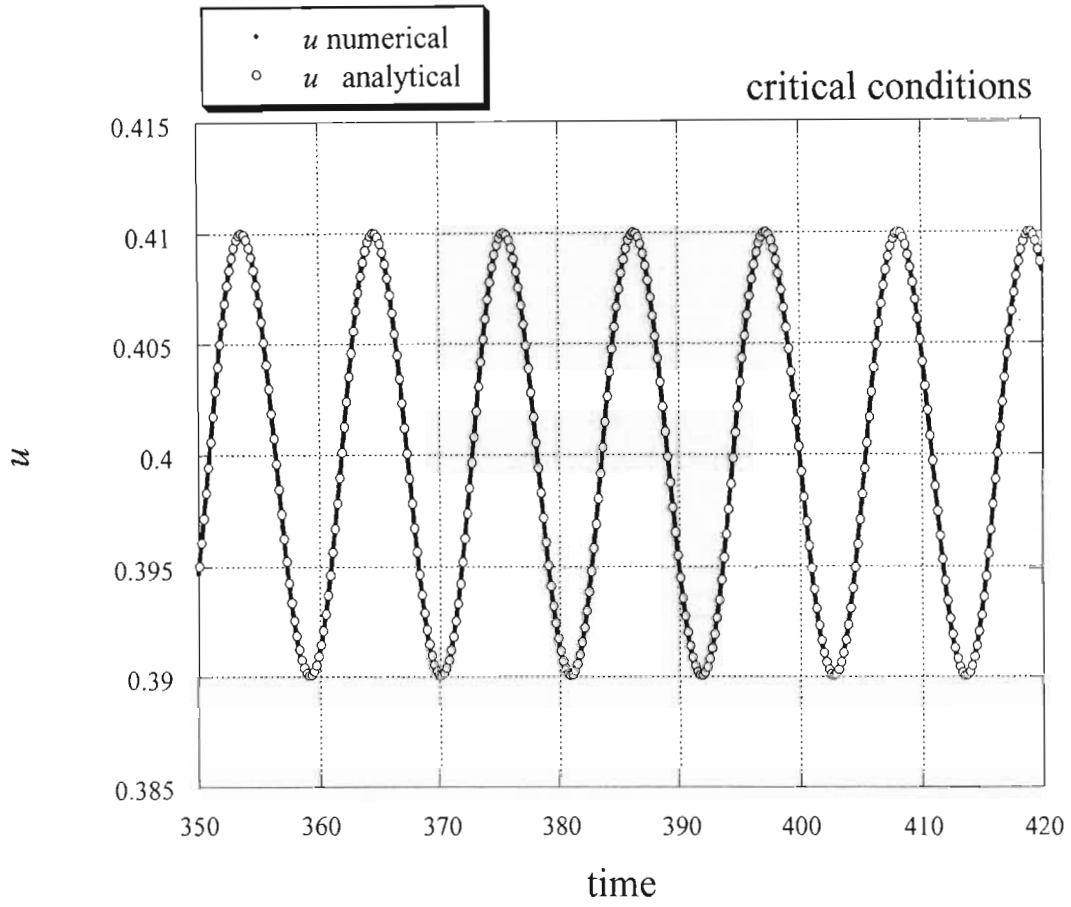


Figure 5.9: Numerical results compared to the weak nonlinear solution for $\gamma_o = 1$ and $R = 5$, $\beta_o = \beta_{o,cr} = 2.5$. Inset into the post-transient time range $350 < t < 420$.

CHAPTER 6

LINEAR STABILITY ANALYSIS TO SPATIALLY HETEROGENEOUS PERTURBATIONS (SHeP)

6.1 Linear Stability of the Nontrivial Stationary Solutions $(u_{s1,2}, v_{s1,2})$

The equations considered in the spatially heterogeneous case are eqs. (2-14) in the form

$$\begin{cases} \frac{\partial u}{\partial t} = \frac{1}{Gn} \nabla^2 u + \left[1 - u + \frac{(v-1)}{(1+Ru)} \right] u & (a) \\ \frac{\partial v}{\partial t} = \frac{1}{Rn} \nabla^2 v + \gamma_o - \beta_o u + \varphi_o v & (b) \end{cases} \quad (6-1)$$

where the dimensionless groups appearing in (6-1) are defined as

$$Gn = \frac{\mu_* H_*^2}{D_*}, \quad Rn = \frac{\mu_* H_*^2}{\alpha_*}, \quad Sn = \frac{k_* \delta_*}{\mu_*^2 m_{o*}}, \quad (6-2)$$

$$R = r_{m*} \delta_*, \quad \gamma = \gamma_o + \gamma_1 u, \quad \beta_o = Sn - \gamma_1$$

where Gn represents a Growth Number, Rn is a Resource Number, Sn is a Storage Number and $R = r_{m*} \delta_*$ is a Biomass Number. It is convenient for the following derivations to represent eqs. (6-1) in the equivalent form obtained by multiplying (6-1a) by $(1+Ru)$ leading to

$$\begin{cases} (1+Ru) \frac{\partial u}{\partial t} = \frac{(1+Ru)}{Gn} \nabla^2 u + \left[(R-1)u - Ru^2 + v \right] u & (a) \\ \frac{\partial v}{\partial t} = \frac{1}{Rn} \nabla^2 v + \gamma_o - \beta_o u + \varphi_o v & (b) \end{cases} \quad (6-3)$$

The boundary conditions applied to this system are represented by (2-10) in the following form

$$\left(\frac{\partial u}{\partial x}\right)_{x=0,L} = \left(\frac{\partial u}{\partial y}\right)_{y=0,1} = 0 \quad (a) \quad (6-4)$$

$$\left(\frac{\partial v}{\partial x}\right)_{x=0,L} = \left(\frac{\partial v}{\partial y}\right)_{y=0,1} = 0 \quad (b)$$

By introducing small, spatially dependent, perturbations $(\varepsilon u_1, \varepsilon v_1)$ around the stationary solutions (u_s, v_s) , u and v take the form

$$u = u_s + \varepsilon u_1(x, y, t) \quad (a) \quad (6-5)$$

$$v = v_s + \varepsilon v_1(x, y, t) \quad (b)$$

where $\varepsilon \ll 1$ stands only to indicate that the perturbations are very small. Substituting (6-5) into (6-3) and neglecting terms that are $O(\varepsilon^2)$ or smaller, yields the linear form of the equations for the perturbations

$$\begin{cases} (1 + R u_s) \frac{\partial u_1}{\partial t} = \frac{(1 + R u_s)}{Gn} \nabla^2 u_1 + [2(R-1)u_s - 3R u_s^2 + v_s] u_1 + u_s v_1 & (a) \\ \frac{\partial v_1}{\partial t} = \frac{1}{Rn} \nabla^2 v_1 - \beta_o u_1 + \varphi_o v_1 & (b) \end{cases} \quad (6-6)$$

Dividing eq. (6-6a) by $(1 + R u_s)$ using the equations for the stationary solution (3-5) and introducing the definitions of β_1 and β_2 from (3-26a,b) yields

$$\begin{cases} \frac{\partial u_1}{\partial t} = \frac{1}{Gn} \nabla^2 u_1 + \beta_1 u_1 + \beta_2 v_1 & (a) \\ \frac{\partial v_1}{\partial t} = \frac{1}{Rn} \nabla^2 v_1 - \beta_o u_1 + \varphi_o v_1 & (b) \end{cases} \quad (6-7)$$

Similarly, the same procedure applied to the boundary conditions (6-4) leads to

$$\left(\frac{\partial u_1}{\partial x}\right)_{x=0,L} = \left(\frac{\partial u_1}{\partial y}\right)_{y=0,1} = 0 \quad (a) \quad (6-8)$$

$$\left(\frac{\partial v_1}{\partial x}\right)_{x=0,L} = \left(\frac{\partial v_1}{\partial y}\right)_{y=0,1} = 0 \quad (b)$$

The linear equations (6-7) can be presented in the following matrix form

$$\frac{d\mathbf{w}_1}{dt} = \mathbf{B}\mathbf{w}_1 \quad (6-9)$$

where $\mathbf{w}_1 = [u_1, v_1]^T$, and the matrix \mathbf{B} stands for

$$\mathbf{B} = \begin{bmatrix} \left(\frac{1}{Gn}\nabla^2 + \beta_1\right) & ; & \beta_2 \\ -\beta_o & ; & \left(\frac{1}{Rn}\nabla^2 + \varphi_o\right) \end{bmatrix} \quad (6-10)$$

The linear system (6-7) has solutions of the following form

$$u_1 = A_1 \cos(\kappa_x x) \cos(\kappa_y y) e^{\lambda t} \quad (a) \quad (6-11)$$

$$v_1 = B_1 \cos(\kappa_x x) \cos(\kappa_y y) e^{\lambda t} \quad (b)$$

The fact that only combinations of cosine functions appear in the linear solution is a result of imposing the boundary conditions (6-8). Substituting these solutions into the equations (6-7) produces the following equation for the eigenvalues

$$\lambda^2 + \left[\frac{\kappa^2}{Gn} + \frac{\kappa^2}{Rn} - (\beta_1 + \varphi_o) \right] \lambda + \frac{\kappa^4}{GnRn} - \left(\frac{\beta_1}{Rn} + \frac{\varphi_o}{Gn} \right) \kappa^2 + (\beta_1 \varphi_o + \beta_o \beta_2) = 0 \quad (6-12)$$

where

$$\kappa^2 = \kappa_x^2 + \kappa_y^2 \quad (6-13)$$

defines the wave number. The following notation is recognized from the linear stability analysis to spatially homogeneous perturbations (SHoP)

$$\psi_A = \beta_1 + \varphi_o \quad (6-14)$$

$$\Delta_A = \beta_1 \varphi_o + \beta_o \beta_2 \quad (6-15)$$

In addition it can be recognized that the coefficient terms appearing in eq. (6-12) represent the trace, ψ_B , and the determinant, Δ_B , of the coefficient matrix \mathbf{B} applied on the solutions (u_1, v_1) as follows

$$\psi_B = \text{trace}(B) = \psi_A - \frac{(Gn + Rn)}{Gn Rn} \kappa^2 \quad (6-16)$$

$$\Delta_B = \det(B) = \Delta_A - \frac{(Gn \beta_1 + Rn \phi_o)}{Gn Rn} \kappa^2 + \frac{\kappa^4}{Gn Rn} \quad (6-17)$$

transforming eq. (6-12) into the following form

$$\lambda^2 - \psi_B \lambda + \Delta_B = 0 \quad (6-18)$$

The solution for the eigenvalues is

$$\lambda_{1,2} = \frac{\psi_B}{2} \left[1 \pm \sqrt{1 - \frac{4\Delta_B}{\psi_B^2}} \right] \quad (6-19)$$

The eigenvalues (6-19) combined with the form of the solutions (6-11) provide the conditions for small perturbations $\varepsilon u_1(x, y, t)$, $\varepsilon v_1(x, y, t)$ around the stationary solutions $(u_{s1,2}, v_{s1,2})$ to grow or decay. When λ is real and negative or complex with a negative real part the perturbations decay and the corresponding stationary solution (u_{s1}, v_{s1}) or (u_{s2}, v_{s2}) is stable to Spatially Heterogeneous Perturbations (SHeP), while if λ is real and positive or complex with a positive real part the perturbations grow exponentially and the corresponding stationary solution is unstable. From eq. (6-19) it is obvious that for stability of the stationary solutions $(u_{s1,2}, v_{s1,2})$ to SHeP one needs to impose the conditions

$$\psi_B < 0 \quad \& \quad \Delta_B > 0 \quad (6-20)$$

The latter guarantees that the eigenvalues λ are real and negative or complex conjugates with a negative real part. Presenting inequalities (6-20) explicitly by using (6-16) and (6-17) yields

$$\psi_A - \frac{(Gn + Rn)}{Gn Rn} \kappa^2 < 0 \quad (6-21)$$

and

$$\Delta_A - \frac{(Gn \beta_1 + Rn \phi_o)}{Gn Rn} \kappa^2 + \frac{\kappa^4}{Gn Rn} > 0 \quad (6-22)$$

Since an assumption is made that the stationary solutions are stable to SHoP implying that $\psi_A < 0$ and since $Gn > 0$, $Rn > 0$, and the κ^2 is positive by definition, the first condition, (6-21), for stability of the stationary solutions to SHeP is unconditionally satisfied. The second condition (6-22) can be presented in the form

$$\kappa^4 - (Gn\beta_1 + Rn\varphi_o)\kappa^2 + GnRn\Delta_A > 0 \quad (6-23)$$

Further expansion of (6-23) leads to

$$Gn(Rn\Delta_A - \beta_1\kappa^2) > Rn\varphi_o\kappa^2 - \kappa^4 \quad (6-24)$$

Inequality (6-24) implies

$$Gn > \frac{(Rn\varphi_o\kappa^2 - \kappa^4)}{(Rn\Delta_A - \beta_1\kappa^2)} \quad \forall \quad Rn\Delta_A > \beta_1\kappa^2 \quad (6-25)$$

and

$$Gn < \frac{(\kappa^4 - Rn\varphi_o\kappa^2)}{(\beta_1\kappa^2 - Rn\Delta_A)} \quad \forall \quad Rn\Delta_A < \beta_1\kappa^2 \quad (6-26)$$

as stability conditions to SHeP. For neutral stability $\lambda = 0$, i.e. $\lambda_1 = \psi_B < 0$ and $\lambda_2 = \Delta_B = 0$ one can define the characteristic (or neutral) value of $Gn = Gn_c$ in the form

$$Gn_c = \frac{(\kappa^4 - Rn\varphi_o\kappa^2)}{(\beta_1\kappa^2 - Rn\Delta_A)} \quad (6-27)$$

This value is a function of the wave number and it has an asymptote at a wave number value of

$$(\kappa^2)_{as} = \frac{Rn\Delta_A}{\beta_1}, \quad (6-28)$$

where the denominator of (6-27) becomes zero. The minimum value of Gn_c in (6-27) as function of κ^2 occurs at some wave number, κ_{cr} , and can be obtained by evaluating $\partial Gn_c / \partial \kappa^2$ and equating it to zero. This minimum value represents the critical value of Gn , i.e. Gn_{cr} , and κ_{cr} is the corresponding critical wave number. This yields

$$\frac{\partial Gn_c}{\partial \kappa^2} = \frac{(2\kappa^2 - Rn\varphi_o)(\beta_1\kappa^2 - Rn\Delta_A) - \beta_1(\kappa^4 - Rn\varphi_o\kappa^2)}{(\beta_1\kappa^2 - Rn\Delta_A)^2} = 0 \quad (6-29)$$

From eq. (6-29) one obtains an equation for the critical wave number in the form

$$\kappa_{cr}^4 - \frac{2Rn\Delta_A}{\beta_1}\kappa_{cr}^2 + \frac{Rn^2\varphi_o\Delta_A}{\beta_1} = 0 \quad (6-30)$$

The solution to the quadratic equation (6-30) is

$$\kappa_{cr}^2 = \frac{Rn\Delta_A}{\beta_1} \left[1 \pm \sqrt{1 - \frac{\beta_1\varphi_o}{\Delta_A}} \right] = \frac{Rn\Delta_A}{\beta_1} (1 \pm S_B) \quad (6-31)$$

where S_B is defined in the form

$$S_B = \sqrt{1 - \frac{\beta_1\varphi_o}{\Delta_A}} \quad (6-32)$$

The critical value of Gn is obtained by substituting (6-31) into (6-27) leading to

$$Gn_{cr} = \frac{Rn\Delta_A}{\beta_1^2} \left[1 \pm \sqrt{1 - \frac{\beta_1\varphi_o}{\Delta_A}} \right]^2 = \frac{Rn\Delta_A}{\beta_1^2} (1 \pm S_B)^2 \quad (6-33)$$

An alternative way to present the stability condition is by using (6-33) to define a critical value of the ratio Gn/Rn in the form.

$$\left(\frac{Gn}{Rn} \right)_{cr} = \frac{\Delta_A}{\beta_1^2} \left[1 \pm \sqrt{1 - \frac{\beta_1\varphi_o}{\Delta_A}} \right]^2 = \frac{\Delta_A}{\beta_1^2} (1 \pm S_B)^2 \quad (6-34)$$

Then the stability condition is expressed by

$$Rg = \frac{Gn}{Rn} = \frac{\alpha_*}{D_*} < \left(\frac{Gn}{Rn} \right)_{cr} = Rg_{cr} \quad (6-35)$$

where the substitution of the definitions of Gn and Rn from eq. (2-8) produced the stability condition in terms of the diffusivity ratio $Rg = \alpha_*/D_*$. Since $\Delta_A > 0$ because the stationary solutions are stable to SHoP it is clear from eq. (6-33) that the critical value of Gn is always non-negative, i.e. $Gn_{cr} \geq 0$. While one may wonder about the double solution for Gn_{cr} and for this purpose also for κ_{cr}^2 , the latter should not be of concern because some minima (or possibly maxima) of $Gn_c(\kappa^2)$ may occur at

negative values of κ_{cr}^2 and should be discarded because there is no physical meaning to negative values of κ^2 . To observe this feature and additional functional forms of $Gn_c(\kappa^2)$, and in particular the critical values Gn_{cr} and κ_{cr}^2 , one can evaluate $Gn_c(\kappa^2)$ based on (6-27) for different values of κ^2 and plot it.

This evaluation was undertaken here for different values of β_1 , $Rn\varphi_o$ (corresponding to $\varphi_o < 0$, $\varphi_o = 0$ and $\varphi_o > 0$) and $Rn\Delta_A$. The results are presented in Figures 6.1-6.8. The stability and instability regions are presented in each Figure. The location of all relevant parameters, e.g. the asymptotic value of κ^2 , $(\kappa^2)_{as} = 2$, its corresponding critical wave number, $\kappa_{cr}^2 = 4.828$ and the critical value of Gn , i.e. $Gn_{cr} = 5.828$, that is applicable to $\varphi_o < 0$ is evident from Figure 6.1. Figure 6.2 presents the neutral curves for conditions applicable to $\varphi_o = 0$, showing a reduction in the value of Gn_{cr} . Figure 6.3 shows the curves for conditions when $0 < Rn\varphi_o < \kappa_{as}^2$, where a further reduction in Gn_{cr} is observed. Figure 6.4 applies to $0 < Rn\varphi_o = \kappa_{as}^2$, quite a degenerated case, resulting from the fact that $Rn\varphi_o = \kappa_{as}^2$ leading to $Gn_c = \kappa^2(\kappa^2 - \kappa_{as}^2)/(\kappa^2 - \kappa_{as}^2)\beta_1 = \kappa^2/\beta_1$, a clear linear function of κ^2 . Figure 6.5 corresponds to $0 < \kappa_{as}^2 < Rn\varphi_o$, showing a substantial qualitative change. All the figures so far considered the indicated parameter values while $\beta_1 = 2 > 0$. In contrast, Figure 6.6 deals with the case when $\beta_1 < 0$ and $\varphi_o > 0$, while Figures 6.7 and 6.8 show the neutral curves as applicable to $\beta_1 < 0$ and $\varphi_o < 0$. The latter clearly show that in the whole physical domain represented by the first quadrant, i.e. $Gn_{cr} \geq 0$ and $\kappa^2 \geq 0$, the stationary solution is stable to SHeP, except for a very narrow domain of low wave numbers and small values of Gn_c in Fig. 6.6, where instability may occur.

One needs to establish at this stage whether oscillatory instability is possible in connection with SHeP. If it is then the possibility of standing and/or travelling waves should be considered. For the latter to occur the eigenvalues have to be complex. From eq. (6-19) it is clear that the condition for complex eigenvalues is

$$1 - \frac{4\Delta_B}{\psi_B^2} < 0 \quad (6-36)$$

which can be expressed in the form

$$4\Delta_B - \psi_B^2 > 0 \quad (6-37)$$

Then the eigenvalues in eq. (6-19) take the form

$$\lambda_{1,2} = \frac{\psi_B}{2} \left[1 \pm i \sqrt{\frac{4\Delta_B}{\psi_B^2} - 1} \right] \quad (6-38)$$

However, in such circumstances $\psi_B < 0$ because $\psi_A < 0$, $Gn > 0$, $Rn > 0$, $\kappa^2 > 0$, and therefore $\psi_B = \psi_A - (Gn + Rn)\kappa^2 / Gn Rn < 0$. One may conclude that the stationary solution (u_s, v_s) is stable to small oscillatory Spatially Heterogeneous Perturbations, because $\psi_B < 0$, and according to (6-38) oscillatory perturbations decay.

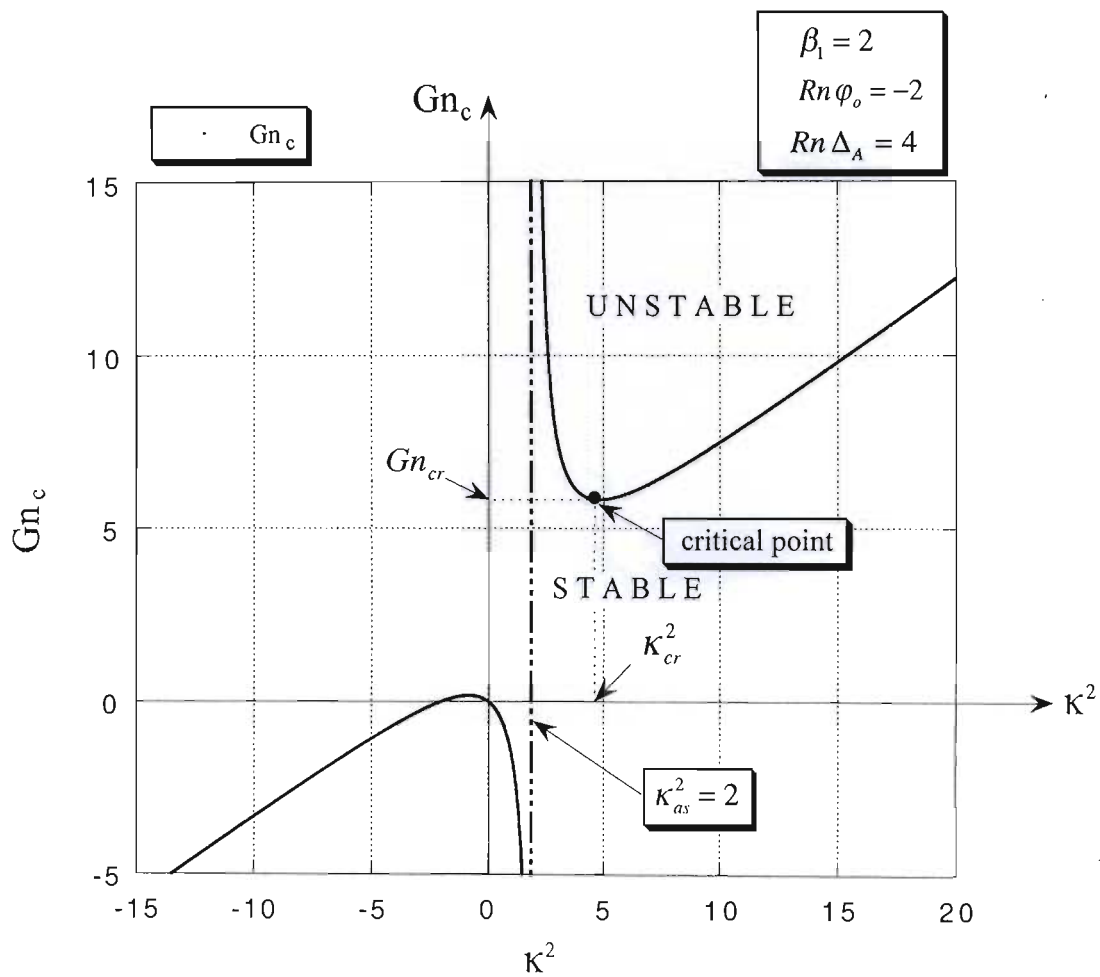


Figure 6.1: Characteristic (neutral) curves corresponding to $\beta_1 = 2$, $\varphi_o < 0$, $Rn\varphi_o = -2$, $Rn\Delta_A = 4$.

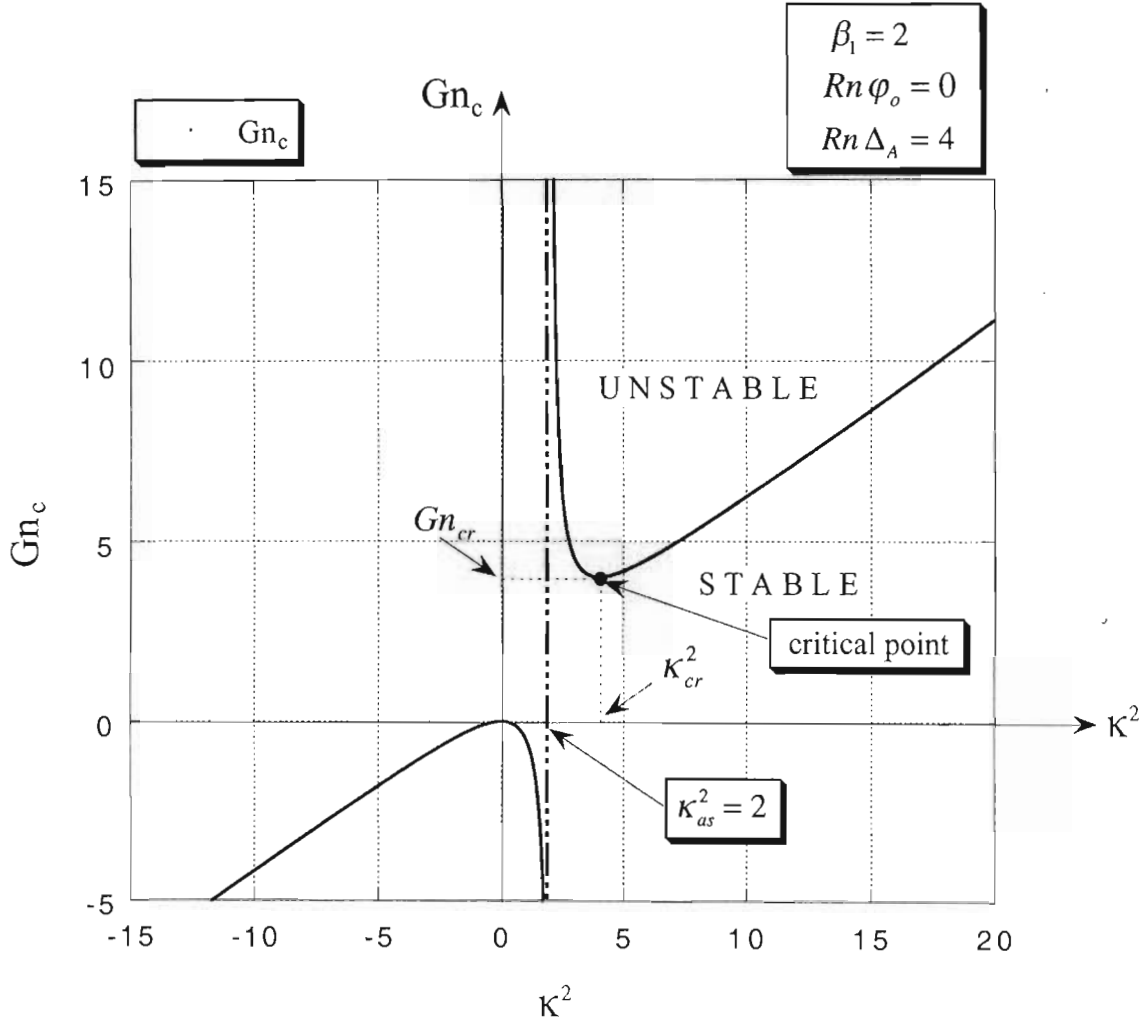


Figure 6.2: Characteristic (neutral) curves corresponding to $\beta_1 = 2$, $\varphi_o = 0$, $Rn \varphi_o = 0$, $Rn \Delta_A = 4$.

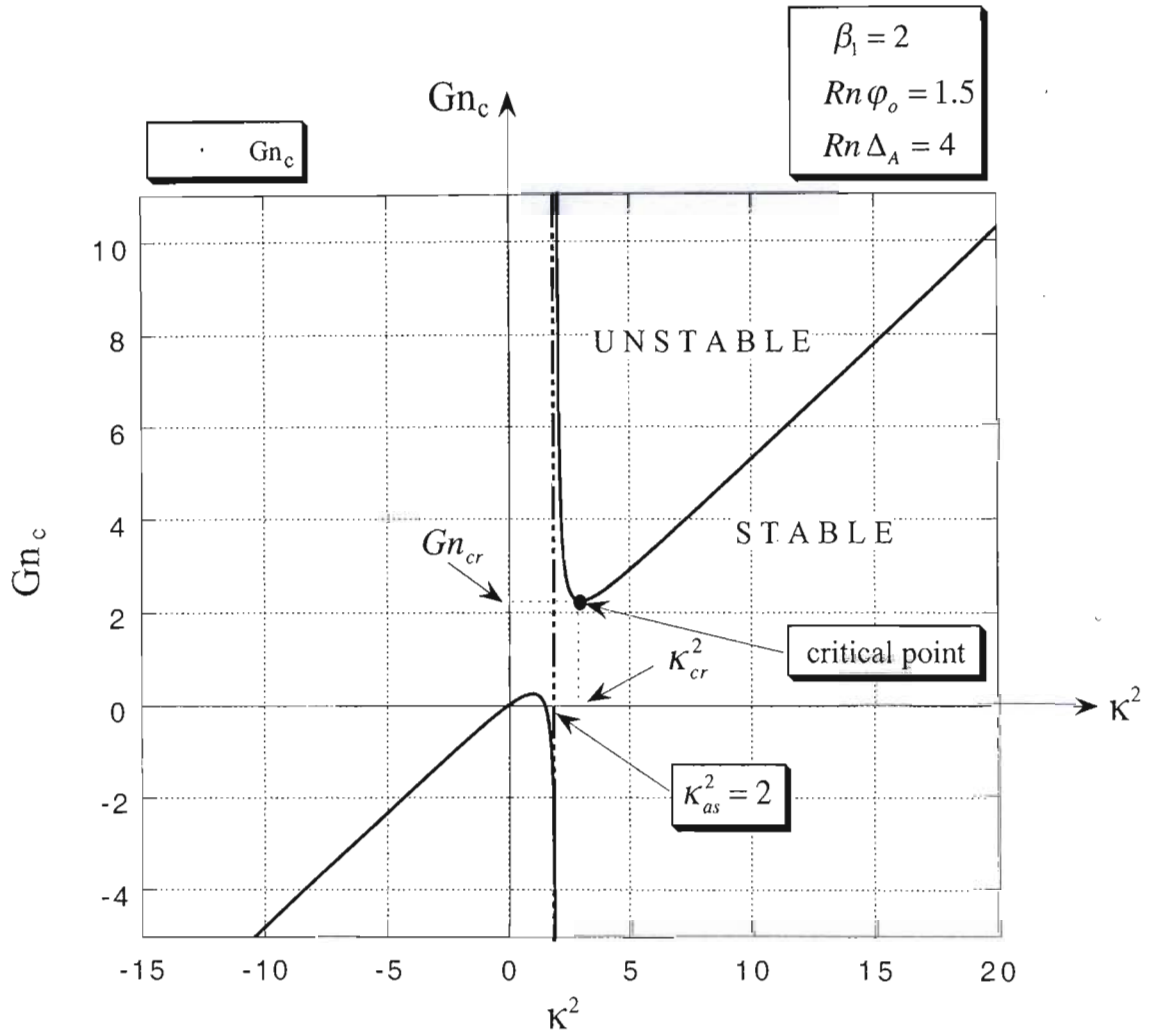


Figure 6.3: Characteristic (neutral) curves corresponding to $\beta_1 = 2$, $0 < \varphi_o < (\kappa_{as}^2)/Rn$, $Rn\varphi_o = 1.5$, $Rn\Delta_A = 4$.

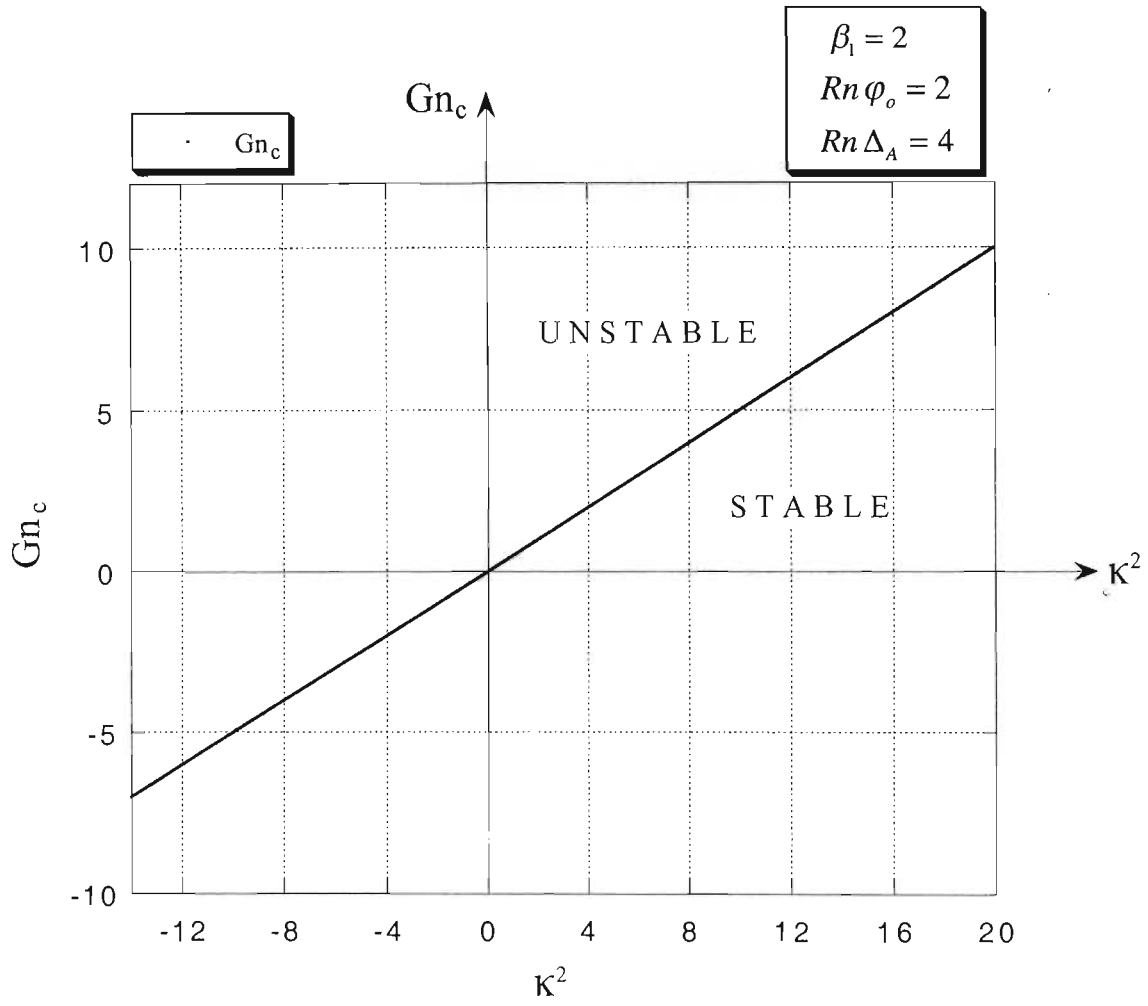


Figure 6.4: Characteristic (neutral) curves corresponding to $\beta_1 = 2$, $0 < \varphi_o = (\kappa_{as}^2)/Rn$, $Rn\varphi_o = 2$, $Rn\Delta_A = 4$.

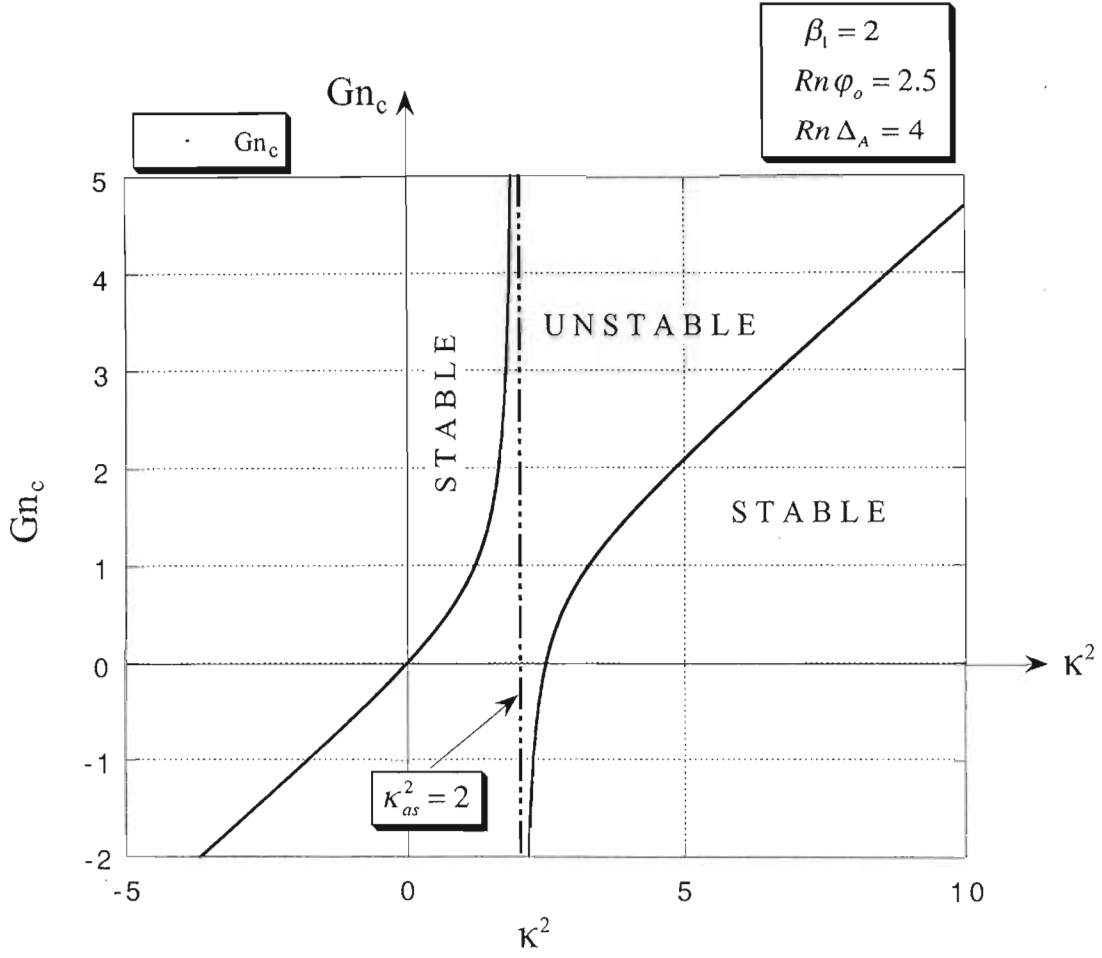


Figure 6.5: Characteristic (neutral) curves corresponding to $\beta_1 = 2$, $0 < (\kappa_{as}^2)/Rn < \varphi_o$, $Rn\varphi_o = 2.5$, $Rn\Delta_A = 4$.

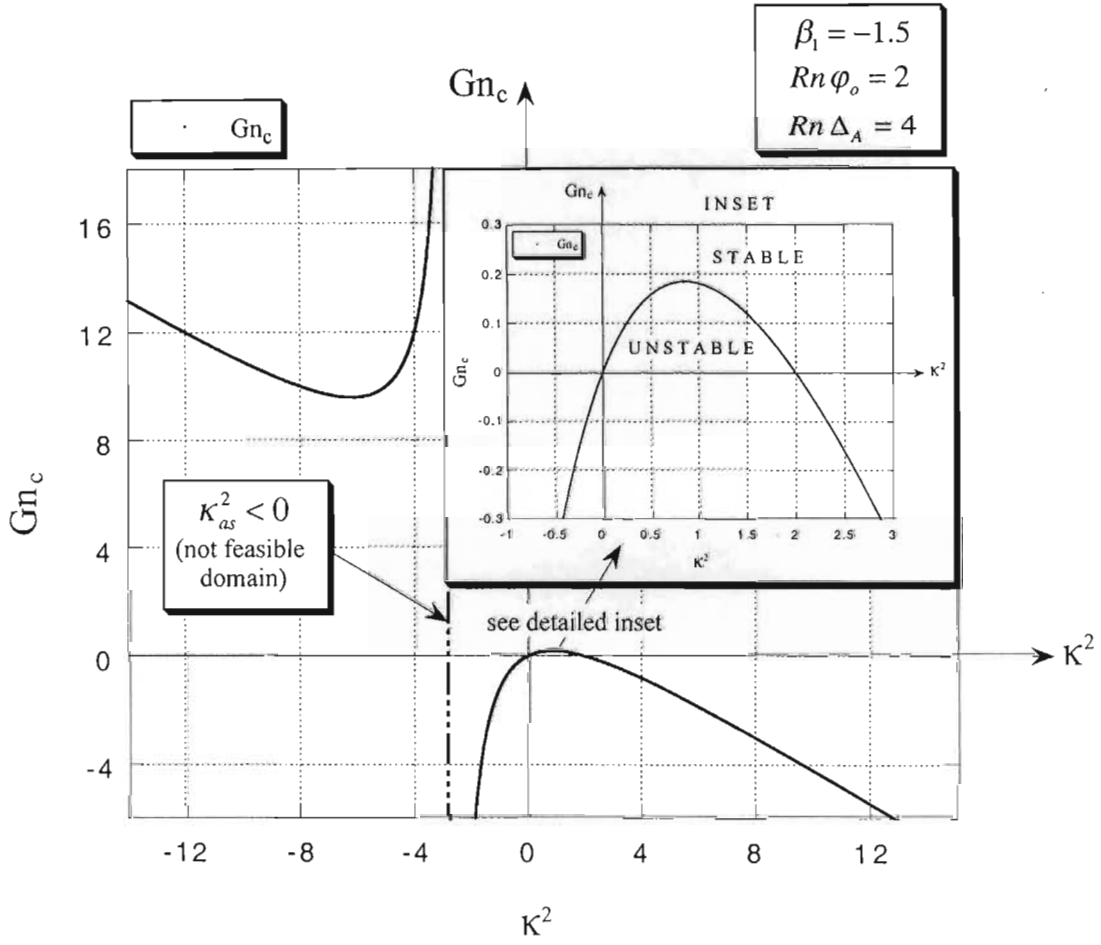


Figure 6.6: Characteristic (neutral) curves corresponding to $\beta_1 = -1.5$, $\phi_o > 0$, $Rn\phi_o = 2$, $Rn\Delta_A = 4$.

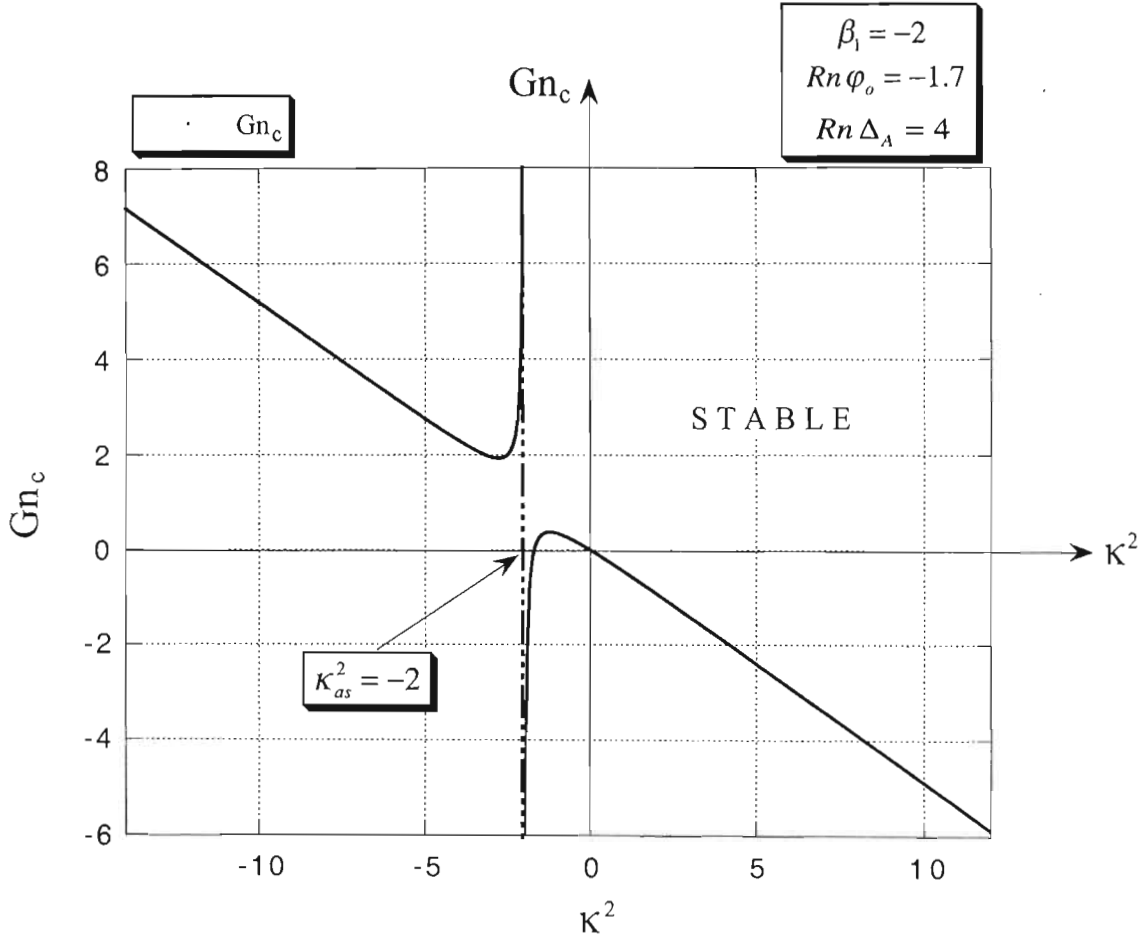


Figure 6.7: Characteristic (neutral) curves corresponding to $\beta_1 = -2$, $\varphi_o < 0$, $Rn\varphi_o = -1.7$, $Rn\Delta_A = 4$.

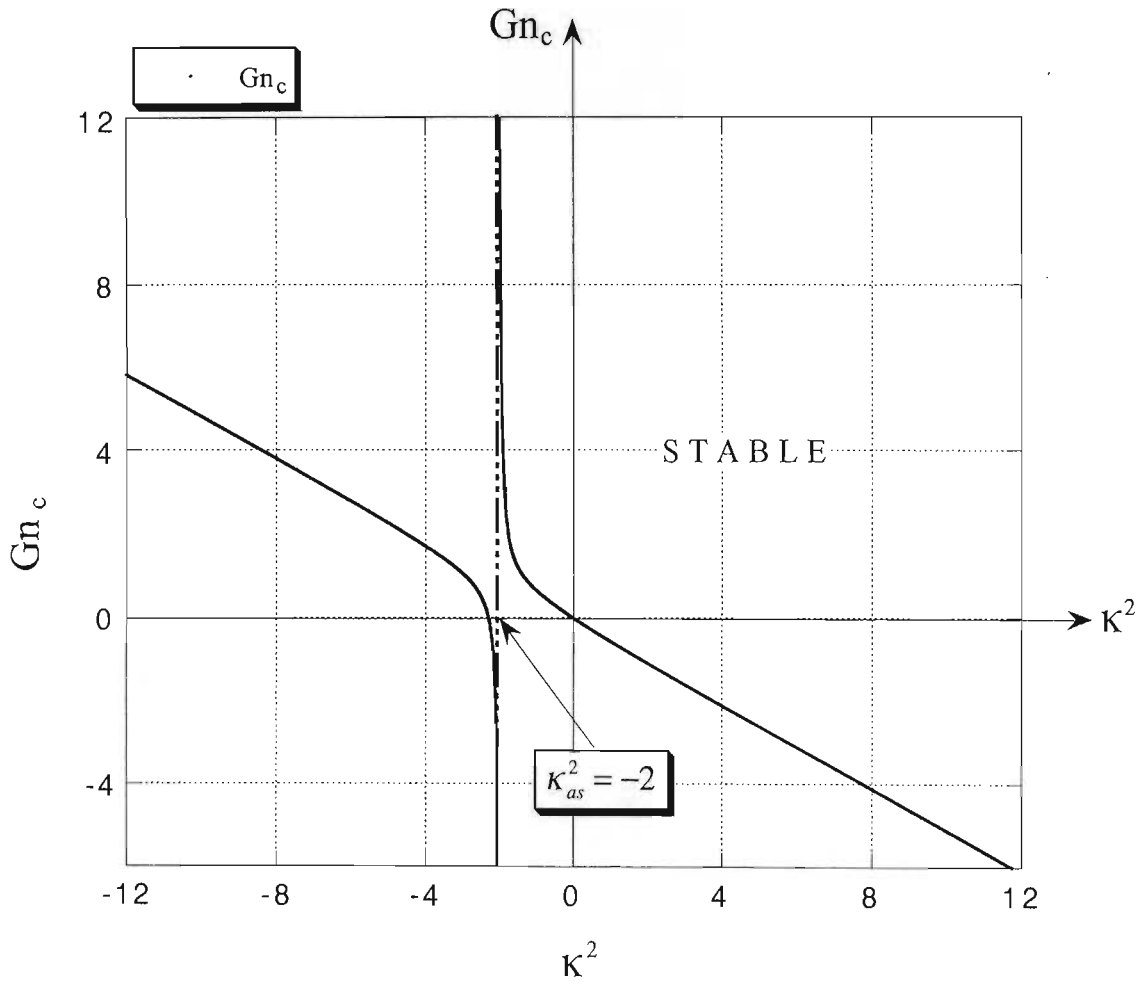


Figure 6.8: Characteristic (neutral) curves corresponding to $\beta_1 = -2$, $\varphi_o < 0$, $Rn\varphi_o = -2.3$, $Rn\Delta_A = 4$.

6.2 Summary of Stability Conditions

The linear stability conditions identified particularly the domain when $\beta_1 > 0$ and $\varphi_o < 0$ as a clear window of parameters when it is obvious that Turing instabilities may occur if

$$Gn > Gn_{cr} \quad (6-37)$$

The critical values are given by

$$\left(\kappa_{cr}^2\right)_1 = \frac{Rn \Delta_A}{\beta_1} \left[1 + \sqrt{1 - \frac{\beta_1 \varphi_o}{\Delta_A}} \right] \quad (6-38)$$

$$\left(\kappa_{cr}^2\right)_2 = \frac{Rn \Delta_A}{\beta_1} \left[1 - \sqrt{1 - \frac{\beta_1 \varphi_o}{\Delta_A}} \right] \quad (6-39)$$

and

$$Gn_{cr,1} = \frac{Rn \Delta_A}{\beta_1^2} \left[1 + \sqrt{1 - \frac{\beta_1 \varphi_o}{\Delta_A}} \right]^2 \quad (6-40)$$

$$Gn_{cr,2} = \frac{Rn \Delta_A}{\beta_1^2} \left[1 - \sqrt{1 - \frac{\beta_1 \varphi_o}{\Delta_A}} \right]^2 \quad (6-41)$$

The linear stability analysis also provided the conclusion that oscillatory instability is not possible in connection to SHeP.

Finally, an additional subtle result can be established from the linear stability analysis to SHeP. The results show that it is not possible to distinguish in terms of linear stability between the wave numbers in the x and y directions. While solutions that include κ_x and κ_y were explicitly considered in eq. (6-11), the results turned out to depend only on the combination $\kappa^2 = \kappa_x^2 + \kappa_y^2$. This degeneracy occurs frequently in this type of problems. It is indeed difficult to indicate a physical or biological reason of why the solution should prefer a particular direction. Therefore, based on this conclusion that no preferred direction can be established, it is appropriate to present the solution as one-dimensional in space, in the form

$$u_1 = A_1 \cos(\kappa_x x) e^{\lambda_1 t} \quad \text{(a)} \quad (6-42)$$

$$v_1 = B_1 \cos(\kappa_x x) e^{\lambda_1 t} \quad \text{(b)}$$

6.3 Conditions for Occurrence of Turing Instability

In this section the interest is focused to formulate the conditions for occurrence of Turing instability. These conditions are just the opposite to the conditions developed for stability of (u_s, v_s) to small Spatially Heterogeneous Perturbations. When the stationary solution is stable to SHoP but unstable to SHeP it is expected to obtain Turing instabilities. For this to occur, from eq. (6-20) it implies that the condition for Turing instability to occur at least one of the following conditions has to be satisfied

$$\psi_B > 0 \quad \text{or} \quad \Delta_B < 0 \quad (6-43)$$

This implies

$$\psi_A - \frac{(Gn + Rn)}{Gn Rn} \kappa^2 > 0 \quad (6-44)$$

or

$$\Delta_A - \frac{(Gn \beta_1 + Rn \varphi_o)}{Gn Rn} \kappa^2 + \frac{\kappa^4}{Gn Rn} < 0 \quad (6-45)$$

It was already established that the first condition, (6-44) is not satisfied (see text following eq. (6-22)) and therefore Turing instability may occur only if (6-45) is satisfied. This implies

$$Gn > Gn_{cr} \quad \forall \quad Rn \Delta_A < \beta_1 \kappa_{cr}^2 \quad (6-46)$$

where the values of Gn_{cr} are given by eqs. (6-40) and (6-41).

CHAPTER 7

WEAK NONLINEAR SOLUTION FOR THE SPATIALLY HETEROGENEOUS PROBLEM

7.1 Governing Equations for the Spatially Heterogeneous Problem

The governing equations considered in this chapter are these corresponding to the spatially heterogeneous case in the form derived in section 6.1 and represented by eqs. (6-3). For convenience of the derivations in what follows they can be expanded further into the form

$$\left\{ \begin{array}{l} Gn(1 + Ru) \frac{\partial u}{\partial t} = (1 + Ru) \nabla^2 u + Gn(R-1)u^2 - GnRu^3 + Gn uv \quad (a) \\ \frac{\partial v}{\partial t} = \frac{1}{Rn} \nabla^2 v + \gamma_o - \beta_o u + \varphi_o v \quad (b) \end{array} \right. \quad (7-1)$$

By applying now the conclusion regarding the lack of a preferred spatial direction, from the linear stability analysis (section 6.2), implying that it is appropriate to treat this problem as one dimensional in space, say in the x direction only, in absence of a criterion of preference, eq. (7-1) transforms into

$$\left\{ \begin{array}{l} Gn(1 + Ru) \frac{\partial u}{\partial t} = (1 + Ru) \frac{\partial^2 u}{\partial x^2} + Gn(R-1)u^2 - GnRu^3 + Gn uv \quad (a) \\ \frac{\partial v}{\partial t} = \frac{1}{Rn} \frac{\partial^2 v}{\partial x^2} + \gamma_o - \beta_o u + \varphi_o v \quad (b) \end{array} \right. \quad (7-2)$$

representing the one dimensional problem in space for heterogeneously distributed populations. These are typical diffusion equations with nonlinear source/sink terms representing the interaction between the population and nutrient i.e. the rate of nutrient consumption/ utilization.

7.2 Asymptotic Expansion, Scales and Parameters

By introducing the definition of the small expansion parameter $\varepsilon \ll 1$ in terms of the relative distance of Gn from its critical value Gn_{cr} as follows

$$\varepsilon^2 = \frac{Gn - Gn_{cr}}{Gn_{cr}} \quad (7-3)$$

one can expand the dependent variables $u(x, t)$ and $v(x, t)$ in the form

$$u = u_s + \varepsilon u_1 + \varepsilon^2 u_2 + \varepsilon^3 u_3 + \dots \quad (7-4)$$

$$v = v_s + \varepsilon v_1 + \varepsilon^2 v_2 + \varepsilon^3 v_3 + \dots \quad (7-5)$$

and express the growth number Gn as a finite expansion resulting directly from eq (7-3) in the form

$$Gn = Gn_{cr} + \varepsilon^2 Gn_{cr}. \quad (7-6)$$

A slow time scale is introduced by replacing t with $t \rightarrow \tau$ (it was established in section 6.2 that oscillatory instability should be excluded as a possibility), where

$$\tau = \varepsilon^2 t \quad (7-7)$$

represents the slow time scale. Substituting the expansions (7-4) and (7-5) into the equations (7-2) yields a hierarchy of differential equations at the different orders. The latter is obtained by grouping terms of like powers of ε . At the leading order one obtains the equations for the stationary solution, at order ε the equations are very similar to the linear stability analysis equations, and its solutions can be obtained up to the value of an unknown amplitude, which changes in time over the slow time scale τ only. At order ε^2 the solutions produce a homogeneous and a particular solution. Finally, at order ε^3 a solvability condition obtained by imposing the requirement of a finite amplitude solution, provides an equation for the time evolution of the $O(\varepsilon)$ amplitude. The latter amplitude equation has a closed form solution that yields a complete analytical result to the problem, however its accuracy is very high only in the neighborhood of the critical value of Gn , i.e. around $Gn \approx Gn_{cr}$, such that $\varepsilon \ll 1$ (see eq. (7-3)) and not too far away from the stationary solution. As one moves away from $Gn \approx Gn_{cr}$, or when the amplitude becomes large so the solution moves quite far

away from the stationary point the accuracy of the analytical solution obtained via the weak nonlinear method is gradually compromised.

Substituting expansions (7-4) and (7-5) as well as (7-6) and replacing t with τ , by using eq. (7-7) in the form $t = \tau/\varepsilon^2$, into the equations (7-2) yields the governing equations in terms of the asymptotic expansion variables. By grouping now the terms containing like powers of ε and requiring that they balance each other, produces a set of separate equations at the different orders.

7.3 Solution at Leading Order $O(1)$

The stationary state equations representing terms that are $O(1)$ can be presented in the form

$$\begin{cases} \frac{(1 + R u_s)}{Gn} \frac{d^2 u_s}{dx^2} + (R - 1) u_s^2 - R u_s^3 + u_s v_s = 0 & (a) \\ \frac{1}{Rn} \frac{d^2 v_s}{dx^2} + \gamma_o - \beta_o u_s + \varphi_o v_s = 0 & (b) \end{cases} \quad (7-8)$$

where $u_s(x)$ and $v_s(x)$ are allowed in general to be functions of x . However, the particular interest in this study is to consider development of spatial patterns from a stable spatially homogeneous state. Therefore, the basic stationary state is taken as represented by the constant stationary solution, $u_s = \text{const.}$ and $v_s = \text{const.}$ derived in section 3.1 and expressed by eqs. (3-11), (3-12), (3-13) and (3-14). They satisfy the stationary state equations

$$\begin{cases} (R - 1) u_s^2 - R u_s^3 + u_s v_s = 0 & (a) \\ \gamma_o - \beta_o u_s + \varphi_o v_s = 0 & (b) \end{cases} \quad (7-9)$$

7.4 Solution at Order $O(\varepsilon)$

At order $O(\varepsilon)$ one collects the terms in the expanded equations that correspond to the power of ε^1 leading to

$$\begin{cases} \left(1 + R u_s\right) \frac{d^2 u_1}{d x^2} + 2(R-1) G n_{cr} u_s u_1 - 3R G n_{cr} u_s^2 u_1 + G n_{cr} (v_s u_1 + u_s v_1) = 0 & (a) \\ \frac{1}{R n} \frac{d^2 v}{d x^2} - \beta_o u_1 + \varphi_o v_1 = 0 & (b) \end{cases} \quad (7-10)$$

Dividing eq. (7-10a) by $(1 + R u_s)$ and using the definitions from eq. (3-26) yields

$$\begin{cases} \left(\frac{d^2}{d x^2} + \beta_1 G n_{cr} \right) u_1 + G n_{cr} \beta_2 v_1 = 0 & (a) \\ -\beta_o u_1 + \left(\frac{1}{R n} \frac{d^2}{d x^2} + \varphi_o \right) v_1 = 0 & (b) \end{cases} \quad (7-11)$$

The solution to the linear system (7-11) takes the form

$$\begin{aligned} u_1 &= A_1(\tau) \cos(\kappa_{cr} x) & (a) \\ v_1 &= B_1(\tau) \cos(\kappa_{cr} x) & (b) \end{aligned} \quad (7-12)$$

By substituting eq. (7-12) into (7-11) produces an equation for the wave number similar to the equation, which was derived by the linear stability analysis, in the form

$$\kappa_{cr}^4 - (G n_{cr} \beta_1 + R n \varphi_o) \kappa_{cr}^2 + R n G n_{cr} \Delta_A > 0 \quad (7-13)$$

leading to the critical values as obtained from linear stability

$$\kappa_{cr}^2 = \frac{R n \Delta_A}{\beta_1} (1 \pm S_B) \quad (7-14)$$

$$G n_{cr} = \frac{R n \Delta_A}{\beta_1^2} (1 \pm S_B)^2 \quad (7-15)$$

where

$$S_B = \sqrt{1 - \frac{\beta_1 \varphi_o}{\Delta_A}} \quad (7-16)$$

A particularly useful relationship in the following derivations is obtained from (7-14) and (7-15) in the form

$$\frac{\kappa_{cr}^2}{Gn_{cr}} = \frac{\beta_1}{(1 \pm S_B)} \quad (7-17)$$

In addition, the substitution of (7-12) into (7-11) leads to the following relationship between the coefficients $A_1(\tau)$ and $B_1(\tau)$ in the form

$$B_1(\tau) = - \frac{\beta_1}{\beta_2} \frac{S_B}{(1 + S_B)} A_1(\tau) \quad (7-18)$$

7.5 Solution at Order $O(\varepsilon^2)$

Collecting the terms in the expanded equations that correspond to the power of ε^2 leads to the equations at order $O(\varepsilon^2)$ in the form

$$\begin{cases} \left(\frac{d^2}{dx^2} + \beta_1 Gn_{cr} \right) u_2 + Gn_{cr} \beta_2 v_2 = -\frac{R}{\beta_4} u_1 \frac{d^2 u_1}{dx^2} - \frac{Gn_{cr} \beta_5}{\beta_4} u_1^2 - \frac{Gn_{cr}}{\beta_4} u_1 v_1 & (a) \\ -\beta_o u_2 + \left(\frac{1}{Rn} \frac{d^2}{dx^2} + \varphi_o \right) v_2 = 0 & (b) \end{cases} \quad (7-19)$$

Equations (7-19a,b) form a coupled linear system. Comparing with eq. (7-11) it is easy to observe that the left-hand-side operator of (7-19a,b) is identical to the one that appears in eq. (7-11) at order $O(\varepsilon)$. The major difference is in the form of the right-hand-side terms. While at order $O(\varepsilon)$ the right-hand-side terms are zero and the equations are homogeneous, the $O(\varepsilon^2)$ equations (7-19) contain terms on their right-hand-side, which depend on the solution at $O(\varepsilon)$. Since the solution at order $O(\varepsilon)$ is known and given by eq. (7-12) it becomes possible to derive the analytical solution to eq. (7-19) at order $O(\varepsilon^2)$. It consists of the superposition between a homogeneous and a particular solution in the form

$$u_2 = u_{2H} + u_{2P} \quad (a) \quad (7-20)$$

$$v_2 = v_{2H} + v_{2P} \quad (b)$$

where (u_{2H}, v_{2H}) is the homogeneous part of the solution and (u_{2P}, v_{2P}) represents the particular solution. The homogeneous part of the solution satisfies the system of equations

$$\begin{cases} \left(\frac{d^2}{dx^2} + \beta_1 Gn_{cr} \right) u_2 + Gn_{cr} \beta_2 v_2 = 0 & (a) \\ -\beta_o u_2 + \left(\frac{1}{Rn} \frac{d^2}{dx^2} + \varphi_o \right) v_2 = 0 & (b) \end{cases} \quad (7-21)$$

while the particular solution satisfies the equations

$$\begin{cases} \left(\frac{d^2}{dx^2} + \beta_1 Gn_{cr} \right) u_{2P} + Gn_{cr} \beta_2 v_{2P} = -\frac{R}{\beta_4} u_1 \frac{d^2 u_1}{dx^2} - \frac{Gn_{cr} \beta_5}{\beta_4} u_1^2 - \frac{Gn_{cr}}{\beta_4} u_1 v_1 & (a) \\ -\beta_o u_{2P} + \left(\frac{1}{Rn} \frac{d^2}{dx^2} + \varphi_o \right) v_{2P} = 0 & (b) \end{cases} \quad (7-22)$$

Since the homogeneous part of the system (7-19) is identical to the equations solved at order $O(\varepsilon)$, the homogenous solution should also have an identical form as eq. (7-12), i.e.

$$u_2 = A_2(\tau) \cos(\kappa_{cr} x) \quad (a) \quad (7-23)$$

$$v_2 = B_2(\tau) \cos(\kappa_{cr} x) \quad (b)$$

where the relationship between the coefficients is similar to eq. (7-18) at order $O(\varepsilon)$ in the form

$$B_2(\tau) = -\frac{\beta_1 S_B}{\beta_2 (1 + S_B)} A_2(\tau) \quad (7-24)$$

To derive the particular solution one needs to decouple equations (7-22a) and (7-22b) in order to obtain one equation for u_{2P} only, and one equation for v_{2P} only. Decoupling the equations is accomplished by using (7-22a) to express v_{2P} in terms of the other variables in the form

$$v_{2P} = -\left(\frac{1}{Gn_{cr} \beta_2} \frac{d^2}{dx^2} + \beta_3 \right) u_{2P} - \frac{R}{Gn_{cr} u_s} u_1 \frac{d^2 u_1}{dx^2} - \frac{\beta_5}{u_s} u_1^2 - \frac{1}{u_s} u_1 v_1 \quad (7-25)$$

and substitute it into eq. (7-22b) to yield

$$\begin{aligned} \beta_o Gn_{cr} \beta_2 u_{2P} + \left(\frac{1}{Rn} \frac{d^2}{dx^2} + \varphi_o \right) \left(\frac{d^2}{dx^2} + Gn_{cr} \beta_1 \right) u_{2P} = \\ \left(\frac{1}{Rn} \frac{d^2}{dx^2} + \varphi_o \right) \left[-\frac{\beta_2 R}{u_s} u_1 \frac{d^2 u_1}{dx^2} - \frac{Gn_{cr} \beta_5}{\beta_4} u_1^2 - \frac{Gn_{cr}}{\beta_4} u_1 v_1 \right] \end{aligned} \quad (7-26)$$

It is convenient to introduce the operator notation

$$\mathcal{L}_1 = \left(\frac{d^2}{dx^2} + \beta_1 Gn_{cr} \right) \quad (7-27)$$

$$\mathcal{L}_2 = \left(\frac{1}{Rn} \frac{d^2}{dx^2} + \varphi_o \right) \quad (7-28)$$

and therefore eq. (7-26) takes the form

$$(\mathcal{L}_1 \mathcal{L}_2 + \beta_o \beta_2 Gn_{cr}) u_{2P} = \mathcal{L}_2 \left[-\frac{R}{\beta_4} u_1 \frac{d^2 u_1}{dx^2} - \frac{Gn_{cr} \beta_5}{\beta_4} u_1^2 - \frac{Gn_{cr}}{\beta_4} u_1 v_1 \right] \quad (7-29)$$

Applying the same process on eq. (7-22b) to isolate u_{2P} yields

$$u_{2P} = \left(\frac{1}{\beta_o Rn} \frac{d^2}{dx^2} + \frac{\varphi_o}{\beta_o} \right) v_{2P} \quad (7-30)$$

which upon substitution into (7-22a) produces

$$(\mathcal{L}_1 \mathcal{L}_2 + \beta_o \beta_2 Gn_{cr}) v_{2P} = -\frac{R \beta_o}{\beta_4} u_1 \frac{d^2 u_1}{dx^2} - \frac{Gn_{cr} \beta_o \beta_5}{\beta_4} u_1^2 - \frac{Gn_{cr} \beta_o}{\beta_4} u_1 v_1 \quad (7-31)$$

Equations (7-29) and (7-31) represent the decoupled form corresponding to the system (7-22). The explicit evaluation of the terms on the right-hand-side of eq. (7-29) is presented in Appendix 4, and the right-hand-side of eq. (7-31) is presented in Appendix 5. These terms act as forcing functions and they impact directly on the form of the solutions u_{2P} and v_{2P} . The results from Appendices 4 and 5 are

$$RHS(7-29) = p_1 \left(\frac{\varphi_o}{2} - \frac{2\kappa_{cr}^2}{Rn} \right) \cos(2\kappa_{cr} x) + \frac{p_1 \varphi_o}{2} \quad (7-32)$$

$$RHS(7-31) = \frac{\beta_o p_1}{2} \cos(2\kappa_{cr} x) + \frac{\beta_o p_1}{2} \quad (7-33)$$

where

$$p_1 = \left(\frac{R\kappa_{cr}^2 - Gn_{cr} \beta_5}{\beta_4} \right) A_1^2 - \frac{Gn_{cr}}{\beta_4} A_1 B_1 \quad (7-34)$$

These forcing functions suggest particular solutions of the form

$$u_{2P} = A_{20} \cos(2\kappa_{cr} x) + C_{20} \quad (a) \quad (7-35)$$

$$v_{2P} = B_{20} \cos(2\kappa_{cr} x) + E_{20} \quad (b)$$

Substituting the particular solution (7-35a) and the RHS expressions (7-32) into (7-29) yields

$$\left[\frac{16\kappa_{cr}^4}{Rn} - 4\kappa_{cr}^2 \left(\varphi_o + \frac{\beta_1 G n_{cr}}{Rn} \right) + \Delta_A G n_{cr} \right] A_{20} \cos(2\kappa_{cr} x) + \Delta_A G n_{cr} C_{20} =$$

$$p_1 \left(\frac{\varphi_o}{2} - \frac{2\kappa_{cr}^2}{Rn} \right) \cos(2\kappa_{cr} x) + \frac{p_1 \varphi_o}{2} \quad (7-36)$$

Equating the terms on the left-hand-side with these on the right-hand-side of (7-36) yields the values of the coefficients of the particular solution in the form

$$A_{20} = \frac{p_1 (Rn \varphi_o - 4\kappa_{cr}^2)}{2[16\kappa_{cr}^4 - 4(Rn \varphi_o + \beta_1 G n_{cr})\kappa_{cr}^2 + Rn G n_{cr} \Delta_A]} \quad (7-37)$$

$$C_{20} = \frac{\varphi_o p_1}{2 G n_{cr} \Delta_A} \quad (7-38)$$

Similarly, substituting the particular solution (7-35b) and the RHS expressions (7-33) into the (7-31) yields

$$\left[\frac{16\kappa_{cr}^4}{Rn} - 4 \left(\varphi_o + \frac{\beta_1 G n_{cr}}{Rn} \right) \kappa_{cr}^2 + \Delta_A G n_{cr} \right] B_{20} \cos(2\kappa_{cr} x) + \Delta_A G n_{cr} E_{20} =$$

$$\frac{\beta_o p_1}{2} \cos(2\kappa_{cr} x) + \frac{\beta_o p_1}{2} \quad (7-39)$$

Equating the terms on the left-hand-side with these on the right-hand-side of (7-39) yields the values of the coefficients of the particular solution in the form

$$B_{20} = \frac{\beta_o Rn p_1}{2[16\kappa_{cr}^4 - 4(Rn \varphi_o + G n_{cr} \beta_1)\kappa_{cr}^2 + Rn G n_{cr} \Delta_A]} \quad (7-40)$$

$$E_{20} = \frac{\beta_o p_1}{2 \Delta_A G n_{cr}} \quad (7-41)$$

The complete solution at this order becomes

$$u_2 = A_2 \cos(\kappa_{cr} x) + A_{20} \cos(2\kappa_{cr} x) + C_{20} \quad (a)$$

$$v_2 = B_2 \cos(\kappa_{cr} x) + B_{20} \cos(2\kappa_{cr} x) + E_{20} \quad (b) \quad (7-42)$$

where the coefficients $A_{20}, C_{20}, B_{20}, E_{20}$, are given by (7-37), (7-38), (7-40) and (7-41), the relationship between B_2 and A_2 is represented by (7-24), and $p_1(A_1, B_1)$ is defined in eq. (7-34).

7.6 Solvability Condition at Order $O(\varepsilon^3)$

At order $O(\varepsilon^3)$ one collects the terms in the expanded equations that correspond to the power of ε^3 leading to

$$\begin{cases} \left(\frac{d^2}{dx^2} + \beta_1 Gn_{cr} \right) u_3 + Gn_{cr} \beta_2 v_3 = RHS31 & (a) \\ -\beta_o u_3 + \left(\frac{1}{Rn} \frac{d^2}{dx^2} + \varphi_o \right) v_3 = RHS32 & (b) \end{cases} \quad (7-43)$$

where the right-hand-sides of these equations, $RHS31$ and $RHS32$, take the form

$$RHS31 = Gn_{cr} \frac{\partial u_1}{\partial \tau} - \frac{R}{\beta_4} \left(u_1 \frac{d^2 u_2}{dx^2} + u_2 \frac{d^2 u_1}{dx^2} \right) - \quad (7-44)$$

$$Gn_{cr} \left[\frac{2\beta_5}{\beta_4} u_1 u_2 + \beta_1 u_1 - \frac{R}{\beta_4} u_1^3 + \frac{1}{\beta_4} (u_1 v_2 + u_2 v_1) + \beta_2 v_1 \right]$$

$$RHS32 = \frac{\partial v_1}{\partial \tau} = \dot{B}_1 \cos(\kappa_{cr} x) \quad (7-45)$$

where $\dot{B}_1 = dB_1/d\tau$.

Equations (7-43) form a coupled linear system. From eq. (7-43) it is easy to observe that the left-hand-side operator of the equations is identical to the one that appears in eq. (7-11) at order $O(\varepsilon)$ and in eq.(7-19) at order $O(\varepsilon^2)$. The major difference is in the form of the right-hand-side terms. Since the solutions at orders $O(\varepsilon)$ and $O(\varepsilon^2)$ are known and given by eq. (7-12) and (7-42) it becomes possible to derive the analytical solution to eq. (7-43) at order $O(\varepsilon^3)$, provided the forcing terms on the right-hand-side do not have a functional form identical to the homogeneous solution. When some of the forcing terms on the right hand sides of eqs. (7-43) have functional forms identical to the homogeneous solution, i.e. $\cos(\kappa_{cr} x)$, they force particular solutions of the form $x \cos(\kappa_{cr} x)$ that are not bounded as the horizontal direction increases, i.e. as $L \rightarrow \infty$. These are conditions recognized as similar to resonance. In order for the solution to be finite one needs to impose the condition that

the coefficients of these “resonant” terms vanish. As a first step, the decoupling of equations (7-43a) and (7-43b) is required.

Decoupling equations (7-43a) and (7-43b) by expressing v_3 from (7-43a) in the form

$$v_3 = \frac{1}{Gn_{cr}\beta_2} \left[RHS31 - \left(\frac{d^2}{dx^2} + \beta_1 Gn_{cr} \right) u_3 \right] \quad (7-46)$$

and substituting it into (7-43b) yields

$$(\mathcal{L}_1 \mathcal{L}_2 + \beta_o \beta_2 Gn_{cr}) u_3 = \mathcal{L}_2 (RHS31) - \beta_2 Gn_{cr} (RHS32) \quad (7-47)$$

Similarly, isolating u_3 from (7-43b) and substituting it into (7-43a) yields

$$(\mathcal{L}_1 \mathcal{L}_2 + \beta_o \beta_2 Gn_{cr}) v_3 = \mathcal{L}_1 (RHS32) - \beta_o (RHS31) \quad (7-48)$$

The interest in these derivations is to obtain the condition that guarantees a finite solution at this order, and not necessarily to derive this solution. Therefore the aim is to evaluate only the “resonant” terms on the right-hand-side of eq. (7-47) or (7-48). The evaluation of these terms is long and tedious and therefore only their final form is presented as follows

$$\begin{aligned} RHS(7-47) = & \left(\varphi_o - \frac{\kappa_{cr}^2}{Rn} \right) \left\{ Gn_{cr} \dot{A}_1 + \frac{R\kappa_{cr}^2}{\beta_4} \left(\frac{5}{2} A_{20} + C_{20} \right) A_1 - \right. \\ & Gn_{cr} \left[\frac{2\beta_5}{\beta_4} \left(\frac{A_{20}}{2} + C_{20} \right) A_1 + \beta_1 A_1 - \frac{3R}{4\beta_4} A_1^3 + \right. \\ & \left. \left. \frac{1}{\beta_4} \left(\frac{B_{20}}{2} + E_{20} \right) A_1 + \frac{1}{\beta_4} \left(\frac{A_{20}}{2} + C_{20} \right) B_1 + \beta_2 B_1 \right] \right\} - \beta_2 Gn_{cr} \dot{B}_1 + n.r.t. \end{aligned} \quad (7-49)$$

where *n.r.t.* stands for “non-resonant terms”. Substituting the relationships for the coefficients defined in eqs. (7-37), (7-38), (7-40), (7-41) and (7-24) and equating these “resonant” terms to zero produces the following equation

$$\left[p_5 + \frac{\beta_1 S_B}{(1 + S_B)} \right] \dot{A}_1 = \frac{\beta_1 p_5}{(1 + S_B)} A_1 - \frac{p_3 p_5}{\beta_4^2} \left[\frac{R \beta_1}{2(1 + S_B)} \left(\frac{5 p_2 \beta_4}{p_4} + \frac{\varphi_o}{\Delta_A} \right) + \right. \quad (7-50)$$

$$\left. \left(\frac{\beta_3 S_B}{2(1 + S_B)} - \beta_5 \right) \left(\frac{p_2 \beta_4}{p_4} + \frac{\varphi_o}{\Delta_A} \right) + 3 R \beta_4 \beta_3 - \frac{\beta_o \beta_4 R n}{2 p_4 G n_{cr}} - \frac{\beta_o}{2 \Delta_A} \right] A_1^3$$

where

$$p_2 = \left[\frac{R n \varphi_o}{G n_{cr}} - \frac{4 \beta_1}{(1 + S_B)} \right] \quad (7-51)$$

$$p_3 = \left[\frac{(\beta_1 R + \beta_3 S_B)}{(1 + S_B)} - \beta_5 \right] \quad (7-52)$$

$$p_4 = \beta_4 \left[\frac{32 \beta_1^2}{(1 + S_B)^2} - 8 \left(\frac{R n \varphi_o}{G n_{cr}} + \beta_1 \right) \frac{\beta_1}{(1 + S_B)} + \frac{2 R n \Delta_A}{G n_{cr}} \right] \quad (7-53)$$

$$p_5 = \frac{G n_{cr}}{R n} \left[\frac{R n \varphi_o}{G n_{cr}} - \frac{\beta_1}{(1 + S_B)} \right] \quad (7-54)$$

By introducing now the following notation

$$\chi = \frac{\beta_1 p_5}{p_5 (1 + S_B) + \beta_1 S_B} \quad (7-55)$$

$$s = \frac{p_3 (1 + S_B)}{\beta_1 \beta_4^2} \left[\frac{R \beta_1}{2(1 + S_B)} \left(\frac{5 p_2 \beta_4}{p_4} + \frac{\varphi_o}{\Delta_A} \right) + \right. \quad (7-56)$$

$$\left. \left(\frac{\beta_3 S_B}{2(1 + S_B)} - \beta_5 \right) \left(\frac{p_2 \beta_4}{p_4} + \frac{\varphi_o}{\Delta_A} \right) + 3 R \beta_3 \beta_4 - \frac{\beta_o \beta_4 R n}{2 p_4 G n_{cr}} - \frac{\beta_o}{2 \Delta_A} \right]$$

into eq. (7-50) one obtains the amplitude equation in the form

$$\dot{A}_1 = \chi [A_1 - s A_1^3] \quad (7-57)$$

where $\dot{A}_1 = dA_1/d\tau$.

7.7 Amplitude Equation, Bifurcation Structure and Solution

The amplitude equation (7-57) can be presented in the form

$$\frac{dA_1}{d\tau} = \chi[A_1 - sA_1^3] \quad (7-58)$$

A further simplification is accomplished by multiplying eq. (7-58) by ε^3 and reintroducing the original time scale by back-substitution of $\tau = \varepsilon^2 t$, to obtain

$$\frac{\varepsilon^2}{\varepsilon^2} \frac{d(\varepsilon A_1)}{dt} = \chi[\varepsilon^2(\varepsilon A_1) - s(\varepsilon A_1)^3] \quad (7-59)$$

By introducing the notation

$$A = \varepsilon A_1 \quad (7-60)$$

into eq. (7-59) it yields

$$\frac{dA}{dt} = \chi[\varepsilon^2 A - sA^3] \quad (7-61)$$

or the alternative form

$$\frac{dA}{dt} = \chi[\varepsilon^2 - sA^2]A \quad (7-62)$$

The steady state solution to the amplitude equation (7-62) corresponding to the post-transient solution of u_1 and v_1 , is obtained by setting the time derivative term in (7-62) equal to zero, in the form

$$[\varepsilon^2 - sA^2]A = 0 \quad (7-63)$$

The solution to (7-63) is

$$A_{(o)} = 0 \quad \forall \quad Gn \leq Gn_{cr} \quad (7-64)$$

corresponding to the case when the stationary solutions are stable, and

$$A^2 = \frac{\varepsilon^2}{s} \quad \forall \quad Gn \geq Gn_{cr} \quad (7-65)$$

or

$$A_{1,2} = \pm \frac{\varepsilon}{\sqrt{s}} \quad \forall \quad Gn \geq Gn_{cr} \quad (7-66)$$

corresponding to the case when the stationary solutions loose stability in the linear sense. Replacing the definition of ε from eq. (7-3) into eq. (7-66) transforms the steady state solution to the form that is explicitly expressed in terms of Gn

$$A_{1,2} = \pm \sqrt{\frac{(Gn - Gn_{cr})}{s Gn_{cr}}} \quad (7-67)$$

The graphical description of the amplitude A based on (7-67) is presented in Figure 7.1 representing a bifurcation diagram. From eq. (7-67) it is evident that for $Gn \geq Gn_{cr}$ the expression under the square root is non-negative as long as $s > 0$. For the values of parameters used in the following calculations $s > 0$ and therefore for this parameter selection the bifurcation is forward. From the bifurcation diagram presented in Figure 7.1 one identifies this type of bifurcation as a pitchfork bifurcation.

From eq. (7-62) the transient solution of A can be derived by direct integration in the form

$$A^2 = \frac{\varepsilon^2}{s \left[1 + \left(\frac{\varepsilon^2}{s r_o^2} - 1 \right) \exp(-2 \chi \varepsilon^2 t) \right]} \quad (7-68)$$

where A_o represents the initial condition of A .

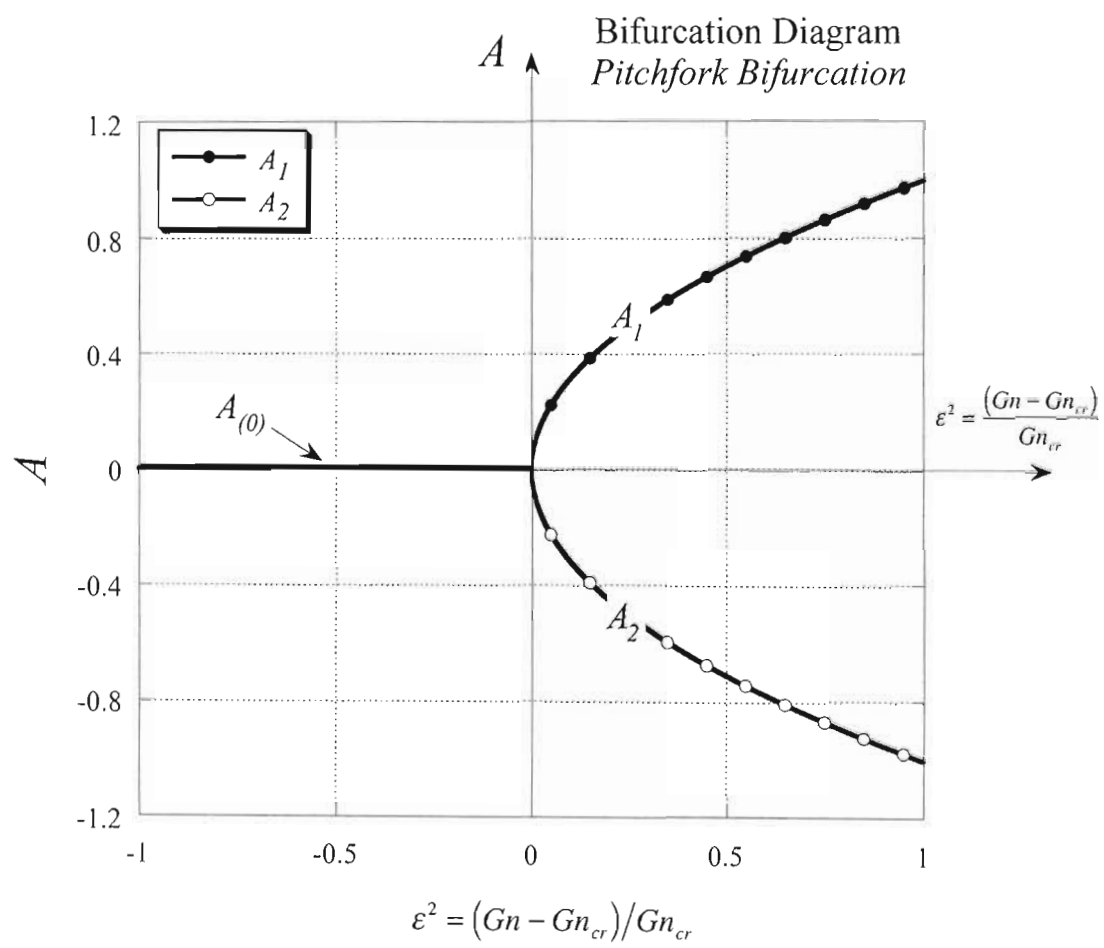


Figure 7.1: Bifurcation diagram identifying a forward pitchfork bifurcation.

7.8 Complete Weak Nonlinear Solution

The complete weak nonlinear solution is obtained by replacing eqs. (7-68), (7-18) and (7-60) into the $O(\varepsilon)$ solutions, eq. (7-12), in the form

$$\varepsilon u_1 = \frac{\varepsilon^2}{\sqrt{s \left[1 + \left(\frac{\varepsilon^2}{s r_o^2} - 1 \right) \exp(-2 \chi \varepsilon^2 t) \right]}} \cos(\kappa_{cr} x) \quad (a)$$

(7-69)

$$\varepsilon v_1 = -\frac{\beta_1}{\beta_2} \frac{S_B}{(1 + S_B)} \frac{\varepsilon^2}{\sqrt{s \left[1 + \left(\frac{\varepsilon^2}{s r_o^2} - 1 \right) \exp(-2 \chi \varepsilon^2 t) \right]}} \cos(\kappa_{cr} x) \quad (b)$$

Then, substituting these solutions into the expansions of u and v , (7-4) and (7-5), up to order $O(\varepsilon)$ yields

$$u = u_s + \varepsilon u_1 = u_s + \frac{\varepsilon^2}{\sqrt{s \left[1 + \left(\frac{\varepsilon^2}{s r_o^2} - 1 \right) \exp(-2 \chi \varepsilon^2 t) \right]}} \cos(\kappa_{cr} x) \quad (7-70)$$

$$v = v_s + \varepsilon v_1 = v_s - \frac{\beta_1}{\beta_2} \frac{S_B}{(1 + S_B)} \frac{\varepsilon^2}{\sqrt{s \left[1 + \left(\frac{\varepsilon^2}{s r_o^2} - 1 \right) \exp(-2 \chi \varepsilon^2 t) \right]}} \cos(\kappa_{cr} x) \quad (7-71)$$

At steady state these complete weak nonlinear solutions take the form

$$u = u_s + \varepsilon u_1 = u_s + \varepsilon \frac{1}{\sqrt{s}} \cos(\kappa_{cr} x) \quad (7-72)$$

$$v = v_s + \varepsilon v_1 = v_s - \varepsilon \frac{\beta_1}{\beta_2 \sqrt{s}} \frac{S_B}{(1 + S_B)} \cos(\kappa_{cr} x) \quad (7-73)$$

7.9 Numerical Method of Solution

The governing equations, in one dimension, to be solved numerically are identical to (7-2) and are presented in the form

$$\left\{ \begin{array}{l} \frac{\partial u}{\partial t} = \frac{1}{Gn} \frac{\partial^2 u}{\partial x^2} + \left[1 - u + \frac{(v-1)}{(1+R u)} \right] u \\ \frac{\partial v}{\partial t} = \frac{1}{Rn} \frac{\partial^2 u}{\partial x^2} + \gamma_o - \beta_o u + \varphi_o v \end{array} \right. \quad \begin{array}{l} \text{(a)} \\ \text{(b)} \end{array} \quad (7-74)$$

The objective of the numerical solution is to use a standard method that provides sufficiently accurate results to compare the weak nonlinear solution to them. Numerical efficiency is not an objective. Therefore, a simple explicit method of solution is used for this purpose. A numerical stability condition on the time step is applied in order to ensure that the results are numerically stable. Since the non-linearity appears in the algebraic terms there is no need for special treatment of this non-linearity. A graphical representation of the numerical grid used in the numerical solution is presented in Figure 7.2. The numerical scheme based on the explicit method for $t_j = j \Delta t$ and $x_i = i \Delta x$, where Δt is the time step and Δx is the step size in the x direction, takes the form

$$\frac{u_{i,j+1} - u_{ij}}{\Delta t} = \frac{1}{Gn} \frac{u_{i+1,j} - 2u_{ij} + u_{i-1,j}}{\Delta x^2} + \left[1 - u_{ij} + \frac{(v_{ij} - 1)}{(1 + R u_{ij})} \right] u_{ij} \quad (7-75)$$

$$\frac{v_{i,j+1} - v_{ij}}{\Delta t} = \frac{1}{Rn} \frac{v_{i+1,j} - 2v_{ij} + v_{i-1,j}}{\Delta x^2} + \gamma_o - \beta_o u_{ij} + \varphi_o v_{ij} . \quad (7-76)$$

By using (7-75) and (7-76) the values of $u_{i,j+1}$ and $v_{i,j+1}$ at the next time step $(j+1)$ are expressed explicitly in terms of known values from the previous time step j , in the form

$$u_{i,j+1} = u_{ij} + \frac{r_\Delta}{Gn} (u_{i+1,j} - 2u_{ij} + u_{i-1,j}) + \Delta t \left[1 - u_{ij} + \frac{(v_{ij} - 1)}{(1 + R u_{ij})} \right] u_{ij} \quad (7-77)$$

$$v_{i,j+1} = v_{ij} + \frac{r_\Delta}{Rn} (v_{i+1,j} - 2v_{ij} + v_{i-1,j}) + \Delta t (\gamma_o - \beta_o u_{ij} + \varphi_o v_{ij}) \quad (7-78)$$

where $r_\Delta = \Delta t / \Delta x^2$. The numerical scheme (7-77) and (7-78) applies to all values of $j=1,2,3, \dots$ and to values of $x_i, \forall i=1,2, \dots, N-1$. Since the explicit boundary values are not known because the boundary conditions are of the form

$$\left(\frac{\partial u}{\partial x} \right)_{x=0,L} = 0 \quad \text{and} \quad \left(\frac{\partial v}{\partial x} \right)_{x=0,L} = 0 \quad (7-79)$$

the following conditions are obtained by introducing “imaginary” grid-points at $x_{-1} = -\Delta x \quad \forall i = -1$ and at $x_{N+1} = (N+1)\Delta x = L + \Delta x \quad \forall i = N+1$, (see Figure 7.2) and discretizing eq. (7-79), in the form

$$\frac{u_{1,j} - u_{-1,j}}{\Delta x} = 0, \quad \frac{u_{N+1,j} - u_{N-1,j}}{\Delta x} = 0, \quad \frac{v_{1,j} - v_{-1,j}}{\Delta x} = 0, \quad \frac{v_{N+1,j} - v_{N-1,j}}{\Delta x} = 0 \quad (7-80)$$

leading to

$$u_{-1,j} = u_{1,j}, \quad u_{N+1,j} = u_{N-1,j}, \quad v_{-1,j} = v_{1,j}, \quad v_{N+1,j} = v_{N-1,j} \quad (7-81)$$

With these derivations the numerical scheme (7-77) and (7-78) can be applied to values of $x_i, \forall i=1,2, \dots, N-1$, while the boundary values are being evaluated using (7-81) in (7-77) and (7-78) in the form

$$u_{0,j+1} = u_{0,j} + \frac{2r_\Delta}{Gn} (u_{1,j} - u_{0,j}) + \Delta t \left[1 - u_{0,j} + \frac{(v_{0,j} - 1)}{(1 + R u_{0,j})} \right] u_{0,j} \quad (7-82)$$

$$u_{N,j+1} = u_{N,j} + \frac{2r_\Delta}{Gn} (u_{N-1,j} - u_{N,j}) + \Delta t \left[1 - u_{N,j} + \frac{(v_{N,j} - 1)}{(1 + R u_{N,j})} \right] u_{N,j} \quad (7-83)$$

$$v_{0,j+1} = v_{0,j} + \frac{2r_\Delta}{Rn} (v_{1,j} - v_{0,j}) + \Delta t (\gamma_o - \beta_o u_{0,j} + \varphi_o v_{0,j}) \quad (7-84)$$

$$v_{N,j+1} = v_{N,j} + \frac{2r_\Delta}{Rn} (v_{N-1,j} - v_{N,j}) + \Delta t (\gamma_o - \beta_o u_{N,j} + \varphi_o v_{N,j}) \quad (7-85)$$

The value of L was selected to be consistent with the critical wave number that was evaluated via the linear stability analysis and weak nonlinear solution, i.e.

$$\kappa_{cr} L = m\pi \quad \forall m = 1, 2, 3, \dots \quad \Rightarrow \quad L = \frac{m\pi}{\kappa_{cr}} = \frac{\pi}{\kappa_{cr}}, \frac{2\pi}{\kappa_{cr}}, \frac{3\pi}{\kappa_{cr}}, \dots \quad (7-86)$$

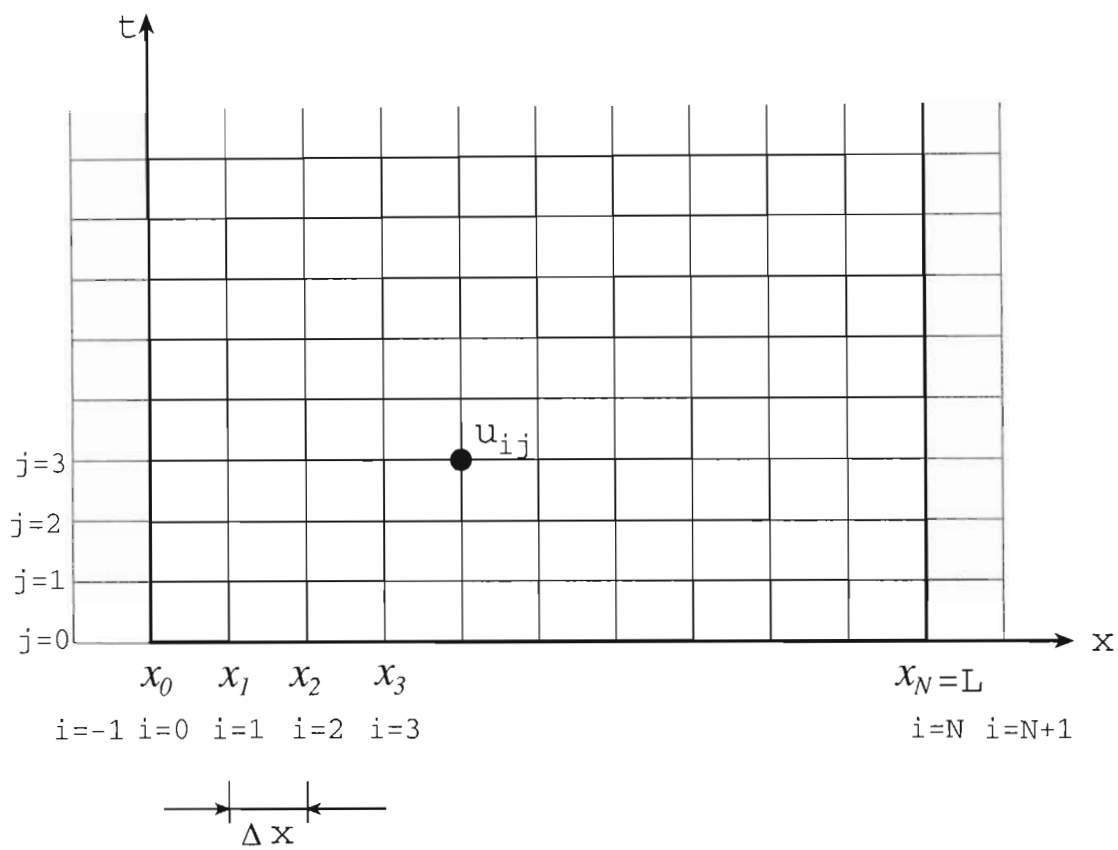


Figure 7.2: Graphical representation of the numerical grid used in the numerical solution.

7.10 Results and Discussion

In all numerical computations a grid size of 201 grid points ($N = 200$) in the x direction was used. The following parameter values were applied to all computations: $Rn = 1$, $R = 10$, $\gamma_o = 0.0675$, $\beta_o = 3$ and $\varphi_o = -0.4$. They correspond to conditions identified in section 4.3.7 as sufficient to guarantee linear stability of the stationary solutions to SHoP. The corresponding values of $\kappa_{cr} = 0.82964$, $Gn_{cr} = 5.70269$, $u_s = 0.225$, $v_s = -1.51875$, $\psi_A = -0.08846 < 0$ and $\Delta_A = 0.083077 > 0$ are consistent with these parameters. The value of L selected to be consistent with the critical wave number was evaluated to be $L = 3.7867$. Therefore the grid size in terms of the size of the increment in the x direction was taken as $\Delta x = 0.0189335$ and the time step was taken as $\Delta t = 10^{-5}$ in all computations. Accordingly, the ratio $r_\Delta = \Delta t / \Delta x^2$ was evaluated to be $r_\Delta = \Delta t / \Delta x^2 = 2.7896 \cdot 10^{-2}$. The latter is a sufficiently small value to guarantee numerical stability over the whole range of values of Gn considered. The value of the parameter Gn was varied gradually from a sub-critical value of $Gn = 5 < Gn_{cr} = 5.70269$ and up to a large supercritical value of $Gn = 25 > Gn_{cr} = 5.70269$. The computations were allowed to run for sufficiently long time until no more changes (to seven significant digits) in the values of u and v occurred. This identified the conditions of steady state. The weak nonlinear solution derived in the previous sections was used to evaluate the analytical values of u and v , which were compared to the numerical results.

The results of this comparison are presented in Figures 7.3-7.22. Initially, a sub-critical value of Gn , i.e. $Gn = 5 < Gn_{cr} = 5.70269$, was used. The results corresponding to this value of Gn are presented in Fig. 7.3 for $u(x)$, in Fig. 7.4 for $v(x)$ and the graphical representation of v vs. u on the phase plane is presented in Fig. 7.5. It is evident from these figures that the solution stabilizes at the stationary solution $u_s = 0.225$, $v_s = -1.51875$, as expected for this sub-critical case. The results corresponding to a slightly super-critical value of Gn , $Gn = 5.71 > Gn_{cr} = 5.70269$, are presented in Fig. 7.6 for $u(x)$, in Fig. 7.7 for $v(x)$ and the graphical representation of v vs. u on the phase plane is presented in Fig. 7.8. The comparison between the weak nonlinear solution and the numerical results show an excellent match. The difference between the two solutions was evaluated and plotted in Figure 7.9

expressed in terms of $\Delta u(x)$. From the figure it is observed that this difference is less than $\pm 2 \cdot 10^{-3}$, an average relative difference of less than 1%. An even larger super-critical value of Gn was used to present the results for $Gn = 7 > Gn_{cr} = 5.70269$. These results are presented in Fig. 7.10 for $u(x)$, in Fig. 7.11 for $v(x)$ and the graphical representation of v vs. u on the phase plane is presented in Fig. 7.12. The comparison between the weak nonlinear solution and the numerical results show again an excellent match. The difference between the two solutions was evaluated and plotted in Figure 7.13, expressed in terms of $\Delta u(x)$. From the figure it can be observed that this difference is less than $\pm 8 \cdot 10^{-3}$. The results corresponding to a large super-critical value of Gn , i.e. $Gn = 15 > Gn_{cr} = 5.70269$, are presented in Fig. 7.14 for $u(x)$, in Fig. 7.15 for $v(x)$ and the graphical representation of v vs. u on the phase plane is presented in Fig. 7.16. The loss of accuracy of the weak nonlinear solution is evident at this value of Gn , which is quite far away from the critical one. Actually, the corresponding value of ε is $\varepsilon = \sqrt{(Gn - Gn_{cr})/Gn_{cr}} = 1.2768$, which certainly violates the asymptotic expansion condition that $\varepsilon \ll 1$. At even larger values of Gn , e.g. $Gn = 20 > Gn_{cr} = 5.70269$, the solution starts showing signs of qualitative change as presented based on numerical results only, in Fig. 7.17 for $u(x)$, in Fig. 7.18 for $v(x)$ and in Fig. 7.19 for the graphical representation of v vs. u on the phase plane. At a value of $Gn = 25$ the numerical solution provides evidence of the appearance of the second Fourier mode, i.e. the weak nonlinear solution takes the form

$$u = u_s + \varepsilon u_1 = u_s + A^{(2)} \cos(2\kappa_{cr} x) \quad (7-87)$$

$$v = v_s + \varepsilon v_1 = v_s + B^{(2)} \cos(2\kappa_{cr} x) \quad (7-88)$$

The results corresponding to this large super-critical value of Gn , i.e. $Gn = 25 > Gn_{cr} = 5.70269$, are presented in Fig. 7.20 for $u(x)$, in Fig. 7.21 for $v(x)$ and the graphical representation of v vs. u on the phase plane is presented in Fig. 7.22, where eqs. (7-87) and (7-88) were used for evaluating the weak nonlinear solution. The second Fourier mode in the solution is evident and is captured also by the weak nonlinear solution although the accuracy of the latter suffers due to the large distance from Gn_{cr} .

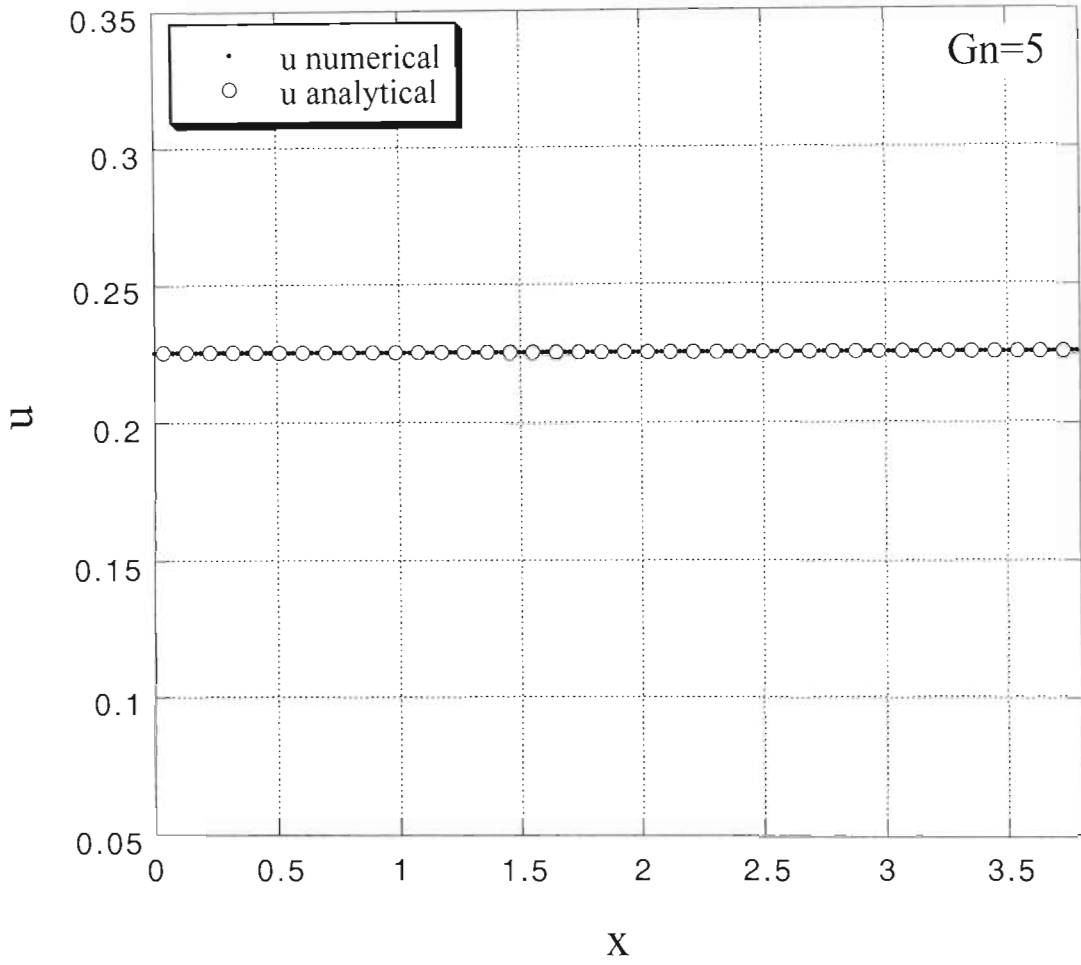


Figure 7.3: Graphical representation of the steady state weak nonlinear solution $u(x)$ compared to the numerical results for a sub-critical value of Gn , i.e. $Gn = 5 < Gn_{cr} = 5.70269$. The solution stabilizes at the stationary solution $u_s = 0.225$.

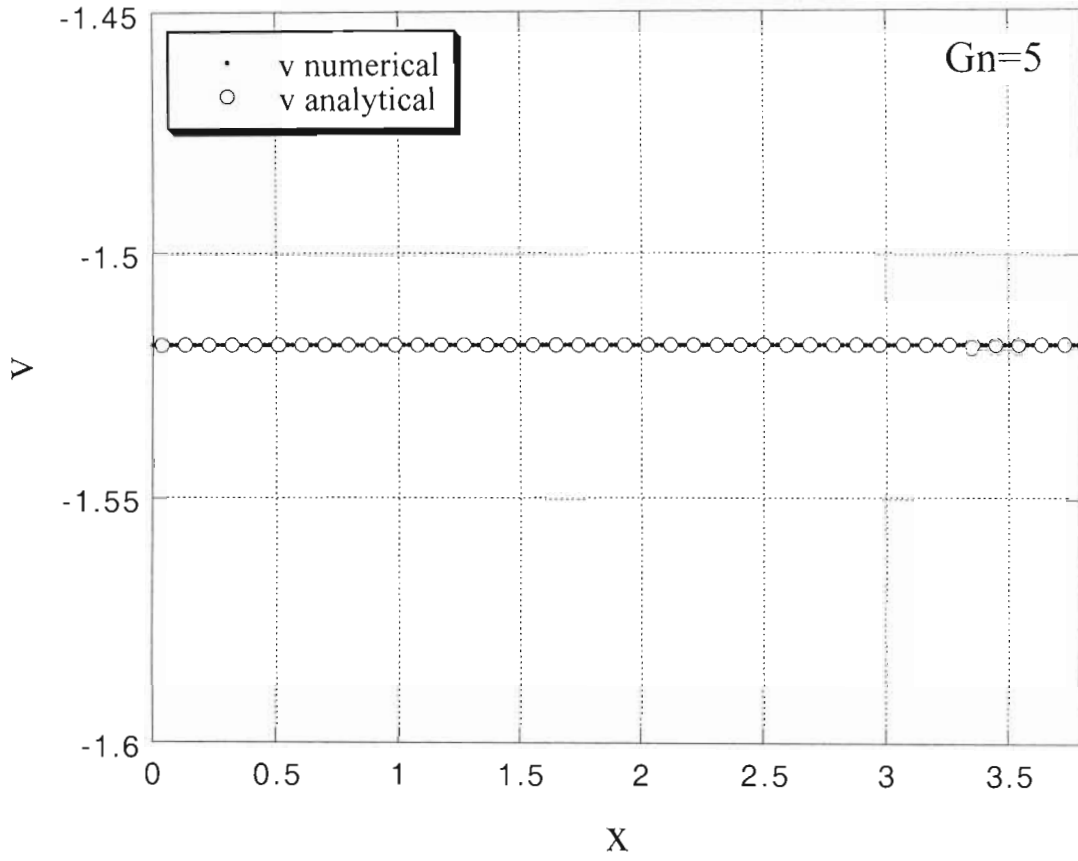


Figure 7.4: Graphical representation of the steady state weak nonlinear solution $v(x)$ compared to the numerical results for a sub-critical value of Gn , i.e. $Gn = 5 < Gn_{cr} = 5.70269$. The solution stabilizes at the stationary solution $v_s = -1.51875$.

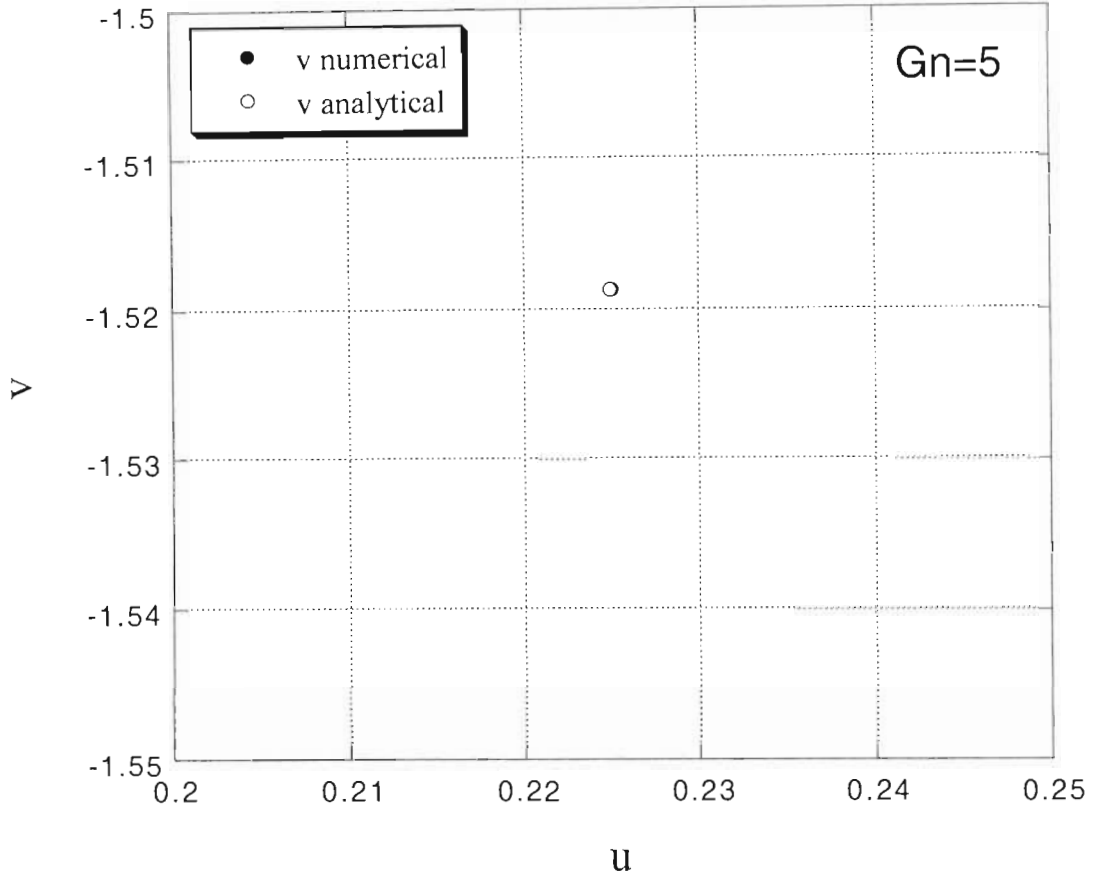


Figure 7.5: Graphical representation of the steady state weak nonlinear solution v vs. u on the phase plane compared to the numerical results for a sub-critical value of Gn , i.e. $Gn = 5 < Gn_{cr} = 5.70269$. The solution stabilizes at the stationary solution $u_s = 0.225$, $v_s = -1.51875$.

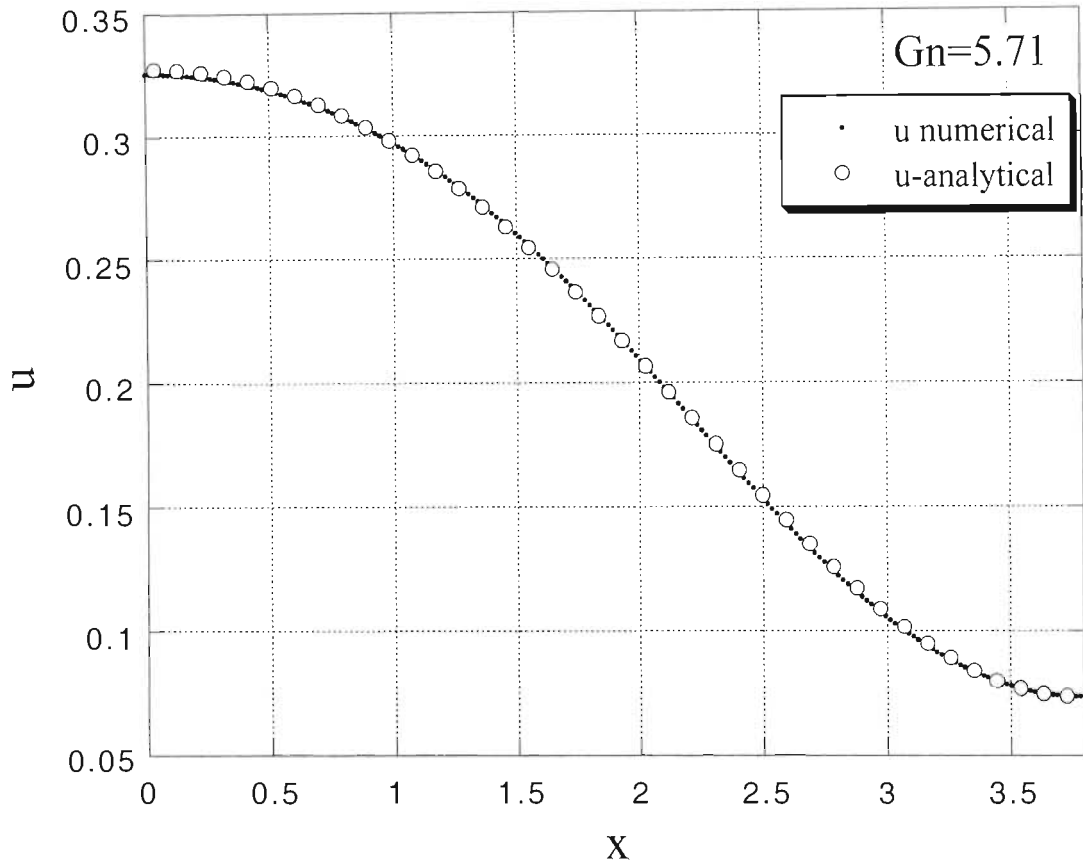


Figure 7.6: Graphical representation of the steady state weak nonlinear solution $u(x)$ compared to the numerical results for a slightly super-critical value of Gn , i.e. $Gn = 5.71 > Gn_{cr} = 5.70269$.

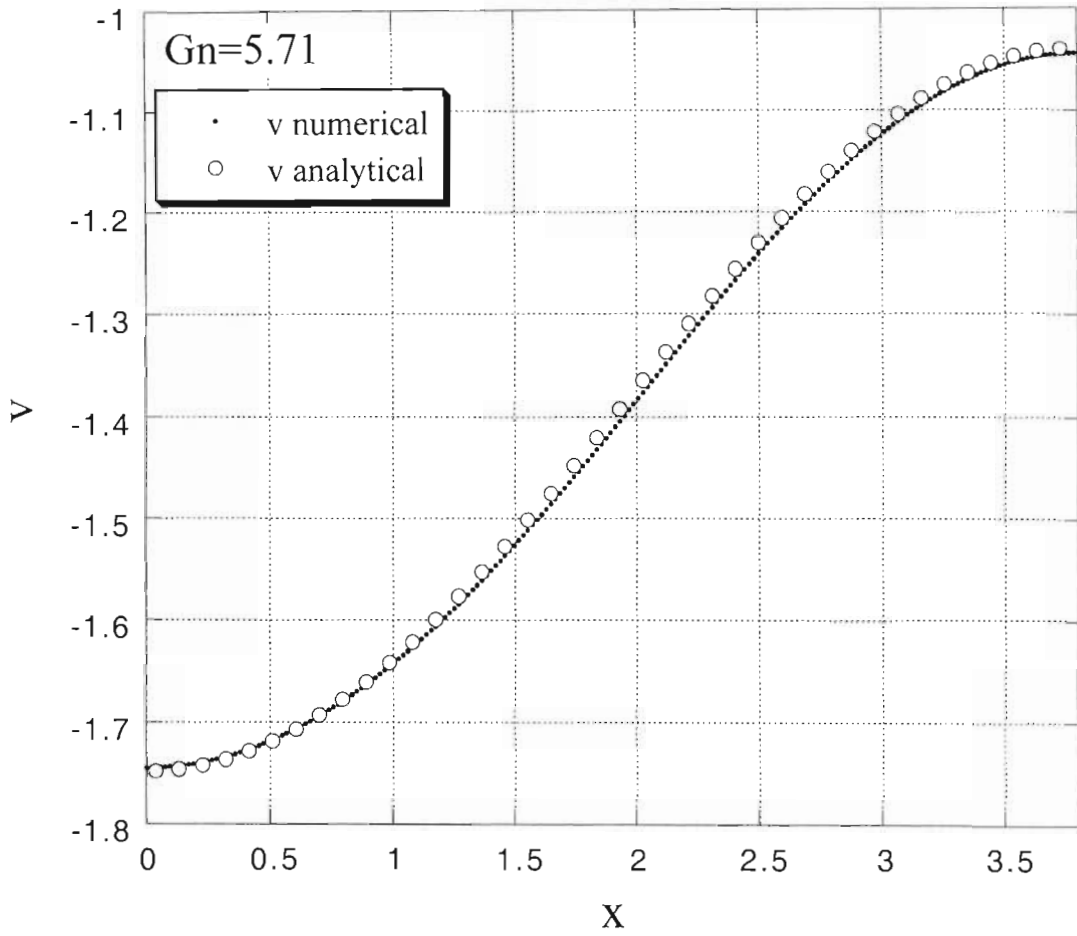


Figure 7.7: Graphical representation of the steady state weak nonlinear solution $v(x)$ compared to the numerical results for a slightly super-critical value of Gn , i.e. $Gn = 5.71 > Gn_{cr} = 5.70269$.

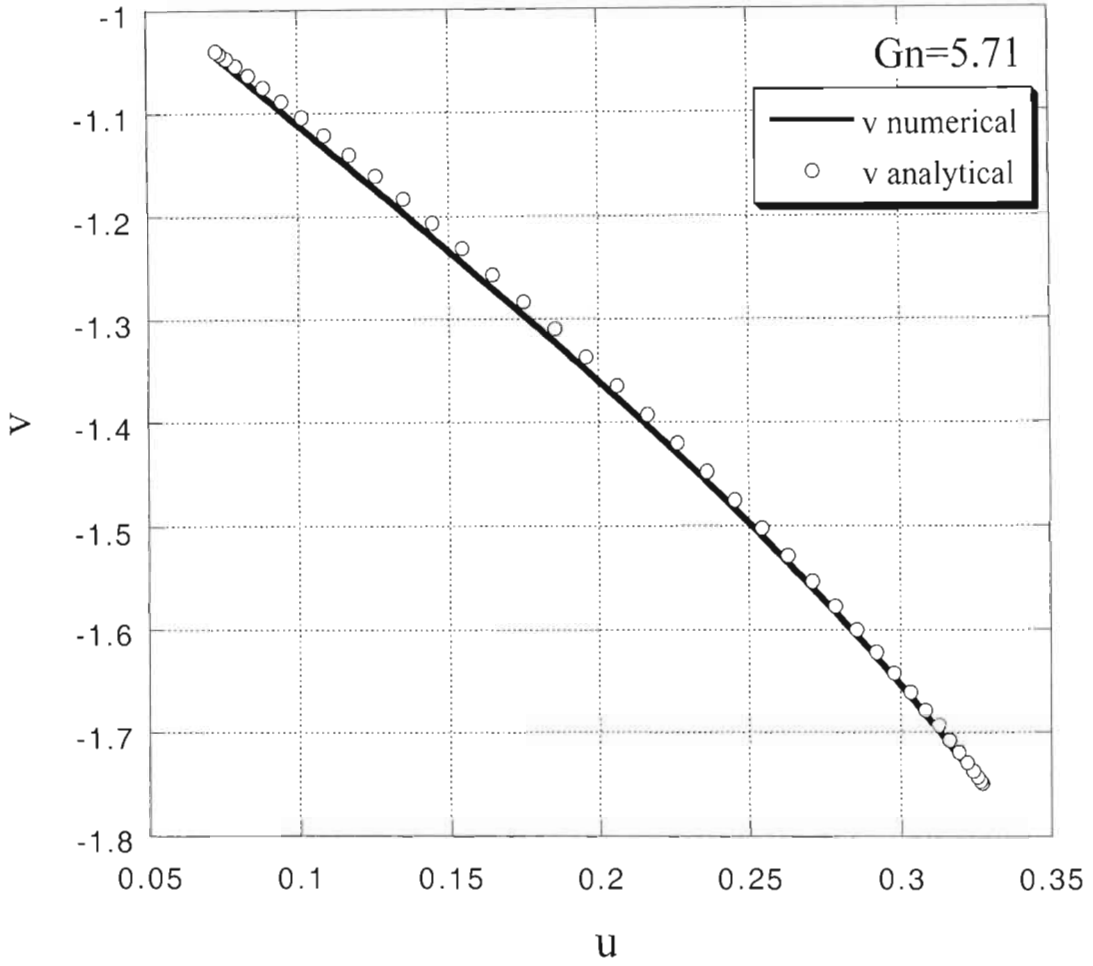


Figure 7.8: Graphical representation of the steady state weak nonlinear solution v vs. u on the phase plane compared to the numerical results for a slightly super-critical value of Gn , i.e. $Gn = 5.71 > Gn_{cr} = 5.70269$.

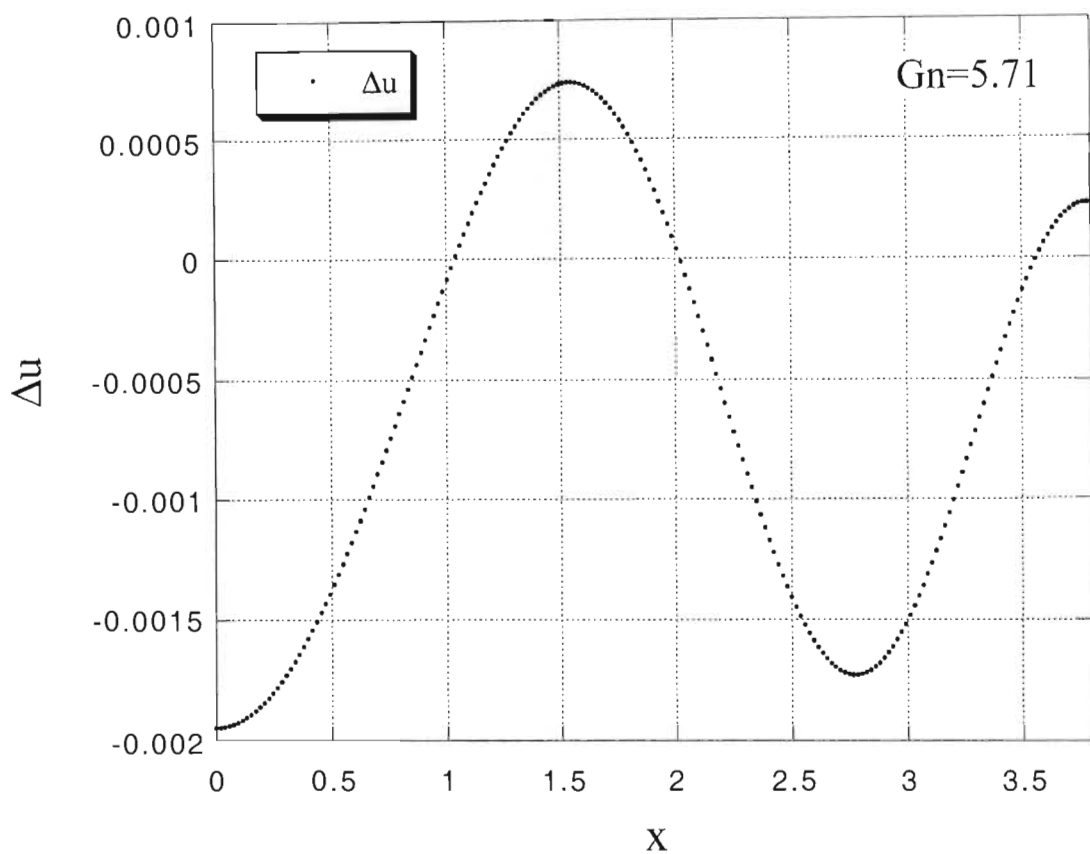


Figure 7.9: Graphical representation of the difference between the steady state weak nonlinear solution and to the numerical results expressed by $\Delta u(x)$, for a slightly super-critical value of Gn , i.e. $Gn = 5.71 > Gn_{cr} = 5.70269$. The difference is less than $\pm 2 \cdot 10^{-3}$.

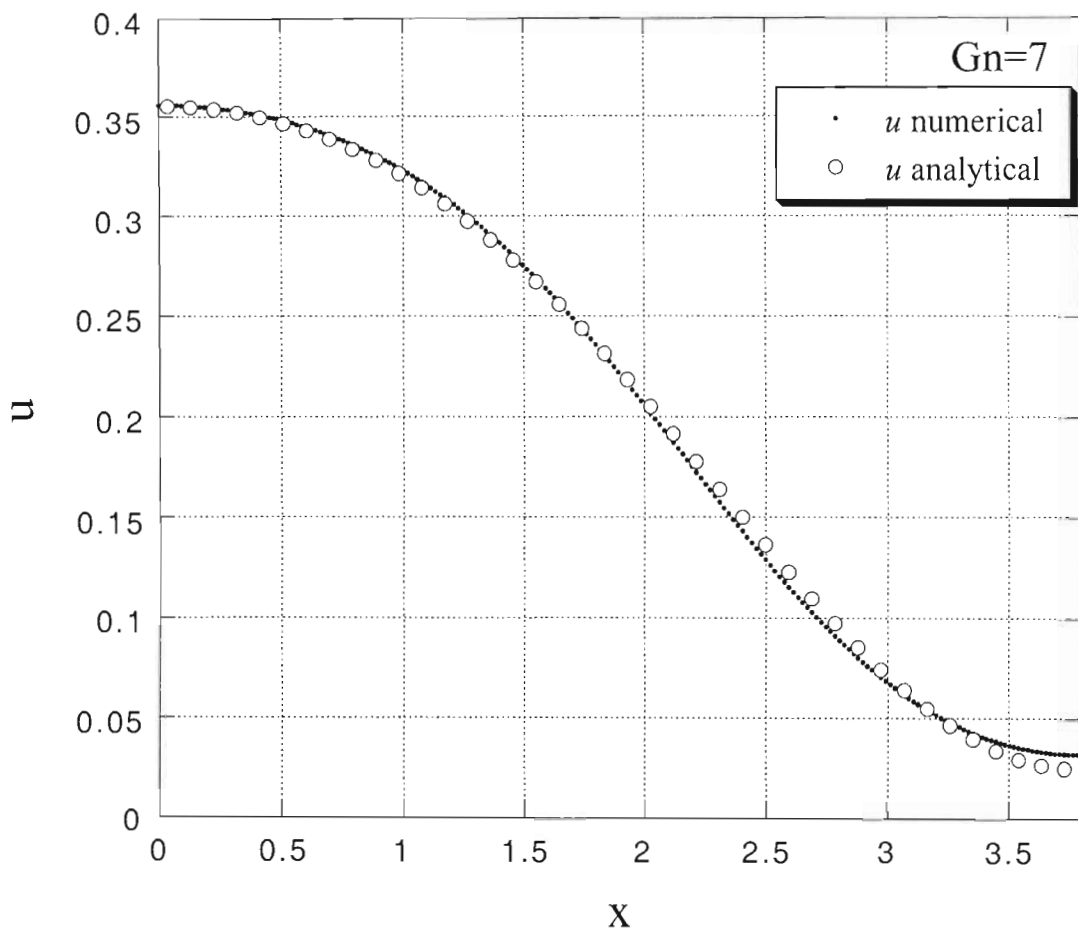


Figure 7.10: Graphical representation of the steady state weak nonlinear solution $u(x)$ compared to the numerical results for a super-critical value of Gn , i.e. $Gn = 7 > Gn_{cr} = 5.70269$.

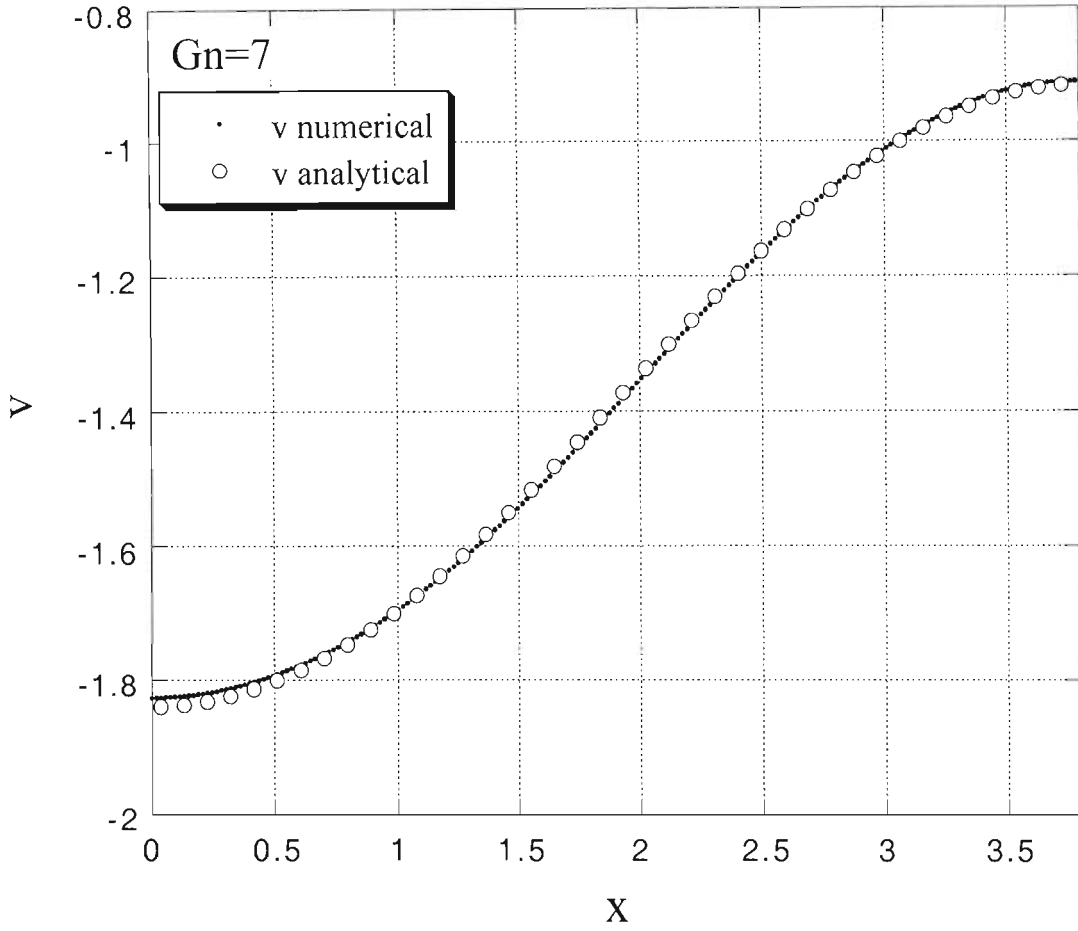


Figure 7.11: Graphical representation of the steady state weak nonlinear solution $v(x)$ compared to the numerical results for a super-critical value of Gn , i.e. $Gn = 7 > Gn_{cr} = 5.70269$.

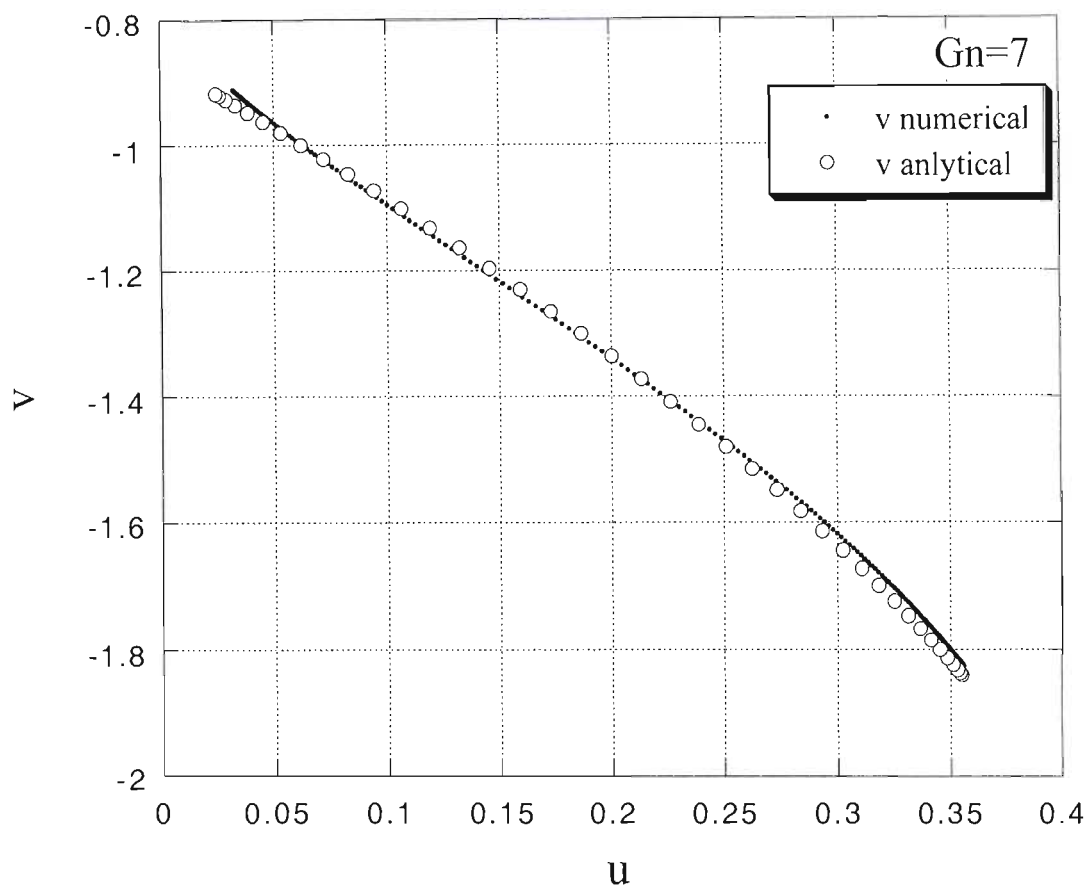


Figure 7.12: Graphical representation of the steady state weak nonlinear solution v vs. u on the phase plane compared to the numerical results for a super-critical value of Gn , i.e. $Gn = 7 > Gn_{cr} = 5.70269$.

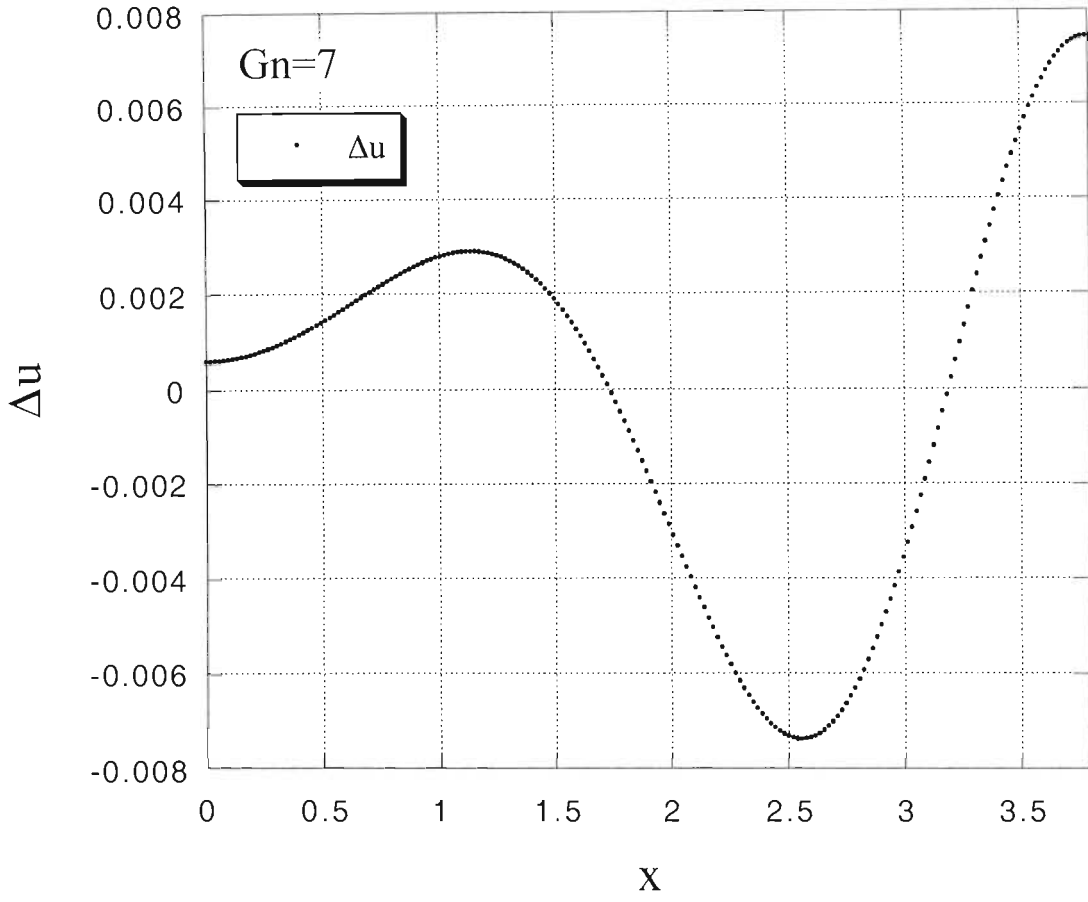


Figure 7.13: Graphical representation of the difference between the steady state weak nonlinear solution and to the numerical results expressed by $\Delta u(x)$, for a super-critical value of Gn , i.e. $Gn = 7 > Gn_{cr} = 5.70269$. The difference is less than $\pm 8 \cdot 10^{-3}$.

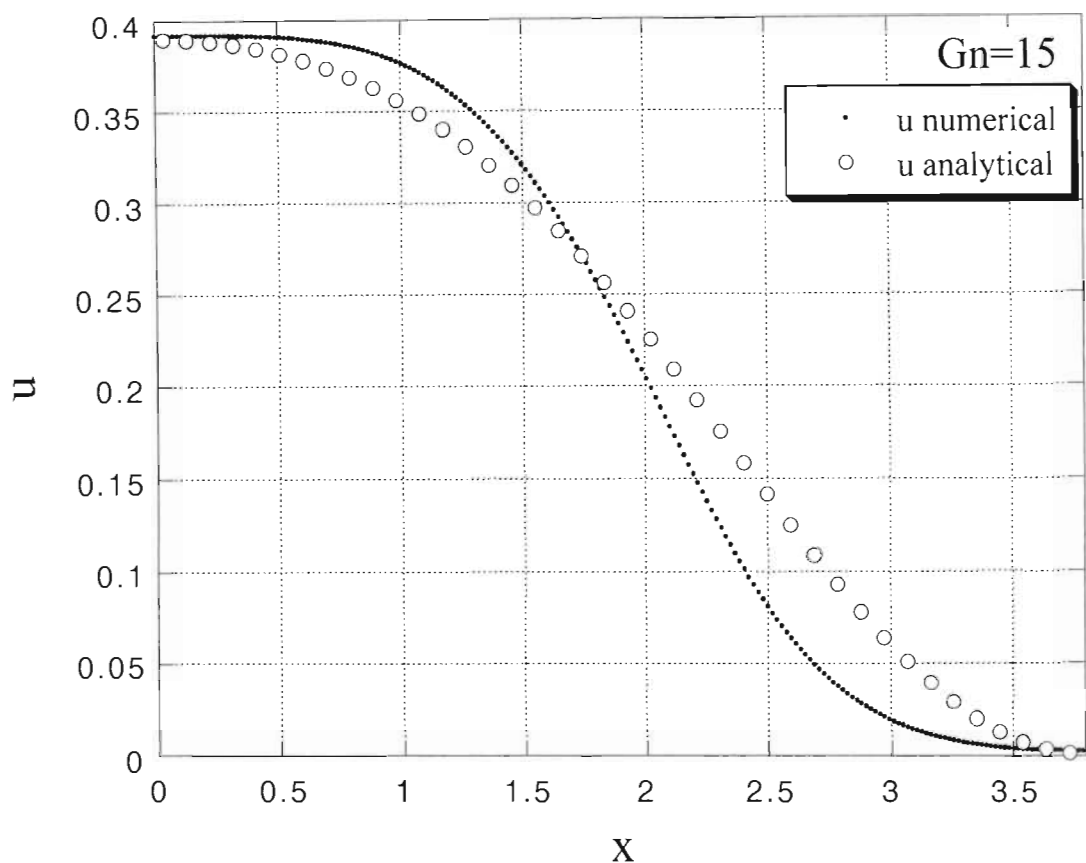


Figure 7.14: Graphical representation of the steady state weak nonlinear solution $u(x)$ compared to the numerical results for a large super-critical value of Gn , i.e. $Gn = 15 > Gn_{cr} = 5.70269$. The breakdown of the accuracy of the weak nonlinear solution is evident.

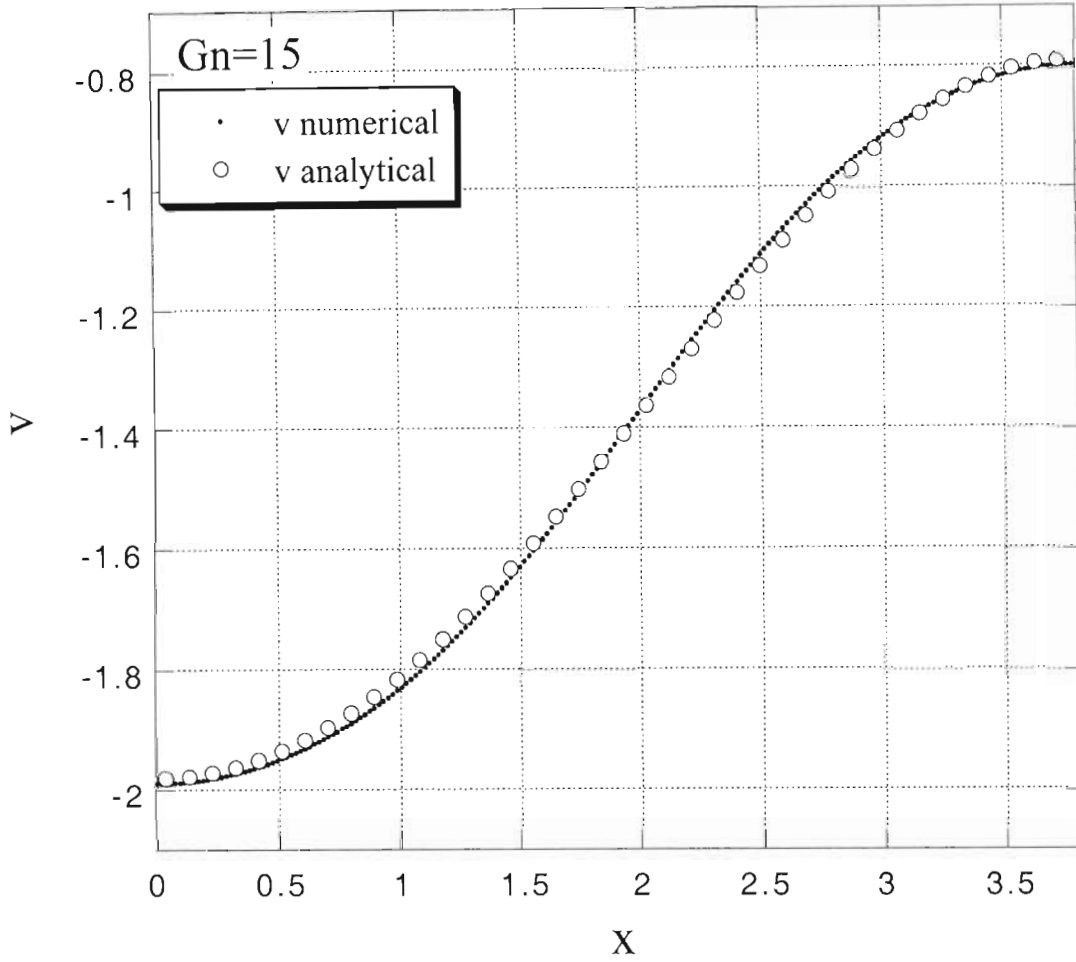


Figure 7.15: Graphical representation of the steady state weak nonlinear solution $v(x)$ compared to the numerical results for a large super-critical value of Gn , i.e. $Gn = 15 > Gn_{cr} = 5.70269$. The breakdown of the accuracy of the weak nonlinear solution is less evident in the solution for $v(x)$.

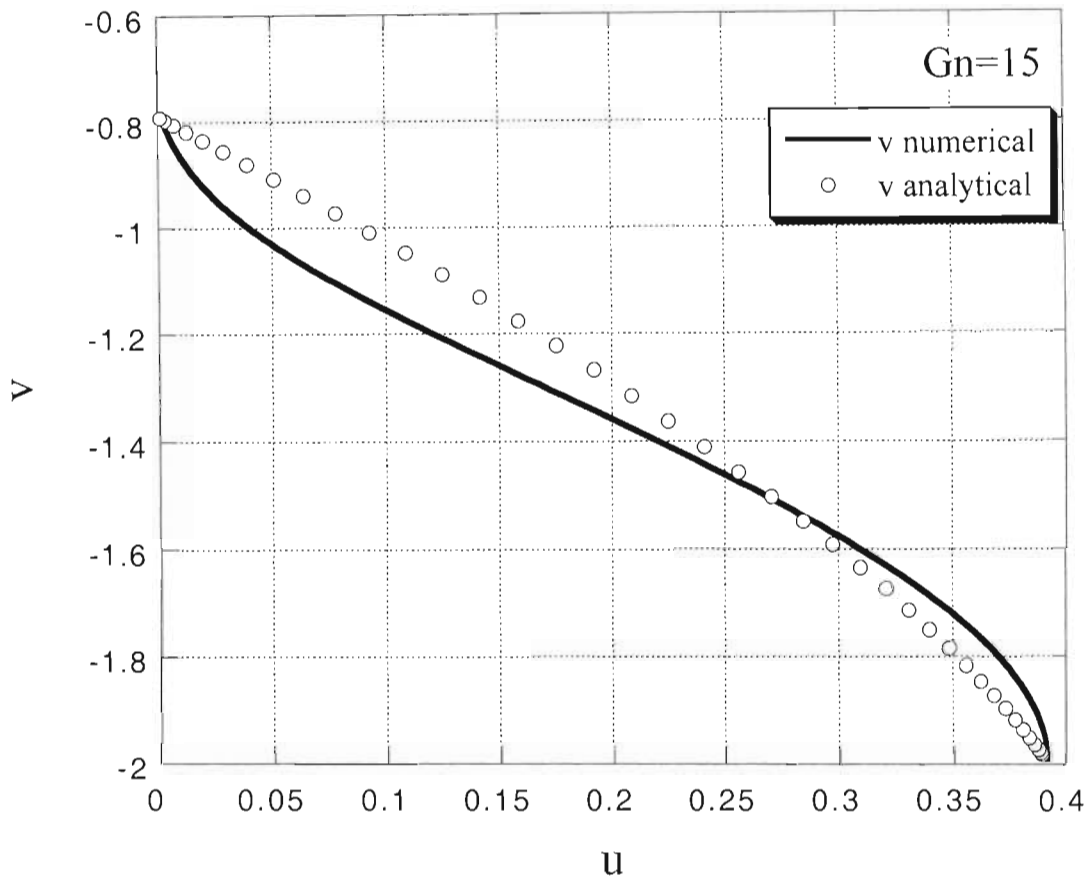


Figure 7.16: Graphical representation of the steady state weak nonlinear solution v vs. u on the phase plane compared to the numerical results for a large super-critical value of Gn , i.e. $Gn = 15 > Gn_{cr} = 5.70269$. The breakdown of the accuracy of the weak nonlinear solution is evident.

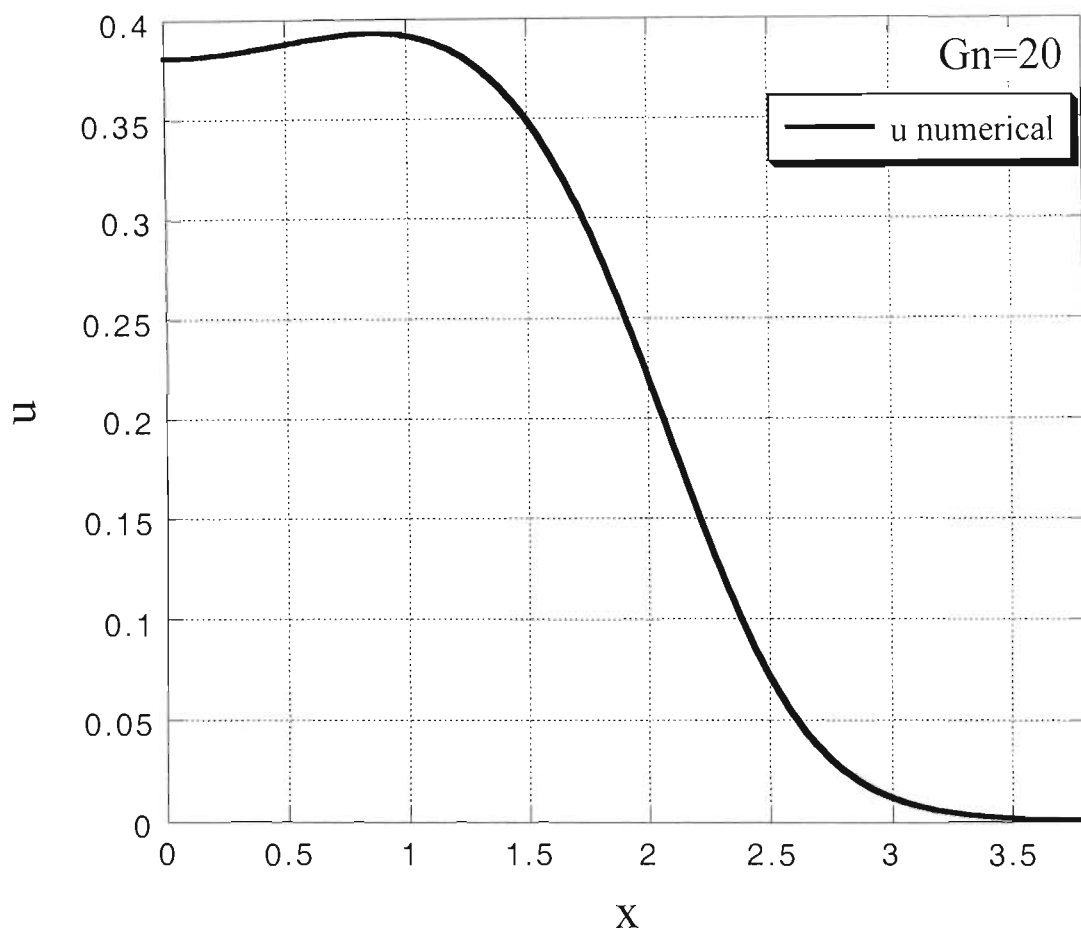


Figure 7.17: Graphical representation of the steady state numerical results of $u(x)$ for a large super-critical value of Gn , i.e. $Gn = 20 > Gn_{cr} = 5.70269$.

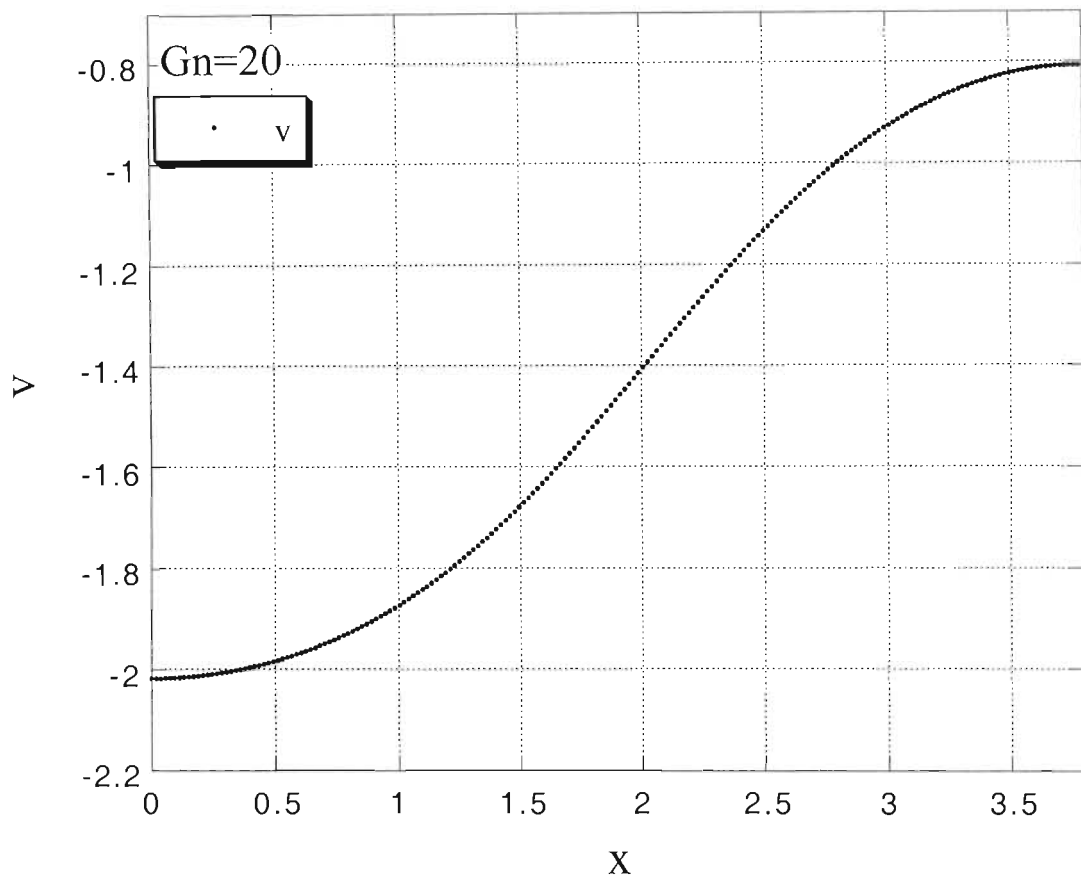


Figure 7.18: Graphical representation of the steady state numerical results of $v(x)$ for a large super-critical value of Gn , i.e. $Gn = 20 > Gn_{cr} = 5.70269$.

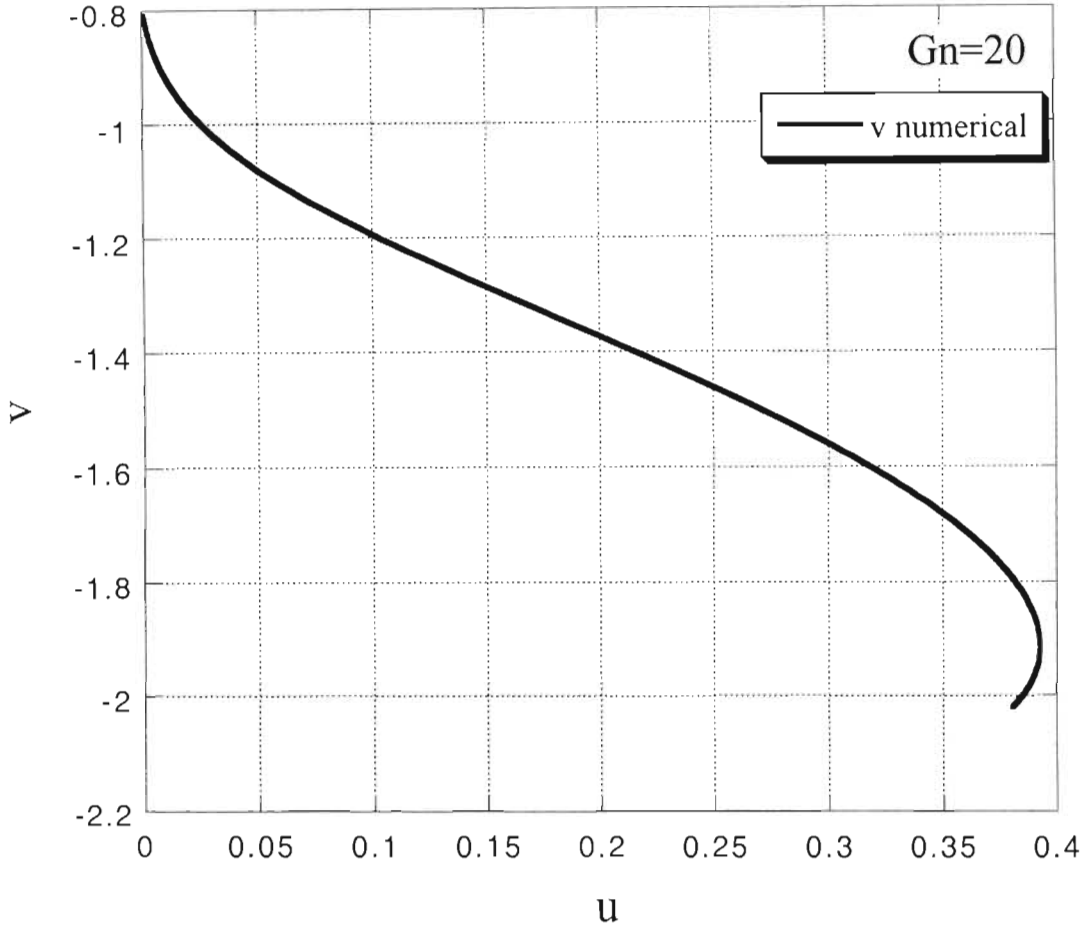


Figure 7.19: Graphical representation of the steady state numerical results v vs. u on the phase plane for a large super-critical value of Gn , i.e. $Gn = 20 > Gn_{cr} = 5.70269$.

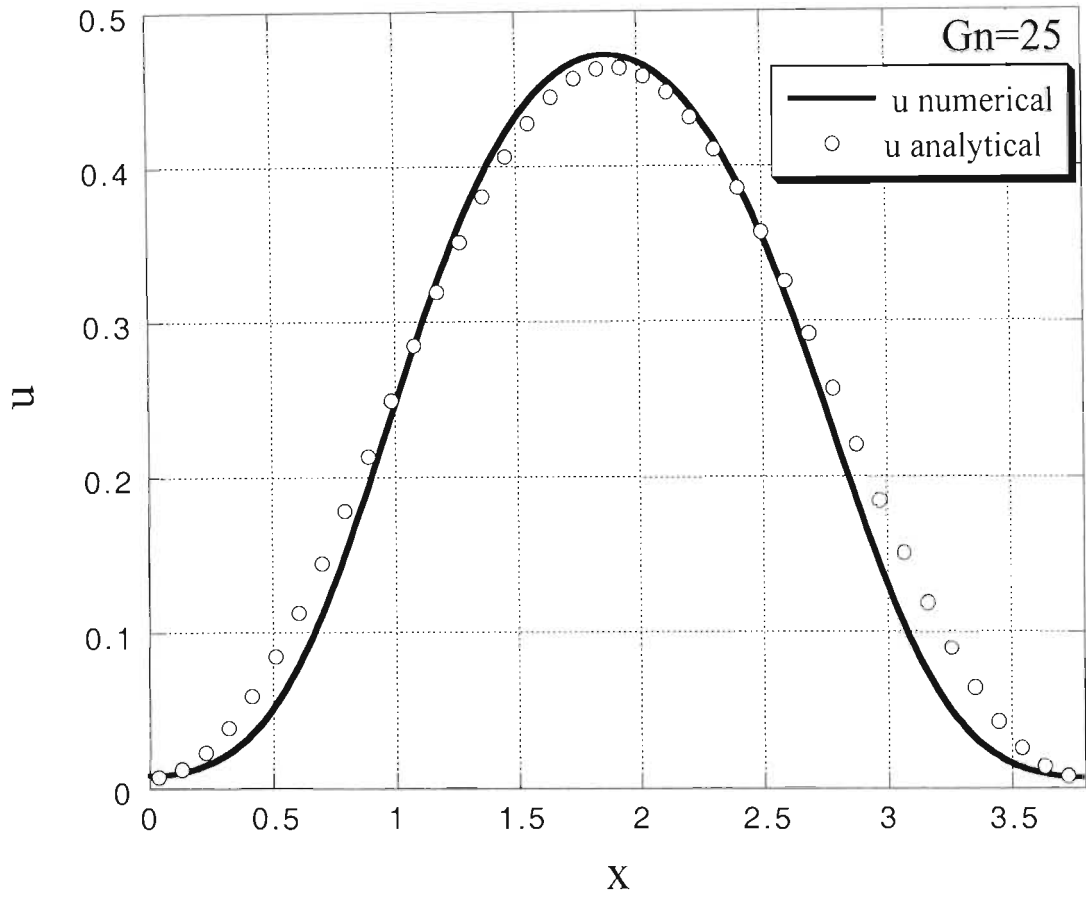


Figure 7.20: Graphical representation of the steady state weak nonlinear solution $u(x)$ compared to the numerical results for a super-critical value of Gn , i.e. $Gn = 25 > Gn_{cr} = 5.70269$. The second Fourier mode in the solution is evident and is captured also by the weak nonlinear solution although its accuracy suffers due to the large distance from Gn_{cr} .

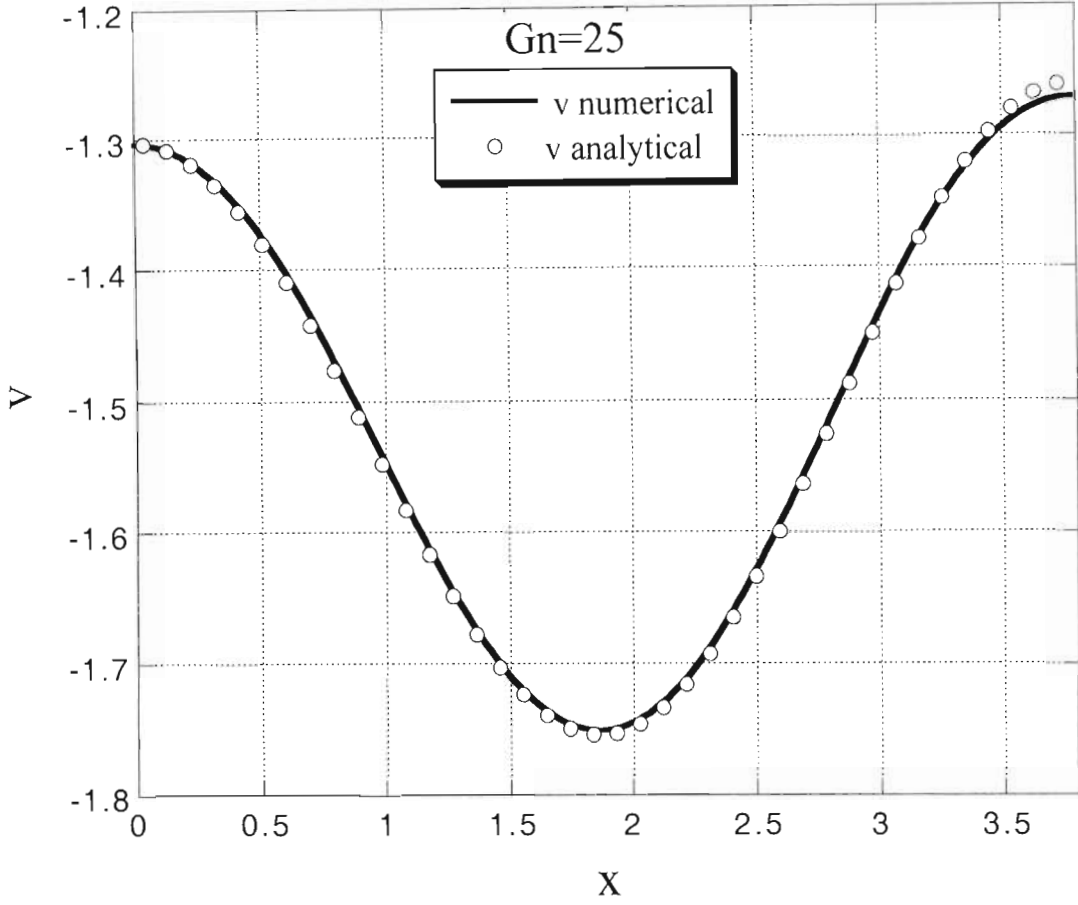


Figure 7.21: Graphical representation of the steady state weak nonlinear solution $v(x)$ compared to the numerical results for a super-critical value of Gn , i.e. $Gn = 25 > Gn_{cr} = 5.70269$. The second Fourier mode in the solution is evident and is captured also by the weak nonlinear solution although its accuracy suffers due to the large distance from Gn_{cr} .

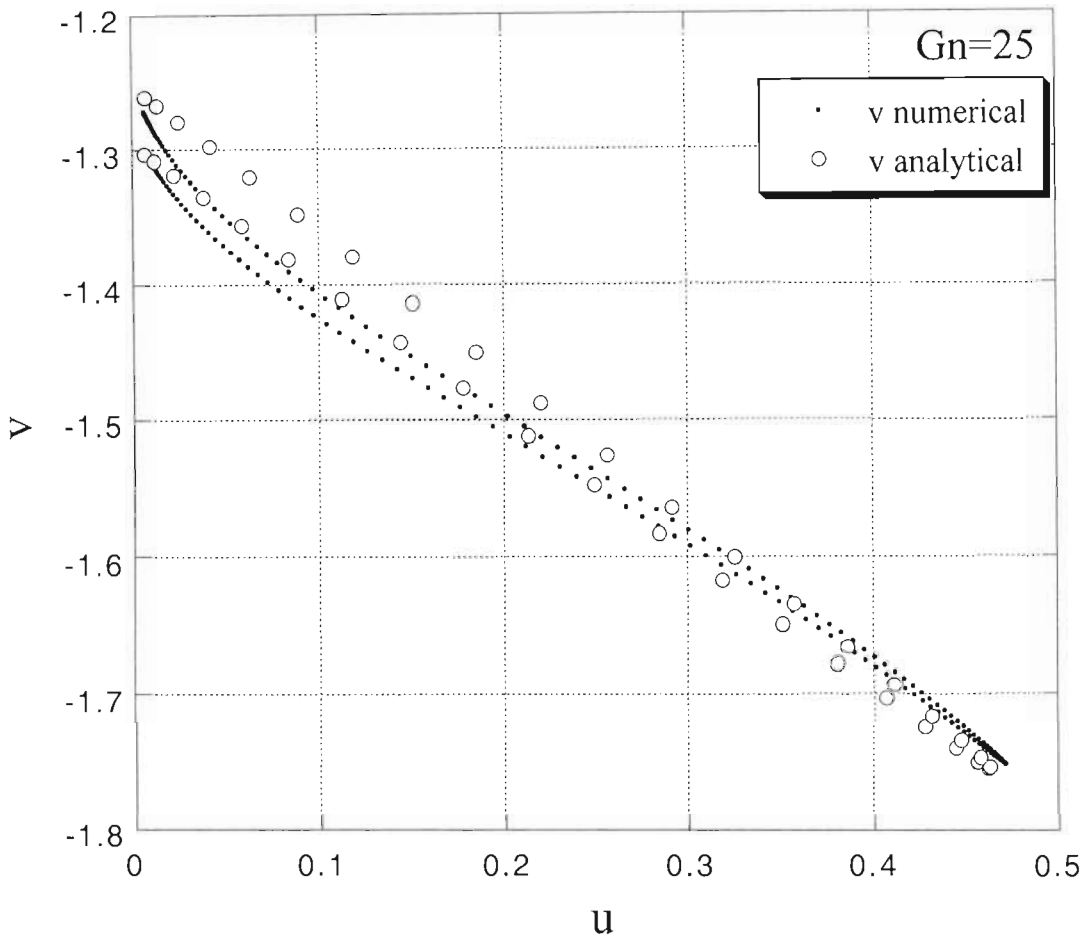


Figure 7.22: Graphical representation of the steady state weak nonlinear solution v vs. u on the phase plane compared to the numerical results for a large super-critical value of $Gn = 25 > Gn_{cr} = 5.70269$.

CHAPTER 8

DISCUSSION AND CONCLUSIONS

A theoretical account of investigating the growth dynamics in heterogeneously distributed populations was presented. In particular the problem of the occurrence of Turing instabilities and spatial pattern formation was considered. Derivation of analytical solutions to the problem of growth of populations in space and in time was performed.

The existing analytical work on Turing instabilities does not go as far as obtaining a complete analytical solution to the problem and therefore is limited to producing stability conditions only.

Complete analytical results even when their accuracy is limited to a narrow parameter range can provide a tool for validation of numerical solutions and can identify the conditions for occurrence or prevention of Turing instability, a tool much needed in planning experiments.

The analytical solutions derived in this study were accomplished by using linear stability analyses and the weak nonlinear method of solution. The analytical solutions were compared to numerical results obtained via standard differential equations solvers showing a very good match within the parameter windows where the analytical solutions are expected to be valid.

This work presents the first application of the Neoclassical Model to the spatially heterogeneous problem. It was demonstrated that the linear stability analysis produce results that might prompt misleading interpretations. The weak nonlinear results provide the complete solution to the nonlinear problem, which are accurate in the neighborhood of the critical value of the controlling parameter and for small amplitudes. The results also show that solutions, which are oscillatory in time, cannot develop spatial heterogeneity, i.e. they are uniform in space.

REFERENCES

- Akçakaya, H.R., Ginzburg, L.R., Slice, D. and Slobodkin, L.B. 1988. The theory of population dynamics – II. Physiological delays, *Bulletin of Mathematical Biology* **50** (5), pp. 503-515.
- Alee, W.C., 1931. *Animal aggregations – A study in General Sociology*, University of Chicago Press, Chicago.
- Allen, J.C., 1975. Mathematical models of species interactions in time and space. *American Naturalist* **109**, p.319.
- Baranyi, J. and Roberts, T.A., 1994. A dynamic approach to predicting bacterial growth in food. *International Journal of Food Microbiology* **23**, pp. 277-294.
- Baranyi, J., Roberts, T.A. and McClure, P.J., 1993. A non-autonomous differential equation to model bacterial growth. *International Journal of Food Microbiology* **10**, pp. 43-59.
- Boiteux, A. and Hess, B., 1978. Visualization of dynamic spatial structures in glycolyzing cell-free extracts of yeast. in *Frontiers of Biological Energetics*, P.L. Dutton, J. Leigh, A. Scarpa (Eds.), Academic Press, New York, pp. 789-798.
- Carlson, T., 1913. Über Geschwindigkeit und Grösse der Hefevermehrung in Würze. *Biochem. Ztschr.* **57**, pp. 313-334.
- Castets, V., Dulos, J., Boissonade, J., DeKepper, P., 1990. Experimental evidence of a sustained standing Turing-type nonequilibrium chemical pattern. *Physical Review Letters* **64**, p. 2953.
- Cross, M.C., Hohenberg, P.C., 1993. Pattern formation outside equilibrium. *Review of Modern Physics* **65**, p. 851.
- Davey, H.M., Davey, C.L., Woodward, A.M., Edmonds, A.N., Lee, A.W. and Kell, D.B., 1996. Oscillatory, stochastic and chaotic growth rate fluctuations in permissively controlled yeast cultures. *BioSystems* **39**, pp. 43-61.

- Edelstein-Keshet, L., 1988. *Mathematical Models in Biology*. Random House, New York.
- Epstein, I., Showalter, K., 1996. Nonlinear chemical dynamics: oscillations, patterns and chaos. *Journal of Physical Chemistry* **100**, p. 13132.
- Fried, H.M. and Fink, G.R., 1978. Electron microscopic heteroduplex analysis of "killer" double - stranded RNA species from yeast. *Proceeding of the National Academy of Science of the USA* **75**, pp. 4224-4228.
- Ginzburg, L.R., 1986. The theory of population dynamics: I. Back to first principles, *J. Theoretical Biology* **122**, pp. 385-399.
- Gompertz, B., 1825. On the nature of the function expressive of the law of human mortality and a new mode of determining the value of life contingencies. *Philosophical Transactions of the Royal Society of London* **115**, pp. 513-583.
- Haken, H., 1979. Pattern formation and pattern recognition – an attempt at a synthesis. in: Haken, H. (Ed.), *Pattern Formation by Dynamic Systems and Pattern Recognition*, Springer-Verlag, Berlin, pp. 2-13.
- Hutchinson, G.E., 1948. Circular casual systems in ecology. *Annals N.Y. Academy Sciences* **50**, pp. 211-246.
- IMSL Library, 1991. *Fortran Subroutines for Mathematical Applications*, Version 2, Houston.
- Klausmeir, C., 1999. Regular and irregular patterns in semiarid vegetation. *Science* **284**, p. 1826.
- Kot, M., 1989. Diffusion-driven period doubling bifurcaations. *BioSystems* **22**, p. 279.
- Krebs, C.J., 1978. *Ecology: The Experimental Analysis of Distribution and Abundance*. 2nd edition, Harper & Row Publishers, New York.
- Levin, S.A., Segel, L.A., 1976. Hypothesis for the origin of planktonic patchiness. *Nature* **259**, p. 659.

- Malthus, T.R., 1798. *An Essay on the Principle of Population*, Penguin, Harmondsworth, England.
- Maron, J.L., Harrison, S., 1997. Spatial pattern formation in an insect host-parasitoid system. *Science* **284**, p. 1826.
- May, M. Sir Robert, 1995. Necessity and change: deterministic chaos in ecology and evolution. *Bulletin of the American Mathematical Society* **32** (3), pp. 291-308.
- May, M. Sir Robert, 1981. Models for single populations. in *Theoretical Ecology*, Sir Robert M. May (Ed.), Blackwell Scientific Publications, Oxford, pp. 5-29.
- May, M. Sir Robert, 1978. Mathematical aspects of the dynamics of animal populations. in: Levin, S. A. (Ed.), *Studies in Mathematical Biology – Part II: Populations and Communities*, Studies in Mathematics **Vol. 16**, The Mathematical Association of America, pp.317-366.
- May, M. Sir Robert, 1973. Time-delay versus stability in population models with two and three trophic levels. *Ecology* **54**, pp. 315-325.
- Meinhardt, H., 1982. *Models of Biological Pattern Formation*, Academic Press, London.
- Mimura, M., Murray, J.D., 1978. On a diffusive prey-predator model which exhibits patchiness. *Journal of Theoretical Biology* **75**, p. 249.
- Murray, J.D., 1989. *Mathematical Biology*, Springer, Berlin.
- Neubert M.G., Caswell, H., Murray, J.D., 2002. Transient dynamics and pattern formation: reactivity is necessary for Turing instabilities. *Mathematical Biosciences* **175**, pp. 1-11.
- Neubert M.G., Kot, M., Lewis, M.A., 1995. Dispersal and pattern formation in a discrete-time predator-prey model. *Theoretical Population Biology* **48**, p. 7.
- Pearl, R., 1927. The growth of populations. *The Quarterly Review of Biology* **II** (4), pp. 532-548.

- Pielou, E.C., 1969. *An Introduction to Mathematical Ecology*. John Wiley & Sons , New York.
- Pirt, S.J., 1975. Growth lag. in *Principles of Microbe and Cell Cultivation*. Blackwell, London.
- Richards, F.J., 1959. A flexible growth function for empirical use. *Journal of Experimental Botany* **10**, pp. 290-300.
- Rohani, P., Ruxton, G., 1999. Diffusion induced instabilities in host-parasitoid metapopulations. *Theoretical Population Biology* **55**, p. 23.
- Segel, L.A., Jackson, J.L., 1975. Dissipative structure: an explanation and an ecological example. *Journal of Theoretical Biology* **37**, p. 545
- Smith, F.E., 1963. Population Dynamics in *Daphnia magna*, *Ecology* **44**, pp. 651-663.
- Strogatz, S.H., 1994. *Nonlinear Dynamics and Chaos*. Perseus Books, Reading MA, pp. 19-20.
- Turing, A., 1952. The Chemical Basis of Morphogenesis. *Phil. Trans. Royal Society of London B* **237**, p. 37.
- Vadasz, A. S., 2000. *Modelling of the Dynamical Interactions of Killer and Sensitive Yeast under Nutritional Stress*, M.Sc. Thesis (*Cum Laude*), University of Durban-Westville, Westville, South Africa.
- Vadasz, A.S., Jagganath, D.B., Pretorius, I.S., Gupthar, A.S., 2000. Electron Microscopy of the K₂ Killer Effect of *Saccharomyces Cerevisiae* T206 on a Mesophilic Wine Yeast. *Antonie van Leeuwenhoek* **78** (2), pp. 117-122.
- Vadasz, A.S., Vadasz, P., Abashar, M.E., Gupthar, A.S., 2001. Recovery of an Oscillatory Mode of Batch Yeast Growth in Water for a Pure Culture. *International Journal of Food Microbiology* **71** / (2-3), pp. 219-234.

- Vadasz, A.S., Vadasz, P., Abashar, M.E., Gupthar, A.S., 2002a. Theoretical and Experimental Recovery of Oscillations during Batch Growth of a Mixed Culture of Yeast in Water. *World Journal of Microbiology & Biotechnology* **18** (3), pp. 239-246.
- Vadasz, A.S., Vadasz, P., Gupthar, A.S., Abashar, M.E., 2002b. Theoretical and Experimental Recovery of Oscillations during Batch Yeast Growth in a Pure Culture Subject to Nutritional Stress. *Journal of Mechanics in Medicine and Biology* **2** (2), pp. 147-163.
- Vadasz, A.S., Vadasz, P., Abashar, M.E. and Gupthar, A.S., 2003. Theoretical and Experimental Evidence of Extinction and Coexistence of Killer and Sensitive Strains of Yeast Grown as a Mixed Culture in Water. *International J. Food Microbiology* **84**, pp. 157-174.
- Vadasz, P., Vadasz, A.S., 2002a. The Neoclassical Theory of Population Dynamics in Spatially Homogeneous Environments – Part I: Derivation of Universal Laws and Monotonic Growth. *Physica A* **309** (3-4), pp. 329-359.
- Vadasz, P., Vadasz, A.S., 2002b. The Neoclassical Theory of Population Dynamics in Spatially Homogeneous Environments – Part II: Non-Monotonic Dynamics, Overshooting and Oscillations. *Physica A* **309** (3-4), pp. 360-380.
- Verhulst, P.F., 1838. Notice sur la loi que la population suit dans son accroissement. *Corr. Math. et Phys. Publ. par A. Quetelet*. T. **X**, pp. 113-121.
- Wangersky, P.J. and Cunningham, W.J., 1957. Time lag in population models. *Cold spring Harb. Symp. Quant. Biol.* **22**, pp. 329-338.
- Wilson, W., Harrison, S., Hastings, A., McCann, K., 1999. Exploring stable pattern formation in models of tussock moth populations. *Journal of Animal Ecology* **68**, p. 94.

APPENDICES

Appendix 1: Derivation of the Right-Hand-Side of eq. (5-41)

This Appendix is dedicated to evaluating the derivation of the terms on the right-hand side of eq. (5-41).

$$RHS(5-41) = -R\beta_2 \left(\frac{du_1^2}{dt} \right) + \frac{1}{\beta_4} \frac{d(u_1 v_1)}{dt} - \frac{R}{\beta_4} \frac{d}{dt} \left(u_1 \frac{du_1}{dt} \right) - \beta_2 \gamma_o \quad (A1-1)$$

Evaluating initially the terms u_1^2 , $(u_1 v_1)$, and $u_1 (du_1/dt)$ by using the $O(\varepsilon)$ solution (5-22) yields

$$u_1^2 = B_1^2 e^{i2\sigma_o t} + B_1^{*2} e^{-i2\sigma_o t} + 2 B_1 B_1^* \quad (A1-2)$$

$$u_1 v_1 = B_1 C_1 e^{i2\sigma_o t} + B_1^* C_1^* e^{-i2\sigma_o t} + B_1^* C_1 + B_1 C_1^* \quad (A1-3)$$

$$u_1 \frac{du_1}{dt} = i\sigma_o (B_1^2 e^{i2\sigma_o t} - B_1^{*2} e^{-i2\sigma_o t}) \quad (A1-4)$$

Therefore taking the time derivatives of (A1-2), (A1-3) and (A1-4) yields

$$\frac{d(u_1^2)}{dt} = i2\sigma_o (B_1^2 e^{i2\sigma_o t} - B_1^{*2} e^{-i2\sigma_o t}) \quad (A1-5)$$

$$\frac{d(u_1 v_1)}{dt} = i2\sigma_o (B_1 C_1 e^{i2\sigma_o t} - B_1^* C_1^* e^{-i2\sigma_o t}) \quad (A1-6)$$

$$\frac{d}{dt} \left(u_1 \frac{du_1}{dt} \right) = -2\sigma_o^2 (B_1^2 e^{i2\sigma_o t} + B_1^{*2} e^{-i2\sigma_o t}) \quad (A1-7)$$

Substituting these terms into eq. (A1-1) produces the result

$$\begin{aligned} RHS(5-41) = & -i2\sigma_o R\beta_2 (B_1^2 e^{i2\sigma_o t} - B_1^{*2} e^{-i2\sigma_o t}) + \\ & \frac{i2\sigma_o}{\beta_4} (B_1 C_1 e^{i2\sigma_o t} - B_1^* C_1^* e^{-i2\sigma_o t}) + \\ & \frac{2\sigma_o^2 R}{\beta_4} (B_1^2 e^{i2\sigma_o t} + B_1^{*2} e^{-i2\sigma_o t}) - \beta_2 \gamma_o \end{aligned} \quad (A1-8)$$

By grouping likewise terms in eq. (A1-8) yields

$$\begin{aligned}
 RHS(5-41) = & \left[\frac{2\sigma_o^2 R}{\beta_4} B_1 + i2\sigma_o \left(\frac{C_1}{\beta_4} - R\beta_2 B_1 \right) \right] B_1 e^{i2\sigma_o t} + \\
 & \left[\frac{2\sigma_o^2 R}{\beta_4} B_1^* - i2\sigma_o \left(\frac{C_1^*}{\beta_4} - R\beta_2 B_1^* \right) \right] B_1^* e^{-i2\sigma_o t} - \beta_2 \gamma_o
 \end{aligned} \tag{A1-9}$$

By substituting the relationships between B_1 and C_1 , and between B_1^* and C_1^* from eqs. (5-27) in the form

$$C_1 = i \frac{\sigma_o}{\beta_2} B_1; \quad C_1^* = -i \frac{\sigma_o}{\beta_2} B_1^* \tag{5-27}$$

produces the result

$$\begin{aligned}
 RHS(5-41) = & \left[\frac{2\sigma_o^2(\beta_2 R - 1)}{\beta_2 \beta_4} - i2\sigma_o R \beta_2 \right] B_1^2 e^{i2\sigma_o t} + \\
 & \left[\frac{2\sigma_o^2(\beta_2 R - 1)}{\beta_2 \beta_4} + i2\sigma_o R \beta_2 \right] B_1^{*2} e^{-i2\sigma_o t} - \beta_2 \gamma_o
 \end{aligned} \tag{A1-10}$$

Equation (A1-10) represents the explicit form of the right hand side of eq. (5-41).

Appendix 2: Derivation of the Right-Hand-Side of eq. (5-43)

This Appendix is dedicated to evaluating the derivation of the terms on the right-hand side of eq. (5-43).

$$RHS(5-43) = R\sigma_o^2 u_1^2 - \frac{\beta_{o,cr}}{\beta_4} u_1 v_1 + \frac{R\beta_{o,cr}}{\beta_4} u_1 \frac{du_1}{dt} \quad (A2-1)$$

The terms u_1^2 , $(u_1 v_1)$, and $u_1 (du_1/dt)$ were evaluated explicitly in Appendix 1 in the form

$$u_1^2 = B_1^2 e^{i2\sigma_o t} + B_1^{*2} e^{-i2\sigma_o t} + 2 B_1 B_1^* \quad (A2-2)$$

$$u_1 v_1 = B_1 C_1 e^{i2\sigma_o t} + B_1^* C_1^* e^{-i2\sigma_o t} + B_1^* C_1 + B_1 C_1^* \quad (A2-3)$$

$$u_1 \frac{du_1}{dt} = i\sigma_o (B_1^2 e^{i2\sigma_o t} - B_1^{*2} e^{-i2\sigma_o t}) \quad (A2-4)$$

Substituting these terms into eq. (A2-1) produces the result

$$\begin{aligned} RHS(5-43) = & R\sigma_o^2 (B_1^2 e^{i2\sigma_o t} + B_1^{*2} e^{-i2\sigma_o t} + 2 B_1 B_1^*) - \\ & \frac{\beta_{o,cr}}{\beta_4} (B_1 C_1 e^{i2\sigma_o t} + B_1^* C_1^* e^{-i2\sigma_o t} + B_1^* C_1 + B_1 C_1^*) + \\ & \frac{R\beta_{o,cr}}{\beta_4} [i\sigma_o (B_1^2 e^{i2\sigma_o t} - B_1^{*2} e^{-i2\sigma_o t})] \end{aligned} \quad (A2-5)$$

By grouping likewise terms in eq. (A2-5) yields

$$\begin{aligned} RHS(5-43) = & \left[R\sigma_o^2 B_1 - \frac{\beta_{o,cr}}{\beta_4} C_1 + \frac{i\sigma_o R\beta_{o,cr}}{\beta_4} B_1 \right] B_1 e^{i2\sigma_o t} + \\ & \left[R\sigma_o^2 B_1^* - \frac{\beta_{o,cr}}{\beta_4} C_1^* - \frac{i\sigma_o R\beta_{o,cr}}{\beta_4} B_1^* \right] B_1^* e^{-i2\sigma_o t} + \\ & 2R\sigma_o^2 B_1 B_1^* - \frac{\beta_{o,cr}}{\beta_4} B_1^* C_1 - \frac{\beta_{o,cr}}{\beta_4} B_1 C_1^* \end{aligned} \quad (A2-6)$$

By substituting the relationships between B_1 and C_1 , B_1^* and C_1^* , and for $B_1 C_1$, $B_1^* C_1^*$, $B_1 C_1^*$ and $B_1^* C_1$ from eqs. (5-27), (5-28) and (5-29) in the form

$$C_1 = i \frac{\sigma_o}{\beta_2} B_1; \quad C_1^* = -i \frac{\sigma_o}{\beta_2} B_1^* \quad (5-27)$$

$$B_1 C_1 = i \frac{\sigma_o}{\beta_2} B_1^2; \quad B_1^* C_1^* = -i \frac{\sigma_o}{\beta_2} B_1^{*2} \quad (5-28)$$

$$B_1 C_1^* = -i \frac{\sigma_o}{\beta_2} B_1 B_1^*; \quad B_1^* C_1 = i \frac{\sigma_o}{\beta_2} B_1 B_1^* \quad (5-29)$$

produces the result

$$\begin{aligned} RHS(5-43) = & \left[R \sigma_o^2 + \frac{i \sigma_o \beta_{o,cr} (R \beta_2 - 1)}{\beta_2 \beta_4} \right] B_1^2 e^{i 2 \sigma_o t} + \\ & \left[R \sigma_o^2 - \frac{i \sigma_o \beta_{o,cr} (R \beta_2 - 1)}{\beta_2 \beta_4} \right] B_1^{*2} e^{-i 2 \sigma_o t} + 2 R \sigma_o^2 B_1 B_1^* \end{aligned} \quad (A2-7)$$

Equation (A2-7) represents the explicit form of the right hand side of eq. (5-43).

Appendix 3: Derivation of the Resonant Terms on the Right-Hand-Side of eq. (5-64)

This Appendix is dedicated to evaluating the derivation of the resonant terms on the right-hand side of eq. (5-64).

$$\begin{aligned}
 RHS(5-64) = \frac{d}{dt} \left[2R\beta_2 u_1 u_2 - \frac{R}{\beta_4} u_1^3 + \frac{1}{\beta_4} u_1 v_2 + \frac{1}{\beta_4} u_2 v_1 - \right. \\
 \left. - \frac{R}{\beta_4} u_1 \frac{du_2}{dt} - \frac{R}{\beta_4} u_2 \frac{du_1}{dt} - \frac{du_1}{d\tau} \right] - \beta_{o,cr} \beta_2 u_1 - \beta_2 \frac{dv_1}{d\tau}
 \end{aligned} \tag{A3-1}$$

Evaluating initially the resonant part of the terms $u_1 u_2$, u_1^3 , $u_1 v_2$, $u_2 v_1$, u_1 , $u_1(du_2/dt)$, $u_2(du_1/dt)$, $(du_1/d\tau)$ and $(dv_1/d\tau)$ by using the $O(\varepsilon)$ and $O(\varepsilon^2)$ solutions (5-22) and (5-55) yields for $RHS1$

$$\begin{aligned}
 RHS1 = \left[2R\beta_2 u_1 u_2 - \frac{R}{\beta_4} u_1^3 + \frac{1}{\beta_4} (u_1 v_2 + u_2 v_1) - \frac{R}{\beta_4} \frac{d(u_1 u_2)}{dt} - \frac{du_1}{d\tau} \right] = \\
 \left[-i \frac{R\sigma_o}{\beta_4} (B_1 B_{20} + B_1^* B_{21}) - \frac{dB_1}{d\tau} - 2R\beta_2 (B_1 B_{20} + B_1^* B_{21}) - \right. \\
 \left. \frac{3R}{\beta_4} B_1^2 B_1^* + \frac{1}{\beta_4} (B_1 C_{20} + B_1^* C_{21} + B_{20} C_1 + B_{21} C_1^*) \right] e^{i\sigma_o t} + c.c. + n.r.t.
 \end{aligned} \tag{A3-2}$$

where *c.c.* stands for identifying “complex conjugate” terms, and *n.r.t.* stands for “non-resonant terms”. Similarly for $RHS2$

$$RHS2 = -\frac{dv_1}{d\tau} - \beta_{o,cr} u_1 = \left(-\frac{dC_1}{d\tau} - \beta_{o,cr} B_1 \right) e^{i\sigma_o t} \tag{A3-3}$$

Taking the time derivative of $RHS1$ and multiplying $RHS2$ by β_2 produces the final form of the right-hand side of eq. (5-64) as follows

$$\begin{aligned}
RHS(5-64) = & \left\{ i\sigma_o \left[- \left(2R\beta_2 + i \frac{R\sigma_o}{\beta_4} \right) (B_1 B_{20} + B_1^* B_{21}) - \frac{dB_1}{d\tau} - \frac{3R}{\beta_4} B_1^2 B_1^* + \right. \right. \\
& \left. \left. \frac{1}{\beta_4} (B_1 C_{20} + B_1^* C_{21} + B_{20} C_1 + B_{21} C_1^*) \right] + \beta_2 \left(- \frac{dC_1}{d\tau} - \beta_{o,cr} B_1 \right) \right\} e^{i\sigma_o t} + \quad (A3-4)
\end{aligned}$$

c.c. + n.r.t.

Equation (A3-4) represents the explicit form of the right hand side of eq. (5-64).

Appendix 4: Derivation of the Right-Hand-Side of eq. (7-29)

This Appendix is dedicated to evaluating the derivation of the terms on the right-hand side of eq. (7-29).

$$RHS(7-29) = \mathcal{L}_2 \left[-\frac{R}{\beta_4} u_1 \frac{d^2 u_1}{dx^2} - \frac{Gn_{cr}\beta_5}{\beta_4} u_1^2 - \frac{Gn_{cr}}{\beta_4} u_1 v_1 \right] \quad (A4-1)$$

By using the solutions at order $O(\varepsilon)$

$$u_1 = A_1(\tau) \cos(\kappa_{cr} x) \quad (a) \quad (A4-2)$$

$$v_1 = B_1(\tau) \cos(\kappa_{cr} x) \quad (b)$$

one evaluates

$$u_1 v_1 = A_1 B_1 \cos^2(\kappa_{cr} x) \quad (A4-3)$$

$$u_1^2 = A_1^2 \cos^2(\kappa_{cr} x) \quad (A4-4)$$

$$\frac{d^2 u_1}{dx^2} = -\kappa_{cr}^2 A_1 \cos(\kappa_{cr} x) \quad (A4-5)$$

$$u_1 \frac{d^2 u_1}{dx^2} = -\kappa_{cr}^2 A_1^2 \cos^2(\kappa_{cr} x) \quad (A4-6)$$

which substituted into (A4-1) to yield

$$RHS(7-29) = \mathcal{L}_2 \left\{ \left[\frac{\kappa_{cr}^2 R}{\beta_4} A_1^2 - \frac{Gn_{cr}\beta_5}{\beta_4} A_1^2 - \frac{Gn_{cr}}{\beta_4} A_1 B_1 \right] \cos^2(\kappa_{cr} x) \right\} = \quad (A4-7)$$

$$\mathcal{L}_2 \left\{ \left[\left(\frac{\kappa_{cr}^2 R - Gn_{cr}\beta_5}{\beta_4} \right) A_1^2 - \frac{Gn_{cr}}{\beta_4} A_1 B_1 \right] \cos^2(\kappa_{cr} x) \right\} = \mathcal{L}_2 [p_1 \cos^2(\kappa_{cr} x)]$$

By substituting the operator \mathcal{L}_2 from eq. (7-28) as well as the trigonometric relationship

$$\cos^2(\kappa_{cr} x) = \frac{1}{2} \cos(2\kappa_{cr} x) + \frac{1}{2} \quad (A4-8)$$

produces

$$RHS(7-29) = \left(\frac{1}{Rn} \frac{d^2}{dx^2} + \varphi_o \right) [p_1 \cos^2(\kappa_{cr} x)] =$$

$$\frac{p_1}{Rn} \frac{d^2 [\cos^2(\kappa_{cr} x)]}{dx^2} + p_1 \varphi_o \cos^2(\kappa_{cr} x) =$$

$$- \frac{2 p_1 \kappa_{cr}}{Rn} \frac{d}{dx} [\cos(\kappa_{cr} x) \sin(\kappa_{cr} x)] + p_1 \varphi_o \cos^2(\kappa_{cr} x) = \quad (A4-9)$$

$$- \frac{p_1 \kappa_{cr}}{Rn} \frac{d [\sin(2\kappa_{cr} x)]}{dx} + \frac{p_1 \varphi_o}{2} \cos(2\kappa_{cr} x) + \frac{p_1 \varphi_o}{2} =$$

$$- \frac{2 p_1 \kappa_{cr}^2}{Rn} \cos(2\kappa_{cr} x) + \frac{p_1 \varphi_o}{2} \cos(2\kappa_{cr} x) + \frac{p_1 \varphi_o}{2}$$

leading to the final result

$$RHS(7-29) = p_1 \left(\frac{\varphi_o}{2} - \frac{2 \kappa_{cr}^2}{Rn} \right) \cos(2\kappa_{cr} x) + \frac{p_1 \varphi_o}{2} \quad (A4-10)$$

Appendix 5: Derivation of the Right-Hand-Side of eq. (7-31)

This Appendix is dedicated to evaluating the derivation of the terms on the right-hand side of eq. (7-31).

$$RHS(7-31) = -\frac{R\beta_o}{\beta_4} u_1 \frac{d^2 u_1}{dx^2} - \frac{Gn_{cr}\beta_o\beta_5}{\beta_4} u_1^2 - \frac{Gn_{cr}\beta_o}{\beta_4} u_1 v_1 \quad (A5-1)$$

By using the solutions at order $O(\varepsilon)$

$$u_1 = A_1(\tau) \cos(\kappa_{cr} x) \quad (a) \quad (A5-2)$$

$$v_1 = B_1(\tau) \cos(\kappa_{cr} x) \quad (b)$$

one evaluates

$$u_1 v_1 = A_1 B_1 \cos^2(\kappa_{cr} x) \quad (A5-3)$$

$$u_1^2 = A_1^2 \cos^2(\kappa_{cr} x) \quad (A5-4)$$

$$\frac{d^2 u_1}{dx^2} = -\kappa_{cr}^2 A_1 \cos(\kappa_{cr} x) \quad (A5-5)$$

$$u_1 \frac{d^2 u_1}{dx^2} = -\kappa_{cr}^2 A_1^2 \cos^2(\kappa_{cr} x) \quad (A5-6)$$

which substituted into (A5-1) and using the trigonometric relationship

$$\cos^2(\kappa_{cr} x) = \frac{1}{2} \cos(2\kappa_{cr} x) + \frac{1}{2} \quad (A5-7)$$

produces

$$RHS(7-31) = \beta_o \left[\frac{R\kappa_{cr}^2}{\beta_4} A_1^2 - \beta_o \frac{Gn_{cr}\beta_5}{\beta_4} A_1^2 - \frac{Gn_{cr}\beta_o}{\beta_4} A_1 B_1 \right] \cos^2(\kappa_{cr} x) = \quad (A5-8)$$

$$\beta_o p_1 \cos^2(\kappa_{cr} x) = \frac{\beta_o p_1}{2} \cos(2\kappa_{cr} x) + \frac{\beta_o p_1}{2}$$

leading to the final form

$$RHS(7-31) = \frac{\beta_o p_1}{2} \cos(2\kappa_{cr} x) + \frac{\beta_o p_1}{2} \quad (A5-9)$$